Downloaded from orbit.dtu.dk on: Apr 17, 2024

DTU Library

Smart Surface Chemistries of Conducting Polymers

for Guiding Cell Behavior in Polymeric Microsystems

Lind, Johan Ulrik

Publication date:
2012

Document Version
Publisher's PDF, also known as Version of record

Link back to DTU Orbit

Citation (APA):
Lind, J. U. (2012). *Smart Surface Chemistries of Conducting Polymers: for Guiding Cell Behavior in Polymeric Microsystems*. Technical University of Denmark.

General rights
Copyright and moral rights for the publications made accessible in the public portal are retained by the authors and/or other copyright owners and it is a condition of accessing publications that users recognise and abide by the legal requirements associated with these rights.

- Users may download and print one copy of any publication from the public portal for the purpose of private study or research.
- You may not further distribute the material or use it for any profit-making activity or commercial gain
- You may freely distribute the URL identifying the publication in the public portal

If you believe that this document breaches copyright please contact us providing details, and we will remove access to the work immediately and investigate your claim.

Smart Surface Chemistries of Conducting Polymers

-for Guiding Cell Behavior in Polymeric Microsystems

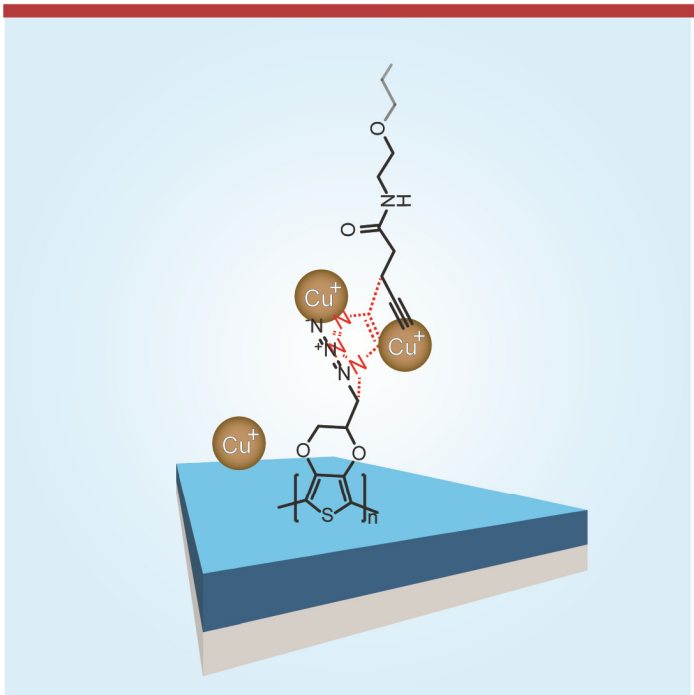

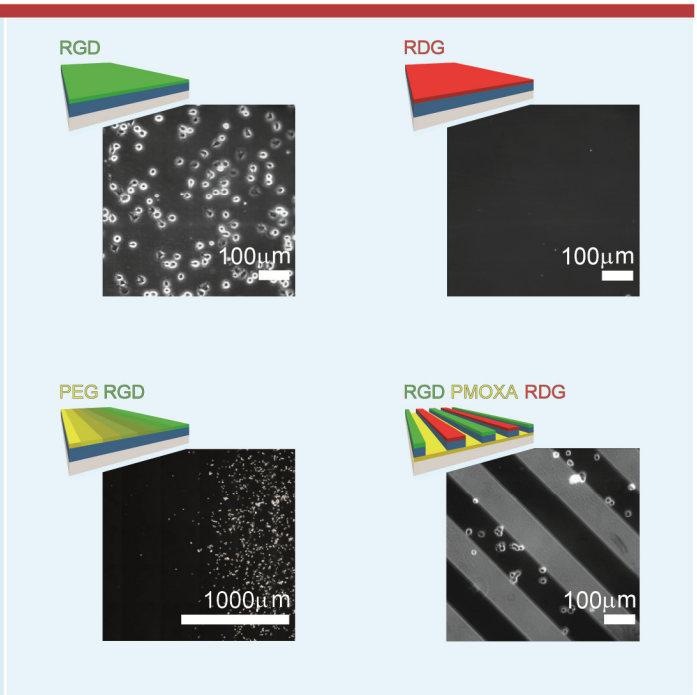

Johan Ulrik Lind

Ph.D. Thesis

DTU Nanotech

Department of Micro- and Nanotechnology

· Ph.D. Thesis · Johan Ulrik Lind ·

· Technical University of Denmark · Department of Micro- and Nanotechnology ·

· February 2012 ·

Abstract

In this thesis we investigate post-polymerization covalent modifications of poly(3,4-dioxythiophene (PEDOT)-type conducting polymers. The aim of the modifications is to gain specific control of the interaction between the material and living mammalian cells. The use of "click-chemistry" to modify an azide-modified PEDOT, poly(3,4-(1-azidomethylethylene)-dioxythiophene) (PEDOT-N_3), is studied in detail, and found to be a valuable approach. This is concluded, as we are able to obtain delicate control of cellular adhesion, by covalently attaching appropriate bio-functional molecules onto PEDOT-N_3 thin film substrates.

Complementing these findings, we introduce a novel technique for fabricating surface chemical gradients on PEDOT-N_3 substrates. The technique is based on applying "electro-click chemistry" to locally induce covalent modifications. Further supplementing these results, we develop a straightforward and in-expensive method for patterning conducting polymer thin films into microelectrodes, without losing control of the surface chemistry of the samples. On the contrary, the method provides direct control of the surface chemistry of both the fabricated micro-electrodes and the gaps between them. The method is based on locally removing PEDOT-type polymers to expose underlying non-conducting functional polymer substrates. Thereby, multifunctional substrates are obtained. By applying this method, we are able to fabricate all-polymer micro-systems with multiple types of localized functional (bio)-chemistries.

In the course of our studies, we find that PEDOT-N_3 thin films undergo a significant yet reversible swelling when exposed to dimethyl-sulfoxide (DMSO). This swelling is found to be of practical use for controlling the reaction density and depth. This, for example, enables the fabrication of dense poly-ethylene-glycol-coatings of the conducting polymer substrates. These coatings render the substrates resistant to protein adsorption. Hence, the choice of solvent is found to be a key parameter for achieving functional post-polymerization modifications of PEDOT-N_3.

The methods developed in this thesis are highly generic, and can therefore be applied for fabricating a diversity of microsystems based on conducting polymers, with multiple types of localized and highly bio-specific surfaces chemistries.

Dansk resumé

I denne afhandling studeres interaktionen mellem ledende polymerer af typen 3,4-dioxythiophene (PEDOT) og levende celler fra pattedyr. Målet med studierne er at fastlægge om samspillet mellem denne type materialer og levende celler, kan kontrolleres ved at foretage kovalente ændringer af polymeren, efter polymerisering. Til dette formål benytter vi en azid-modificeret PEDOT: Poly(3,4-(1-azidomethylethylene)-dioxythiophene) (PEDOT-N_3). Dette sætter os i stand til at forankre forskellige typer af overfladekemi til polymeren ved at hjælp af ”klik”-kemi med forskellige alkyn-reaktanter. Denne ”klik”-kemi-tilgang viser sig højst anvendelig til at kontrollere interaktionen mellem materialet og levende celler. Vi er således i stand til at fremstille overflader hvor vedhæftningen af celler kan kontrolleres biologisk specifikt, ved at forankre passende funktionelle molekyler til PEDOT-N_3 substraterne.

Som supplement til disse resultater, præsenterer vi en ny teknik til at fabrikere overfladekemiske gradienter på PEDOT-N_3-tyndfilm. Teknikken er baseret på at anvende "elektro-klik kemi" til lokalt at inducere en kovalent forankring af alkyn-reaktanter. Som yderligere supplement til disse resultater, udvikler vi en simpel og billig metode til at fremstille mikroelektroder af ledende polymerer, hvor den direkte kontrol over overfladekemien af prøverne bevares. Metoden gør det således muligt at kontrollere overfladekemien af både de fabrikerede mikroelektroder samt mellemrummene mellem dem. Metoden er baseret på lokalt at fjerne PEDOT tyndfilm så underliggende ikke-ledende funktionelle polymerer eksponeres, og der derved fremstilles multifunktionelle substrater. Ved at anvende denne metode, fremstiller vi mikrosystemer baseret udelukkende på polymerer, hvor flere typer af funktionel (bio)-kemi præsenteres lokalt.

Igennem vores studier står det klart at PEDOT-N_3 tyndfilm kvælder betydeligt, men reversibelt, når de udsættes for dimethyl-sulfoxid (DMSO). Denne kvældning kan anvendes til at kontrollere reaktionstætheden og reaktionsdybden. Dette muliggør eksempelvis fremstillingen af tætte poly-ethylen-glycol belægninger af PEDOT-N_3 substraterne. Sådanne belægninger gør substraterne modstandsdygtige over for adsorption af proteiner. Altså viser valget af opløsningsmiddel sig at være centralt for, om funktionelle kovalente ændringer af PEDOT-N_3 kan opnås.

Metoderne vi har udviklet i denne afhandling er i høj grad almengyldige, og kan derfor anvendes til at fremstille en mangfoldighed af mikrosystemer baseret på ledende polymerer, med flere typer af lokal og biologisk specifik overfladekemi.

Table of contents

List of abbreviations & nomenclature 1

Chapter 1: Introduction 3

Chapter 2: Covalent Modification of PEDOT-N_3 Thin Films for Controlled Interaction with Living Cells 17

Chapter 3: Covalent Modifications of PEDOT-N_3 Studied by XPS analysis 27

Chapter 4: The Swelling of PEDOT-N_3 in DMSO/Water Mixtures 41

Chapter 5: Solvent Composition Directs Reaction Depth and Density of PEDOT-N_3 Thin Tilms 49

Chapter 6: Bio-Active Surface Chemical Gradients on PEDOT-N_3 Substrates 63

Chapter 7: PEDOT Microelectrodes Fabricated through Printed Dissolution 79

Chapter 8: All-Polymer Microsystems with Multiple In-Register Surface Chemistries 99

Chapter 9: Conclusion 115

References 120

Acknowledgements 128

External communication activities 129

Appendix 1: Syntheses of Alkyne Reactants

Appendix 2: Syntheses of Modified Polystyrene Polymers

Appendix 3: “Complex Surface Concentration Gradients by Stenciled “Electro Click Chemistry””

Appendix 4: “Solvent Composition Directing Click-Functionalization at the Surface or in the Bulk of Azide-Modified PEDOT”

Appendix 5: “Facile Micropatterning of Functional Conductive Polymers with Multiple Surface Chemistries in Register”

List of abbreviations & nomenclature

AFM	Atomic force microscopy
Alkyne-PEG-GRDGS	Peptide containing mixed natural and non-natural amino-acids, linked with peptide bonds. Sequence: *Pentyne-PEG$_{11}$-Glycine$_5$-Phenylalanine(4-iodo)-Glycine-Arginine-Aspartate-Glycine-Serine*
Alkyne-PEG-GRGDS	Peptide containing mixed natural and non-natural amino-acids, linked with peptide bonds. Sequence: *Pentyne-PEG$_{11}$-Glycine$_5$-Phenylalanine(4-iodo)-Glycine-Arginine-Glycine-Aspartate-Serine*
APTMS	(3-Aminopropyl)-trimethoxysilane
BSA	Bovine serum albumin
COC	Cyclic olefin copolymer
CuAAC	Copper(I)-catalyzed azide-alkyne Huisgen 1,3-dipolar cycloaddition
DBS	Dodecylbenzenesulfonate
DCM	Dichloromethane
DHB	2,5-dihydroxy benzoic acid
DMAP	4-Dimethylaminopyridine
DMF	Dimethyl-foramide
DMSO	Dimethyl-sulfoxide
EBTB	1-Ethynyl-3,5-bis(trifluoromethyl)benzene
EDC	1-Ethyl-3-(3-dimethylaminopropyl)carbodiimide
EDOT	3,4-ethylenedioxythiophene
EDOT-N_3	3,4-(1-azidomethylethylene)-dioxythiophene)
EDOT-OH	3,4-(1-hydroxymethylethylene)-dioxythiophene)
ELISA	Enzyme-linked immunosorbent assay
FGF	Fibroblast growth factor
Fmoc	Fluorenylmethyloxycarbonyl
GRDGS	Glycine-Arginine-Aspartate- Glycine-Serine
GRGDS	Glycine-Arginine-Glycine-Aspartate-Serine
HATU	Hexafluorophosphate-Methanaminium
HBSS	Hank's balanced saline solution
HRP	Horse radish peroxidase
HRP-IgG	Horse-radish peroxidase conjugated to Immunoglobulin G IgG
HSA	Humane serum albumin
IgG	Immunoglobulin G
MeOx	2-methyl-2-oxazoline
NaAsc	Sodium ascorbate
NGF	Nerve growth factor

NHS	N-hydroxysuccinimide
NTA	Nitrilotriacetic acid
NTA-alkyne	Prop-2-ynyl 5-(N,N-bis(carboxymethyl)amino)-5-(S)carboxypentanecarbamate)
OTS	Octadecyltrichlorosilane
PANI	Polyaniline
PBS	Phosphate buffered saline
PC-12	Pheochromocytoma-12
PDMS	Poly(dimethylsiloxane)
PEDOT	Poly(3,4-ethylenedioxythiophene)
PEDOT-N_3	Poly((3,4-(1-hydroxymethylethylene)-dioxythiophene)
PEDOT-OH	Poly((3,4-(1-hydroxymethylethylene)-dioxythiophene)
PEDOT:PSS	P-doped PEDOT containing PSS anions
PEDOT:TsO	P-doped PEDOT containing TsO anions
PEDOT-N_3:TsO	P-doped PEDOT-N_3 containing TsO anions
PEG	Poly-ethylene-glycol
PEG-alkyne	α-Methoxy-poly(ethylene glycol)-ω-pent-4-ynamide
PET	Poly(ethylene terephthalate)
PLL	Poly(L-lysine)
PLLA	Poly(L-lactic acid)
PMOXA	Poly(2-methyl-2-oxazoline)
PPy	Polypyrrole
PS	Polystyrene
PS-alkyne	Poly-[(4-prop-2-yn-1-yloxy)-styrene-ran-styrene]
PS-N_3	Poly(4-(azidomethyl)styrene
PSS	Poly(styrene-sulfonic acid)
RGD	Arginine – Glycine - Aspartate
RIE	Reactive ion etching
RP-HPLC	Reverse phase high performance liquid chromatography
RPMI	Roswell park memorial institute
SAM	Self-assembled monolayer
TFA	Tri-fluoro-acetic-acid
TIPS	Tri-isopropyl silane
TMB	Tetramethylbenzidine
TRIS	Tri-(hydroxymethyl)aminomethane
TsO	Tosylate
XPS	X-ray photoelectron spectroscopy

Chapter 1

Introduction

Motivation

Advanced polymer devices for improved cell handling and culturing

Culturing and handling of living cells is becoming increasingly important in modern day medical research and therapy. Although impressive research breakthroughs have been made using conventional plastic culture dishes, the results are difficult to translate into clinical use for the general public. This is due to the need for expensive and time consuming analytical equipment, and more importantly; the need of a highly skilled specialist staff. These limitations can be overcome by developing more advanced cell culturing systems. Such systems should be automated and contain multiple functions performing analysis and accurate control of cell development, with a minimum requirement of skilled labor. Additionally, the systems should be sufficiently in-expensive to enable practical use in the clinic.

Automated polymer micro-fluidic systems offer such an alternative to the conventional culture dishes. In principle, they allow a much higher degree of control of the local cell environment and stimuli than conventional culture dishes. This enables a higher degree of accuracy in cell culturing and handling. However, to fully realize this potential, there is a demand for development of novel functional materials and accompanying processing methods, which can allow fabrication of systems with concurrent delicate control of the cell environment and stimuli and integrated analysis of cell development.

Conducting polymers: Smart materials for advanced polymer cell handling devices

There is an extensive pool of materials available when producing polymer-based micro-fluidic systems.[1] The choice of materials is defined by which properties are demanded for a given task. Electric conductance is a material property which can drastically add functionality to a micro-fluidic system.[2-4] For introducing conductance to the systems, conducting polymers is an exciting class of materials that in some cases can act as in-expensive alternative to metals and semiconductors. Equally important, conducting polymers have a number of attractive unique characteristics that make them particularly well-suited for the use in bio-medical devices. These include the ability to act both as an ionic and an electronic conductor, optical transparency, and the potential for altering the chemical appearance of the polymers by simply altering the defining monomer.[5-11] For bio-medical purposes, conducting polymers have further valuable features, such as the potential for capturing bio-molecules on or within the polymer, and specifically release these molecules upon electrical stimuli, and the potential for electrochemically control of cellular adhesion.[12-16] Poly(3,4-dioxythiophene) (PEDOT) is a particularly attractive conducting polymer, due to its ease of handling, high conductance, chemical stability, and cellular compatibility.[5, 6, 17]

Controlling the interaction between conducting polymers and living cells

One of the central aspects of controlling cell development is controlling the microenvironment of the cell. The microenvironment is defined by a number of factors. These include the contents of the liquid in the cell proximity and the surface chemical properties, the physical properties, and the shape of the materials in contact with the cell. The content of the liquid in the cell proximity can be accurately controlled in micro-fluidic systems, as they offer a very precise control of liquid movement and exchange. This important aspect has been, and still is, the center of numerous studies.[2, 4, 18, 19] In this thesis we focus on another central aspect of the cellular environment; namely surface chemical properties of the materials applied in the micro-fluidic system. Specifically, the central focus has been the surface chemical properties of PEDOT-type conducting polymers, and how the surface chemistry can be altered to facilitate highly specific interactions between the material and living mammalian cells. Our approach to adjusting the surface chemical properties has been to apply post-polymerization functionalization of a modified PEDOT polymer. Mainly, we have applied an azide modified PEDOT, Poly(3,4-(1-azidomethylethylene)-dioxythiophene) (PEDOT-N_3), which can be specifically modified with functional alkyne reactants through click chemistry.

We have found that a highly controlled interaction with cells can indeed be obtained using this approach. We have further found that the choice of solvent can be used as a simple method for controlling the depth and density of the functionalizations. Along with these findings, we have developed a method for patterning active surface chemistries into gradient patterns on conducting polymer substrates. In addition to this, we have investigated how functional PEDOT-types can be processed and combined with other functional polymeric materials, to create advanced all-polymeric cell handling systems with multiple localized bio-functional surface chemistries.

The structure of this thesis

In the remainder of this introduction we first present the rationale for our choice of methodology for adjusting the relation between PEDOT-type polymers and living cells. Subsequently, a short overview of the general properties and uses of PEDOT-type polymers will be given. We will then give a number of examples from the recent literature of valuable approaches to modifying PEDOT to facilitate a specific use of the material. In doing so, modifications aimed at tailoring the interaction with living cells will be emphasized. This overview will highlight that there is a wide range of different methodologies available that may serve as supplements or alternatives to the approach which we have taken. Following the introduction, our central findings will be presented and discussed in seven Chapters.

In Chapters 2-5 we present results related to uniform functionalizations of PEDOT-N_3 thin films:

In Chapter 2 we show how a finely controlled cellular adhesion onto PEDOT-N_3 substrates can be achieved through covalent modification with appropriate alkyne reactants.

In Chapter 3 we illustrate how X-ray photo-electron spectroscopy (XPS) was used for confirming and quantifying the surface chemical modifications of the PEDOT-N_3 substrates.

In Chapter 4 we show that PEDOT and especially PEDOT-N_3 thin films undergo a violent yet reversible swelling when exposed to solvent mixtures with high dimethyl-sulfoxide (DMSO) contents.

In Chapter 5 we present a simple method for controlling the reaction depth and density, when functionalizing PEDOT-N_3 thin films. The method is based on the swelling characteristics of PEDOT-N_3 which are outlined in Chapter 4. We show how dense poly-ethylene-glycol (PEG) coatings for limiting the adsorption of proteins can be made in this manner without compromising the conductance of the substrate.

Chapters 6-8 will be centered on methods for laterally localizing specific surface chemistries onto different parts of a sample, and on the combination of PEDOT-type polymers with other functional polymers:

In Chapter 6 we present a method for directing surface chemistries, including the cell active chemistries presented in Chapter 2, into gradient patterns on PEDOT-N_3 substrates.

In Chapter 7 a simple method for locally removing PEDOT-type polymer films from an underlying substrate is presented. Importantly, the method thereby exposes the surface chemistry of the underlying support in an unperturbed form. We further show how this can be applied to fabricate PEDOT microelectrodes where the surface chemistries in the gaps between the electrodes can be directly controlled.

In Chapter 8 we combine the patterning procedure introduced in Chapter 7 with the surface chemistries introduced in Chapter 2, to fabricate all-polymer microfluidic devices, with multiple types of localized, in register, covalently attached, bio-functional surface chemistries.

In Chapter 9, a collected conclusion of the entire work will be given.

Methodology: Click chemistry on PEDOT

A central aim of this thesis is to explore whether post-polymerization covalent modifications is a viable approach to controlling the interaction between PEDOT-type polymers and living cells. As will be outlined below, numerous interesting and successful studies using non-covalent approaches have been published, whereas drastically fewer studies have consider covalent approaches. Although non-covalent approaches in many cases have proven to be of great value, we suggest covalent modification holds a number of advantages that makes this approach attractive as an alternative and as a supplement to the non-covalent approaches. One major advantage should be that the bond strength ensures that multiple active molecules can be attached without the risk of one molecule out-competing the other for example due to a stronger adsorption onto the material. This should facilitate the design of substrates with complex surface chemical compositions. Equally important, attaching a (bio)-molecule covalently permits control of the orientation of the molecule, which can be essential to its function. Additionally, the covalent bond also allows large density functionalizations of specifically oriented molecules. For instance, we have exploited this for fabricating cell- and protein-resistant PEG surface coatings of PEDOT-type substrates.

We chose to apply a post-polymerization functionalization route where specific chemical handles for further modification were introduced in the PEDOT monomer. This approach has the benefit that various chemical entities can be introduced without the need to synthesize new PEDOT monomers. It furthermore allows vertical localization of the chemical functionalities, for instance, for functionalizing only the surface of a film, without interfering with its bulk properties. Additionally, as we will show in this report, laterally localized chemical modifications are also facilitated by this approach. However, for many chemical reactions, specific solvents or elevated temperatures are needed, which make them in-compatible with bio-molecules. Thus, an appropriate choice of chemical reaction is central for enabling biologically functional modifications. One example of such a reaction is to apply activation of carboxylic acid groups with N-hydroxysuccinimide (NHS) to allow reaction with amine reactants in aqueous environments. This approach was used in three recent studies by Luo *et al.*, Sekine *et al.,* and Xie *et al.* to anchor amine containing bio-molecules onto a carboxylic acid modified PEDOT.[20-22] We have similarly followed a biocompatible approach in our studies, and applied "Click chemistry" for covalently functionalizing an azide modified PEDOT: PEDOT-N_3, see Figure 1. "Click chemistry" is a popular term being used to categorize a number of chemical reactions, which have a number of common favorable traits. The most important of these traits are quantitative reaction yields, no reaction by-products, and mild reaction conditions, ideally allowing aqueous solutions and non-elevated reaction temperatures.[23] The reaction between an azide group and a terminal alkyne; the copper(I)-catalyzed azide-alkyne Huisgen 1,3-dipolar cycloaddition (CuAAC), is by far the most popular example of such a click chemical reaction. Consequently, the reaction has

been successfully used in a multitude of settings, including in post-polymerization modification of polymers.[24-29]

Within the last four years, there have been several reports on the fabrication of PEDOT-type polymers containing alkyne and azide side chain groups, and on the subsequent functionalization of these species using CuAAC.[9-11, 30-32] However, none of these reports treat functionalization of PEDOT with bio-active molecules for controlling the interaction with cells and other biological entities. In our group, a 3,4-(1-azidomethylethylene)-dioxythiophene (EDOT-N_3) monomer was developed prior to the work presented in this thesis. It was found that EDOT-N_3 could be chemically oxidized to yield p-doped PEDOT-N_3 films containing tosylate (TsO) anions.[17] These PEDOT-N_3 films were found to be stable, insoluble, and were functionalized with a range of alkyne reactants.[10] The conductivity of the PEDOT-N_3 films were found to be ~$6 \cdot 10^1$ S/cm, which is in the common range of conducting polymers, but lower compared to similar films of native PEDOT, which have conductivity of ~$7 \cdot 10^2$ S/cm.[5, 10, 17] These PEDOT-N_3 substrates have served as an ideal starting point for both investigating post-polymerization chemical modification aiming at achieving highly specific biologically active PEDOT-type substrates as well as how such PEDOT-type substrates can be patterned and processed to make them valuable materials for all-polymer micro-fluidic systems.

The conducting polymer PEDOT: Properties and applications

Since the discovery of poly-acetylene in the mid-seventies, conductive polymers have developed into a diverse class of materials. The extended conjugated system in the polymer backbone is a preserved common feature, while variations in the side-chain structure and the introduction of hetero-atoms provide the different polymers with distinct physical and chemical properties. These modifications, for example, have served to fabricate polymers that are not flawed by the low stability in air and difficult processing that is hampering poly-acetylene.[5] Figure 1A displays a few of the most commonly used conducting polymers, along with PEDOT-N_3.

The extended conjugated system in the conducting polymers gives rise to a filled valence band and an empty conducting band separated by a small band-gap. Accordingly, conducting polymers are semiconductors. Native PEDOT, for example, has a band gap of ~1.5 eV.[33] Similar to in-organic semiconductors, conducting polymers can be doped to increase the conductivity; p-doping by partial oxidation typically being the relevant method. These doped conducting polymers typically have conductivities in the order of 10^1 S/cm-10^3 S/cm.[5] For comparison, metals have conductivities in the 10^4-10^6 S/cm range. When doping a conducting polymer, net charge is introduced in the polymer backbone, thus counterions will concurrently be introduced into the material to ensure charge neutrality.

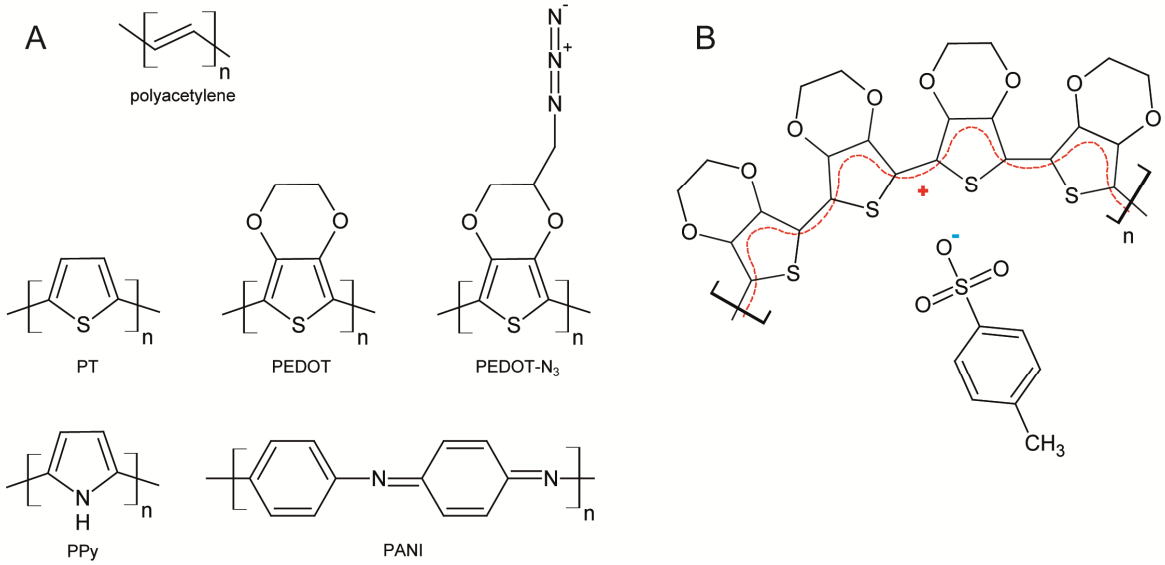

Figure 1 conducting polymers

A: Selected conducting polymers and their abbreviations. PT: polythiophene, PPy: polypyrrole, PANI: polyaniline PEDOT: poly(3,4-ethylenedioxythiophene), PEDOT-N_3: poly(3,4-(1-azidomethylethylene)-dioxythiophene). **B**: p-doped PEDOT containing tosylate anions. A ratio of one tosylate per PEDOT monomer is typically found. The positive charge is dislocated in the conjugated system, here highlighted in red.

The choice of counterion influences the properties of the material, and can therefore serve as a variable for tailoring the properties of a conducting polymer. The PEDOT films which have mainly been investigated in this thesis, contain tosylate counterions and are stable and insoluble, see Figure 1B. However, if poly-anionic Poly(styrene-sulfonic-acid) (PSS) counterions are applied instead of tosylate, PEDOT can be found as water soluble colloids. PEDOT:PSS is thus commercially available as aqueous dispersions.[5] As we generally have applied tosylate ions throughout this thesis, we will not specify the counterion directly, but simply write PEDOT and PEDOT-N_3. In cases where we find that there is a risk of confusion, or where we find it important to emphasize that a particular counterion was used, we will use the nomenclature PEDOT:TsO or similar.

Conducting polymers have not replaced metals and semiconductors. In addition to the lower conductivity, a lower long-term stability of conducting polymers makes metals superior for many applications.[5] However, conducting polymers as a group does hold a number of advantages, such as the low price, easy processing, and perhaps most importantly: The possibility of tailoring the electronic, optical, chemical or even biological properties of the polymer to suit a given problem. Due to these benefits, conducting polymers have today found use in a number of applications. PEDOT is for example being employed in solar cells,[34, 35] organic light emitting electrodes,[36] photographic films,[5] fuel cells,[37, 38] and actuators.[39, 40] Recently, PEDOT has even shown promise for substituting platinum in fuel cells.[37] Within the bio-medical area, PEDOT has been

investigated for use in electrochemical bio-sensors for detecting various relevant biological entities such as oligo-nucleotides,[41, 42] proteins,[20] pH,[43] glucose,[44] and morphine.[45]

Many conducting polymers, including PEDOT, have been found to have great cell-compatibility, and there has consequently been an increasing interest in applying PEDOT and other conducting polymers for handling, analyzing, and culturing of living cells.[6, 46-51] Especially the culturing of neural, epithelial and muscle cells has gathered interest, as the conductance of the substrate can be used for electric or electro-mechanical stimulation of the cells.[51-54] Along these lines, there has been a great interest in the use of conducting polymers as coatings for neural electric recording probes, and in neural implants.[6, 53, 55-57] Most relevant for the use in polymeric cell culturing devices, PEDOT microelectrodes are being investigated for following cell development over time through impedance spectroscopy.[58, 59] Additionally, the high conductance which can be achieved for PEDOT, has allowed the fabrication of all-polymeric electroporation devices.[60] These reports underline that PEDOT is a versatile multifunctional material with great relevance to cell culturing and handling applications.

Tailoring the properties of PEDOT

Similar to all polymers, conducting polymers are defined by the monomers constituting the polymer. By making minor changes in the repeating unit, the properties of a polymer can be drastically changed. In addition, by mixing different monomers, randomized or block co-polymers can be fabricated, these again displaying completely different properties to those of the polymers based on the individual monomers alone. By using these classical methods, conducting polymers with various properties can be produced, and tailored to facilitate a specific application. In fact, PEDOT is itself a successful modification of polythiophene. The introduction of the cyclic ethylene-di-oxy motif leads to a “polythiophene” with a highly stable and highly conductive p-doped state.[5] Following this trend, it has become a highly popular praxis to further modify the EDOT monomer in the ethylene part of the EDOT molecule. As this is not part of the pi-conjugated backbone of PEDOT, numerous new functionalities have been successfully introduced without disrupting the conductance of the polymer, see Figure 2.[9-11, 20, 42, 43, 61-69] The modifications typically either aim at changing the properties of PEDOT directly,[42, 43, 62-67, 69] or at introducing small (bio)-chemical handles, which can be specifically functionalized after polymerization.[9-11, 20, 61, 68] In addition to these approaches aimed at direct functionalization of PEDOT, functionalities can also be added to PEDOT by non-covalent means. This can for example be done by adsorbing functional molecules onto the PEDOT surface,[70] or incorporating functional molecules into the PEDOT matrix; the latter often being done during the polymerization process.[71-73] The modifications of PEDOT, covalent as well as non-covalent, serve to alter the properties of the material. Below, an assortment of relevant examples is given.

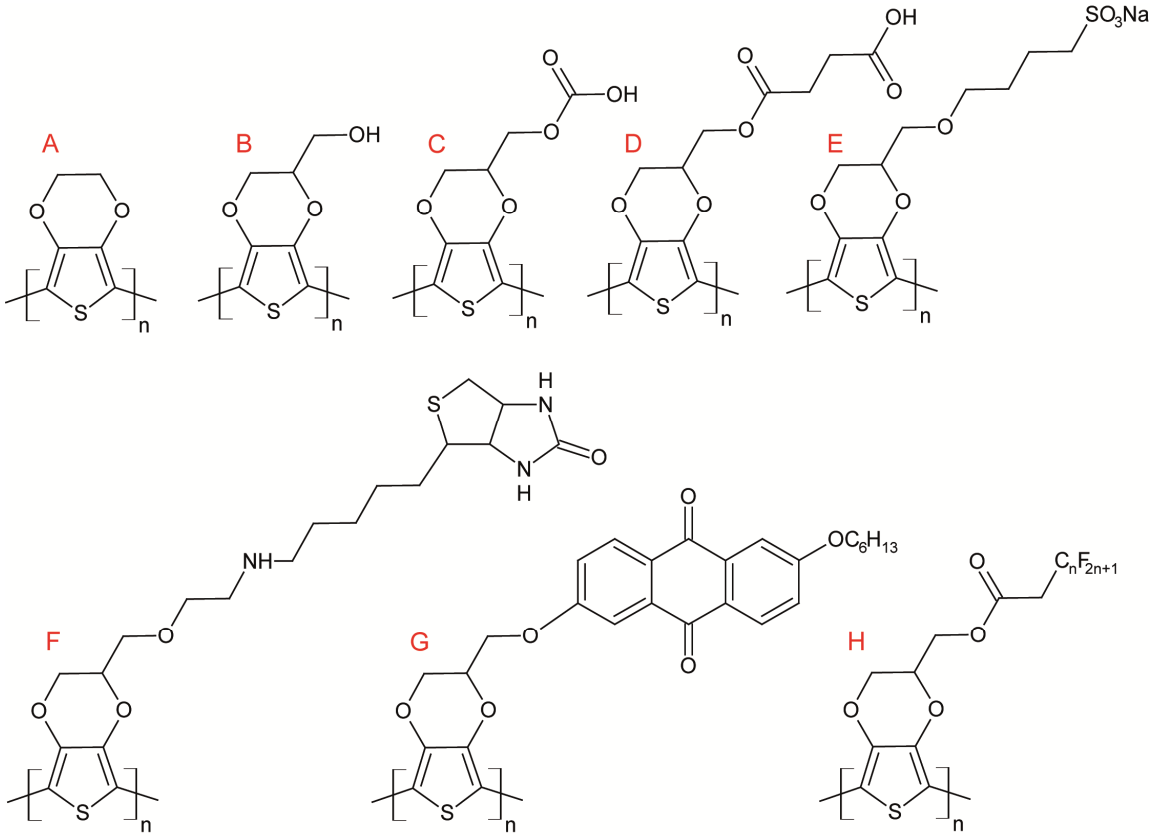

Figure 2 Modified PEDOT-type polymers

A: Regular PEDOT, **B**: Commercially available hydroxyl modified PEDOT, **C**: Carboxylic acid modified PEDOT used by Luo *et al.*[21], **D**: Carboxylic acid modified PEDOT used by Muoffouk & Higgins[42], **E**: Sulfonate modified PEDOT used by Cutler *et al.*[64], **F**: Biotinylated PEDOT used by Muoffouk & Higgins [68], **G**: Anthraquinone modified PEDOT used by Segura *et al.* [63] **H**: Fluorinated PEDOT used by Darmanin *et al.,* n= 4,6,8 [65]

A frequent aim of the modifications of PEDOT is to tune the electro-chemical and optical properties of the material. For example, Segura *et al.* covalently introduced a number of different electron acceptor groups such as anthraquinone into the EDOT monomer side-chain, see Figure 2G. Thereby they obtained PEDOT-type polymers with donor-acceptor redox behavior and an increased light absorption cross-section.[63, 67] Using a vastly different approach, Berggrens group showed that adsorption of tetrakis(dimethylamino)ethylene onto PEDOT films lowered the surface work function without influencing the conductance of the bulk film. Such a modification is relevant if PEDOT is to be used as electron-injecting layers, in addition to the widespread use of PEDOT as a hole-injection layer in photo-voltaic and electro-chromic devices.[70, 74]

Another goal of PEDOT modifications can be to change the intrinsic film-forming properties of the material. For example, Cutler *et al.* covalently modified the EDOT monomer to incorporate a 1-butanesulfonic acid motif in the polymer side-chain, see Figure 2E. Thereby, a capable counterion for the p-doped state was introduced directly into the monomer, allowing the

fabrication of "self-doped" films. In addition, this modification allowed the fabrication of ordered layer-by-layer structures with cationic polymers.[64] Surface chemical properties of PEDOT, such as the hydrophilicity, can similarly be changed by altering the EDOT monomer. This has, for instance, been done by Darmanin *et al.* They incorporated a poly-fluorinated side-chain into the monomer, displayed in Figure 2H. Upon electro-polymerization and concurrent doping with a hexafluorophosphate anion, they obtained superhydrophobic films with a >150° contact angle of water.[65] Non-covalent approaches can also be used to alter the surface energy of PEDOT films. For example, Döbbelin *et al.* fabricated hydrophobic PEDOT:PSS films by introducing cationic molecules with hydrophobic tails into the conducting polymer matrix. The additional positive charge which was thereby introduced was balanced by surplus anionic charge from PSS not engaged balancing the p-doping of PEDOT.[66] PEDOT has also been modified multiple times in order to gain specific sensing capabilities. As an example, Mouffouk and Higgins used a post-polymerization functionalization approach to graft oligo-nucleotides onto a co-polymerized substrate of EDOT and a carboxylic acid modified EDOT, displayed in Figure 2D. Complimentary nucleotide strands could be specifically detected as a shift in the oxidation peak of the film during a cyclic voltametry scan.[42] Similarly they fabricated a biontinylated PEDOT, shown in Figure 2F, which was capable of binding and sensing avidin.[68] In addition to such studies aimed at tailoring the electronic, optical, physical, or sensing properties of PEDOT, there has been an increasing interest in modifying PEDOT, and other conducting polymers, to achieve controlled influence on living cells. These are of special interest to this thesis and will be highlighted in the section below.

Conducting polymers tailored to living cells

Non-covalent methods for changing the biological activity of conducting polymers

One of the most successful approaches to tuning the biological activity of conducting polymers has been to incorporate bio-active molecules into the conducting polymer matrix during the polymerization.[6, 75] This approach was pioneered with polypyrrole (PPy), see Figure 1. The initial studies focused on entrapment of smaller anionic molecules, which could simultaneously balance the p-doping of the polymer and add a biological function to the material. Since then, numerous biologically active macromolecules, such as proteins, have successfully been entrapped in this polymer without losing their function. The bio-molecules presented on the conducting polymer surfaces in this manner have been shown to improve the bio-compatibility of the conducting polymer substrates with various cells.[6, 13, 76-78] In addition to this surface effect, a slow passive release of bio-molecules from the interior of the films has also been observed, which can likewise be of great interest when culturing cells.[6] Most interestingly, it has also been shown that a number of different bio-active molecules entrapped within conducting polymers, such as anti-inflammatory drugs and the protein Nerve growth factor (NGF), can be specifically released upon electrical stimulation.[12, 79, 80]

For many applications PEDOT is a more appealing candidate than PPy due to a superior conductance and stability. However, in contrast to pyrrole, which is water soluble, EDOT has a very low water-solubility. This can naturally be an issue when performing entrapment of bio-molecules in PEDOT during polymerization. Green *et al.* circumvented this by adding a co-solvent such as acetonitrile to aqueous solutions, and co-polymerized laminin-derived peptides and NGF with PEDOT.[49, 81] Suspensions of EDOT in water without any added surfactant have, however, recently been applied successfully to entrap ATP molecules, glucosaminoglycans, and proteins into electro-polymerized PEDOT films.[72, 82-85] For example, Asplund *et al.* incorporated fibrinogen, heparin, and hyaluronate into PEDOT and investigated the *in vitro* and *in vivo* cell compatibility of the fabricated films. Here they observed no *in vitro* cytotoxicity for fibroblast and neuroblastoma cells cultured on the films, and no increased *in vivo* cytotoxicity of PEDOT:heparin covered platinum implants in rats.[82, 83]

As an alternative to introducing bio-functional molecules into conducting polymer films during the polymerization, they can be adsorbed or even incorporated into the film after the polymerization process. Such adsorption or incorporation of bio-molecules, in particular proteins, has been found to rely significantly on the oxidation state of the polymer, and can thus be directed through electrochemistry. For example, Che *et al.* were able to introduce the neurotransmitter glutamate as counterion for p-doped PEDOT, by first reducing a preformed PEDOT film, initially containing tosylate counterions, and then electrochemically re-oxidizing the film in the presence of glutamate.[86] This incorporation of glutamate was reported to attract and anchor neural cells, which showed an improved attachment to the PEDOT:glutamate compared to the native PEDOT:TsO.

In a number of interesting studies, Berggren, Jager and co-workers have compared cell proliferation on reduced and oxidized conducting polymer films. These studies highlight the importance of protein adsorption onto surfaces as determinant for cellular attachment and proliferation. In one study, it was found that the reduction of PEDOT:TsO lead to a decrease in the number of neural stem cells attaching to the surface, by a factor of two.[14] The decreased cell attachment was found to be caused by an increased adsorption of human serum albumin (HSA) onto the reduced film. The adsorbed HSA block the adsorption of other proteins, and thereby limit cellular attachment. Remarkably, in another study, a significantly *increased* cellular adsorption of epithelial cells was obtained on reduced PEDOT:TsO surfaces. This was achieved by pre-adsorbing fibronectin onto the samples. It was thus found that the adsorption characteristics of fibronectin on the reduced surface favored the attachment of epithelial cells, probably due to a more accessible binding site.[15]

In a related study on PEDOT:heparin, they reported that the inherent association of growth factors to heparin could be adjusted by changing the oxidation state of PEDOT:heparin. When reducing the substrate, they found that heparin became less tightly associated with PEDOT,

and, as a consequence, more accessible to binding growth factors. This finding was used for controlling neural stem cell development, by exploiting that neural stem cells remain in an undifferentiated and proliferating state when exposed to fibroblast growth factor (FGF)2. When a PEDOT:heparin film was locally reduced in the presence of FGF2, and neural stem cells were subsequently cultured on the substrates, it was observed that neural stem cells cultured on the reduced part of the film remained undifferentiated, while cells cultured on the oxidized part showed differentiation into neural cell types, and a decreased proliferation. This observation is most likely due to FGF2 binding to a larger extent to the reduced PEDOT:heparin.[87] In addition to PEDOT, the group also studied cell proliferation on PPy samples. In a recent study, they reported that the doping anion had prominent influence on the viability of neural stem cells. Cells cultured on PPy films doped with dodecylbenzenesulfonate (DBS) showed a markedly improved viability compared to those cultured on films doped with tosylate, chloride, and perchlorate. Additionally, they found that reduction of the DBS-doped films could lead to cell death, serving as an electric switch for cell survival. Again, these differences were likely, to some extent, induced by changes in protein adsorption.[88]

Other groups have similarly exploited reduction of PEDOT:TsO for controlling protein adsorption onto the substrates, for the purpose of guiding cell behavior. For example, Gumus *et al.* recently fabricated a gradient of surface associated fibronectin by varying the electric potential along a PEDOT:TsO film. Fibronectin was here found to adsorb in larger concentration in the reduced areas. Surprisingly, haptotactic migration of endothelial cells along the substrate was found to be directed towards lower concentration of fibronectin. This observation was explained by suggesting that an increased cell adhesion to the oxidized PEDOT might counteract the established protein surface gradient.[89] Electrochemical control of macromolecule adsorption has also been investigated for layer-by-layer assembly of alternating anionic and cationic species onto PEDOT:PSS substrates. Collazos-Casteo *et al.* induced association of Poly(L-lysine) (PLL) by reducing the film. The PLL could in turn be used for binding negatively charged heparin to the surfaces. Heparin was then used for used for binding spermine or FGF, the spermine activating neural cell growth, while FGF induced proliferation of precursor cells.[90]

Biologically un-specific adsorption largely dominated by electrostatic attraction has evidently proved to be a useful mechanism for controlling the adsorption of biomolecules onto conducting polymer surfaces. An original alternative approach was put forward by Sanghvi *et al.* They applied phage display to discover peptide sequences with high affinity for PPy:Cl. Subsequently, they fabricated peptide constructs containing a PPy-recognizing segment linked by a spacer to the Arginine-Glycine-Aspartate (RGD) amino acid motif. Peptides containing this motif are known to mimic the function of fibronectin and induce attachment of cells expressing appropriate integrin membrane proteins.[91] The group found that the peptide construct was able to bind to the PPy surface, and furthermore, that the peptide was capable of inducing an increased cell attachment of the investigated pheochromocytoma (PC)12 cells.[92]

Covalent methods for changing the biological activity of conducting polymers

The number of studies using covalent modification of conducting polymers to alter the surface bio-chemistry is significantly lower than the number of studies using non-covalent approaches. There is, however, some interesting studies, which indicate that covalent approaches do hold an exciting potential for controlling cell-material interaction for conducting polymers. Before the studies for this thesis were initiated, Lee *et al.* had shown that a carboxylic acid modified PPy could be directly functionalized with RGD-peptides after polymerization. They found that the surfaces modified with this cell-anchoring motif showed increased adhesion and spreading for endothelial cells when comparing to native PPy and carboxylic acid-modified PPy.[93] More recently, Xie *et al.* attached aptamers with affinity for thrombin covalently to carboxylic acid modified PEDOT nanotubes. Doing so, they succeeded in fabricating a conducting polymer field effect transistor sensor for detection of thrombin.[20] Very recently, Sekine *et al.* used a similar carboxylic acid modified PEDOT to covalently anchor streptavidin to PEDOT substrates. This enabled capture of biotinylated antibodies onto the substrates. By selecting antibodies for specific cells, they were able to capture appropriate cells on the surface. Fascinatingly, they found that this specific capture was only seen for substrates with nanometer scaled roughness. They fabricated such rough substrates through a controlled electro-polymerization of the polymer. [22]These studies thus highlight the importance of structure in controlling cell-material relation.

Covalent modifications of PEDOT have also been used to fabricate PEDOT substrates with other characteristics that make them attractive for cell applications. For example Persson *et al.* fabricated a PEDOT substrate for culturing living cells, which could be disintegrated upon electric reduction, allowing cellular detachment without the use of enzymes. The basis of this platform was a self-doped PEDOT containing sulfonic acid groups introduced in the side-chain of the monomer,[16] similar to that fabricated by Cutler *et al.* displayed in Figure 2E.

Structure and biological activity of conducting polymers

The micrometer and nanometer scale structure of a material surface can have a major effect on the biological activity of the material.[94-96] This holds true for conducting polymers as well. Accordingly, the study by *Sekine et al.*, which was outlined above, does not stand alone. Other studies on various conducting polymers generally suggest that nanometer scaled surface roughness induces cellular adhesion.[53, 97, 98] In a study by Abidian *et al.*, PPy and PEDOT nanotubes were applied to induce the attachment of primary neurons onto neural probes. The conducting polymer nanotubes were made by applying electrospun poly-(L-lactic acid) (PLLA) nano-fibers as templates during electro-polymerization of the conducting polymers. When comparing the attachment of neurons on these nano-structured conducting polymer substrates with that found on the native probes, an increased cellular attachment and neurite outgrowth could be observed.[53]

In addition to the surface structure, the lateral patterning of a conducting polymer can also significantly influence the interaction with cells.[52, 54] Patterning can for example serve as a method for confining cells into defined patches. Such an approach was used by Hsiao *et al.* in a recent study. They applied photo-lithography to pattern PEDOT:PSS thin films into microelectrode arrays with electrode widths down to 20 μm. In the gaps between the electrodes, polyethylene-glycol/polypropylene-glycol oxide/ polyethylene-glycol tri-block co-polymers were adsorbed to hinder cellular attachment to these areas. Thus, cellular attachment and neurite outgrowth of the cultured PC12 cells were confined to the electrodes. This confinement effectively made the cells develop directionally elongated phenotypes.

Summary

A wide range of approaches can be taken towards tailoring the surface chemical properties of PEDOT-type conducting polymers for cell-culturing and -handling applications. Non-covalent approaches based on either the incorporation of functional molecules into the conducting polymer matrix during polymerization or on electrochemically induced surface adsorption have so far been studied in most detail, and have shown promising results. On the other hand, the use of covalent modifications of PEDOT-type polymers to address the issue has only been scarcely investigated prior to this thesis. Investigating the applicability of CuAAC post-polymerization functionalization of PEDOT-N_3 with functional alkyne reactants was therefore chosen as the central topic of this thesis.

Chapter 2

Covalent Modification of PEDOT-N_3 Thin Films for Controlled Interaction with Living Cells

Introduction

One of the most important subjects considering the interaction between a material and a living cell is whether the cell can adhere and proliferate on the material surface. Specifically controlling the adhesion of a distinct cell type is a complex matter, as some cells types adhere readily onto a variety of material surfaces, while others do not. Also, different cell types recognize and adhere onto different specific biological motives, and with varying strengths. Furthermore, the same cell line can gain or lose such specific recognition in the course of its development.[99] Thus, the ability to capture specific cell-types, while avoiding attachment of other cells, is a highly valuable material property both when culturing and analyzing cell populations. As outlined above, most studies on controlling the cell adhesion on conducting polymer surfaces aim at inducing the adhesion of a given cell type by presenting specific bio-molecules on the material surface.[6] Typically, this has been done using non-covalent methods, either by electrochemically inducing the surface adsorption of a bio-molecule,[15, 87, 90] or by incorporating bio-molecules during the polymerization process.[49, 81-83] Covalent anchoring of bio-functional molecules has also been used. For example, RGD-peptides have been attached onto the surface of PPy to induce cellular adhesion.[93] However, the vast majority of the studies have not addressed the issues of *limiting* cell adhesion, and of tailoring the adhesion strength of a particular cell. These issues are nevertheless of large importance in cell-handling and -culturing devices. In such devices, the ability to select particular cells from mixed populations, being either different cell types or a single cell type in different development stages, are of great value. Likewise, the ability to tune cell adhesion strength onto a surface can allow, for example, for the selection of particular cell phenotype during culturing or for transient cell capture for analytical purposes.

To address these issues, we chose an approach which aimed at initially limiting cell adhesion onto the conducting polymer surface, and subsequently presenting selected cell binding motives at controlled concentration on such a background. Specifically, we have functionalized PEDOT-N_3 substrates with PEG-alkyne reactants to fabricate PEG surface coatings that limit cell adhesion. On this PEG-coating background, we have introduced RGD cell binding motives. These were found to re-induce cellular binding. Importantly, similar surfaces presenting a scrambled, *RDG* peptide were not capable of inducing cell binding, showing that the cellular attachment was indeed bio-specific. Finally, one experiment indicated that the cellular adhesion strength onto mixed PEG / RGD surface can be controlled by varying the RGD concentration. Thus, our studies have shown that a highly delicate control of cellular adhesion onto conducting polymer surfaces can be achieved through post-polymerization covalent modifications.

Covalent modification of PEDOT-N_3 can provide bio-specific control of cellular attachment

We applied 3T3 mouse fibroblasts as model cells for studying cellular attachment. These cells were chosen as they are known to be an adherent cell type. They can thus serve as a relevant model for investigating unspecific cellular attachment. Also, 3T3 fibroblasts express integrin types that can be directly addressed to induce specific cellular attachment. In our initial studies, we seeded 3T3 fibroblasts onto native PEDOT-N_3 films. We found that the cells adhered and spread on the substrates within 45 min, see Figure 3 for examples. This suggests that the films are biocompatible. In support of this, we did not observe any apparent toxicity when 3T3 cells were kept for a day or longer on PEDOT-N_3 samples. However, we did not conduct systematic long term studies of cell proliferation on the films. This is demanded if rigid conclusions are to be drawn considering the biocompatibility of PEDOT-N_3. Studies on the toxicology of other PEDOT-class polymers have been performed several times in the literature, and generally PEDOT substrates have been reported to be highly biocompatible.[6] The introduction of organic azide functionality in PEDOT-N_3 might however influence the biocompatibility, although we did not see any indications of such issues.

As 3T3 cells were found to adhere readily onto PEDOT-N_3 surfaces, they can serve as a model for potential situations where attachment of a particular cell type has to be limited. In order to limit cell adhesion, it is essential to control protein adsorption. For the case of PEDOT, this has been highlighted in studies by Berggren and co-workers, who found that cell attachment was intimately linked to the protein adsorption characteristics of the film.[14, 15] Biologic samples normally contain large amounts of various proteins, and more so, living cells continuously secrete proteins. A most common methodology for limiting protein adsorption onto a material is to cover the surface of the material with a dense layer of PEG molecules.[100, 101] PEG coatings limit protein adsorption due to a combination of different effects: Overall, a dense PEG coating serves as a steric hindrance between a protein and an underlying substrate. Also, the direct interaction between proteins and PEG itself is negligible. Additionally, PEG molecules have a high hydrophilicity, and have tightly bound hydrations shell in water. Finally, there is an entropic loss associated with confining a polymer to a smaller conformational space.[101] A complete discussion of the importance of each of these effects is however beyond the scope of this thesis.

We synthesized PEG-alkyne molecules with a molecular weight of 815 Da as described in Appendix 1. The PEG-alkyne molecules were subsequently covalently attached to PEDOT-N_3 thin films using CuAAC. In contrast to the native PEDOT-N_3 films, 3T3 fibroblasts did not adhere onto the PEG-functionalized PEDOT-N_3 films, See Figure 3.

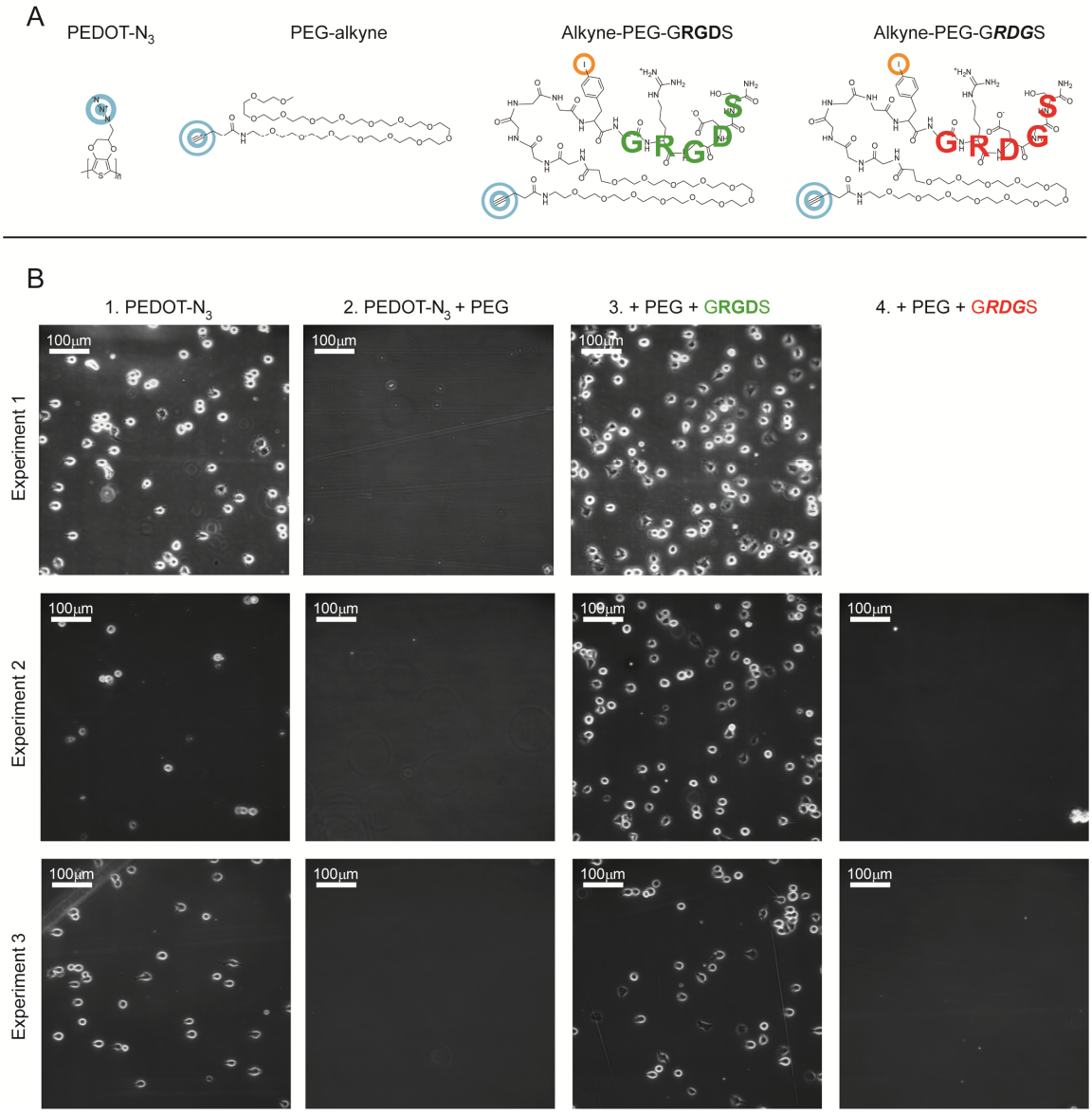

Figure 3 Controlling the adhesion of 3T3 fibroblasts to PEDOT-N_3 through covalent modification

A: Molecular structure of PEDOT-N_3 and the functional alkyne molecules which were attached to the PEDOT-N_3 substrates to specifically control cell adhesion. CuAAC-reactive groups have been highlighted with blue concentric circles. Two peptides were tested for their ability to induce cellular adhesion. The C-terminal amino-acid sequence is highlighted in each of the peptides: The G**RGD**S peptide is expected to induce cellular adhesion, whereas the G***RDG***S is not expected to. In each of the peptides, an iodine hetero-atom XPS marker was introduced. This is highlighted by an orange circle. **B**: Phase-contrast microscope images of 3T3 fibroblasts attached to native and functionalized PEDOT-N_3 substrates. Each row represents one cell adhesion experiment. In each experiment areas functionalized with different surface chemical composition were examined in parallel. See experimental section for reaction conditions used to functionalize PEDOT-N_3. For all experiments, 3T3 cells were seeded in a concentration >1 mio cells/ml, and allowed to adhere for 45 min. Unattached cells were then removed by flowing buffer through the flow chamber, at a gradually increasing rate. For Experiment 1 a GRDGS area was not included. Images displayed were acquired after washing 2 min at 2 ml/min, which is equivalent to a shear stress of 1.25 Pa. Most cells in the PEG-functionalized areas were removed at lower flow rates, whereas the shear was increased to 10 Pa without removing the cells in the G**RGD**S areas.

The successful anchoring of the PEG-alkynes to the PEDOT-N_3 substrates was confirmed by XPS studies, which will be presented in Chapter 3. In order to achieve a functional PEG-coating it is central that the coating is *dense*.[101] We found that the choice of solvent had a significant influence on the density of the PEG-coatings fabricated by anchoring PEG-alkynes onto PEDOT-N_3 from solution. We will investigate this topic in Chapters 3-5. The adsorption of proteins, and consequently the adhesion of cells, onto PEDOT films doped with TsO, has been reported to be drastically influenced by the oxidation state of the film.[14, 15] We did not, however, investigate if cell adhesion could be limited by oxidizing or reducing the polymer. On the contrary, all cell adhesion experiments were done on oxidized p-doped substrates. This approach was taken as we envision that for future potential applications using the conductivity of the material, e.g. for electrical analysis or stimulation of cells, the highly conductive p-doped state is the most relevant.

To achieve a specifically induced cellular attachment, we combined cell binding resistant PEG films with bio-functional peptide motives. On a dense PEG background coating, we presented peptides containing the sequence RGD which can induce attachment of 3T3 fibroblasts and other cells expressing the appropriate integrins.[91] The amino acid sequence Glycine-Arginine-Glycine-Aspartate-Serine (G**RGD**S) has been found to be effective when the RGD-motif is located at the C-terminal of a peptide.[91] We synthesized molecules that contained this amino acid sequence connected via a short PEG spacer to an alkyne group, (alkyne-PEG-GRGDS). The molecule also contained a few additional Glycine residues and a non-natural iodine-marked phenylalanine residue, see Figure 3. This iodine made it possible to directly estimate the amount of peptide on a substrate in XPS, as we will show in Chapter 3. The synthesis is described in Appendix 1. We fabricated mixed surfaces by reacting PEDOT-N_3 substrates first with alkyne-PEG-GRGDS, and subsequently with the PEG-alkyne. The second reaction was performed to ensure that the entire surface was covered by a dense PEG coating. The introduction of the peptides on the PEG background was observed to drastically induce binding and spreading of 3T3 fibroblasts, see Figure 3. Thus, the adhesion of 3T3 fibroblast onto PEDOT-N_3 can be both limited and induced by covalently attaching appropriate molecules. Following this finding, an important question was whether the induced cell binding seen for the RDG surfaces was indeed bio-specific, and not, for instance, caused by the peptides leading to an increased protein adsorption. To elucidate this, we synthesized a control peptide containing the scrambled amino acid sequence R-D-G. The molecule was identical to alkyne-PEG-GRGDS, apart from this exchange of two amino acids. The synthesis is described in Appendix 1. PEDOT-N_3 substrates functionalized with this peptide instead of the alkyne-PEG-GRGDS did not show any induced cellular binding, see Figure 3. This implies that the increased binding observed for the GRGDS peptides is indeed caused by specific biological recognition.

As for the PEG-surfaces, the successful coupling of both the alkyne-PEG-G**RGD**S and the alkyne-PEG-G***RDG***S to PEDOT-N_3 were confirmed by XPS. The XPS data will be discussed thoroughly in Chapter 3. Here we will only note that as both peptides contained an iodine hetero-atom, it was

possible to directly estimate the amount of peptide on a substrate in XPS, also on the mixed surfaces. Thus the G**RGD**S and G***RDG***S surfaces in Figure 3B, contained similar amount of iodine, in addition to a similar overall elemental composition. This confirm that the differences seen in cellular binding is not an artifact caused e.g. by differences in reaction kinetics of the two peptides. The surfaces *do* contain similar amounts of peptides, and are overall chemically equivalent. However, the surfaces have drastically different biological properties, as one heavily induces adhesion of 3T3 Fibroblast while the other limits adhesion of the same cells. Taken as a whole, our studies show that a very high degree of control of PEDOT-N_3 interaction with living cells can be achieved through covalent modification of the conducting polymer substrates. Importantly such modifications were not found to disrupt the conductance of the films, as we will discuss in Chapter 5.

Adjusting the RGD to PEG ratio on PEDOT-N_3 substrates can regulate the adhesion of cells

Having established that specific cellular attachment can be achieved by introducing alkyne-PEG-G**RGD**S on a PEG background, we briefly explored if the adhesion of 3T3 fibroblasts on mixed alkyne-PEG-GRGDS/PEG-alkyne (GRGDS/PEG) substrates could be adjusted by changing the concentration of the peptide. The adhesion of 3T3 fibroblasts onto two mixed GRGDS/PEG surfaces with different concentrations of the peptide is compared in Figure 4. The amount of iodine on each sample was measured on duplicates of the samples using XPS. As the amount of iodine is proportional to the amount of peptide on the surfaces, the experiment suggested that the number of attached cells is larger for samples that contain a high peptide concentration. As will be outlined in Chapter 3, the iodine signal, in combination with the remaining elemental XPS composition, can be used for estimating the percent of the reactants on the surface that are peptides. According to these estimates, ~5% and ~40% of the reactants are peptides, on each of the two surfaces displayed in Figure 4, respectively. In Chapter 6, samples with gradually increasing GRGDS/PEG ratios are investigated. In these experiments, the adhesion of 3T3 cells was observed to follow the same trend as that seen in Figure 4. Thus, our experiments overall indicate that the mixed GRGDS/PEG approach is a highly sensitive procedure for controlling cell adhesion. We suggest that it might be possible to design surface compositions with adhesion strength matching specific purposes, such as weakly attaching surfaces for transient adhesion, for example for purification of cell populations. We did not, however, further investigate such possibilities.

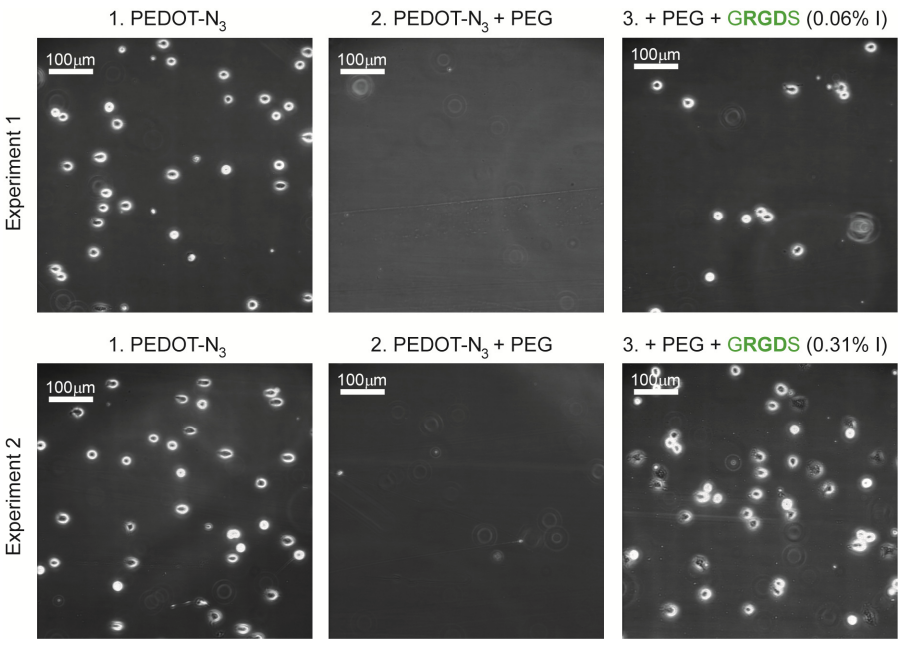

Figure 4 Cellular adhesion on mixed PEG/peptide surfaces with different amounts of peptide
Phase-contrast microscope images of 3T3 fibroblasts attached to native and functionalized PEDOT-N_3 substrates. GRGDS-functionalized areas containing two different peptide concentrations were compared to the native substrate and a PEG-functionalized area, in two separate experiments. See experimental section for reaction conditions used for functionalizing the substrates. The iodine contents of the GRGDS areas were estimated by investigating duplicates of the samples in XPS. The XPS analyses were performed on samples which were not re-oxidized, whereas the cell attachment studies were performed on re-oxidized samples. In each cell adhesion experiment the cell solution and environment was the same for all areas. For all experiments, 3T3 cells were seeded in a concentration >1 mio cells/ml, and allowed to adhere for 45 min. Unattached cells were subsequently removed by flowing buffer through the flow chamber at a gradually increasing rate. Images displayed were acquired after washing 2 min at 2 ml/min, equivalent to a shear stress of 1.25 Pa.

Conclusion

We have demonstrated that making CuAAC post-polymerization modifications of PEDOT-N_3 can serve as highly sophisticated approach for controlling the interaction between this PEDOT-type conducting polymer, and living mammalian cells. Surfaces that resist adhesion of 3T3 fibroblast cells were made by forming PEG coatings of the PEDOT-N_3 substrates. Additionally, by introducing G**RGD**S peptides on such PEG backgrounds, an induced cellular adhesion was achieved. Scrambled G***RDG***S peptides did not induce any cellular attachment. This confirmed that the cellular attachment found for the G**RGD**S substrates was highly bio-specific. The covalent anchoring of the functional molecules further allowed for the fabrication of surfaces with different cell binding capability by changing the G**RGD**S to PEG ratio. Based on our success on controlling cellular adhesion through covalent modification of PEDOT-N_3 substrates, we suggest that similar covalent approaches are applicable for designing conducting polymer surfaces with even more complex surface characteristics, such as surfaces capable of inducing specific cell developments.

Experimental

Preparation of Cyclic Olefin Copolymer supports

Cyclic Olefin Copolymer (COC) supports of the TOPAS brand were made using injection molding. We applied in-house fabricated circular supports with 5 cm diameter and 2 mm thickness. We also applied rectangular shaped supports, with the dimensions of a standard microscope slide: 25 mm x 75 mm and 1 mm thickness. Both types of supports were made using a commercial injection molding machinery; ENGEL VC 80/45, Schwertberg, Austria. TOPAS 5013 substrates were made at 130 °C, using 4 min cooling.

PEDOT-N_3 thin films fabrication

EDOT-N_3 was synthesized in accordance with an earlier reported procedure.[10] PEDOT-N_3 thin films were fabricated by spin-coating and polymerizing on cyclic olefin copolymer (COC) supports as described previously.[10, 17] PEDOT-N_3 substrates were prepared by *in situ* polymerization of EDOT-N_3 on injection molded COC (TOPAS 5013, TOPAS Advanced Polymers, Frankfurt, Germany) substrates, either circular Ø 5 cm discs or microscope slides. The substrates were cleaned with acetone, isopropanol, ethanol, and water prior to spin-coating. EDOT-N_3 (20 mg, 0.15 mmol), CLEVIOS C-B40 (0.48 mL, 40 wt% Fe(III)tosylate in 1-butanol, H.C. Starck, Goslar, Germany), and 1-butanol (0.48 mL) were mixed and spin-coated onto the substrates (20 s at 700 rpm). The samples were placed in an oven or at hot plate at 70 °C for 2 min and subsequently washed with water and blown dry in a nitrogen flow, yielding films with a thickness of approximately 150 nm.

Alkyne reagents

The syntheses of the PEG-alkyne (815 Da), alkyne-PEG-GRGDS, alkyne-PEG-GRDGS are described in Appendix 1.

Post-polymerization CuAAC-reactions on PEDOT-N_3

7.5 mm x 7.5 mm poly(dimethylsiloxane) (PDMS) frames, or 10 mm x 10 mm *in situ Gene frame* from Thermo Scientific were used to contain the reaction solution. 150-200 µl reaction solution was typically used. For the formation of the Cu(I) catalyst for the CuAAC reactions, we used a most common procedure of applying a Cu(II) salt and adding surplus sodium ascorbate (NaAsc) reducing agent.[102] Reactions were stopped by rinsing in de-ionized water followed by re-oxidizing the PEDOT-N_3 by rinsing in a 10 vol% aqueous solution of Clevios C-B40, and rinsing in de-ionized water again. All samples used in cell experiments were re-oxidized.

Alkyne-PEG-GRGDS / alkyne-PEG-GRDGS Figure 3: 4 h with 1 mM alkyne-PEG-GRGDS, 2 mM $CuSO_4$, 27 mM NaAsc in 50 mM NaCl. For samples used in cell experiment, the samples were subsequently reacted with PEG-alkyne as described below. Surfaces which were used in cell

experiments prior to XPS analysis were rinsed thoroughly in 5 vol% Tween-20 solution and large amounts of Milli-Q water, before applying XPS.

PEG-alkyne reactions for cell adhesion experiments displayed in Figure 3: 6 h with 20 mM PEG-alkyne 0.7 mM $CuSO_4$ 27 mM NaAsc in 50 mM NaCl solution.

Alkyne-PEG-GRGDS Figure 4: 4 h with 1 mM alkyne-PEG-GRGDS, 2 mM CuSO4, 27 mM NaAsc in 50 mM NaCl, or 0.002 mM alkyne-PEG-GRGDS, 0.13 mM $CuSO_4$, 27 mM NaAsc in 50 mM NaCl. After the reactions the samples were subsequently reacted with PEG-alkyne:

PEG-alkyne reactions Figure 4: 6 h with 40 mM PEG-alkyne 0.7 mM $CuSO_4$ 27 mM NaAsc in 50 mM NaCl solution.

Fibroblast adhesion studies

Fibroblast adhesion studies were performed in a Rectangular Parallel Plate Flow Chamber kit from Glycotech. The flow chamber has the outer dimensions 15 mm x 25 mm x 75 mm (*h,w,l*) the inner dimensions 0.127 mm x 10 mm x 60 mm (*h,w,l*). The chamber was assembled on top of a microscope slide shaped COC substrate covered by a functionalized PEDOT-N_3 film.

The flow experiments were conducted in a Hanks balanced saline solution (HBSS) buffer containing Mg(II) and Ca(II). 200 µL of a >1 mio cells/mL suspension of 3T3 fibroblasts in a Roswell park memorial institute (RPMI) media was injected into the flow chamber. The cells were allowed to adhere for 45 min. HBSS buffer was then flowed through the chamber, increasing the flow rate gradually every 2 min. The final flow corresponded to a surface shear stress of 10Pa. This was maintained for 1 min. During the experiment, the flow through the chamber was adjusted using a NE-1000 syringe pump (New Era Pump Systems) equipped with at 50 mL syringe. Images were acquired on a Zeiss Axiovert S100 microscope (Carl Zeiss, Oberkochen, Germany), equipped with LD Plan-NEOFLUAR 20x/0.4 objective, applying an iXon camera (Andor Technology, Belfast, Northern Ireland). The pump flow and the image acquisition were controlled by dedicated software running under LabView. The software was made specifically for the setup by Dr. David Selmeczi.

Chapter 3

Covalent Modifications of PEDOT-N_3 Studied by XPS Analyses

Introduction

X-ray Photoelectron Spectroscopy (XPS) is a highly sensitive method for evaluating the surface chemical composition of a substrate. Accordingly, it is a commonly used technique for examining the surface chemical composition of PEDOT thin films,[10, 11, 74, 103, 104] and polymeric substrates in general.[105] Throughout this thesis, XPS have served as the main method for following the surface chemical modifications that were made. A cornerstone in our studies has been the CuAAC functionalization of PEDOT-N_3 thin films with alkyne molecules. In this Chapter we show how XPS was used for validating and quantifying these reactions. The results presented confirm that the highly tailored interactions observed between functionalized PEDOT-N_3 substrates and living cells, which were presented in Chapter 2, were indeed caused by the functionalization of PEDOT-N_3 with appropriate functional molecules. The data also highlight the influence the solvent exerts on the density of these functionalizations of PEDOT-N_3.

We initially show how the high resolution XPS signal of nitrogen has been highly useful for monitoring the CuAAC functionalization of PEDOT-N_3. We then show that the high resolution carbon signal can serve to validate that appropriate reactants have been coupled onto a PEDOT-N_3 substrate. Subsequently, we exemplify how the high resolution sulfur signal can be used for estimating the oxidation state and doping degree of PEDOT-N_3. After the analysis of these high resolution spectra, we show how the overall elemental composition of a sample is valuable for showing the presence of appropriate reactants on the surface, and for determining the composition of PEDOT-N_3 samples functionalized with two reactants. Finally, we show how XPS was used for detecting unspecific adsorption of peptides reactants, and for validating a procedure for removing these un-specifically adsorbed reactants.

High resolution nitrogen 1s XPS analysis

The Azide group found in PEDOT-N_3 has a highly distinct XPS signal, which was used for following the CuAAC reactions. The cause of this distinct XPS signal is the partially positively charged nitrogen atom in the azide group. The electrons of this nitrogen have an unusually high binging energy, leading to the separate peak in the XPS signal at binding energy of ~404.5eV.[106] Thus, for the pure PEDOT-N_3 films, a 1:2 doublet was observed in the nitrogen signal, see Figure 5A. When the azide participates in a CuAAC reaction with an alkyne molecule, a triazole is formed, and this high energy peak disappears.[10, 107] The high resolution nitrogen XPS signal can therefore be used for verifying that the CuAAC-reaction is taking place, and for monitoring the reaction degree.

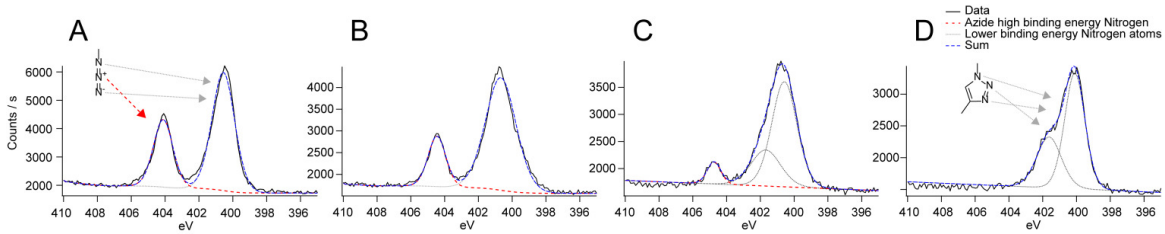

Figure 5 High Resolution nitrogen XPS signal of PEDOT-N_3 before and after CuAAC-reaction
When a CuAAC-reaction takes place, the unique XPS-signal from the azide disappears. The red dotted lines indicate a fit to the azide high energy nitrogen peak at ~404.5 eV. Grey dotted lines are fits to the low binding energy nitrogen found in un-reacted azides, and in the triazoles. Blue lines are the sum of the fits. **A:** PEDOT-N_3 surface prior to reaction **B:** 4 h reaction with 10 mM PEG-alkyne in Milli-Q water **C:** 6 h reaction with 20 mM PEG-alkyne in 50 mM NaCl solution **D:** 6 h reaction with PEG-alkyne in 33 mM NaCl solution of 2/3vol. water and 1/3vol. DMSO. See experimental section for detailed reaction conditions.

Figure 5A displays the high resolution nitrogen XPS spectrum from a native PEDOT-N_3 film. In Figure 5B-D the spectra from three PEDOT-N_3 films that have been functionalized with PEG-alkyne using different protocols is displayed. For each of the three protocols a decrease in the high binding energy XPS signal from azide can be seen, thus confirming that a CuAAC reaction is taking place. Notably, the extent of this decrease is highly dependent on the protocol, especially on the solvent used. In Figure 5B, a reaction in pure water leads to a partial removal of the azide signal. In Figure 5C a reaction in a salt buffer removes the majority of the azide signal, while in Figure 5D, the entire azide signal is removed after a reaction in a salt buffer containing 33 vol% DMSO. The influence of the solvent on the reaction degree and depth of CuAAC functionalization of PEDOT-N_3 films is a point which we will return to in Chapter 5. The protocol used for anchoring PEG-alkyne onto PEDOT-N_3 in Figure 5C, is identical to that which was used for functionalizing the PEDOT-N_3 films which were analyzed for cellular adhesion in the experiments displayed in Chapter 2, Figure 3. The high resolution nitrogen XPS signal accordingly confirms that a CuAAC click-reaction was successfully made on these substrates. Note that even for a complete surface functionalization of PEDOT-N_3 with PEG-alkyne, it is expected that a residual azide signal is observed. This is due to the sampling depth of the XPS measurement. The sampling depth of an XPS measurement is determined by the depth at which photo-emitted electrons leave the sample with the same energy as they had upon emission. This is depth is naturally linked to the inelastic mean free path of an electron in the material, but also elastic processes influence the probability of emitted electrons leaving the material without energy loss.[105] These scattering processes collectively give rise to the sampling depth represented by an exponentially decreasing function $\propto e^{-x/L_{char}}$. For polymeric samples, the characteristic length scale L_{char} of this function, is in the order of a few nanometers.[105] Therefore, the complete removal of the azide signal observed in Figure 5D indicates that a deeper functionalization of PEDOT-N_3 with PEG is taking place.

Similar to the functionalization of PEDOT-N_3 with PEG-alkyne, CuAAC modifications with other alkyne reactants were followed by examining the decrease in the azide signal in the high resolution nitrogen XPS spectrum. For reactions with alkyne-PEG-GRGDS reactants, or

other alkyne reactants containing numerous nitrogen atoms, the decrease in the high-binding energy azide signal was concerted by a drastic increase in the low-binding energy signal, due to the introduction of additional nitrogen. Such a signal was e.g. observed for surfaces reacted with alkyne-PEG-G***RGD***S or alkyne-PEG-G***RDG***S similar to those tested for cellular adhesion in Chapter 2, Figure 3. This again confirmed that successful click-reactions had taken place.

High resolution carbon 1s XPS analysis

Similar to the high resolution nitrogen XPS signal, the high resolution carbon signal was also valuable for following the functionalization of PEDOT-N_3 with alkyne reactants. This is exemplified in Figure 6. Figure 6A displays the signal from a native PEDOT-N_3 substrate, Figure 6B displays the signal after reaction with PEG-alkyne, and Figure 6C displays the spectrum after reaction with alkyne-PEG-G**RGD**S. The reaction conditions were identical to those used for preparing the functionalized PEDOT-N_3 surfaces which were tested for cellular adhesion in Chapter 2, Figure 3. It can be observed in Figure 6B that the reaction with PEG-alkyne leads to the appearance of a pronounced peak in the carbon spectrum at a binding energy of ~286.5 eV. This peak corresponds well to the signal from carbon atoms sharing one covalent bond with an oxygen atom.[105] Such carbon atoms are introduced in large numbers when PEG is attached to the surface. Therefore the carbon spectrum confirms that PEG-alkyne is present on the surface. Similarly, after reaction with alkyne-PEG-GRGDS, a new local peak in the carbon signal was observed at ~288.5 eV, see Figure 6C. Such high energy carbon signal arises from carbon atoms sharing three or more bonds with electro-negative elements.[105]

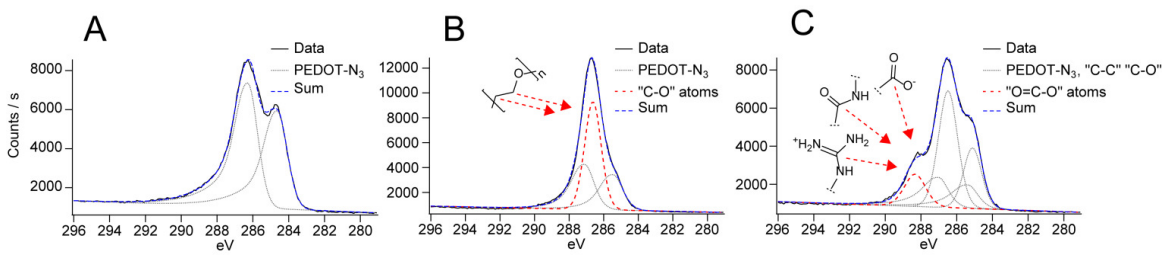

Figure 6 High resolution carbon XPS spectra of PEDOT-N_3 before and after reaction with PEG-alkyne and alkyne-PEG-GRGDS

A: A pure PEDOT-N_3 surface. The tail into the high binding energy region is caused by the partial positive charge found on the carbon atoms in the PEDOT-N_3 back-bone in the p-doped state. The grey lines indicate two fitted peaks with equivalent tails into the high binding energy range. **B:** A PEDOT-N_3 substrate after reaction for 6 h with PEG-alkyne. The red dotted line indicates a fit to the C-O peak at ~286.5 eV which has been added to the peak used in A. **C:** A PEDOT-N_3 substrate after reaction for 4 h with alkyne-PEG-GRGDS. The red dotted line indicates a fit to the high binding energy carbon at ~288.5 eV which has been added to the peak fit used in B. An aliphatic carbon peak was also included. In all the spectra, the blue lines are the sum of the fits. The fits were not used for quantitative analysis, but serve to highlight the differences in the three spectra. The samples B and C were not re-oxidized prior to XPS evaluation. See experimental section for detailed reaction conditions.

This is the case for the carbon atoms found in the amide, carboxylic acid, and guanidinium motives in the peptides. Thus, the carbon signal indicates that alkyne-PEG-G**RGD**S is found on the surface. In combination with the high resolution nitrogen signal which showed that a CuAAC reaction took place, the carbon signal confirm that the appropriate reactants, and not, for instance, small alkyne-containing impurities, were attached to the surface during the reaction.

High resolution sulfur 2p XPS analysis

The CuAAC click reactions were performed in a reducing environment. Sodium ascorbate (NaAsc) were added in surplus to reduce Cu(II) ions to the catalytic Cu(I) ions. The surplus NaAsc also reduces the partially oxidized PEDOT-N_3, thereby lowering the conductance of the film. This can be observed in the high resolution sulfur XPS signal, as tosylate anions diffuse out of the PEDOT matrix upon reduction, see Figure 7. To restore the conductance of the films after reaction, they were ”re-oxidized” in an aqueous solution containing 10 vol% of a 40 wt% solution of iron(III)tosylate in n-butanol. This restored the conductance, and tosylate anions were again observed in the XPS signal, see Figure 7C. We also tested the re-oxidization procedure on PEDOT-N_3 substrates which were reduced without any alkyne reactant being present. The re-oxidized substrates were observed to have an elemental composition identical to that observed for the native p-doped substrates prior to reduction. For samples containing alkyne-PEG-GRGDS or alkyne-PEG-GRDGS, leftover iron was occasionally seen in the XPS after re-oxidization, see Table 4. This illustrated that an insufficient rinsing procedure had been applied after the re-oxidization. No iron was observed for the samples which where reacted a second time with PEG-alkyne before re-oxidization. Accordingly, iron was not present on the samples tested for cellular adhesion in Chapter 2, Figure 3.

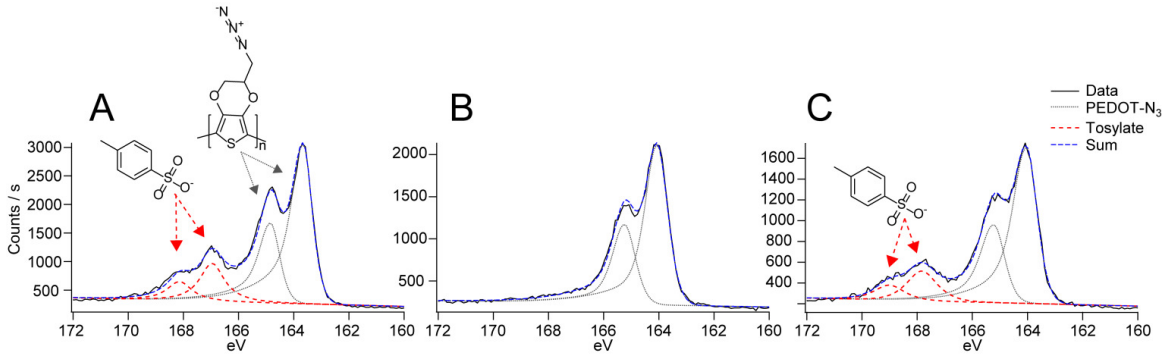

Figure 7 High resolution XPS 2p sulfur signal of PEDOT-N_3 samples in native, reduced and re-oxidized state following a CuAAC-reaction

A: Native PEDOT-N_3 substrate **B**: PEDOT-N_3 substrate after CuAAC-reaction with PEG-alkyne in reducing environment. **C**: PEDOT-N_3 substrate after CuAAC-reaction with PEG-alkyne in a reducing environment, followed by re-oxidization in 10 vol% Baytron C-B40 in Milli-Q water. The red dotted line indicates a fit to the sulfur doublet arising from tosylate anions in the p-doped PEDOT-N_3 matrix. Grey lines are fits to the sulfur atoms found in the backbone of the PEDOT polymer. In all the spectra, the blue lines are the sum of the fits. See experimental section for detailed reaction conditions.

The degree of doping of the PEDOT-N_3 film could also be estimated from the sulfur 2p spectrum. Due to the spin-orbit coupling, the energy levels in a p-orbital are split into two levels with a 2:1 ratio difference in degeneracy, giving rise to a doublet with a 2:1 ratio in intensity in the XPS spectrum.[105] From our data, the split between the two peaks was found to be ~1.2 eV, which is in fine correspondence with literature.[104, 108, 109] Two doublets are easily identified in Figure 7. The low binding energy doublet arises from PEDOT-N_3, and the high binding energy doublet arises from TsO, which is bound to three electron withdrawing oxygen atoms. In a similar analysis of PEDOT, Zotti *et al.* reported the offset value from the first PEDOT sulfur peak to the first TsO peak to be ~3.4 eV.[110] This is in good correspondence with our data for PEDOT-N_3. As for the carbon 1s spectrum, the mobile positive charge in PEDOT-N_3 backbone gives rise to slightly increased binding energies of the sulfur atoms in PEDOT-N_3. This was accounted for by allowing the sulfur peaks of the PEDOT sulfur atoms to contain a tail into the higher binding energy range.[103, 104, 108, 109] Using these estimates, a ratio between the two doublets of 4:1 was typically found for both PEDOT-N_3 and re-oxidized PEDOT-N_3. This agrees well with what has earlier been reported for the PEDOT:TsO doping level of about one charge/tosylate per ~4 PEDOT monomers.[5, 104, 108, 109, 111]

Elemental composition XPS analysis

In addition to the analysis of the individual elemental XPS spectra, the overall atomic composition of the functionalized PEDOT-N_3 samples was also used for validating the CuAAC modifications. Upon reaction, the elemental composition of a sample should change from resembling that of pure PEDOT-N_3 to becoming increasingly similar to that of the reactant. For example, for reactions with PEG-alkyne the carbon and oxygen surface content should increase, and the nitrogen and sulfur content should decrease. This can be observed indeed to be the case in Table 1 and Table 2. In Table 1 the elemental composition of an oxidized PEDOT-N_3 substrate is compared with that seen after reaction with PEG-alkyne and re-oxidization. In Table 2 the elemental composition of a reduced PEDOT-N_3 substrate is compared with that seen after reaction with PEG-alkyne prior to re-oxidization. For both the reduced and the oxidized cases a significant drop in the nitrogen and sulfur content and a concurrent increase the in oxygen and carbon content was observed, compared to the relevant reference. While the diminished azide signals observed in the high resolution nitrogen spectra showed that CuAAC reaction takes place, the overall elemental composition, in concert with the high resolution carbon spectrum, confirmed that the reactant was indeed the expected PEG-alkyne molecule. Notably, the CuAAC-reaction conditions of entrance B in Table 2 were identical to those used for the samples tested for cellular adhesion in Chapter 2, Figure 3, again verifying that the observed decrease in cellular attachment was causes by the attachment of PEG-alkyne onto PEDOT-N_3. Similar to what was observed in the high resolution nitrogen spectra; it can also be seen from the elemental compositions displayed in Table 1 and Table 2 that an increased concentration of DMSO in the reaction solvent leads to an increased reaction degree. We will return to this cause of this effect in Chapter 4 and 5. In both Table 1 and Table 2, silicon impurities can be seen for most of the samples. As the oxygen content was generally found to be higher than expected, we suspect that the impurity also contain oxygen. We suggest that silicone, for example PDMS, is a likely source of the impurities. Similar impurities were observed throughout the work presented in this thesis. The amount of the impurities varied from sample to sample, and the source of the impurity was not found. Such impurities might constitute a significant problem for achieving substrates with controlled biological properties. However, we did succeed in fabricating highly bio-specific substrates, despite this potential problem.

Experimental			XPS atomic composition in %				
Sample	Substrate	Description	C	O	S	N	Si
A	PEDOT-N_3	No reaction, native substrate	56.16	18.09	9.2	16.55	0
B	PEDOT-N_3	PEG in 30vol% DMSO sol.	60.52	23.79	5.14	10.04	0.51
C	PEDOT-N_3	PEG in 50vol% DMSO sol.	64.58	26.56	2.34	5.8	0.71
	-	Theoretical values from PEG	67.8	30.4	0	1.8	0

Table 1 Elemental composition of PEDOT-N_3 before and after reaction with PEG

A: Native PEDOT-N_3 substrate **B:** 4 h with 10 mM PEG-alkyne in 30% DMSO in Milli-Q water. **C:** 4 h with 10 mM PEG-alkyne in 50 vol% DMSO in MQ water. Both samples were re-oxidized. See experimental section for detailed reaction conditions.

Experimental			XPS atomic composition in %				
Sample	Substrate	Description	C	O	S	N	Si
A	PEDOT-N_3	No reaction, reduced substrate	55.47	19.18	8.09	16.47	0.79
B	PEDOT-N_3	PEG in 50mM NaCl	60.16	23.79	4.77	10.11	1.02
C	PEDOT-N_3	PEG in 33mM NaCl in 33vol% DMSO sol.	63.47	26.99	2.28	6.26	1
	-	Theoretical values from PEG	67.8	30.4	0	1.8	0

Table 2 Elemental composition of PEDOT-N_3 before and after reaction with PEG, no re-oxidization

A: Native PEDOT-N_3 substrate **B:** After reaction for 6 h with 20 mM PEG-alkyne in 50 mM NaCl solution. **C:** After reaction for 6 h with 20 mM PEG-alkyne in 33 mM NaCl solution of 2/3vol. water and 1/3vol. DMSO. See experimental section for detailed reaction conditions.

Similar to the reactions with PEG-alkyne, the functionalizations of PEDOT-N_3 with the peptide molecules alkyne-PEG-G**RGD**S and alkyne-PEG-G***RDG***S were confirmed by the elemental compositions obtained in XPS. As expected from the theoretical composition of the peptide reactants, an increased carbon and oxygen signal, and a decreased sulfur signal, was observed after reaction. This is displayed in Table 3 for the re-oxidized case and in Table 4 for the reduced case. As noted earlier, the alkyne-PEG-G**RGD**S and alkyne-PEG-G***RDG***S contained a non-natural iodine-substituted phenylalanine residue. This iodine served as a direct marker for the peptides as can be seen in both Table 3 and Table 4.

Experimental			XPS atomic composition in %						
Sample	Substrate	Description	C	O	S	N	Si	I	Fe
A	PEDOT-N_3	No reaction, native substrate	56.16	18.09	9.2	16.55	0	0	0
B	PEDOT-N_3	GRGDS in 50vol% DMSO sol.	59.44	22.49	3.61	12.31	1.44	0.49	0.21
	-	Theoretical value from GRGDS	60.18	24.78	0	14.16	0	0.88	0

Table 3 Elemental composition of PEDOT-N_3 before and after reaction with GRGDS peptides

A: Native PEDOT-N_3 substrate. ***B:*** Overnight with 3 mM in 50 vol% DMSO solution. See experimental section for detailed reaction conditions.

Experimental			XPS atomic composition in %						
Sample	Substrate	Description	C	O	S	N	Si	I	Fe
A	PEDOT-N_3	No reaction, reduced substrate	55.47	19.18	8.09	16.47	0.79	0	0
B	PEDOT-N_3	GRGDS in 50mM NaCl	60.06	20.51	4.73	14.33	0	0.38	0
	-	Theoretical value from GRGDS	60.18	24.78	0	14.16	0	0.88	0

Table 4 Elemental composition of PEDOT-N_3 before and after reaction with GRGDS peptides, no reoxidation

A: Native PEDOT-N_3 substrate. **B:** Reaction for 4 h with 0.25 mM alkyne-PEG-GRGDS in 50 mM NaCl solution. See experimental section for detailed reaction conditions.

Elemental composition XPS analysis on mixed GRGDS/PEG substrates

The iodine marker that was incorporated in the peptides, was especially useful when analyzing surfaces containing both PEG-alkyne and alkyne-PEG-G**RGD**S or alkyne-PEG-G***RDG***S. Without a direct marker for the peptides, the elemental composition, or high resolution carbon spectrum, will not necessarily give a clear answer to the composition of such mixed surfaces, i.e. the amount of each of the two alkynes on the sample. Table 5 displays the elemental composition of a mixed alkyne-PEG-G**RGD**S/PEG-alkyne and a mixed alkyne-PEG-G***RDG***S/PEG-alkyne surface that were both used in the cell adhesion experiments that were displayed Chapter 2, Figure 3. It can be seen that the surfaces have similar elemental composition, and contain similar amounts of iodine. This validates that the same amount of peptides is present on the two surfaces. The lack of cellular attachment observed for the alkyne-PEG-G***RDG***S surfaces was thus caused the loss of bio-specific recognition of the RGD motif, and not by other changes the in chemistry of the samples.

Experimental			XPS atomic composition in %						
Sample	Substrate	*Description*	C	O	S	N	Si	I	Fe
A	PEDOT-N_3	No reaction, native substrate	56.16	18.09	9.2	16.55	0	0	0
B	PEDOT-N_3	G**RGD**S + PEG used in cell experiments	66.3	21.35	2.09	9.24	0.86	0.16	0
C	PEDOT-N_3	G***RDG*** S + PEG used in cell experiments	66.6	21.79	2.39	8.48	0.61	0.13	0

Table 5 Elemental composition mixed PEG/peptide PEDOT-N_3 surfaces used in cellular adhesion experiments
A: Native PEDOT-N_3 substrate **B/C:** PEDOT-N_3 surfaces functionalized with PEG-alkyne and alkyne-PEG-G**RGD**S/G***RDG***S, used in cell experiments displayed in Chapter 2, Figure 3. The samples were rinsed thoroughly in 5 vol% Tween-20 solution and Milli-Q water, before being analyzed in XPS. See experimental section for detailed reaction conditions.

We considered if it was possible to finely control the amount of alkyne-PEG-GRGDS on a mixed alkyne-PEG-GRGDS/PEG-alkyne (GRGDS/PEG) surface. The mixed GRGDS/PEG substrates which were tested for cellular adhesions in Chapter 2, Figure 4, were fabricated by performing two separate reactions: First, a reaction with the peptide was conducted, and then a second reaction with PEG-alkyne was made to ensure a complete PEG-coverage of the substrate. When using this approach, different peptide concentrations were defined by adjusting the amount of peptide reactant and catalyst present in the first reaction step. Although this approach could indeed be used for making mixed surfaces with different GRGDS/PEG ratios, we suspected that it would be difficult to attain fine control of the GRGDS/PEG ratio by using this approach. As an alternative, we tested competitive mixed reactions containing both alkyne-PEG-GRGDS and PEG-alkyne. An example of this approach is shown in Figure 8A. Here, we were able to control of the amount of iodine, and thus the amount of peptide found on the surfaces, by varying the GRGDS/PEG ratio in the reaction solution. The amount of iodine measured on each surface was used for estimating the amount of both alkyne-PEG-GRGDS and PEG-alkyne on the substrates. The data was recalculated to obtain the percent of the total XPS signal arising from each of the two reactants. In

these calculations, the iodine signal was used as a direct measure for the XPS signal arising from the peptide. By multiplying the percent signal from iodine with the total number of XPS active atoms in the peptide, the percent of the XPS signal arising from the peptide was estimated:

$$\%_{atom}Iodine \cdot \frac{no_{XPS\ active\ atoms/peptide}}{no_{Iodine\ atoms/peptide}} = \%_{atom}Peptide$$

$$\%_{atom}Iodine \cdot \frac{113}{1} = \%_{atom}Peptide$$

Following a similar logic, sulfur was used as a direct measure for total XPS signal arising from PEDOT-N_3 matrix. For PEDOT-N_3 in a reduced state this is given by:

$$\%_{atom}Sulfur \cdot \frac{no_{XPS\ active\ atoms/PEDOTN3monomer}}{no_{Sulfur\ atoms/PEDOTN3monomer}} = \%_{atom}PEDOTN_3$$

$$\%_{atom}Sulfur \cdot \frac{13}{1} = \%_{atom}PEDOTN_3$$

For the oxidized state the amount of TsO had to be taken into account. This was done by assuming that 1 TsO was found per 4 EDOT-N_3 monomers:

$$\%_{atom}Sulfur \cdot \frac{no_{XPSactive\ atoms/(PEDOTN3monomer+\frac{1}{4}TsO)}}{no_{Sulfur\ atoms/(PEDOTN3monomer+\frac{1}{4}TsO)}} = \%_{atom}(PEDOTN_3 + \frac{1}{4}TsO)$$

$$\%_{atom}Sulfur \cdot \frac{15.75}{1.25} = \%_{atom}(PEDOTN_3 + \frac{1}{4}TsO)$$

The residual XPS signal was ascribed to PEG:

$$\%_{atom}PEG = 100 - \%_{atom}Peptide - \%_{atom}PEDOTN_3$$

As impurities were occasionally observed on the samples, this procedure has the obvious flaw that it does not take these into account. It therefore overestimates the amount of PEG-alkyne found on the surface, as the entire signal which cannot be directly assigned to PEDOT-N_3 or alkyne-PEG-GRGDS, is attributed to PEG-alkyne. A more valid estimate of PEG concentration might be established by peak fitting to the high resolution carbon data, or by a careful analysis of the elemental composition of the surfaces. This was however considered beyond our scope, and was not conducted. From the estimated percent of the XPS signal arising from each of the two reactants, the corresponding relative number of peptides/PEG molecules can be calculated. This is done by taking the difference in number of atoms in each reactant into account:

$$\frac{no.Peptide}{no.PEG} = \frac{\%_{atom}Peptide}{\%_{atom}PEG} \cdot \frac{56}{113} \Leftrightarrow \frac{no.PEG}{no.Peptide} = \frac{\%_{atom}PEG}{\%_{atom}Peptide} \cdot \frac{113}{56}$$

From this we calculated the percent of the reactants being peptides, out of the total number of reactants:

$$\%_{reactant}Peptide = 100 * \frac{no.Peptide}{no.PEG + no.Peptide} = \frac{1}{\frac{\%_{atom}PEG}{\%_{atom}Peptide} \cdot \frac{113}{56} + 1}$$

$$= 100 * \frac{\%_{atom}Peptide}{\%_{atom}PEG \cdot 113/56 + \%_{atom}Peptide}$$

The iodine data for the mixed GRGDS/PEG surfaces displayed in Figure 8A, was recalculated in manner just outlined. Figure 8B displays the percent alkyne-PEG-GRGDS of the total amount of reactants on the surface. For the reaction which contained equal amounts of PEG-alkyne and alkyne-PEG-GRGDS, slightly less than 50% of the reactants found on the surface were calculated to be peptides. This might indicate that the PEG-alkyne has slightly faster reaction kinetics than the alkyne-PEG-GRGDS. This could however easily be an artifact caused by overestimation of the amount of PEG on the surface. Additionally, it appears that for low concentrations of peptide, the peptide has faster reaction kinetics than the PEG-alkyne. Evidently, the overall picture is far from simple. There were however a number of uncontrolled parameters in the experiments. For example, the total concentration of reactant was not constant in the samples, whereas the concentration of Cu(I) catalyst was. Furthermore the total amount of data is overall low. Therefore we find it of little use to discuss the potential differences in reaction kinetics of PEG-alkyne and alkyne-PEG-GRGDS on this basis. Still, on the qualitative level, the data displayed in Figure 8 show that it is indeed possible to fabricate mixed GRGDS/PEG functionalized PEDOT-N_3 with highly variable ratios of GRGDS/PEG.

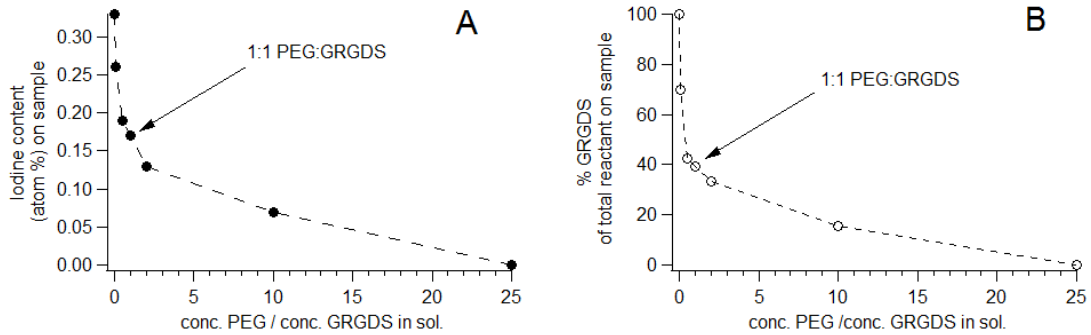

Figure 8 Controlling the amount of peptide on a mixed reactions of alkyne-PEG-GRGDS and PEG-alkyne

A: The iodine content found in XPS analysis of a series of mixed reactions of alkyne-PEG-GRGDS and PEG-alkyne were made by keeping the concentration of peptide constant at 0.25 mM and varying the concentration of PEG between 0 and 6.25 mM. Reactions were performed in Milli-Q water solutions. After the reaction, the samples were rinsed in DMF to removed un-specifically adsorption peptides. **B:** Corresponding percentage alkyne-PEG-GRGDS of the total amount of reactants on the surface. See experimental section for detailed reaction conditions.

Unspecific adsorption of peptide molecules can be avoided through appropriate washing

We observed that alkyne-PEG-GRGDS and alkyne-PEG-GRDGS could adsorb un-specifically onto PEDOT-N_3. When control reactions were conducted with these reactants, but without the Cu(II) catalyst, we saw a significant iodine signal, which could not be removed by rinsing the sample with water. We found that the un-specifically adsorbed peptides be removed by rinsing the surfaces in Dimethyl-formamide (DMF) or an aqueous solution of Tween-20 detergent, see Table 6. For studies where a second reaction of PEG was performed, as in the cell experiments in Chapter 2, Figure 3 and Figure 4, such washes were not performed.

Experimental				
Sample	Substrate	Description	Wash	I
A	PEDOT-N_3	Click reaction with GRGDS peptide	Milli-Q water	0.51
B	PEDOT-N_3	Click reaction solution ***without*** Cu catalyst	Milli-Q water	0.13
C	PEDOT-N_3	Click reaction with GRGDS peptide	0.1% Tween-20	0.39
D	PEDOT-N_3	Click reaction solution ***without*** Cu catalyst	0.1% Tween-20	0
E	PEDOT-N_3	Click reaction with GRGDS peptide	DMF	0.38
F	PEDOT-N_3	Click reaction solution ***without*** Cu catalyst	DMF	0

Table 6 Unspecific adsorption of GRGDS peptides, in CuAAC-reaction environments

When performing CuAAC-reactions with alkyne-PEG-GRGDS in reducing environments, adsorption of the peptides can be observed, even when copper is not present in the reaction solution. Iodine content in the XPS is displayed as a measure of this unspecific adsorption. By rinsing in DMF of 0.1% Tween-20 solution, the unspecific adsorption could be removed. Following these washes the surfaces were rinsed in Milli-Q water to remove these solvents. 4 h reaction with 0.25 mM alkyne-PEG-GRGDS, 6.7 mM NaAsc, +/- 0.5 mM $CuSO_4$ was used. See experimental section for detailed reaction conditions.

Conclusion

We have shown that XPS analyses are well-suited for confirming the covalent attachment of alkyne reactants to PEDOT-N_3 substrates. The disappearance of the high binding energy azide signal in the nitrogen spectrum served as a direct indication of successful CuAAC reactions. Other methods, including the incorporation of hetero atom XPS markers, served to show that the correct reactant(s) was indeed found on each of the functionalized surfaces. Furthermore XPS analysis could be used for investigating the doping state of the films, and confirming that the p-doping of the films, which are lost during the CuAAC reactions that take place in a reducing environment, can be reestablished by a subsequent re-oxidization with Fe(III)tosylate. Finally, we found that unspecific adsorption of alkyne-PEG-GRGDS molecules could be monitored in XPS,

and that such adsorbed molecules could be removed by washing with organic solvent or aqueous detergent solutions.

Experimental

PEDOT-N_3 Samples on COC supports
Samples were prepared as described in Chapter 2.

Post-polymerization CuAAC-reactions on PEDOT-N_3 substrates
7.5 mm x 7.5 mm PDMS frames or 10 mm x 10 mm *in situ Gene frame* from Thermo Scientific, were used to contain the reactant solutions. 150-200 µl reaction solution was typically used. Reactions were stopped by rinsing in de-ionized water followed by re-oxidizing the PEDOT-N_3 by rinsing in a 10 vol% aqueous solution of Clevios C-B40, and rinsing in de-ionized water again. All samples used in cell experiments were re-oxidized. Where indicated in the Figure caption, samples applied for XPS investigations were not re-oxidized.
Alkyne-PEG-GRGDS / alkyne-PEG-GRDGS, Figure 6C, Table 4B, Table 5B/C: 4 h with 1 mM alkyne-PEG-GRGDS, 2 mM $CuSO_4$, 27 mM NaAsc in 50 mM NaCl. For samples used in cell experiments, the samples were subsequently reacted PEG-alkyne as described below. Surfaces used in cell experiments prior to XPS analysis were rinsed thoroughly in 5 vol% Tween-20 solution and copious amounts of Milli-Q water, before applying XPS.
PEG-alkyne reactions for experiments displayed in Figure 5C, Figure 6B, Table 2B, Table 5B/C: 6 h with 20 mM PEG-alkyne 0.7 mM CuSO4 27 mM NaAsc in 50 mM NaCl solution.
PEG reaction conditions Figure 5D, Table 2C: 6 h with 20 mM PEG-alkyne 0.7 mM $CuSO_4$ 27 mM NaAsc in 33 mM NaCl solution of 2/3vol. water and 1/3vol. DMSO.
PEG reaction conditions Figure 5B: 4 h with 10 mM PEG-alkyne 2 mM $CuSO_4$ 40 mM NaAsc in Milli-Q water
PEG reaction conditions Table 1B, Figure 7C: 4 h with 10 mM PEG-alkyne 2 mM $CuSO_4$ 40 mM NaAsc in 30% DMSO in Milli-Q water.
PEG reaction conditions Table 1C: 4 h with 10 mM PEG-alkyne 2 mM $CuSO_4$ 40 mM NaAsc in 50% DMSO in Milli-Q water
Alkyne-PEG-GRGDS Table 4B: overnight with 3 mM alkyne-PEG-GRGDS, 0.6 mM $CuSO_4$ 6 mM NaAsc in 50 vol% DMSO solution. After reaction overnight the sample was rinsed in DMF and re-oxidized
Alkyne-PEG-GRGDS Table 6: 4 h with 0.25 mM alkyne-PEG-GRGDS, 0.5 mM $CuSO_4$ 6.7 mM NaAsc in 50 mM NaCl solution after reaction the sample was rinsed in DMF
Alkyne-PEG-GRGDS-PEG mixed reaction Figure 8: 0.25 mM alkyne-PEG-GRGD, PEG-alkyne 0, 0.025, 0.125, 0.25, 2.5 or 6.25 mM. Milli-Q water solutions, reaction time of 4 h, 6.7 mM NaAsc and 0.5 mM $CuSO_4$ were used in all reaction. Samples were rinsed in DMF and Milli-Q after reaction.

XPS investigations

XPS experiments were conducted using a Thermo Fisher Scientific K Alpha (East Grinstead, UK). A 400 μm spot on each sample was irradiated using monochromatized aluminum Kα radiation, and survey (pass energy 200 eV) and high resolution (pass energy 25 eV) spectra of relevant elements were acquired. Flood-gun charge compensation was used for all samples. Data analyses of the XPS spectra were performed using the Avantage software package supplied by the manufacturer.

Chapter 4

The swelling of PEDOT-N_3 in DMSO/Water Mixtures

Introduction

In the preceding Chapter, we found that when functionalizing PEDOT-N_3 substrates with alkyne reactants, the solvent had a notable influence on the surface reaction degree. The addition of DMSO to the reaction solution increased the surface reaction degree of PEG-alkyne. In this Chapter we have investigated the basis of this finding. We have found that PEDOT-N_3 films undergo a significant and reversible swelling in DMSO/water mixtures with a high DMSO content. A similar but less pronounced behavior was observed for regular PEDOT. For thin films of PEDOT containing PSS anions, PEDOT:PSS, it has been reported that washing with DMSO, and other polar organic compounds, can increase conductance of the films significantly, possibly by allowing reorganization of the polymeric chains.[112-114] Thus, the observation of drastic changes in the structure of PEDOT type thin films upon exposure to DMSO is not new. We did not observe any notable changes in the conductivity of PEDOT and PEDOT-N_3 films containing TsO anions after exposure to DMSO.

The central findings of this Chapter were presented in the paper: "Solvent Composition Directing Click-Functionalization at the Surface or in the Bulk of Azide-Modified PEDOT" *Macromolecules*, 44 (3), pp. 495–501 (2011), and the following Chapter contains entire continuous sections taken from this paper.

PEDOT-N_3 films undergo significant and reversible swelling in high DMSO concentration DMSO/water mixtures

We investigated swelling of PEDOT-N_3 and PEDOT thin films upon exposure to DMSO and water in a series of atomic force microscopy (AFM) measurements, see Figure 9. In these measurements we found that PEDOT-N_3 undergo a substantial swelling in DMSO compared to in water. The measurements were performed by initially exposing the thin films to pure water and subsequently gradually increasing the DMSO content of the solvent until reaching pure DMSO. The films were then exposed to pure water again to probe the reversibility of the swelling process. The thicknesses of both PEDOT-type polymers increased with increasing DMSO content. For PEDOT-N_3 in solvent mixtures with ≤50 vol% DMSO in water, the relative increase in film thickness is of <5% compared to the thickness in pure water. For >50 vol% DMSO in water, thickness increases strongly with DMSO content up to a maximum in pure DMSO of ~260% of the film thickness found in water. Importantly, immersion in water of the maximally swelled film resulted in the thickness returning to its original value in water. The corresponding effect on

PEDOT films is less pronounced with a measured thickness in pure DMSO of ~150% of that in pure water. The thickness of PEDOT also decreases upon re-exposure to water, although is cannot be determined with certainty from these measurements if it returns to its original value in water. Interestingly, the swelling of the PEDOT and PEDOT-N_3 films appeared to have little influence of the roughness of the substrates. AFM analysis of the film surface morphology after repeated exchange of the immersion liquids thus showed very little dependence on the degree of swelling, with mean and RMS roughness values of less than 10 nm for all the conditions explored, see Figure 10 and Table 7.

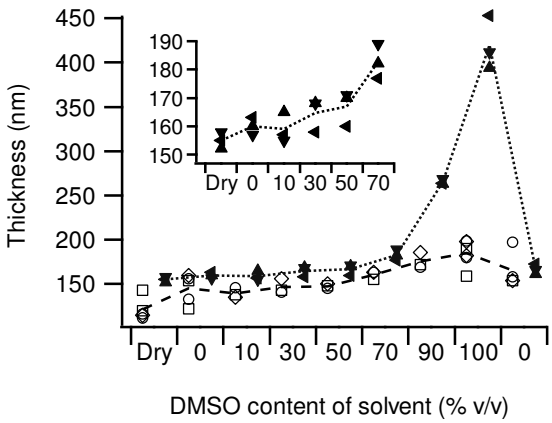

Figure 9 PEDOT-N_3 and PEDOT swell upon exposure to high DMSO concentration solvents

The thickness of PEDOT (open symbols) and PEDOT-N_3 (solid symbols) thin films were measured by AFM for gradually increasing DMSO content. The thickness was first measured in dry condition and then in mixtures of water and DMSO, starting from pure water and increasing the DMSO content until reaching pure DMSO. The films were then re-immersed in pure water. For each film at least three different areas were measured with each symbol corresponding to one of the areas. The lines show average thickness of these points. Insert: The thickness of PEDOT-N_3 films at low DMSO contents shown at larger magnification.

Substrate	Roughness R_a				Roughness R_{rms}			
	Dry	Water	DMSO	Water after DMSO	Dry	Water	DMSO	Water after DMSO
PEDOT-N_3:TsO	2.1	5.7	3.1	2.8	2.9	8.6	3.9	3.6
PEDOT:TsO	1.5	2.7	4.3	4.5	1.9	4.1	4.9	6.1

Table 7 Surface roughness of PEDOT-N_3 and PEDOT swelled in DMSO

Surface roughness of PEDOT-N_3 tosylate and PEDOT tosylate films prior to immersion in liquid, immersed in water, then immersed in DMSO, and finally after drying, respectively. Analysis proceeded using the roughness analysis routine of the Gwyddion software package.

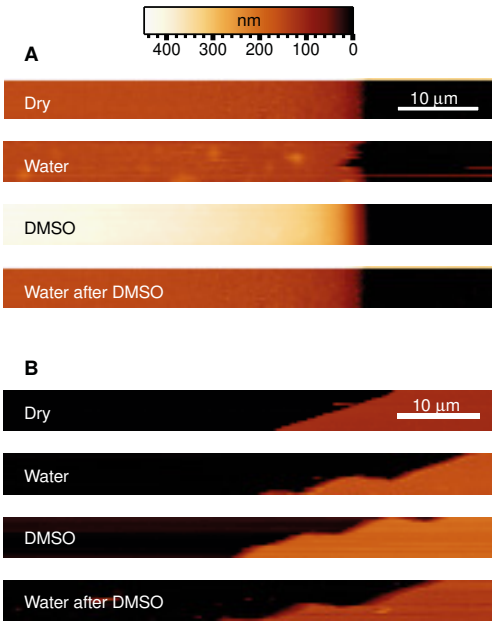

Figure 10 AFM micrographs of PEDOT-N_3 and PEDOT swelled in DMSO and water

AFM micrographs of **A**: PEDOT-N_3:TsO or **B**: PEDOT:TsO films immersed in liquid environments and measured across a mechanically induced surface defect. The color legend corresponds to the measured heights with all images being presented using the same height-to-color scaling, and with each image vertically shifted to have zero height at the substrate surface (black areas).

We also investigated whether the swelling of PEDOT-N_3 and PEDOT thin films was associated with changes in light absorption. Absorption spectroscopy showed small variations in a broad absorption peak centered at 530 nm after exposure of PEDOT-N_3 films to different liquid environments, see Figure 11A. No changes in visible and near-infrared absorption were found for PEDOT films exposed to the same treatments, see Figure 11B.

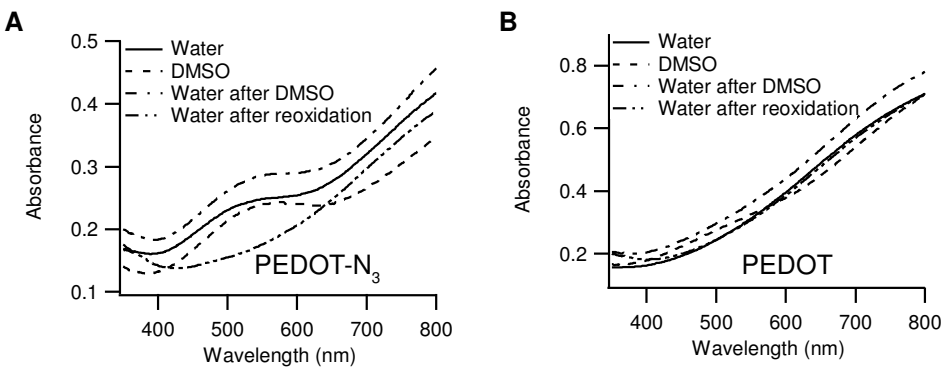

Figure 11 Absorption profiles of PEDOT-N_3 and PEDOT washed in water and DMSO

Optical absorbance of **A**: PEDOT-N_3:TsO or **B**: PEDOT:TsO film after immersion in water, immersion in DMSO, immersion in DMSO followed by washing in water, or re-oxidation in Fe(III)tosylate followed by washing in water, respectively.

DMSO increases the conductance of PEDOT:PSS, but not PEDOT:TsO or PEDOT-N_3:TsO

As we mentioned in Chapter 1, PEDOT is usually employed in a p-doped state with counter anions ensuring charge neutrality. Tosylate (TsO) or polymeric poly(styrene-sulfonic acid) (PSS) counterions are commonly used,[5] and the PEDOT and PEDOT-N_3 films primarily investigated throughout this thesis, were *in situ* polymerized, and contained tosylate counterions.[5, 17] PEDOT with polymeric PSS counterions (PEDOT:PSS) is widely used commercially available alternative. For comparison, this type of film was included in the AFM and conductivity analysis. Table 8 compares thickness and sheet resistance of PEDOT:PSS in the dry state, in water, and in DMSO, respective, to the corresponding values found for PEDOT-N_3 with tosylate (PEDOT-N_3:TsO) or PEDOT with tosylate (PEDOT:TsO).

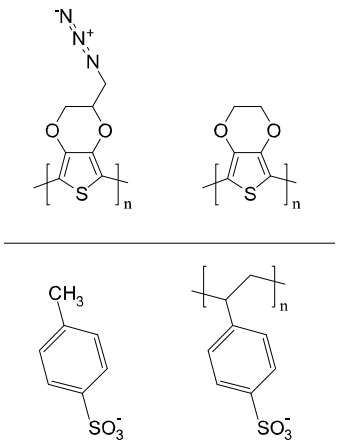

Figure 12 PEDOT, PEDOT-N_3 and PSS and TsO counterions
Structure of PEDOT-type polymers and counterions. Top left: PEDOT-N_3. Top right: PEDOT. Bottom left: Tosylate counterion. Bottom right: Poly(styrene sulfonate) counterion.

Substrate	Film thickness in nm[a]			Film sheet resistance in kOhms/square[b]					
	Dry[c]	Water[d]	DMSO[e]	Dry[c]	Water[d]	Dry after water[f]	Dry[c]	DMSO[e]	Dry after DMSO[g]
PEDOT-N_3:TsO	155	160	420	0.71	1.15	1	0.77	1.33	1.34
PEDOT:TsO	121	145	185	0.08	0.11	0.11	0.09	0.1	0.1
PEDOT:PSS	266	2087	1879	267	[h]	241	218	1.1	0.45

Table 8 Swelling and conductance characteristics of PEDOT:TsO, PEDOT-N_3:TsO and PEDOT:PSS
Thickness and sheet resistance of PEDOT-N_3:TsO, PEDOT:TsO, and PEDOT:PSS thin films prior to immersion in liquid, immersed in liquid, and after drying, respectively. [a] Average value of at least three different areas on each film measured by AFM after ≥30 min exposure. [b] Average of two four-point probe measurements of perpendicular orientations obtained after ≥10 min exposure. [c] Film in dry state before immersion in liquids. [d] Film immersed in water. [e] Film immersed in DMSO. [f] Film dried in a stream of nitrogen after immersion in water. [g] Film washed in water and dried in a stream of nitrogen after immersion in DMSO. [h] The PEDOT:PSS film immersed in water did not produce stable sheet resistance values.

Our AFM studies revealed very large swelling of PEDOT:PSS in both DMSO and water. In both solvents the measured thicknesses were >700% of the dry state thickness. This finding is not surprising as it is well established that PEDOT:PSS is both hygroscopic and capable of absorbing large amounts of DMSO.[114, 115] The interaction between DMSO and PEDOT:PSS has attracted considerable attention, as DMSO and a number of other polar organic solvents can be used to drastically increase PEDOT:PSS conductance.[112, 114, 116] Addition of these solvents to aqueous suspensions of PEDOT:PSS during or after spin-casting of films improves the conductance by orders of magnitude.[114, 116, 117] We similarly observe a ~500 times lower sheet resistance of a preformed PEDOT:PSS film after immersion in DMSO followed by washing in water and drying (see Table 8, columns "Dry" vs. "Dry after DMSO"). It is worth noting that even the heavily swelled state of PEDOT:PSS during DMSO treatment exhibit ~200 times lower sheet resistance (columns "Dry" vs. "DMSO"). In contrast, PEDOT-N_3:TsO and PEDOT:TsO films show small increases in sheet resistance of ~1.75 times and ~1.1 times, respectively, upon DMSO treatment. In this comparison, it should be noted that the initial and final sheet resistance of the latter films are actually both close to the resistance for PEDOT:PSS after solvent treatment.

Mechanistic considerations on PEDOT-N_3 swelling in high DMSO concentration DMSO/water mixtures

It has been proposed that for PEDOT:PSS, DMSO can induce a re-organization of the PSS and PEDOT domains with respect to each other, and change the conformation of the individual PEDOT chains, leading to the observed increased conductance. [112-114] Ouyang[112] *et al.* proposed that interaction between the dipole moment of DMSO with dipoles and/or positive charges in the PEDOT backbone, in concert with hydrogen bonding to protonated sulfuric acid groups in PSS, is the driving force for such reorganization. Additionally, Bagchi and Menon[113] showed that the PEDOT polymer chains acquire extended conformations in DMSO compared to water. Hence, a favored interaction between PEDOT type polymers and DMSO is not a new phenomenon. We observed much stronger swelling of PEDOT:PSS than of PEDOT:TsO in both water and DMSO. The large volume fraction of hygroscopic PSS in PEDOT:PSS compared to the volume fraction of tosylate in PEDOT:TsO[103] likely accounts for most of this difference. We therefore considered if the larger swelling of PEDOT-N_3:TsO than of PEDOT:TsO in DMSO could reflect differences in the doping levels and tosylate content of the two polymers. However, estimation of the tosylate content from XPS analysis of the sulfur peak[103, 104] as outlined in Chapter 3, does not indicate markedly different levels in PEDOT:TsO and in PEDOT-N_3:TsO. Another explanation for their different swelling properties might be the presence or absence of the azide functionality. In a recent study by Sando *et al.* [118] on the vibrational behavior of the inorganic azide ion in DMSO and water, no preferential solvation of the azide towards water or DMSO was reported. We can therefore only suggest that the azide group in organic polymers may have a favorable interaction

with DMSO, perhaps in synergy with other interactions such as those suggested by Ouyang.[112] Finally, it should be noted that the difference in the EDOT vs. EDOT-N_3 monomers leads to different polymerization behaviors, which is reflected in the slightly different polymerization conditions.[10] Thus, the chain lengths of PEDOT-N_3 might be of different from those of the regular PEDOT, which could affect the swelling properties.

Conclusion

We have observed a distinctive swelling behavior for PEDOT-N_3:TsO thin films in DMSO solutions. In water, the polymer film swelled only a few percent, whereas in DMSO the thickness increased to ~260% of the thickness found in the dry state. Importantly, this swelling in DMSO could be reversed by exposing the film to water again. PEDOT containing tosylate as counterions displayed a similar but less pronounced effect, while PEDOT with polymeric PSS counterions swelled to more than seven times its original thickness in both water and DMSO.

Experimental

Solvents
Ultrapure water of resistivity >18.2 MΩ cm (Milli-Q water) was produced on a Millipore Quantum system (Millipore, MA, USA). DMSO (>99% purity) was obtained from Merck (Darmstadt, Germany). DMSO concentrations in DMSO/water solutions are given in volume percent throughout the text.

Cyclic Olefin Copolymer supports
COC substrates were fabricated as described in Chapter 2.

Preparation of functional microscope glass substrates
In the AFM studies, octadecyltrichlorosilane (OTS) treated glass microscope slides were used as substrates for PEDOT:TsO and PEDOT-N_3:TsO films. (3-aminopropyl)-trimethoxysilane (APTMS) treated glass microscope slides were used as substrates for PEDOT:PSS film. OTS treatment proceeded by immersion of the glass slides in a 0.5% solution of OTS (Sigma-Aldrich) in toluene for at least 15 min. After treatment the slides were rinsed in toluene, ethanol, and Milli-Q water. APTMS treatment was done by placing the microscope slide for 2 h in a 0.1 M solution of APTMS (Sigma-Aldrich) in 2-propanol containing 1.5 M water, and rinsing in 2-propanol, ethanol and Milli-Q water.

PEDOT-N_3 thin films fabrication
As described in Chapter 2.

PEDOT thin films fabrication

PEDOT films were prepared by *in situ* polymerization of EDOT on injection molded COC (TOPAS 5013, TOPAS Advanced Polymers, Frankfurt, Germany) substrates, or microscope glass slides substrates, cleaned with acetone, isopropanol, ethanol and water. 6.5 mL CLEVIOS C-B40 (H.C. Starck, Goslar, Germany), 2 mL 1-butanol, 0.15 mL pyridine, and 0.22 ml CLEVIOS M (H.C. Starck), were mixed in the stated order and spin-coated on the COC discs (20 s at 700 rpm). The samples were placed in an oven or at a hot plate at 70 °C for 2 min and subsequently washed with water and blown dry in a nitrogen flow, yielding films with a thickness of approximately 140 nm.

PEDOT:PSS thin films fabrication

PEDOT:PSS films for AFM investigation were made by spin-coating a 1.2-1.4% PEDOT:PSS aqueous solution (483095, Sigma-Aldrich) at 1000 rpm onto a glass microscope slide. Following spin-coating the film was annealed on a hot plate at 200°C for 30 min.

AFM measurements

AFM measurements were performed on a PSIA XE-150 (Park Systems, Suwon, Korea) operating in intermittent contact mode and using Tap300Al and Tap75Al cantilevers (Budget Sensors, Sofia, Bulgaria). Liquid measurements used a liquid probe hand (Park Systems) and a homemade sample chamber permitting complete immersion of the substrate. Film thicknesses were determined by measuring the step height of a step produced either by cutting a narrow line with a scalpel, or through masked oxygen plasma etching of part of the film (Plasmatherm 740, Unaxis, St Petersburg, FL, USA). The step heights of at least 3 points on each sample were measured. For measurement series using a sequence of solvent mixtures, the same measurement areas were probed in each step of the series. Exchange of DMSO/water mixtures proceeded by washing the sample chamber twice with the new mixture and waiting for a period of at least 30 min before analysis to allow the film to adjust. The DMSO content was increased in each step of the measurement series, except for the final re-immersion in pure water. The surface morphology of PEDOT-N_3:TsO and PEDOT:TsO films in liquid environments were analyzed using the open source software package Gwyddion (gwyddion.net): A surface area of 8 µm by 30 µm was extracted from each AFM image, background corrected using a first-order plane fit, and analyzed by the "Statistical quantities" function.

Optical absorption of PEDOT-N_3 and PEDOT films in liquid environments

PEDOT:TsO or PEDOT-N_3:TsO films on COC supports were immersed for 10 min in Milli-Q water or DMSO, respectively, before measuring their absorbance spectra. Reoxidation of the films were performed by brief immersion in 10% Fe(III)tosylate in butanol (CLEVIOS CB-40, Heraeus, Germany) in Milli-Q water followed by thorough washing with Milli-Q water. Absorbance spectra were recorded on a Shimadzu UV-1700 spectrophotometer.

Chapter 5

Solvent Composition Directs Reaction Depth and Density of PEDOT-N_3 Thin Films

Introduction

In Chapter 4 we showed that PEDOT-N_3 thin films undergo a violent but reversible swelling when exposed to DMSO. We also showed that the swelling of the films in DMSO/water mixtures could be gradually increased by increasing the DMSO content. In this Chapter we show how these findings can be exploited for controlling reaction degree and depth of CuAAC modifications of PEDOT-N_3 thin films. Specifically, by using AFM and XPS analysis we have found that the reaction observables can be adjusted by changing the solvent composition for a number of different alkyne reactants. The general principle for using the solvent composition for directing reaction depth is illustrated in Figure 13. Larger concentration of DMSO leads to larger swelling of the conducting polymer film and deeper and denser reactions of the alkyne reactants.

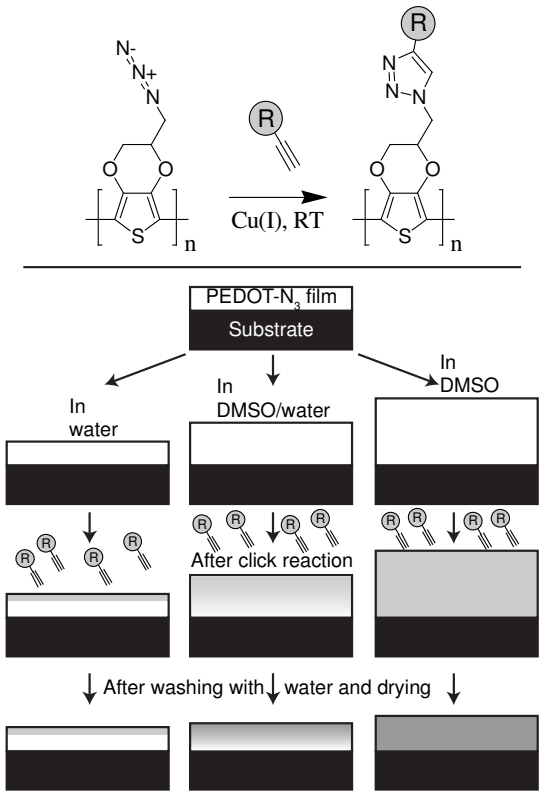

Figure 13 Principle for applying solvent composition for directing functionalization depth for PEDOT-N_3 films
Top: Cu(I)-catalyzed click reaction between the azide of PEDOT-N_3 and an alkyne reactant. *Bottom:* Illustration of the swelling of PEDOT-N_3 thin films (white) in water, in water/DMSO mixtures, and in pure DMSO, respectively, and the resulting degrees of reaction (gray) at the surface and in the bulk of the film in its swelled state after reaction, or after washing with water and drying.

We initially show this principle for PEG-alkyne. Often, the formation of a high-density surface layer of PEG molecules by grafting from solution can be difficult due to steric hindrance by initially bound PEG molecules.[119] Here we find that addition of DMSO to the aqueous solution results in a much denser PEG film, probably due to the swelling of the PEDOT-N_3 that increases the number of accessible reactive azide groups. Such a dense PEG coverage can be achieved at

intermediate DMSO concentrations without compromising the conductivity of the PEDOT-N_3, whereas the use of very high DMSO concentrations leads to a substantial bulk modification and concomitant decrease of the film conductivity. Importantly, we have found that the protein adsorption is significantly lowered for samples covered with PEG using intermediate amounts of DMSO. As mentioned earlier, for many potential bio-applications, avoiding the long or short term unspecific adsorption of proteins is essential. Nevertheless, covalently functionalized PEDOT type film showing this property has, to our knowledge, not been reported earlier. After this detailed investigation of the functionalization of PEDOT-N_3 with PEG-alkyne, we show that the solvent directed functionalization principle is applicable to other alkyne reactants, illustrating the generality of the method.

There are other approaches that can be taken to directing functional chemistries towards the surface or the bulk of the films. For example in the studies by Berggrens group mentioned in Chapter 1, the surface work function of PEDOT type thin films were altered by adsorbing specific molecules onto the material surface,[70, 74] whereas in studies by Segura *et al.*,[67] the electrochemical properties of the entire film were changed by covalently altering the monomer. The solvent directed functionalization however provides a simple method for changing either only the surface properties of a film, or the properties of the entire film, using the same substrate for numerous localized functionalities. It further allows intermediate functionalizations of the films gradually changing the bulk properties.

The central findings of this Chapter were presented in the paper "Solvent Composition Directing Click-Functionalization at the Surface or in the Bulk of Azide-Modified PEDOT" *Macromolecules*, 44 (3), pp. 495–501 (2011), and the following Chapter contains entire continuous sections taken from this paper.

The swelling of PEDOT-N_3 in DMSO/water mixtures controls the reaction depth of PEG-alkyne

We investigated the functionalization of PEDOT-N_3 films with PEG-alkyne by applying XPS and AFM. These analyses were performed on a number of PEDOT-N_3 films functionalized with PEG-alkyne at varying DMSO concentration and fixed concentrations of PEG-alkyne, $CuSO_4$, and sodium ascorbate. To analyze the reaction degree, we applied the high resolution nitrogen signal. As was illustrated in Chapter 3, Figure 5, the doublet peak which is characteristic for azide groups, is removed upon conversion of the azide to a triazole group. The intensity ratio of the higher binding energy peak to the lower binding peak is 1:2 for azide groups, whereas the ratio becomes less than 1:2 upon reaction. We used this nitrogen doublet peak ratio as a direct measure of the surface reaction degree. In Figure 14 this ratio is presented for the prepared PEG-reacted films. We analyzed both the front *and* the back of the functionalized films to detect if bulk reaction took place.

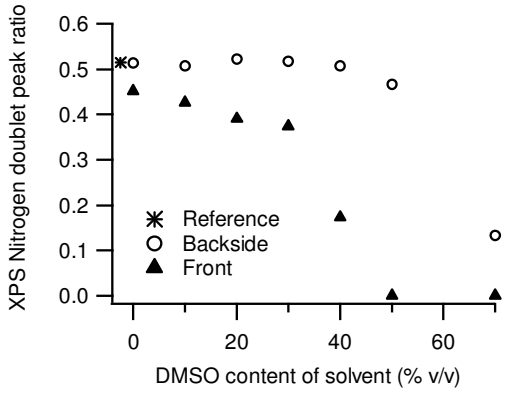

Figure 14 XPS analysis of the degree of reaction on PEDOT-N_3 films modified by PEG-alkyne as a function of DMSO concentration

All reactions used 10 mM PEG-alkyne, 2 mM $CuSO_4$, 40 mM sodium ascorbate, and a fixed reaction time of 4 h. A nitrogen peak intensity ratio of ½ corresponds to zero degree of reaction, while full conversion of the azides yields a peak ratio of 0. Nitrogen peak analysis was performed both on the front side (facing the reaction solution; solid triangles) and on the back side (facing the substrate; open circles) of the film, with the reference (asterisk) being a freshly prepared PEDOT-N_3 film.

The analysis shows that some reaction occurs on the front of the film in pure water after 4 h reaction time. However, the resulting PEG layer is of low density. If the characteristic length of the XPS sampling profile in is set to 2.5 nm, which is the common range for organic materials,[105] the nitrogen peak ratio found for the reaction in pure water corresponds to a surface PEG layer with a thickness of <0.5 nm in the vacuum conditions applied during the XPS measurement. Addition of DMSO to the aqueous solvent leads to gradually increasing degrees of reaction until no azides can be found on the front of the film within the XPS sampling depth. On the backside of the film, no reaction is seen for the pure water samples or for DMSO concentrations below 50%. However, for DMSO concentrations ≥50%, reaction occurs even on the back of the film. Thus, the increased swelling at high DMSO concentrations does indeed allow reaction to occur deep into the film. Figure 14 also shows that smaller DMSO concentrations have an effect. This effect is either increasing the surface density of reacted groups and/or permitting reaction deeper into the film. However, the degree of reaction in the film interior cannot easily be determined by XPS analysis, since the obvious option of performing XPS depth profiling may adversely affect the azide functionality.

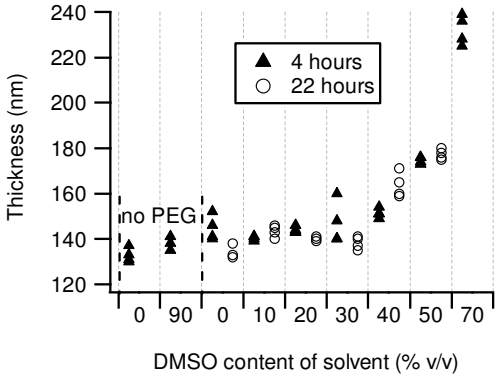

Figure 15 AFM analysis of the PEDOT-N_3 film thickness after reaction with PEG-alkyne at varying DMSO concentrations and reaction times

(4 h: solid triangles; 22 h: open circles), followed by washing with water, and drying the samples. All reactions used 10 mM PEG-alkyne, 2 mM $CuSO_4$, and 40 mM sodium ascorbate. The two controls to the left in the graph underwent all process steps except for the addition of PEG-alkyne.

Stable coupling of PEG-alkyne to azides in the bulk of the PEDOT-N_3 film will result in a larger film volume. We therefore measured the film thickness after reaction, washing with water, and drying, to use the thickness as an indirect measure of the average degree of reaction. The PEDOT-N_3 film thickness in dry condition after reaction with PEG-alkyne was measured by AFM for a range of DMSO concentrations and reaction times of 4 and 22 h, respectively, see Figure 15. Some minor in-homogeneities in the film structure could be observed during the AFM measurements. Still, a correlation between the thickness of the film and the DMSO content of the reaction solvent is evident for both the 4 h and the 22 h series. For the 4 h reaction at 50% DMSO, the thickness was ~175 nm and at 70% DMSO it was 230 nm, equivalent to respectively 130% and 175% of the thickness of the reference areas without PEG. This clearly shows that bulk reaction does indeed take place for higher DMSO concentrations. A similar bulk reaction of a PEDOT-N_3 film had been observed in an earlier study on modifying PEDOT-N_3 with an alkyne modified fluorescein in DMF.[10] Notably, for the low DMSO concentrations and for pure water, no significant thickness increase is observed even for the 22 h reaction time, indicating the absence of bulk reaction. The importance of the reaction time for bulk reaction at high DMSO concentrations is stressed by the missing point at 70% DMSO for the 22 h series: This experiment was in fact performed, but the film was not sufficiently mechanically stable after the PEG-alkyne reaction to perform the height analysis procedure. In general the films often became unstable for reactions conducted in ≥70% DMSO. We take this as an indication that upon heavy PEG functionalization the material loses its cohesive strength and fractures during the rinsing steps. The swelling process itself is not responsible for the loss of mechanical stability, since the control sample of immersed in 90% DMSO without adding PEG-alkyne, see left side of Figure 15, remained perfectly stable after washing with water and drying.

In-depth functionalization with PEG-alkyne does not disrupt the conductivity of PEDOT-N_3

Global and local volumetric expansion of the PEDOT-N_3 film upon covalent coupling of alkynes in the film interior may adversely affect its conductive properties in addition to its mechanical properties. The sheet resistance of the films after PEG modification is displayed in Figure 16. The conductivity is only weakly influenced by the reaction steps up to reaction conditions affecting the overall film stability, ≥ 70% DMSO, cf. Figure 15. Remarkably, the AFM measurements in Figure 15 indicate incorporation of significant amounts of material in the film using 40-50% DMSO in the reaction solution and yet only small increases in the sheet resistance are observed in Figure 16, in particular for the shorter reaction time of 4 h. These findings are in good agreement with earlier reports that large amounts of a second molecular (PEG) or polymeric (poly(methyl methacrylate)) material can be incorporated into PEDOT without compromising its conductivity.[120, 121]

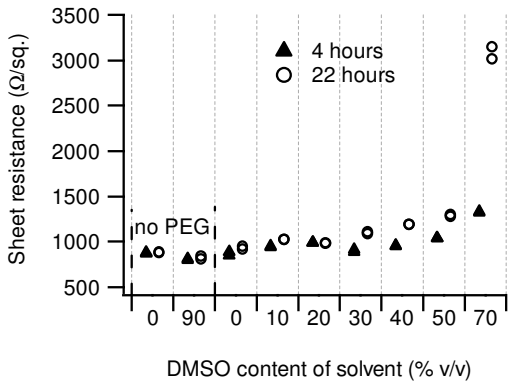

Figure 16 Sheet resistance of the PEDOT-N_3 film after reaction with PEG-alkyne at varying DMSO concentrations and reaction times

(4 h: solid triangles; 22 h: open circles). All reactions used 10 mM PEG-alkyne, 2 mM $CuSO_4$, and 40 mM sodium ascorbate. Prior to the resistance measurement all films had been rinsed and re-oxidized as described in the Experimental section, since the CuAAC reactions are performed in a chemically reducing environment. The two controls to the left in the graph underwent all process steps except that no PEG-alkyne was added to the reaction solution.

Protein adsorption onto PEDOT-N_3 can be limited through functionalization with PEG-alkyne

The XPS data in Figure 14 indicates that PEG-alkyne can be grafted at higher density in solvents with larger DMSO concentrations. Increased PEG coverage is expected to reduce the protein adhesiveness of the PEDOT-N_3 film surface[119] and thereby approach an ideal "non-fouling" surface. We tested this concept by means of adsorption of horse-radish peroxidase conjugated to Immunoglobulin G IgG (HRP-IgG) as test protein. The enzymatic HRP part allows for easy detection of the amount of adsorbed protein by following the formation of a colored product of the enzymatic process, similar to in a direct enzyme-linked immunosorbent assay (ELISA) experiment. The results are displayed in Figure 17. Only a small reduction in protein adsorption was found for the PEDOT-N_3 film modified by PEG-alkyne in water, whereas increasing the DMSO content leads to decreasing protein adsorption. The minimum adsorption is found for film surfaces reacted in ≥50% DMSO. This is a very good agreement with the XPS analysis presented in Figure 14, which showed complete reaction of the azide groups within the XPS sampling depth for ≥50% DMSO in the reaction solution. An intermediate DMSO concentration of 40%-50% in the reaction solution may consequently be employed to form a dense PEG surface layer that strongly reduces protein adsorption without adversely affecting the conductive properties of the PEDOT-N_3, cf. Figure 16.

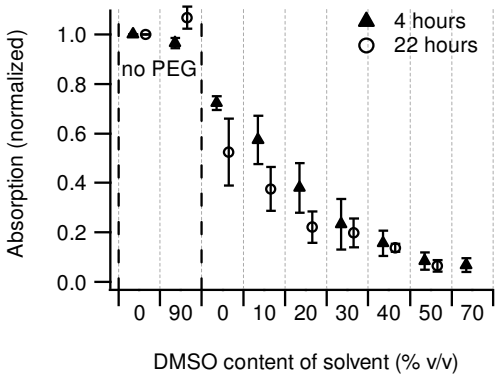

Figure 17 Protein adsorption to PEDOT-N_3 functionalized with PEG at varying DMSO concentration and reaction times

(4 h: solid triangles; 22 h: open circles). The ability of the films to resist protein adsorption was tested using IgG-HRP. The relative adsorption of IgG-HRP was determined via the turnover of the HRP-substrate TMB and measured by light absorption at 450 nm. Four independent experiments were conducted. All results are normalized to the highest protein adsorption measured, i.e. for the reference point at 0% DMSO with no added PEG-alkyne. Error bars show the standard error of the mean (n=4).

PEDOT-N_3 swelling in DMSO/water mixtures can be control the reaction depth of various alkynes

The observed dependence on DMSO content might be unique for the PEG-alkyne, for instance by the DMSO influencing the solubility of the PEG-domain.[119] We examined the generality of our approach by reacting PEDOT-N_3 films with several other alkyne reactants. Figure 18 shows XPS analysis of the reaction of PEDOT-N_3 films with pentynoic acid. Again, the ratio of the two peaks in the high resolution nitrogen signal was employing as a direct measure for the reaction degree. Reaction in solvent mixtures containing ≤50% DMSO results in intermediate reaction on the front side and no reaction on the back side of the film. Higher DMSO content leads to increasing degrees of reaction on the back side of the film, in full agreement with the results obtained for PEG-alkyne, cf. Figure 14. As pentynoic acid, being negatively charged and containing a short hydrophobic segment, is a fairly dissimilar reactant to PEG-alkyne, we suggest that the controlled swelling of the PEDOT-N_3 is most likely the main source of the observed bulk reactions.

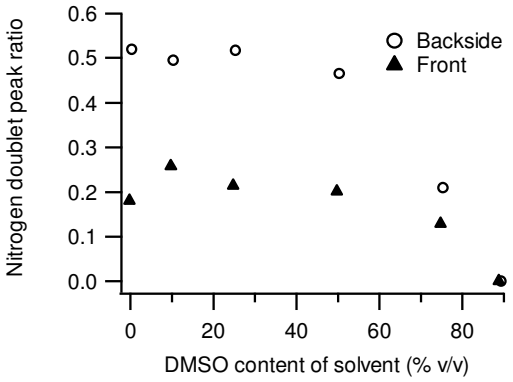

Figure 18 XPS analysis of the degree of reaction on PEDOT-N_3 films modified by pentynoic acid as a function of DMSO concentration

All reactions used 10 mM pentynoic acid, 2 mM $CuSO_4$, 40 mM sodium ascorbate, and a reaction time of 18 h. A nitrogen peak intensity ratio of ½ corresponds to zero degree of reaction, while full conversion of the azides yields a peak ratio of 0. Nitrogen peak analysis was performed both on the front side (solid triangles) and back side (open circles) of the film.

Three other alkynes spanning a range of molecular weights, propargyl alcohol (MW 42 Da), an alkyne modified Ni(II)-chelating nitrilotriacetic acid (NTA-alkyne, MW 344 Da), and alkyne-PEG-GRGDS (MW 1727 Da), were reacted with the PEDOT-N_3 using different DMSO concentrations, and evaluated using XPS analysis of the nitrogen doublet peak. These reagents all showed an increasing degree of reaction with increasing DMSO concentration; see Figure 19 - Figure 21. This confirms that the method is applicable for a wide range of reactants. The modification of PEDOT-N_3 by NTA-alkyne and alkyne-PEG-GRGDS was further independently probed by quantitative XPS analysis of hetero-atoms which were specific to the two reagents

(nickel and iodine, respectively; see Figure 20 and Figure 21). For both reactants the reaction trends observed by these analyses were in agreement with those from the nitrogen peak fit analysis.

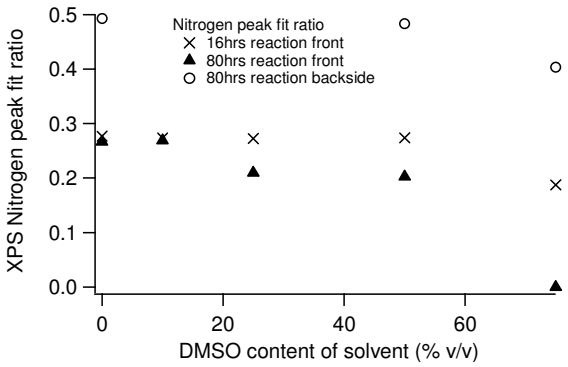

Figure 19 XPS analysis of the degree of reaction on PEDOT-N_3 films modified by propargyl alcohol as a function of DMSO concentration

The longer reaction time of 80 h used 12. 5 mM propargyl alcohol, 1.25 mM CuSO4, and 50 mM sodium ascorbate (front side: closed triangles; backside: open circles). The shorter reaction time of 16 h (crosses) used 10 mM propargyl alcohol, 1 mM CuSO4, and 40 mM sodium ascorbate. A nitrogen peak intensity ratio of ½ corresponds to zero degree of reaction, while full conversion of the azides yields a peak ratio of 0. Nitrogen peak analysis was performed both on the front side and backside of the film. The signal from the backside suggests some degree of reaction throughout the film thickness for the highest DMSO concentration.

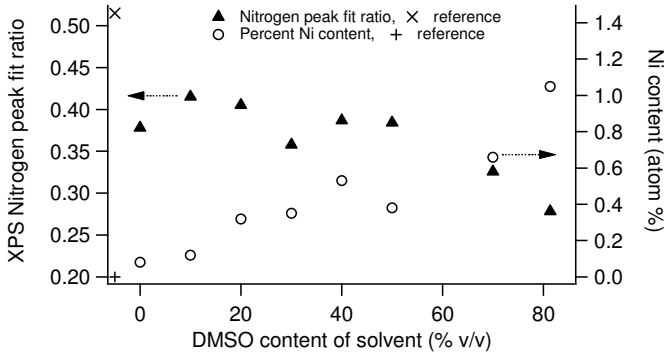

Figure 20 XPS analysis of the degree of reaction on PEDOT-N_3 films modified by NTA-alkyne as a function of DMSO concentration

Nitrogen doublet peak ratio (solid triangles; reference: cross) and the surface concentration of nickel (open circles; reference: plus) were used for determining the reaction degrees. All reactions used 10 mM NTA-alkyne, 2 mM CuSO4, 40 mM sodium ascorbate, and a reaction time of 4 h. The NTA moiety can chelate transition row metals such as Ni(II), which was used as an independent XPS assay of the degree of reaction in addition to the nitrogen peak ratio analysis. For the Ni(II) assay, the samples were immersed in 50 mM EDTA in 50 mM Tetramethylbenzidine (TRIS) buffer for 30 min, reacted with 100 mM Ni(II)SO4 in Milli-Q water for 30 min, and rinsed with Milli-Q water before drying in a stream of nitrogen. Left axis: A nitrogen peak intensity ratio of ½ corresponds to zero degree of reaction, while full conversion of the azides yields a peak ratio of 0. Right axis: Increasing nickel content corresponds to higher degrees of reaction. The reference is a freshly prepared PEDOT-N_3 film.

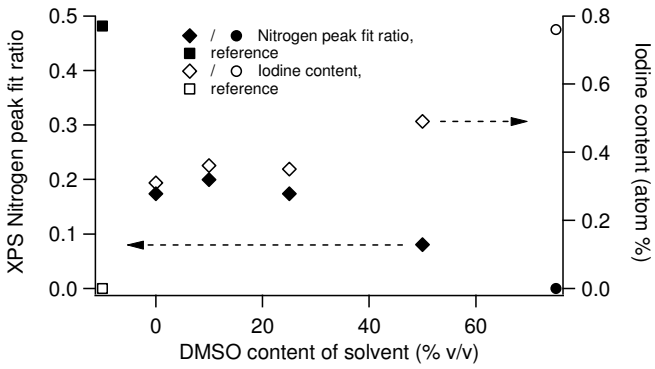

Figure 21 XPS analysis of the degree of reaction on PEDOT-N_3 films modified by alkyne-PEG-GRGDS as a function of DMSO concentration

The nitrogen doublet peak ratio (solid points; reference: solid square) and the surface concentration of iodine (open points; reference: open square) were used for determining the reaction degrees. All reactions used 3 mM alkyne-peptide, 0.6 mM CuSO4, 6 mM sodium ascorbate, and overnight reaction time. The samples were rinsed in DMF after reaction. For the highest DMSO concentration (circles) point, which used 5 mM alkyne-peptide, 1 mM CuSO4, 20 mM sodium ascorbate was used, and no DMF wash was performed. Left axis: A nitrogen peak intensity ratio of ½ corresponds to zero degree of reaction, while full conversion of the azides yields a peak ratio of 0. The nitrogen peak ratio will also be influenced by coupling of the nitrogen-rich peptide fragment, and is therefore less straight-forward to interpret for this molecule. Right axis: Increasing iodine content reliably corresponds to higher degrees of reaction as only the alkyne-peptide contains iodine as hetero-atom. The reference is a freshly prepared PEDOT-N_3 film.

An important final consideration is that there might be other effects than just the swelling of the PEDOT-N_3 increasing the in-depth reaction. DMSO could have a general accelerating effect on the CuAAC-reaction, independent of the type of alkyne. DMSO is often employed as solvent or co-solvent for CuAAC reactions, it is a better solvent for the catalytic Cu(I) ion than water,[24, 122, 123] and it has served to accelerate a number of reactions.[124] However, even when increasing the reaction time to 80 h for the smallest of the reactants (propargyl alcohol) we did not see any noticeable change in the degree of reaction for low DMSO concentrations, compared to a much shorter reaction time of 16 h (see Figure 19). Thus, we maintain that film swelling is of key importance for the increased reaction depth observed upon adding DMSO, although changes in the reaction kinetics may play a secondary role.

High concentrations of DMSO in solvent increases reaction degree of PEG-alkyne on PS-N_3

We speculated earlier that the introduction of the azide functionality might be important to the observed swelling behavior of PEDOT-N_3 and the associated high accessibility of the azides for click reactions with alkynes. If so, other polymers containing azide groups should exhibit a similar behavior. As a simple test case, we performed preliminary tests of a click-reaction between an azide-modified polystyrene (PS-N_3), see Figure 22, and PEG-alkyne at varying DMSO content in the reaction solution, see Figure 23.

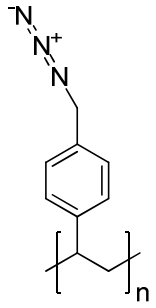

Figure 22 Molecular structure of the applied azide-modified polystyrene PS-N_3

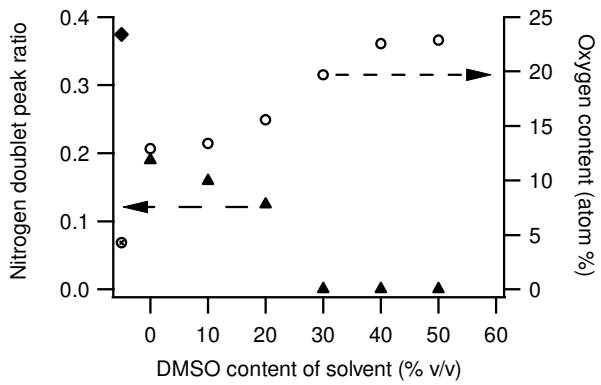

Figure 23 XPS analysis of the degree of reaction on PS-N_3 films modified by PEG-alkyne as a function of DMSO concentration

The nitrogen doublet peak ratio (solid triangles; reference: solid diamond) and the surface concentration of oxygen (open circles; reference: cross in circle) were used as measures for the surface reaction degree. All reactions used 5 mM PEG-alkyne, 1 mM CuSO4, 20 mM sodium ascorbate, and overnight reaction time. Left axis: A nitrogen peak intensity ratio of ½ corresponds to zero degree of reaction, while full conversion of the azides yields a peak ratio of 0. Right axis: Increasing oxygen content corresponds to higher degrees of reaction as only the alkyne-peptide contains oxygen as hetero-atom. A dense surface layer of reacted PEG-alkyne in a largely stretched conformation would approach an oxygen content of ~30 atom%. The reference is a freshly prepared PS-N_3 film.

The results show a strong dependence on the DMSO content with complete conversion of azides at the surface occurring for ≥40% DMSO and a two-fold increase in the surface density of PEG chains over the reaction performed in pure water. Although it is likely that the increased swelling of the PS-N_3 in high DMSO concentrations is not caused directly by the azide of the polystyrene, but general for polystyrene polymers, the approach of partially swelling a polymeric substrate before grafting PEG from solution, appear to be generally applicable, and not only applicable for PEDOT-N_3 substrates. The variation from the expected 1:2 ratio for azide groups found for the native PS-N_3 was found to originate from decomposition of the azide during the XPS analysis. This is due to the fact that the PS-N_3, being a non-conductive substrate, undergoes significant charging during XPS analysis which has to be counter-acted by applying an electron-source flood-gun, which leads to partial decomposition of the azides.

Conclusion

We have shown how the drastic and reversible swelling which occurs for PEDOT-N_3 thin films in DMSO/water mixtures with high DMSO content, can be exploited for directing a post-polymerization functionalization of PEDOT-N_3 thin films. In pure water and in water with low DMSO content, reaction was found only to take place on the surface. Increasing DMSO content resulted in gradually larger swelling that lead to higher degree of bulk reaction. Such controlled reaction depth was demonstrated for a number of alkyne reactants. The modification with PEG-alkyne served to illustrate how such control of the degree of reaction via the swelling of the film can be employed to fabricate a conducting polymer film surface with minimal protein adhesiveness without adversely affecting the film conductivity. This property of resisting protein adsorption is a most useful characteristic for future potential bio-applications. As we showed in Chapter 2, it is possible to present specific biological motives on such a PEG-background. It should thus be feasible to specifically capture small biological entities, in addition to the whole cells presented in Chapter 2, onto covalently modified PEDOT-N_3 surfaces, while limiting the adsorption of unwanted molecules. This might enable sensitive detection of bio-molecules, such as a protein, in samples containing large amounts of bio-material, such as whole blood samples. Although an interesting perspective, we did not further investigate these possibilities.

Another interesting perspective is the possibility for fabricating bi-functional films having one type of functionality at the material surface and another in the bulk. We suggest that this should be possible by initially adding one type of functionality to the surface of the film, by performing a reaction in a non-swelling state, followed by adding a second function to the bulk state, by reaction in a swelled state.

Experimental section

Cyclic Olefin Copolymer supports
COC substrates were fabricated as described in Chapter 2.

PS-N_3 synthesis
PS-N_3 was synthesized as described in Appendix 2 by Dr. A.E. Daugaard

Spin-coating of PS-N_3 onto COC substrates.
A 10 mg / mL solution of PS-N_3 in dioxane was made. 500 µL of the solution was spin-coated onto a COC substrate a 1000 rpm.

Alkyne reagents

The syntheses of the PEG-alkyne, alkyne-PEG-GRGDS, alkyne-PEG-GRDGS and NTA-alkyne reagents are described in Appendix 1. The NTA-alkyne was synthesized by Dr. A.E. Daugaard. Propargyl alcohol and 4-pentynoic acid were purchased from Sigma-Aldrich.

Post-polymerization CuAAC-reactions on PEDOT-N_3

All reactions were performed in a home-made reaction well system. The wells were defined by circular holes of 5-7 mm in diameter in a 2 mm thick silicone rubber film (Leewood Elastomer, Skogaas, Sweden) which was attached to the substrates via double-sided adhesive tape (ARcare 90106, Adhesive Research, Glen Rock, PA, USA). Holes of 4-6 mm in diameter were punched in the adhesive tape and placed in registry with the holes of the silicone rubber film. This system allowed for the exchange of the well sidewalls in later protein adsorption studies, thereby eliminating the influence of non-specific protein adsorption to the sidewalls. In each reaction well 70-75 µl of reaction solution was added. Unless otherwise noted, 10 mM alkyne reagent, 2 mM $CuSO_4$, and 40 mM sodium ascorbate were used. The reaction time and the DMSO content of the reaction solution were varied. During reaction each well was covered by a piece of poly(ethylene terephthalate) (PET) foil to limit the access of air. After reaction the wells were rinsed in Milli-Q water, re-oxidized and rinsed in Milli-Q water again.

Modification of PS-N_3 with PEG-alkyne

The reactions were conducted as described above for PEDOT-N_3, using varying DMSO content in the reaction solution.

AFM measurements

AFM measurements were performed as described in Chapter 4.

XPS investigations

XPS investigations were performed as described in Chapter 3. Data analyses of the XPS spectra were performed using the Avantage software package supplied by the manufacturer. The elemental composition was obtained and a peak fit of the nitrogen high resolution data was conducted from which the height ratio between the high energy azide peak and the lower energy major peak was obtained. The back side of the PEDOT-N_3 films was made available for analysis by stripping the entire film off its OTS-coated glass substrate after reaction, using a piece of double-sided adhesive tape.

Conductivity measurements

Conductivity measurements were done using a four-point probe (Jandel Engineering, Linsdale, UK) connected to a Keithley 2400 source-meter (Cleveland, OH, USA). Two measurements in perpendicular orientations were performed on each sample. Measurements in water or DMSO were performed by immersing the contact pins of the four-point probe into a droplet of the solvent placed on top of the substrate. Control experiments were conducted on a non-conducting

substrate with Milli-Q water and DMSO droplets, respectively. The control experiments verified that the conductivity of DMSO and of Milli-Q water did not significantly contribute to the values measured on the polymer films.

Protein adsorption studies

PEDOT-N_3 films reacted with PEG-alkyne were tested for their protein adhesiveness. The CuAAC reaction proceeded in a chemically reducing environment, and the samples were subsequently re-oxidized by immersion in ~4% Fe(III)tosylate in 10% 1-butanol/ 90% Milli-Q water for 10 min. The surface was then immersed in DMSO for 10 min and finally rinsed in Milli-Q. Phosphate buffered saline (PBS) (25 µl) was added to each well for 5 min, followed by addition of 25µl of 7.5 µg/ml HRP-Rabbit Anti-Goat IgG (611620 Invitrogen, Camarillo, CA, USA) in PBS solution that was left to adsorb for 15 min. The protein solution was removed and the samples were washed twice with 0.1% Tween-20 in PBS for 5 min. As final procedure step, the samples were washed with Milli-Q water and blown dry in a stream of compressed nitrogen gas. The wells were then removed and replaced with a new set of silicone wells. Quantification of the adsorbed HRP-containing protein was performed by adding 100µl of 3,3',5,5'-tetramethylbenzidine solution (TMB, Sigma Aldrich) to each well and letting the enzymatic reaction run for 4 min on a rocking table. The solutions were then transferred to a 96-well plate and the light absorption at 450 nm was evaluated using a Wallac Victor 1420 plate reader (Perkin Elmer, USA).

Chapter 6

Bio-Active Surface Chemical Gradients on PEDOT-N_3 Substrates

Introduction

In Chapter 5 we showed that our post-polymerization functionalization approach allowed the covalent attachment of alkyne reactants to be directed either to the bulk or to the surface of PEDOT-N_3 thin films, by choosing an appropriate reaction solvent. In this Chapter we show that the post-polymerization functionalization approach also allows lateral confinement of reactants in designated areas of the thin films. Specifically, we demonstrate that functional alkyne reactants can be attached in gradient patterns on PEDOT-N_3 thin films by using electro-click chemistry,[125-127] in a process which we have named "stenciled electro-click chemistry". We demonstrate that the amplitude, width, and steepness of the fabricated gradients can be varied by choosing appropriate reaction parameters, and apply the method to fabricate substrates with gradually changing surface bio-chemistries. Such surface gradients of various molecules, in addition to related solution gradients, are frequently observed in the biological world. They are, for example, of central importance in animal tissue development[128] and are required for guiding cell homing of immune cells in the mammalian immune system.[129]

The working principle for fabricating surface chemical gradients using stenciled electro-click chemistry is shown in Figure 24. A PEDOT-N_3 thin film is kept at a defined spacing from a copper top electrode which is partially covered by an insulator. A DMSO solution containing an alkyne reactant and $CuSO_4$ is injected into the gap. A potential of -0.5 V vs. the copper electrode is then applied to the PEDOT-N_3 film. The applied potential reduces Cu(II) to the catalytically active Cu(I) on the PEDOT-N_3 surface. Where the current density is largest, most Cu(I) will be formed, and most CuAAC click-reactions will take place. For the areas of the PEDOT-N_3 substrate in closest proximity to the top electrode, the total resistance will be lower than for areas further away from the exposed top electrode. Thus, a surface chemical gradient of the alkyne-reactant will be established on the PEDOT-N_3 substrate, following the current density pattern.

Due to the large interest in the study of cellular responses to bio-molecule gradients, a large number of *in vitro* methods have been developed for generating concentration gradients in solution, in gels, or at surfaces to mimic various *in vivo* cell environments. Stable, covalently bound, and well-defined surface gradients in complex patterns are however not easily fabricated by existing procedures. Procedures for making surface gradients have been reviewed e.g. by Genzer and Bhat.[130] A common method for generating surface gradients is through unspecific adsorption of proteins, using diffusion between reservoirs of different concentrations to generate a concentration gradient.[130, 131] Gradients based on Self-Assembled Monolayers (SAMs) on gold using diffusion,[132, 133] gradient based on using controlled ozone exposure,[134] and based on applying an in-plane voltage drop,[135] have likewise been described. The popular diffusion based gradients are generally limited to simple linear gradients and unspecific binding. As an alternative, light-assisted photo-coupling has been demonstrated as a method for generating complex surface gradients.[136, 137] The main advantage of such light controlled gradients is the ability to produce complex structures with high resolution. The drawbacks of this approach are the need for

expensive and advanced equipment, and the requirement for highly special chemicals. With the existing literature in mind, we suggest five main advantages of our stenciled electro-click chemistry approach: I) The principle is based upon the well known CuAAC that offer a high degree of versatility and a high number of available reagents; II) very complex gradients can be established with multiple functionalities, e.g. overlapping gradients of orthogonal ligand chemistry on the same substrate; III) the species are covalently bound to support long term stability; IV) the substrate is conducting and can therefore be combined with electrical analysis tools like impedance spectrometry; V) the conducting polymer substrate can easily be micro-patterned before or after the gradient fabrication as we will demonstrate in Chapter 7 and 8 of this thesis.

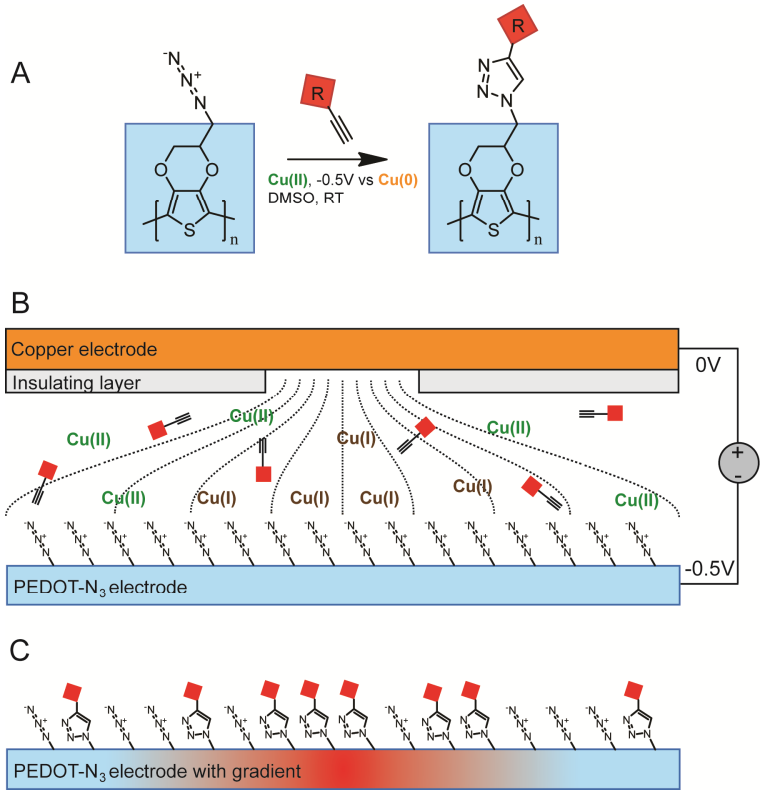

Figure 24 Schematic representation of the stenciled electro-click chemistry process

A: The azide/alkyne click chemistry reaction depends on electrochemically generated Cu(I) from dissolved Cu(II). **B**: A copper counter electrode with a patterned insulating coating forms a "stencil" for the fan-out of electrical field lines to the click reactive PEDOT-N_3 electrode. Applying a negative bias to the PEDOT-N_3 will lead to local generation of Cu(I) in a current dependent manner. **C**: The local current and accordingly the rate of formation of Cu(I) depends on the distance to the exposed copper electrode, resulting in a gradual change in areal density of alkynes clicked onto the azides.

For PEDOT, the difference in macromolecule adsorption onto the oxidized and reduced material,[14, 15, 90] which we discussed in Chapter 1, can serve as an additional route to fabricate surface gradients. Indeed, Gumus *et al.* recently fabricated a gradient of passively adsorbed fibronectin by varying the electric potential along a PEDOT film. The fibronectin was here found to adsorb in larger concentration in the reduced areas, but surprisingly the haptotactic migration of endothelial cells along the substrate was found to be directed towards the oxidized PEDOT rather than towards a higher fibronectin concentration.[89] This illustrates a benefit of our covalent

approach, namely that the covalent attachment allows the substrate to be re-oxidized or uniformly reduced after the attachment of the gradient molecules, thereby generating a homogeneous surface chemical background for the gradient.

In the presented studies, we initially show that the parameters of the setup can be varied to obtain gradients with a multitude of controlled shapes, and discuss the role of the choice of solvent. Subsequently, we show that the functional alkyne molecules introduced in Chapter 2 can be patterned into cell adhesive gradients on a uniform PEDOT-N_3 substrate. These studies also serve as a basis for a discussion of the stability of highly functionalized PEDOT-N_3 films. Finally we show that the procedure is also well-suited for fabricating surface gradients of proteins. These have been made by attaching an alkyne modified nitrilotriacetic acid (NTA) molecule, to specifically capture His-tagged proteins.

Most of the central findings of this Chapter were presented in the paper: "Complex Surface Concentration Gradients by Stenciled "Electro Click Chemistry"" Langmuir, 26, pp. 16171-16177 (2010). This Chapter contains entire continuous sections taken from this paper. The paper was a shared first author paper with Dr. Thomas S. Hansen. A large part of the work in the paper was thus conducted by Dr. Hansen. For completion, results taken from experimental work performed by Dr. Hansen will also be included. Whenever this is the case, it will be noted in the text and in figure captions.

Stenciled surface chemical gradients on PEDOT-N_3 substrates

The shape of the gradient produced by stenciled electro-click chemistry on PEDOT-N_3 substrates is influenced by a number of factors. These include the applied concentrations, the geometry of the setup, the electrical potential, and the reaction time. We examined the importance of each of these factors, as displayed in Figure 25. We applied a fluorine-containing alkyne, 1-ethynyl-3,5-bis(trifluoromethyl)benzene (EBTB), as reactant, see insert in Figure 25A. EBTB contains 6 fluorine atoms per molecule and can therefore be detected with high sensitivity and specificity using XPS. Experiments were performed using varying reaction times, distances to top electrode, electrical potentials, EBTB (alkyne reactant) concentrations, and $CuSO_4$ (catalyst precursor) concentrations. Each of the fabricated gradients was analyzed using XPS line-scans, taking the fluorine content as a direct measure of the reaction degree. *These experiments were performed by Dr. T.S. Hansen*. Figure 25A shows that changing the alkyne reactant concentration mainly affects the maximum surface concentration (amplitude) of the gradient without affecting its width, as long as the reactant concentration is kept ≤1 mM. The alkyne concentration is therefore well-suited for controlling the steepness and height of the gradient. Reaction time and electrode spacing primarily influences the width of the gradient, as can be deduced from Figure 25 B and C. Small electrode separations and short reaction times should consequently be used if one wishes to generate multiple gradients with sub-millimeter separations. In fact, we were able to fabricate

multiple gradient designs in a fast and reproducible manner by adjusting these parameters, as we will describe further below. A more complex influence on the gradient shape, was found when the Cu(II) concentration was varied (Figure 25D). In the lower end of the range investigated, ≤1 mM, small changes in the gradient amplitude were observed. However, for a concentration of Cu(II) of 10 mM, a limiting maximum amplitude appeared to be reached, and a distinctive broadening of the gradient was observed. The relatively small influence of the $CuSO_4$ at low concentrations may arise from Cu(II) ions being generated at the copper counter electrode, thereby making Cu(II) available at a higher concentration than that which was added. The origin of the odd gradient shape at 10 mM $CuSO_4$ might be related to the role of Cu(II) as both a catalyst precursor and the major contributor to the solvent conductivity. To investigate this aspect, we substituted 90% of the $CuSO_4$ with $NiSO_4$ in Figure 25E. The Ni(II) ion has no catalytic effect on the CuAAC reaction, and the maximum available amount of catalyst is thus lowered by a factor of 10, while the solvent conductivity is expected to be similar to that of the 10 mM $CuSO_4$ sample. The shape of the obtained gradient was found to have the same characteristic broadening as was found for 10 mM $CuSO_4$, suggesting that the broadening is caused by increasing the conductivity of the solvent. The effect of varying the applied potentials was also investigated. When no potential difference was applied, no reaction was observed, while more negative potentials lead to a slight overall broadening of the gradient profiles, see Figure 25F. In summary, our studies on EBTB illustrate that a wide range of gradients can be fabricated using stenciled electro chemistry.

To support the experimental findings of which parameters are well suited for changing the gradient appearance, numerical simulations were conducted. These simulations could indeed reproduce the trends observed in the experiments with EBTB. The simulations were performed entirely by *Dr. T.S. Hansen* and will not be presented here.

All electro-clicked gradients were fabricated in DMSO solutions containing minute amounts of water. DMF was also an applicable solvent,[126] but electro-click reactions in pure water, applying various hydrophilic alkyne reactants, were not successful. As we demonstrated in Chapter 4, the conductivity of the PEDOT-N_3 does not change in water compared to in DMSO. We therefore suggest that the failure to perform electro-click reactions in water is most likely caused by the differences between the electrochemistry of copper in water and DMSO. As mentioned earlier, due to a better solvation, the Cu(I) ion has higher stability in DMSO than in water.[122] This influences the electrochemical properties significantly. The electrochemical reduction of Cu(II) to Cu(0) takes places in two steps: Cu(II) is reduced to Cu(I), and Cu(I) is reduced to Cu(0).[138-140] The stability of Cu(I) in DMSO allows the electrochemical reduction of Cu(II) to take place in two well separated steps.[138, 141, 142] Thus solubilized catalytic Cu(I) will be formed in significant amounts. In water however, Cu(I) is less stable and consequently the second reduction step is fast, allowing only transient presence of Cu(I).[138, 140, 142]

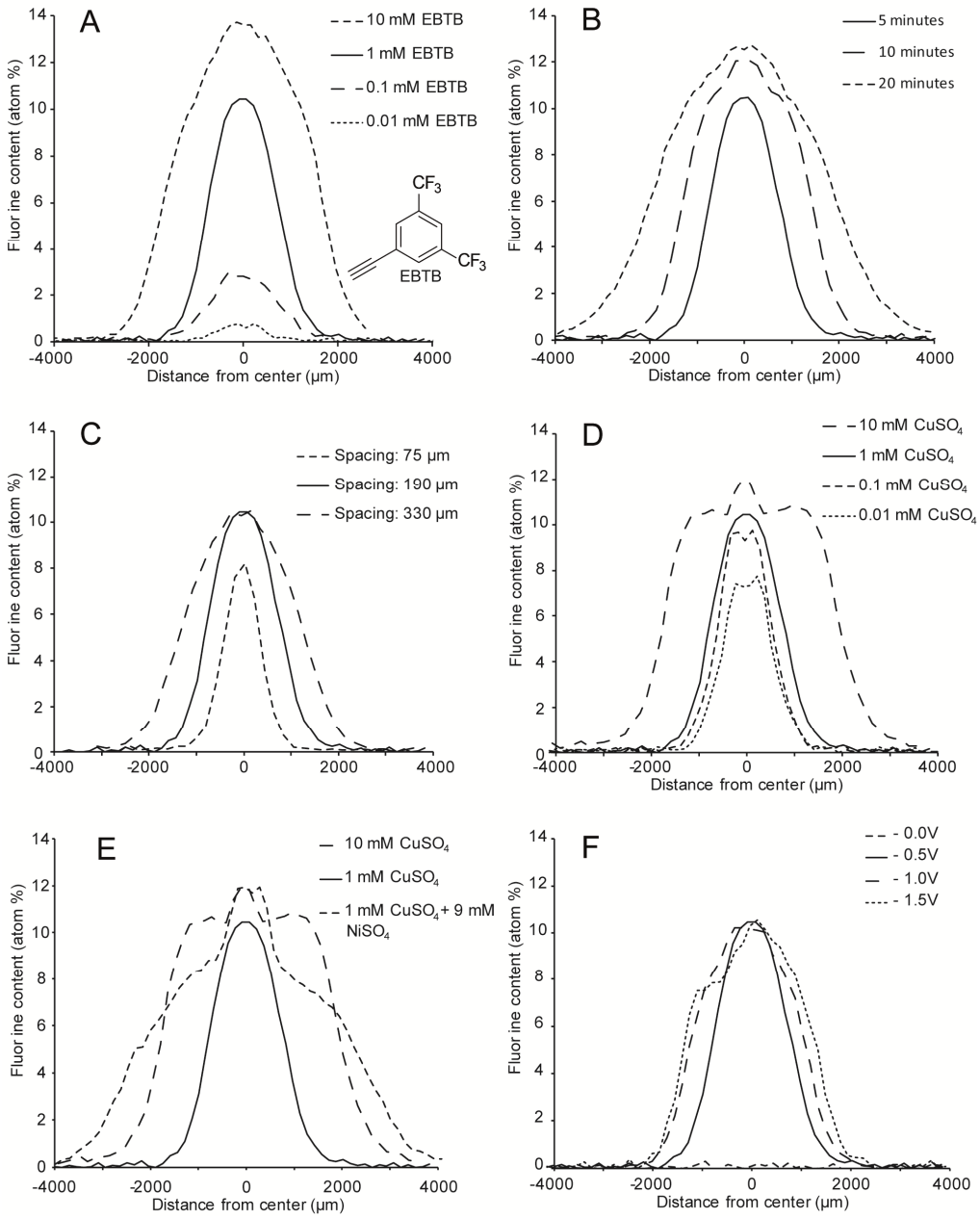

Figure 25 Electro-clicked gradients of EBTB on PEDOT-N_3 made using varying reaction parameters

EBTB (insert in A) was electro-clicked onto PEDOT-N_3 substrates using varying parameters. Reaction conditions except for the varied parameter were 1 mM EBTB, 1 mM $CuSO_4$, a potential of -0.5 V on the PEDOT-N_3 electrode, a reaction time of 5 min, and a distance to the top electrode of 190 µm. The gradients were analyzed using XPS-line scans, taking the fluorine content as a direct measure for the reaction degree. **A:** Changing the EBTB concentration has a high impact on the amplitude of the gradient and, for the highest concentration used, also on the width. **B:** Reaction time mainly affects the width of the gradient **C:** The distance to the top electrode also affects the width of the gradient. **D:** The $CuSO_4$ concentration has little overall influence except for the highest concentration employed. **E:** A solution containing 9 mM of the catalytically inert $NiSO_4$ was used to test the influence on electrolyte conductivity on the gradient profile. The profile of the 1 mM $CuSO_4$ + 9 mM $NiSO_4$ was comparable to 10 mM $CuSO_4$ profile, indicating that the shape of the 10 mM $CuSO_4$ is most likely linked to the conductivity of the electrolyte. **F:** Increasing the potential from -0.5 V to -1.5 V leads to a small widening of the gradient. If no potential is applied, no reaction is observed. *Experiments in this figure were made by Dr. T.S .Hansen*

For water/DMSO mixed solutions it has thus been reported that increasing the amount of DMSO leads to an increased formation of Cu(I) during the reduction of Cu(II). A similar behaviour was reported for DMF/water mixtures,[139] in agreement with our finding that the electro-click reactions also run well in DMF. Other effects than the electrochemical behavior of copper, might however also play a role. The significant swelling of PEDOT-N_3 in DMSO, outlined in Chapter 4 - 5, may increase the reaction kinetics of the surface functionalization due to a larger accesibility of the reactive azide groups.

Considering the choice of solvent for the reaction, it is also worth noting that along with the fabrication of a surface gradient, a vertical gradient is most probably also established. As the reaction takes place in DMSO, the PEDOT-N_3 will be in a significantly swelled state, and therefore bulk reaction likely occur as seen in Chapter 5. In our original report of the stenciled electro-click chemistry,[127] displayed in Appendix 3, we did not consider this aspect, as we only later became aware of the swelling properties of PEDOT-N_3 in DMSO.

Stenciled cell-adhesive surface chemical gradients on PEDOT-N_3 substrates

Stenciled electro-click chemistry was used to form biologically active gradients of the functional alkyne reactants introduced in Chapter 2. An alkyne-PEG-GRGDS gradient was initially established on the PEDOT-N_3 substrate using stenciled electro-click chemistry, and the remaining azide functional groups were subsequently coupled to PEG-alkyne in a regular CuAAC click reaction step. As the alkyne-PEG-GRGDS contains an iodine-marked phenylalanine residue, the concentration of the peptides on the surface could be followed via the iodine signal in XPS, see Figure 26A. We investigated the adhesion of 3T3 fibroblasts on such GRGDS gradient-modified PEDOT-N_3 substrates. Similar to in Figure 3 and Figure 4 in Chapter 2, the 3T3 fibroblast cells were allowed to adhere to the surface and un-attached cells were washed off the substrate after 1 h of incubation. Figure 26C displays a mosaic of phase contrast images of the central channel parts, with the remaining cells appearing bright. As outlined in Chapter 3, the surface concentration of peptide can be estimated from the iodine signal, and presented in a number of manners. In our original paper,[127] displayed in Appendix 3, the density of peptides was represented by the percentage of the total reactant signal in the XPS which arose from the peptides. Here, a slightly different representation is used, namely the percentage of peptides of the total number of reactants on the surface, see Figure 26B. When comparing these values to the number density of the cells on the surface, we observed a clear correlation of GRGDS density and the ability of the cells to adhere to the surface. This is in great correlation with the studies on cell attachment to uniform mixed-reactant surfaces that was presented in Chapter 2, Figure 4. For the areas where ≥10% of the reactants attached to the surface are peptides, the number of attached cells appears to

vary within the same range, whereas markedly lower cellular adhesion is seen for areas with below 5% peptide.

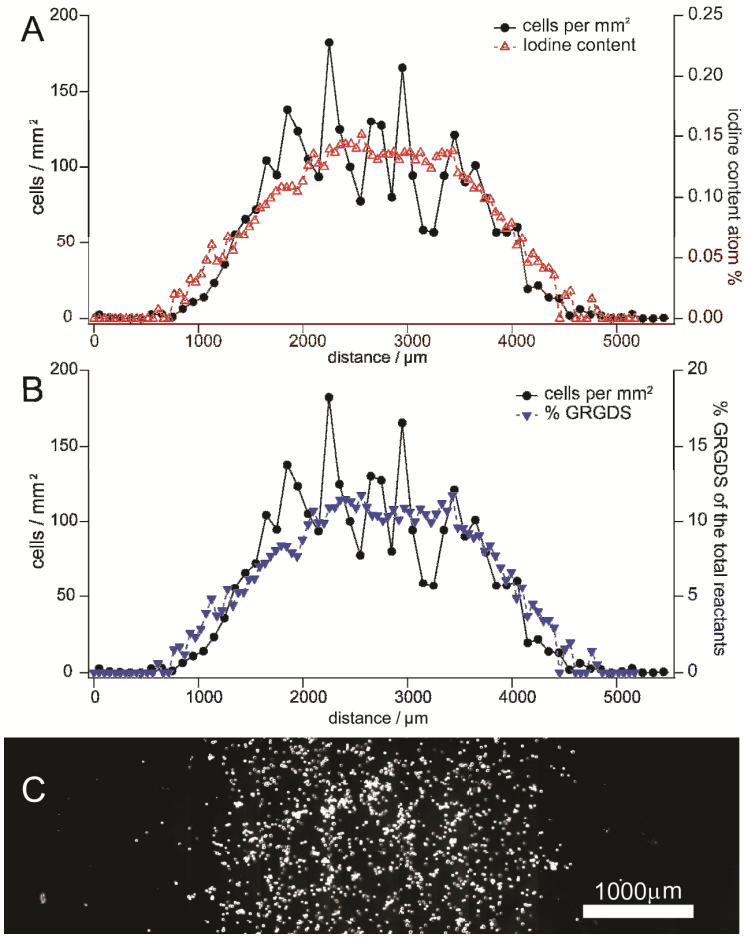

Figure 26 Cell adhesion to a PEDOT-N_3 substrate functionalized with a RGD gradient on a PEG background
A Surface gradient of alkyne-PEG-GRGDS was made on a PEDOT-N_3 substrate and the remaining azide groups were functionalized with PEG-alkyne. Subsequently, adhesion of 3T3 fibroblast was tested. The cells were allowed to adhere for 1 h and non-adhered cells were washed off at a surface shear stress of 0.1 Pa. **A**: Iodine XPS signal compared to the adhered cell density observed in a flow chamber experiment on this surface. **B:** Comparison of the percent of the surface reactants being alkyne-PEG-GRGDS, calculated from XPS investigation of the substrate, to the adherent cell density observed in a flow chamber experiment on this surface. The scaling between the iodine signal and the calculated percentage alkyne-PEG-GRGDS of reactants on the surface is not linear, as variations in the sulfur signal are also taken into account in the calculation. **C:** Mosaic of phase contrast microscopy images of 3T3 fibroblast cells adhered to the alkyne-PEG-GRGDS gradient.

The alkyne-PEG-GRGDS gradients on the PEG-background were fabricated by sequential click-reactions, where the second PEG-alkyne click reaction was performed similar to those used in Chapter 2 and 3. When examining alkyne-PEG-GRGDS gradients fabricated using stenciled electro-click chemistry in XPS, we discovered that a large amount of the peptide attached in the electro-click reaction, appeared to be removed during the second reaction with PEG-alkyne. This was observed as a significant lowering of the iodine signal of the fabricated gradients.

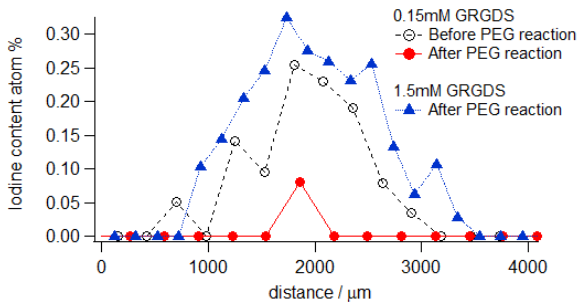

Figure 27 Removal of an electro-clicked alkyne-PEG-GRGDS gradient during subsequent PEG-alkyne reaction
A surface gradient of alkyne-PEG-GRGDS on PEDOT-N_3 was almost completely removed when the sample was subsequently reacted with PEG-alkyne, taking the iodine signal in XPS as a direct measure for the amount of alkyne-PEG-GRGDS on the substrate. By increasing the concentration of the alkyne-PEG-GRGDS reactant in the electro-click reaction from 0.15 mM to 1.5 mM, a notable iodine gradient can be seen on the surface even after the PEG reaction.

Furthermore, for gradients with a low initial amount of peptide, an almost complete removal of the iodine signal could be observed, as displayed in Figure 27. As could be expected from the EBTB studies, increasing the amount of alkyne reactant increased the amplitude of the GRGDS gradients, and we found that when doing so, a clear iodine gradient could be observed even after the PEG reaction, see Figure 27. The removal of the alkyne-PEG-GRGDS molecules during the PEG-alkyne reaction appears to be caused by a number of different factors. In Chapter 3 we noted that some unspecific adsorption of the peptides occurs for the standard CuAAC click-reaction with alkyne-PEG-GRGDS. However, washing the samples in DMF as described in Chapter 3 did not lead to any removal of the peptides. Unspecific adsorption onto the surfaces is therefore not a likely explanation for the removal of the peptides during the second reaction with PEG-alkyne. In Chapter 5, we observed that performing CuAAC-reactions with PEG-alkyne in high DMSO contents over extended time, could lead to extremely high degrees of functionalization of the PEDOT-N_3 films, causing the films to become unstable and to disintegrate. Similarly, we propose that some areas of the outermost parts of the films which have a very high degree of functionalization with alkyne-PEG-GRGDS after the electro-click reaction can become unstable during the second reaction with PEG-alkyne.

The mechanism for such a removal of parts of the PEDOT-N_3 film is not obvious. One proposal could be that the outermost part of the films is continuously removed during the PEG-reaction. This could explain why an alkyne-PEG-GRGDS gradient with larger initial amplitude is not removed entirely during the PEG-alkyne reaction, whereas those with lower amplitude were removed. To test this hypothesis we investigated the removal of the peptides during the PEG-alkyne reaction, at varying reaction times. In these studies we only saw minor differences between 15 min and 20 h reaction time, see Figure 28. The GRGDS was clearly being removed more rapidly during the first 15 min. Also, we did not see any thinning of the PEDOT-N_3 films. Overall, we therefore do not find it likely that the PEDOT-N_3 film is stripped continuously during the PEG-alkyne reaction time. As an alternative to a continuous removal, one might propose that the electro-click reaction inherently make the film less stable. However, this suggestion does not fit well with the observation that gradients with large amplitudes appear to have a larger resistance

than gradients with smaller amplitudes. One could also propose that the outermost film is inherently less stable, possibly due to shorter PEDOT-N_3 chain lengths being made during the *in situ* polymerization. We did not investigate this hypothesis.

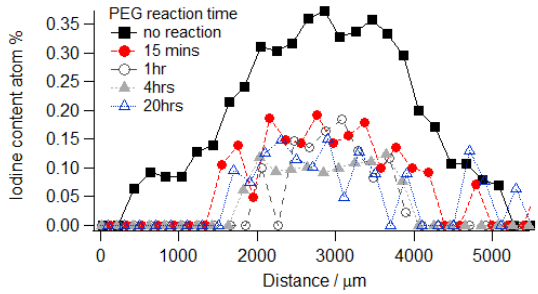

Figure 28 Time dependence of the removal of alkyne-PEG-GRGDS gradients during PEG-alkyne reaction
Surface gradients of alkyne-PEG-GRGDS on PEDOT-N_3 appears mainly to be diminished during the first part of a subsequent reaction with PEG-alkyne, taking the iodine signal in XPS as a direct measure for the amount of alkyne-PEG-GRGDS on the surface.

It is worth noting that since the PEG-alkyne CuAAC takes place in a reducing environment, the p-doping of the film is lost during the reaction. Although this doping can easily be re-established, as described in Chapter 3, the loss of the doping during the reaction might make the functionalized PEDOT-N_3 films less stable. In the doped state internal coulomb attractions are found within the films between the holes in the PEDOT-N_3 backbone and associated tosylate anions, whereas during the CuAAC reaction these attractions are lost. Figure 29 shows the effect of exposing an alkyne-PEG-GRGDS gradient sample to the reducing environment used for the click-reaction with PEG-alkyne, but without the reactant being present. It can be seen that a significant part of the gradient was removed even without the PEG present. Although we did not observe any complete removal of small amplitude GRGDS-PEG-alkyne gradients when these were not exposed to PEG-alkyne, the prolonged reduction of the film clearly plays a significant role in the removal of the alkyne-PEG-GRGDS from the samples. This is somewhat surprising as the film is also reduced during the electro-click reaction.

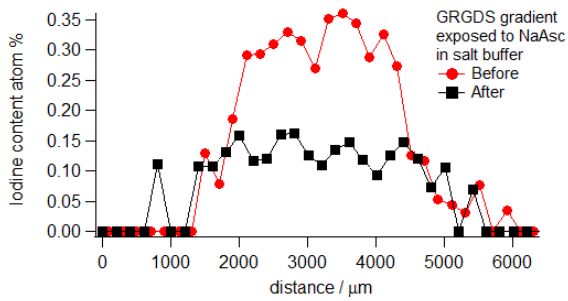

Figure 29 Removal of alkyne-PEG-GRGDS gradient by prolonged exposure to reducing conditions.
A surface gradient of alkyne-PEG-GRGDS on PEDOT-N_3 was exposed to the reducing reaction conditions used for PEG-alkyne CuAAC reactions for 6 h, but without adding any PEG-alkyne. The gradient is diminished notably when exposed to these conditions. The iodine signal in XPS was used as a direct measure for the amount of alkyne-PEG-GRGDS on the sample.

So far, we have mainly considered scenarios where the alkyne-PEG-GRGDS functionalized PEDOT-N_3 film is partially removed during the second CuAAC reaction. However, many other mechanisms for the observed drop in alkyne-PEG-GRDGS XPS signal can be put forward. One proposal could be that a part of the alkyne molecules are trapped in the top part of the PEDOT-N_3 film during the electro-click reaction, and that the reduced state conditions found in the second CuAAC reaction allow these to be washed out. As most of the potential mechanisms remain highly speculative, we will end the discussion by noting that, from a practical standpoint, fabricating gradients with larger amplitudes during the first electro-click reaction step, served as a viable solution for making functional alkyne-PEG-GRGDS gradients on a PEG-alkyne functionalized PEDOT-N_3 background.

As will be presented in Chapter 8, we also applied electro-click reactions for functionalizing PEDOT-N_3 microelectrodes. Here we observed a similar instability of alkyne-PEG-GRGDS functionalized PEDOT-N_3 electrodes when performing a second CuAAC reaction in reducing environments. Also here the practical problem could be solved by achieving a higher degree of functionalization in the first reaction step. As a side-note, the introduction of additional functional polymeric substrate did not allow the electro-click reaction in Chapter 8 to be performed in pure DMSO, and 10 vol% water was therefore added to the electro-click reaction solutions. Electro-click reaction in pure water was however still not found to be applicable.

Protein surface gradients on PEDOT-N_3 substrates

The stenciled electro-click approach can also be used for fabricating surface chemical gradients of larger bio-active molecules than the alkyne-PEG-GRGDS. We fabricated gradients of His-tagged proteins, through a two-step process. In the first step, a gradient of prop-2-ynyl 5-(N,N-bis(carboxymethyl)amino)-5-(S)carboxypentanecarbamate (NTA-alkyne) was made. The NTA motif is well known for capturing His-tagged proteins via chelated Ni(II), a method that is highly popular for proteins purification,[143-145] and for targeting proteins onto surfaces.[145] In the second step a His-tagged protein is captured onto NTA functionalized parts of the film. As the His-tag is widely used for purification of proteins, a large number of proteins that incorporate this motif are commercially available. This expands the applicability of our approach significantly. Figure 30 illustrates an example of the approach. *The experiment was performed by Dr. T.S. Hansen.* Figure 30A displays a schematic illustration of a 2D array of 100 µm diameter holes fabricated in an insulating layer on the copper counter electrode. Such a stencil was employed to fabricate NTA-alkyne gradients on the PEDOT-N_3 surface. The gradient surface was then immersed in a Ni(II) containing solution, before finally being exposed to a solution containing His-tagged enhanced green fluorescent protein (eGFP). The resulting gradients of His-tagged eGFP could be visualized by fluorescence microscopy, see Figure 30B. The individual gradients emerge radially, and aligned with the stencil openings. For the fabrication of these gradients, an electrode spacing of only 25 µm and a reaction time of 2 min were used. These values were applied to limit the lateral extent of

each separate gradient, in accordance with the results found when using EBTB as alkyne reactant in Figure 25. As can be observed, the 2D protein gradients were successfully formed, illustrating how the geometry can be adjusted by simply changing the accessibility of the solution to the top electrode. The successful fabrication of protein gradients make the method highly interesting as protein gradients are of significant biological interest. One example is that this enables the fabrication of chemokine gradients. Chemokines are proteins responsible for guiding cell homing to the different compartments of the body, through increasing and decreasing concentrations. The ability to mimic such patterns is a valuable tool, e.g. for evaluating the ability of cultured dendritic cells of the adaptive immune defense to home to the lymph nodes.[129, 146] This is an important issue for allowing dendritic cell based cancer immunotherapy.[147, 148]

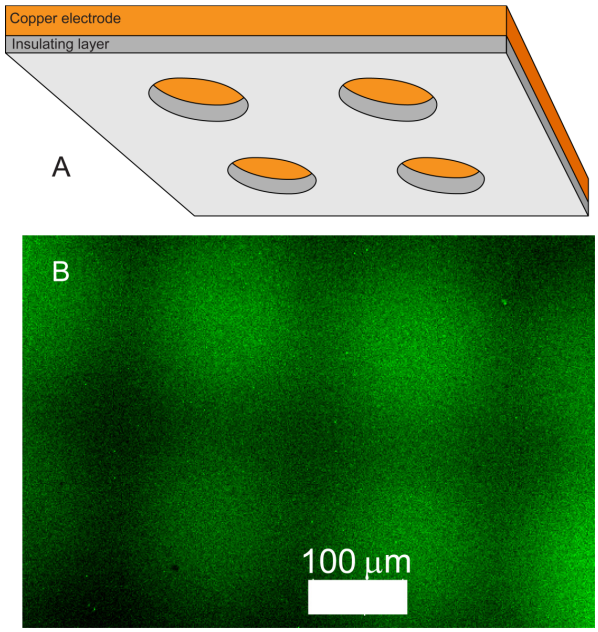

Figure 30 Circular 2D gradients of fluorescent protein on PEDOT-N_3 substrates

A: Schematic of a stenciled copper counter electrode designed to establish separate microscopic surface gradients in a regular 2D array. The hole diameters are 100 µm, and the holes are placed in a square grid with a center-to-center distance of 200 µm. **B:** Fluorescence microscopy image of 2D gradients of NTA-alkyne formed on a PEDOT-N_3 surface, visualized by subsequent capture of His-tagged eGFP. *The experiment presented in this figure was performed by Dr. T.S. Hansen*

Conclusion

We have demonstrated a method for fast production of gradients on an electrically conductive surface using stenciled electro-click chemistry. The method can be used to make linear and complex 2D gradients of covalently bound molecules. The characteristics of the gradient fabrication technique have been examined using XPS, and these studies confirm that a wealth of gradient patterns can be formed by varying simple parameters of the setup. Surface gradients of cell-binding or selective protein-binding moieties have been formed without adversely affecting their targeted interactions with biological entities. The method is well-suited for making fast, reproducible and complex gradients for investigations and manipulations of biological systems. These studies exemplify that our approach of using CuAAC-based post-polymerization modifications of PEDOT-N_3 is highly relevant for fabricating advanced surface biochemistries of conducting polymers. We further suggest that the method is not only of interest to biological research and cell handling systems based on conducting polymers: The generality of the electro-click reaction should make it applicable to any conducting substrate presenting click-reactive moeities, e.g. azidated or alkynated self-assembled monolayers.

Experimental

Cyclic Olefin Copolymer supports
PEDOT-N_3 Samples on COC supports
Samples were prepared as described in Chapter 2.

Syntheses of the alkyne reactants
Syntheses are described in Appendix 1

Alkyne-PEG-GRGDS and EBTB gradient samples fabrication.
A copper plate was partially covered with a transfer adhesive (ARcare 90106, Adhesive Research, Glen Rock, PA, USA) in which a 0.5 mm slit was cut using a CO_2 laser (48-5S carbon dioxide laser, Synrad inc. USA) to form the pattern stencil. The copper electrode was placed above a PEDOT-N_3 film using a 380 µm thick spacer, see Figure 31. The functionalization was done using a DMSO solution of 1 mM alkyne-PEG-GRGDS and 1 mM $CuSO_4$, and application of a potential of -0.5 V on the PEDOT-N_3 vs. the copper electrode for 5 min. The PEDOT-N_3 samples were then treated with a 50 mM NaCl aqueous solution containing 20 mM PEG-alkyne, 0.67 mM $CuSO_4$ and 27 mM sodium ascorbate. Reaction time was 6 h unless otherwise noted. The EBTB (1-ethynyl-3,5-bis (trifluoromethyl)benzene, Figure 25A insert) gradients were fabricated by an equivalent procedure, only replacing the alkyne-PEG-GRGDS with EBTB and varying the reaction parameters. For the alkyne-PEG-GRGDS gradients in Figure 27, a slightly different electro-click

procedure was used, instead of DMSO, DMF was used as solvent, -0.3 V was applied for 5 min, and 0.1 mM $CuSO_4$ was used. 0.15 mM and 1.5 mM alkyne-PEG-GRGDS was used. All samples functionalized with alkyne-PEG-GRGDS were rinsed in DMF and re-oxidized as described in Chapter 2 and 3, prior to the second click-reaction with PEG, or investigation in XPS.

Flow chamber 3T3 fibroblast adhesion studies.

The cellular adhesion studies were overall conducted as described in Chapter 2. A homemade flow chamber with rectangular channel dimensions of 0.140 mm x 5 mm x 32 mm (*h*, *w*, *l*) was used. The chamber is assembled by connecting two homemade COC substrates, one containing the gradient and the other defining inlets and outlets, with a strip of transfer adhesive. The adhesive was cut using a CO_2-laser to define the lateral geometry of the channel. The thickness of the adhesive defined the height of the channel. The flow experiments were conducted in HBSS buffer (Lonza) containing Mg(II) and Ca(II) to permit integrin binding to RGD. 250 µl of a 5 mio cells / mL suspension of 3T3 fibroblasts was injected into the flow chamber. The cells were allowed to adhere for 1 h. The flow rate was gradually increased to a flow corresponding to a surface shear stress of 0.1 Pa for 2 min.

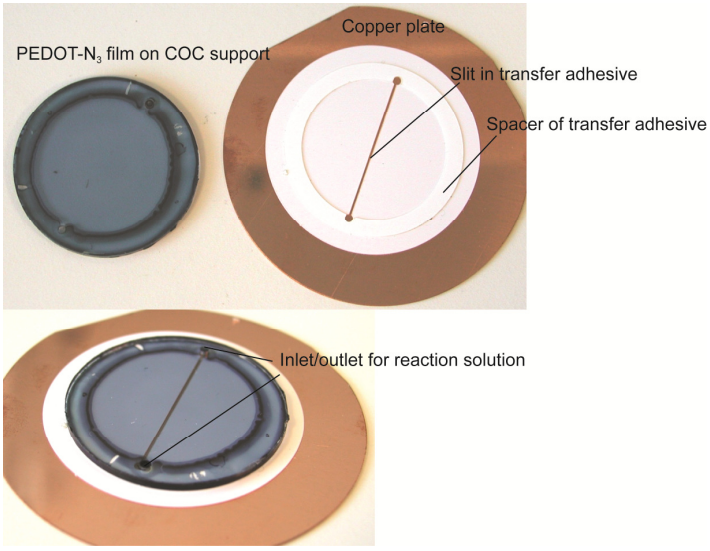

Figure 31 Setup used for fabricating EBTB and alkyne-PEG-GRGDS gradients

Top: The PEDOT-N_3 coated TOPAS disc (left) and the copper plate with transfer adhesive (right). A slit has been cut in the transfer adhesive using a CO_2-laser. The rim is also made of transfer adhesive and is used for defining the spacing between the PEDOT-N_3 surface and the copper electrode. Bottom: The assembled setup without clamps and connectors. The TOPAS disc has two holes for inlet and outlet of the alkyne reactant / $CuSO_4$ solution. *Photography and device design was conducted by Dr. T.S .Hansen*

NTA / eGFP gradient fabrication.

A micro-patterned stencil was produced by photolithography and subsequent reactive ion etching in a thin film of COC deposited on an evaporated copper electrode: A 4 inch silicon wafer was coated by 500 nm copper using electron beam evaporation, before spin coating with COC mr-I T85 (Micro Resist Technology, Berlin, Germany) at 3000 rpm for 30 s to yield a 4.5 µm thick layer, as measured with an Ambios XP-2 (Ambios Technology, Inc., Santa Cruz, US) profilometer using a stylus force of 1 mg. After baking at 80°C for 10 min a layer of ma-P 1275 (Micro Resist Technology, Berlin, Germany) was spin coated on top at 3000 rpm for 30 s, and the sample was re-baked at 80°C for 10 min. The photoresist was exposed through a chrome mask in a Karl Süss MA4 mask aligner (Munich, Germany) with a dose of 400 mJ/cm2. The photo resist was developed using ma D 331 (Micro Resist Technology, Berlin, Germany) for 60 s. The wafer was then etched in a Reactive Ion Etcher (Plasmatherm 740, Unaxis, St Petersburg, FL) for 15 min at 300 W and 7 Pa O2. Finally the remaining photoresist was removed by washing in acetone, isopropanol, ethanol, and Milli-Q water. The PEDOT-N_3 surface was functionalized using a spacer thickness of 25 µm and a reaction time of only 2 min to produce steep gradients. A solution of 1 mM CuSO4 and 1 mM NTA-alkyne was used. After functionalization the sample was re-oxidised in ~4 wt% Fe(III)tosylate in 90:10 water:butanol and placed in 50 mM EDTA/ 50 mM Tetramethylbenzidine (TRIS) buffer pH 7.5 for 30 min. The sample was then immersed in 100 mM $NiSO_4$ for 30 min, washed with a solution of 150 mM NaCl and 10 mM TRIS pH 7.5, and blocked with a block buffer containing 150 mM NaCl, 10 mM TRIS pH 7.5 and 2 wt% bovine serum albumin (BSA). Reaction with 5 µM His-tagged eGFP (enhanced Green Fluorescent Protein, Cell Sciences, Canton, MA, USA) in 150 mM NaCl and 10 mM TRIS occurred over night at 4°C. The sample was finally thoroughly washed with 1 M NaCl and 0.1 wt% Tween-20 in Milli-Q water.

X-ray Photoelectron Spectroscopy (XPS) studies.

XPS investigations were overall performed as described in Chapter 3. Line-scan studies were performed using step sizes from 40 µm to 100 µm and employing an x-ray spot size equal to the step size. Spectra of the relevant elements were collected at each spot using data collection times varying from 10 to 80 s per spectrum depending on the element being sampled.

Chapter 7

PEDOT Microelectrodes Fabricated through Printed Dissolution

Introduction

In this Chapter, we will turn focus from controlling the surface chemical properties of PEDOT-ype polymers to how such polymers can be processed and combined with other functional material to fabricate multifunctional microsystems. Here, we introduce a versatile procedure: "*printed dissolution*" for patterning PEDOT thin films into micro-electrodes. The central benefit of the procedure is that it locally removes the conducting polymer from a given substrate, and re-exposes the surface chemistry of the underlying substrate in an unperturbed form. Chemical functional groups such as azide and alkyne have been found to be resistant to the conditions applied in the patterning. These functionalities have accordingly been found to be re-exposed upon patterning, allowing direct covalent functionalization of the gaps between the microelectrodes. Currently, when conducting polymers are patterned, for example for uses in microsystems, photolithography and other clean room processes are typically used.[149, 150] In addition to being an in-expensive alternative, the ability to preserve an underlying surface chemistry separates our method, printed dissolution, further from standard lithographic processes such as reactive ion etching (RIE), in which any predefined specific organic chemistry below a film being patterned will typically be removed. The conjugated backbone of PEDOT in which the oxidation takes place, is a universal feature in conducting polymers. Correspondingly, over-oxidation of this backbone has been used in numerous other patterning/local deactivation schemes for a variety of conducting polymers.[149-152] Our printed dissolution concept is in essence based on exploiting that the over-oxidation changes the solubility parameters of the polymer. We therefore find it likely that a similar scheme could be applied for locally removing other conducting polymers and other PEDOT type polymers than those tested here.

The central concept of the *printed dissolution* patterning is displayed Figure 32. A PEDOT-type thin film is physically contacted with a micro-structured agarose stamp containing the oxidizing agent sodium hypochlorite (NaOCl), Figure 32A. In earlier reported work in our group, it was found that such stamping can be used for locally removing the conductivity of the PEDOT, as the over-oxidization breaks the conjugated system of the PEDOT backbone, thereby removing the conductance.[110] When doing so, a stable film of over-oxidized PEDOT is left in the gaps between the electrodes, as illustrated in Figure 32B. However, we here show that by applying a non-ionic detergent either directly in the agarose stamp, or in a subsequent washing step, this leftover over-oxidized PEDOT can be removed from the supporting substrate, exposing it for potential subsequent functionalization, Figure 32C. In this Chapter we initially show how PEDOT and thin films can be locally removed from polymeric and non-polymeric supports, and discuss the limitations to the printed dissolution technique. We then show how re-exposed azide-modified substrates can be directly modified using CuAAC after the patterning. Finally we compare the printed dissolution of PEDOT and PEDOT-N_3 on various substrates, to clarify the reasoning behind the methodology, and to expose strength and weaknesses of the printed dissolution method. In Chapter 8 we will show how the technique can be combined with surface chemical

modifications of the conducting polymer electrodes, to fabricate multifunctional all polymeric microsystems. In Chapter 8 we will further discuss the advantages of the printed dissolution technique, compared to other micro-patterning procedures. The central findings of this Chapter are presented in the newly submitted manuscript: "Facile micropatterning of functional conductive polymers with multiple surface chemistries in register" and the following Chapter contains entire continuous sections taken from this manuscript.

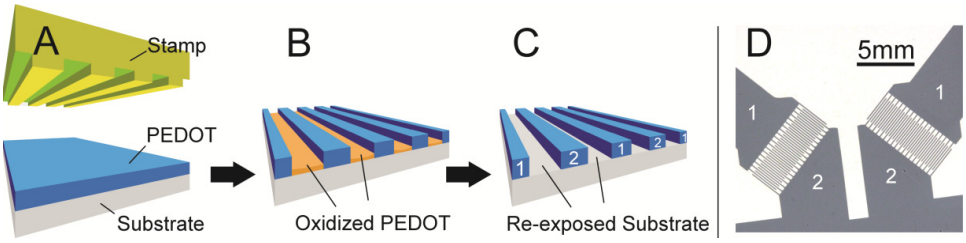

Figure 32 Principle of PEDOT micro-removal by printed dissolution using an agarose stamp.
A: An agarose hydrogel stamp with a predefined microstructure, soaked in a solution containing NaOCl, is brought into contact with a PEDOT thin film. **B**: After the stamping, over-oxidized and non-conducting PEDOT is found in the contacted areas. **C**: The over-oxidized PEDOT can be removed from the substrate by washing the sample in a solution containing Triton X-100, or by adding Triton X-100 directly to the NaOCl solution used for soaking the stamp. See experimental section for details. **D**: Optical micrograph of a PEDOT thin film on a COC substrate patterned into two sets of inter-digitated 100 µm wide electrodes, using this technique. (Inserted numbers 1 and 2 mark independent electrodes). One agarose stamp can be used multiple times, and can define circuits on areas of several cm^2.

Printed dissolution can locally re-expose unperturbed substrate chemistry on a micrometer scale

When PEDOT films are exposed to an agarose stamp soaked in an aqueous solution containing the oxidizing agent NaOCl, a stable, transparent and non-conducting material is formed. This can be used for making micrometer sized patterns of PEDOT and non-conductive PEDOT.[110] We found that by adding a non-ionic detergent to the stamp, or to a subsequent washing step, the over-oxidized material can be dissolved, thereby exposing the underlying substrate. This is shown for PEDOT on COC substrates in Figure 33. In these studies, PEDOT films were stamped with a flat agarose stamp, and the effect of applying the detergent Triton-X100 was examined using XPS and contact angle measurements. PEDOT substrates stamped with no detergent were found to be hydrophilic, to contain significant amounts of oxygen and sulfur. These substrates were homogeneous indicating the presence of a coherent film. When detergent was introduced either in the stamp and/or in a subsequent wash, the stamped films became dissolvable and could be washed off, exposing the underlying COC. The surface chemical characteristics of the samples exposed to detergent, accordingly resembled those of homogeneous COC, and not PEDOT or over-oxidized PEDOT.

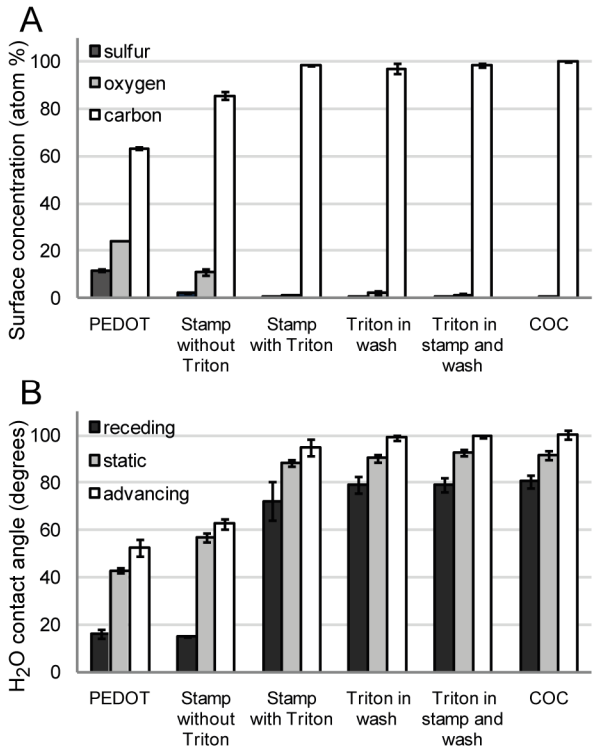

Figure 33 PEDOT removed from COC by printed dissolution

PEDOT thin films on COC substrates were stamped with flat unstructured agarose stamps, and the effect of applying Triton-X100 detergent investigated. **A**: Elemental composition obtained from XPS **B**: Contact angle measurements. Both techniques indicate that applying Triton-X100 detergent in the agarose stamp and/or in a subsequent wash leads to the re-exposure of the underlying COC substrate. See experimental section for details.

The printed dissolution method was also found to be well-suited for removing PEDOT locally by using a micro structured agarose stamp, as illustrated in Figure 34 and Figure 35. Here a PEDOT thin film was patterned into two sets of 100 µm wide and 0.5 cm long electrodes with 100 µm spacing on a COC substrate; see Figure 34. In Figure 35 a XPS line-scan was conducted across the electrodes, where the atomic content of a 40 µm spot was evaluated every 30 µm. When comparing the atomic composition in the middle of each electrode in Figure 35 with that found for the continuous PEDOT film shown in Figure 33, the compositions can be observed to be equivalent, indicating that the PEDOT electrodes are not influenced by the stamping. Correspondingly, the atomic composition measured in the points between the electrodes matches that of pure COC, as observed for the macroscopic stamped areas in Figure 33. Thus, the printed dissolution can be used for removing PEDOT, also on a micrometer scale. A 100 µm electrode pattern similar to that used in Figure 35 was used for all the electrode experiments presented in this Chapter and Chapter 8. This electrode width was chosen as it is well-suited for evaluation using XPS line-scans, which for the applied instruments is limited to a spot size of 40 µm.

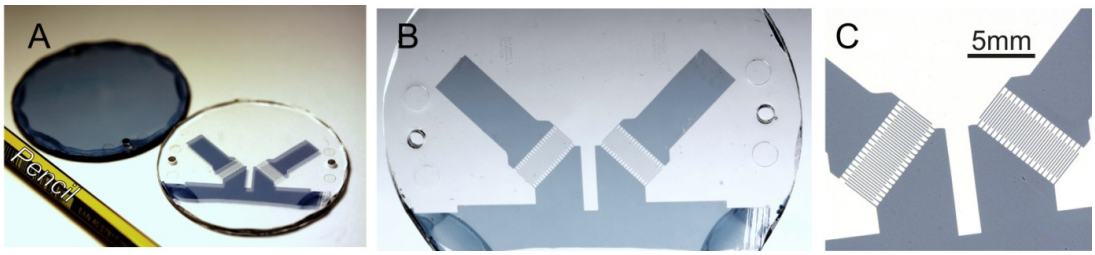

Figure 34 PEDOT thin films on COC substrates patterned by printed dissolution

A PEDOT film on a COC substrate patterned by stamping with an agarose stamp soaked in a solution of 1.5 wt% NaOCl and 0.1 vol% Triton-X100 for 4 min, followed by washing. Pictures **A**-**C** taken at increasing magnification. A pencil is included as scale. See experimental section for details

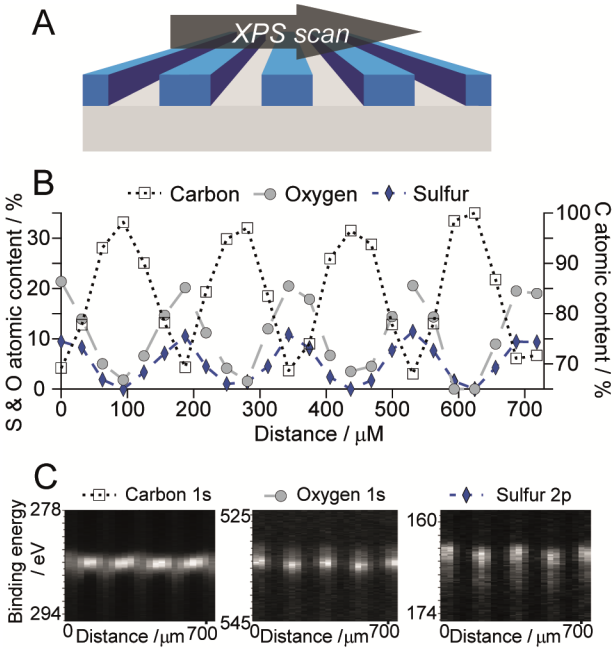

Figure 35 100 µm wide electrodes PEDOT spaced by 100 µm COC investigated by XPS

A PEDOT thin film on a COC substrate was patterned using the printed dissolution procedure. See experimental section for details on sample preparation. **A**: Sketch of XPS line-scan across five electrodes. Note well that the sketch is not drawn to scale as the film thickness is only ~150 nm and the electrodes are 100 µm wide **B**: Experimentally observed localized atomic composition obtained from XPS line-scan C: Raw XPS line-scan data.

Yet, it is important to point out that significantly smaller structures can be made using agarose stamp PEDOT patterning. Indeed, as small as 2µm structures were made using the similar concept without detergent.[110] These studies indicated that to reliably achieve very small features, it can necessary to use shorter stamping times and lower NaOCl concentrations than those applied here, as lateral diffusion of the oxidant can otherwise limit the size of the obtained features.[110] Studies of the consequence of lowering the stamping time and NaOCl concentration are presented in Table 9.

Experimental				Contact Angles					
				No washing			With washing		
Substrate	film	% NaOCl in stamp	Stamp time / mins	Static	Adv	Re	Static	Adv	Re
COC	PEDOT	2.5	1	84	91	61	90	98	82
COC	PEDOT	2.5	4	75	92	71	90	92	80
COC	PEDOT	2.5	8	82	88	71	89	91	80
COC	PEDOT	1.25	1	68	82	54	86	97	78
COC	PEDOT	1.25	4	84	97	74	88	93	82
COC	PEDOT	1.25	8	90	92	75	84	93	78
COC	PEDOT	0.625	1	72	88	63	84	91	78
COC	PEDOT	0.625	4	79	82	68	88	100	78
COC	PEDOT	0.625	8	83	93	68	84	93	78
COC	PEDOT	0.25	1	51	43	<15	46	46	<15
COC	PEDOT	0.25	4	74	88	65	88	95	80
COC	PEDOT	0.25	8	82	87	64	86	91	72
COC ref.	none			92	100	81	92	100	81

Table 9 Efficiency of removal of PEDOT from COC for varying stamping times and NaOCl concentrations
All tested NaOCl concentrations resulted in comparable removal of PEDOT, when using stamping times of 4-8 min. A stamping time of 1 min yielded similar results for NaOCl concentrations ≥ 0.625 wt%, whereas 0.25 wt% NaOCl did not efficiently remove the over-oxidized PEDOT. Contact angles were measured before and after a wash with Triton-X100 detergent. Note that a slightly different washing and stamping procedure, compared to that used in Figure 35 and Figure 33 was applied, see experimental section for details.

From the data in Table 9, it can be seen that the removal of PEDOT from COC was equally efficient for shorter stamping times and lower concentrations of NaOCl. It could further be concluded that when detergent was applied in a subsequent washing step, even lower NaOCl concentrations and shorter stamping times were applicable. For the case where detergent was only applied in the stamp, it can be seen that when stamping for 4 min, which was used as a standard when patterning PEDOT thin films into 100 µm electrodes with an equidistant spacing, the NaOCl concentration could be lowered to 0.625 wt% without significantly affecting the removal of the PEDOT. As 1.0-2.5 wt% was typically used, it should be possible to lower the NaOCl concentration significantly. If detergent is also included in a subsequent washing step, the results are even more promising: An even lower NaOCl concentration of 0.25 wt% appears to be sufficient and if 0.625 wt% NaOCl is used, the stamping time can be lowered to at least 1 min without notably affecting the removal of the PEDOT. We therefore conclude that it should be possible to fabricate significantly smaller structures, while still removing the PEDOT from the support.

Azide-modified supports are re-exposed upon printed dissolution patterning of PEDOT and can be specifically functionalized

Having established that PEDOT thin films can be removed from COC substrates on a micrometer scale to re-expose unperturbed COC, we now turn to showing micro-scale patterning of PEDOT on more delicate substrates containing functional chemical groups. We show that these functional groups are available after patterning, and can be directly covalently functionalized with appropriate reactants. In Figure 36**,** a PS-N_3 film initially hidden bellow the PEDOT is thus directly functionalized. After the printed dissolution patterning, the characteristic XPS-signal for the azide group could be observed in the high resolution nitrogen XPS spectra in the areas between the electrodes. This indicates that the PS-N_3 was exposed without damaging the functional chemical groups. The azides could be used for anchoring molecules containing alkynes specifically to the areas between the electrodes, using click-chemistry. This was illustrated by applying 5-Iodo-pentyne as a hetero atom XPS marker for completed click-reaction. Accordingly, a clear iodine signal can be seen between the PEDOT electrodes after the reaction. The electrodes can be identified by the presence of sulfur. The printed dissolution patterning scheme can thus be used for fabricating polymeric microelectrodes with directly controlled surface chemistry of the spacing between micro-electrodes of PEDOT, in a simple and inexpensive manner. In Chapter 8 we will expand on this finding by applying additional functional polymeric substrates, and furthermore incorporate controlled surface chemistries to the microelectrodes by applying PEDOT-N_3 and a hydroxyl- modified PEDOT, poly((3,4-(1-hydroxymethylethylene)-dioxythiophene) (PEDOT-OH).

The printed dissolution technique, in addition to being well-suited for fabricating all-polymeric systems, also appeared to be applicable for non-polymeric substrates. In Figure 37 we tested the printed dissolution patterning of PEDOT into 100 μm electrodes on a microscope glass substrate. Prior to spin coating PEDOT onto the substrate, the glass substrate was functionalized with azide groups using silane chemistry. Similar to the PS-N_3 substrate in Figure 36, the glass substrate was covalently coupled to 5-Iodo-pentyne after the printed dissolution patterning, and subsequently analyzed in XPS.

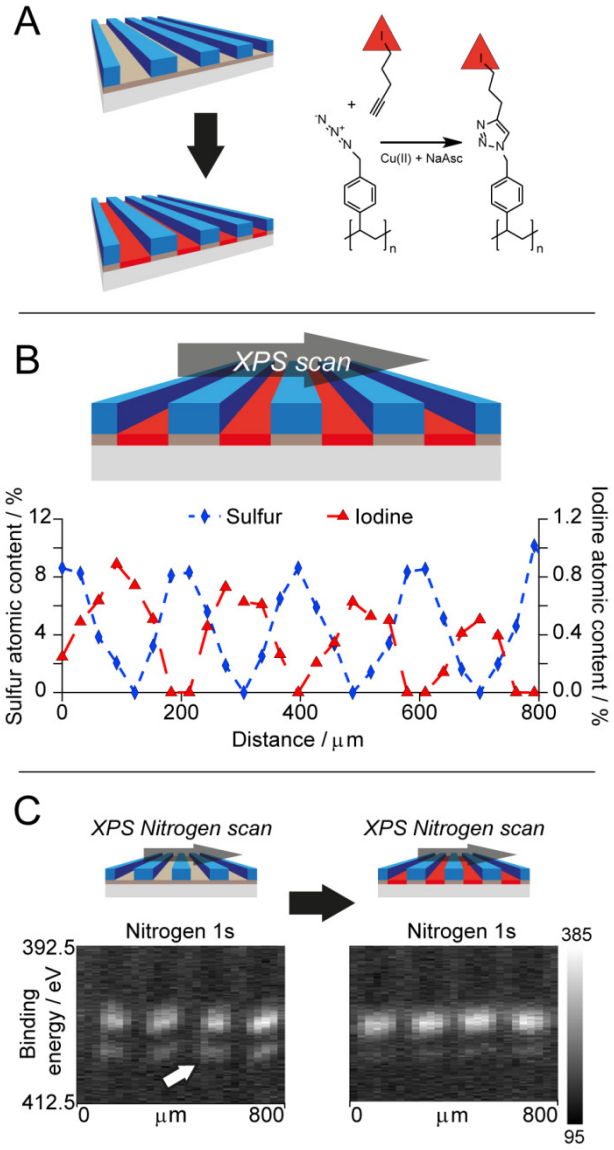

Figure 36 Functionalization of a re-exposed functional PS-N_3 polymer substrate

PS-N_3 re-exposed upon patterning of PEDOT into 100 µm electrodes using printed dissolution, is functionalized with 5-iodo-pentyne. **A**: Click-reaction scheme, see experimental section for details. **B**: XPS line-scan across five electrodes, showing the local atomic content of sulfur and iodine, the iodine being placed specifically at the PS-N_3 between the electrodes (indicated by sulfur). **C**: Raw line-scan high resolution nitrogen spectrum before and after the reaction. The presence of azides is indicated by the presence of a 1:2 doublet. The minor peak of the doublet is indicated with an inserted white arrow. After the reaction this minor peak is notably decreased relative to the major peak, due to the conversion of the azides in the top layer of PS-N_3 to 1-4-triazoles upon click-reaction.

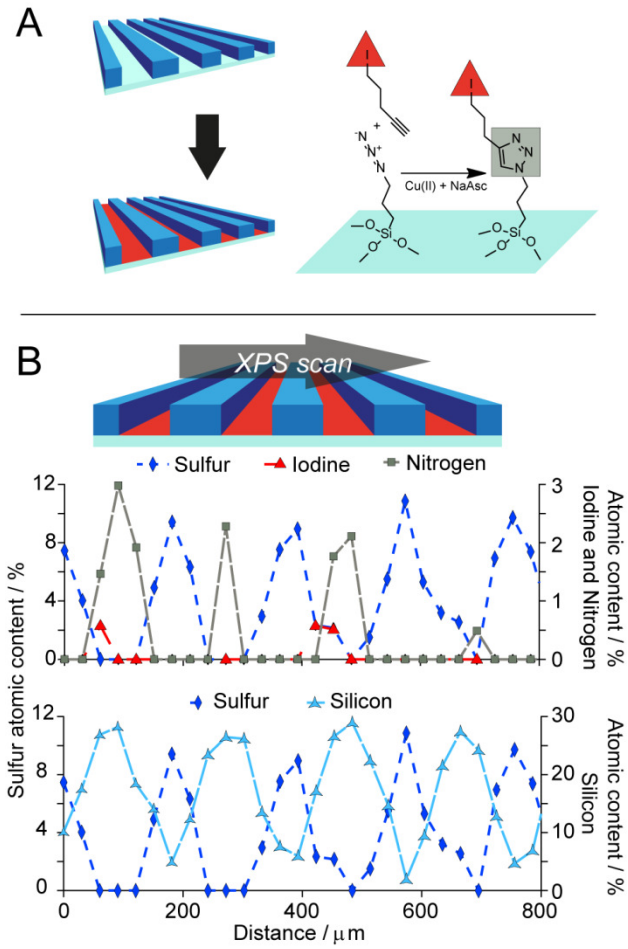

Figure 37 Functionalization of re-exposed azide modified glass substrate

An azide modified microscope glass substrate was covered with a PEDOT thin film, which was subsequently locally removed from the substrate to fabricate into 100 µm electrodes, using printed dissolution. The re-exposed substrate was functionalized with 5-iodo-pentyne **A:** Click-reaction scheme, see experimental section for details. **B**: XPS line-scan across five electrodes, showing the local atomic content of sulfur, nitrogen, iodine, and silicon. The iodine signal was overall weak and only local traces was found between the PEDOT electrodes. However, a nitrogen signal from the Triazole could be found between the electrodes. Judging from the sulfur signal and the silicon signal the substrate is exposed during the printed dissolution procedure, confirming that the printed dissolution technique is also applicable for non-polymeric substrates.

From the sulfur signal it could be concluded that the printed dissolution successfully removed the PEDOT from the substrates, exposing the silicon of the glass substrate. The subsequent functionalization of the substrates with the iodine marker molecule could, however, not be confirmed with certainty. Trace amounts of iodine could be seen between some electrodes, but in general the signal to noise ratio was low. Consequently, we could not consistently observe iodine between all electrodes. We suggest that this is due to a low density azide coating of the substrates, leading to a weak iodine signal. To examine if the azide coating of the glass substrates was found between the electrodes after the stamping procedure, we investigated the nitrogen content between the electrodes. This content is expected to be 3 times larger than the iodine in the case of

complete click-functionalization of the azide coating. Indeed nitrogen was more reliably found between the electrodes. Interestingly, the nitrogen signal was found to be lower when examining the surfaces prior to click-functionalization. This made it difficult to observe the characteristic azide 1:2 doublet in the nitrogen spectrum. This was attributed to the partial decomposition of the Azide group during the XPS measurement which was also observed for the non-conducting PS-N_3 substrates as mentioned in Chapter 5. We conclude that the printed dissolution technique appears to be applicable for modified functional glass substrates. However, in order to confirm this, and in order to be of practical use, the density of the fabricated azide coatings must be improved.

Printed dissolution methodology considerations

Prior to testing detergents, various solvents were assessed for their ability to dissolve the over-oxidized PEDOT-type films. The films were observed to be resistant to a number of regular polar solvents such as water, ethanol, iso-propanol, n-butanol, acetone, acetonitril and 1-4-dioxane. On the other hand, DMSO and DMF both had a notable effect: When patterning PEDOT-N_3 films with an agarose stamp soaked in NaOCl, coherent light-brown films were found. These films could be thinned significantly to give a transparent film by washing with DMF or DMSO. XPS confirmed that the majority of the over-oxidized film was in fact removed. This corresponds well with our earlier finding presented in Chapter 4 that PEDOT and especially PEDOT-N_3 undergoes as violent swelling in DMSO.[153] However, for fabricating all-polymeric microsystems, a solvent system that dissolve the over-oxidized material without affecting other polymeric components, is required. Since DMF and DMSO are quite effective solvents for a number of polymers, the applicability of these solvents for removal of the stamped PEDOT material is limited. For example they both dissolve the azide-modified polystyrene PS-N_3 and an alkyne-modified polystyrene that will be introduced in Chapter 8. We found that addition of small amounts of water to DMSO could prevent such functional polystyrenes from dissolving. Consequently, DMSO/water mixtures of up to up to 90 vol% DMSO were investigated for their ability to remove the over-oxidized PEDOT and PEDOT-N_3 material. Three types of substrates were investigated: COC, PS-N_3 and PS-N_3 covalently coated with an alkyne modified version of the hydrophilic polymer poly(2-methyl-2-oxazoline) (PMOXA), displayed in Figure 38. PMOXA was investigated as it is an attractive alternative to PEG for making anti-fouling coatings.[154-157] Some major benefits of PMOXA compared to PEG are a higher hydrophilicity and better resistance to oxidative degradation and chain cleavage, thereby offering higher resistance to non-specific protein adsorption.[154-158] We hypothesized that the stability of PMOXA in oxidative environments would be sufficient to allow a preformed PMOXA film hidden below a PEDOT film to be exposed and remain functional after stamping.

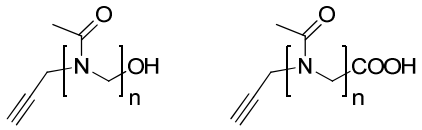

Figure 38 Alkyne modified PMOXA molecules
Alkyne modified PMOXA molecules Left: Containing a hydroxide terminal group, Right: Containing a carboxylic acid terminal group. Generally a 4000 Da hydroxyl-terminal PMOXA was used in our studies.

The results from our studies on applying water/DMSO mixtures to remove over-oxidized PEDOT and PEDOT-N_3 films are displayed in Table 10. Note, that no detergent was used in any step of the process. A number of interesting conclusions can be drawn from Table 10. For both PEDOT and PEDOT-N_3 leftover over-oxidized conducting polymer material could be found on the samples, even when using 90 vol% DMSO in the washing step. Judging from the XPS, this was especially evident for the PS-N_3 substrates. Additionally, the contact angle measurements showed that all COC and PS-N_3 substrates remained hydrophilic after the wash. Thus, the mixed DMSO/water solvent approach was not found to be useful for these substrates. From Table 10 it may also be concluded that over-oxidized PEDOT and PEDOT-N_3 were removed significantly more efficiently from for the PS-N_3 substrates which had been functionalized with PMOXA, than from the native PS-N_3 substrates. In the XPS, a significantly lower sulfur signal was accordingly observed on the PMOXA substrates. A final observation which could be made from Table 10 was that PEDOT-N_3 appeared to oxidize slower than PEDOT, and that in general more material was left on the substrates after patterning. In the studies presented in Chapter 8, we fabricated PEDOT-N_3 electrodes by printed dissolution. Here the larger adhesion of the over-oxidized PEDOT-N_3 was counteracted by applying slightly higher NaOCl concentrations for PEDOT-N_3 samples, and introducing a PEDOT film below all PEDOT-N_3 films.

Prior to the studies presented in Table 10, the PMOXA coatings had been tested for their resistance to the oxidative environment that is present during the stamping. Two types of PMOXA coatings with different end groups, along with a PEG coating made using a PEG-alkyne, were tested. (The PEG-alkyne used in this Chapter and Chapter 8 was a commercially available variant, which was identical to the in house synthesized PEG-alkyne used in the preceding Chapters.) The PMOXA and PEG films were contacted directly with a NaOCl-soaked agarose stamp, without any PEDOT or PEDOT-N_3 film present. Following an aqueous rinse, the substrates were investigated in XPS. The results are displayed in Table 11. The XPS atomic composition of the films was found to be identical for both types of PMOXA coatings, before and after stamping. This confirmed that these coatings were well-suited for being re-exposed upon printed dissolution of a PEDOT-type film. Surprisingly, also the PEG-coated sample appeared to be intact. However, when applying a similar scheme to that which was successfully used for re-exposing PMOXA from below a PEDOT film, we did not observe any re-exposure of the PEG surface. This suggests that there are differences in how PMOXA and PEG interact with PEDOT, either during PEDOT polymerization or during the stamping procedure, and that these

differences determine that PMOXA-coatings are suited to be re-exposed, and the PEG-coatings are not.

Experimental			Obs.	Contact Angles			XPS atomic composition							
Substrate	film	Wash sol DMSO %	Visible Film	Static	Adv	Re	C	O	S	N	Si	Na	Cl	Fe
COC	PEDOT	**0**	No	52	62	<15	85.03	11.27	2.56		0.35	0.33	0.45	
COC	PEDOT	**50**	No	73	72	15	89.84	8	1.6		0.56			
COC	PEDOT	**80**	No	82	84	38	92.63	5.86	1.51					
COC	PEDOT	**90**	No	80	86	40	94.2	4.61	1.19					
COC	PEDOT-N_3	**0**	Yes	66	72	<15	53.91	25.72	5.87	12.57	0.97	0.46	0.5	
COC	PEDOT-N_3	**50**	Yes	58	71	<15	53.11	24.8	6.05	13.93	0.99	0.65	0.47	
COC	PEDOT-N_3	**80**	Shade	63	72	<15	65.52	17.86	5.12	10.69	0.45	0.36		
COC	PEDOT-N_3	**90**	No	69	75	<15	74.3	15.85	2.48	4.85	1.66			0.86
COC ref.	none			92	100	81	99.9	0.1						
PS-N_3	PEDOT	**0**	no	65	62	<15	72.95	14.1	3.27	8.4			0.48	0.8
PS-N_3	PEDOT	**50**	Shade	56	61	<15	74.22	11.61	2.85	10.32			0.37	0.62
PS-N_3	PEDOT	**80**	Shade	58.5	71	<15	77.38	9.44	2.63	10.09				0.47
PS-N_3	PEDOT	**90**	Shade	50	66	<15	76.56	10.48	2.74	9.48				0.74
PS-N_3	PEDOT-N_3	**0**	Yes	65	69	<15	52.49	26.56	5.99	13.58	0.82	0.56		
PS-N_3	PEDOT-N_3	**50**	Yes	66	70	<15	52.37	25.79	5.89	13.81	0.93	0.53	0.32	0.36
PS-N_3	PEDOT-N_3	**80**	No	53	67	15	61.41	18.11	5.02	15.16				0.3
PS-N_3	PEDOT-N_3	**90**	No	67	72	<15	65.14	15.6	4.08	14.17		0.35		0.67
PS-N_3 ref.	none			80	86	71	80.5			19.5				
PMOXA	PEDOT	**0**	No	41	57	<15	73.79	10.88	1.46	12.87			0.52	0.48
PMOXA	PEDOT	**50**	No	32	35	<15	77.25	8.03	0.78	13.94				
PMOXA	PEDOT	**80**	No	20	23	<15	76.97	8.24	1.04	13.75				
PMOXA	PEDOT	**90**	No	29	28.5	<15	82.05	7.35	0.67	9.93				
PMOXA	PEDOT-N_3	**0**	Yes	66	70	18	55.95	24.26	5.23	12.28	0.92	0.92	0.44	
PMOXA	PEDOT-N_3	**50**	Yes	64	73	<15	53.11	25.29	5.82	13.66	1.19	0.69	0.24	
PMOXA	PEDOT-N_3	**80**	No	50	47	15	66.56	14.74	3.48	14.78		0.43		
PMOXA	PEDOT-N_3	**90**	No	45	45	<15	74.34	9.41	1.25	14.63		0.36		
PMOXA ref	none			19	20	<15	72.5	9.7		17.8				

Table 10 DMSO/water washes is not effective for removing over-oxidized PEDOT and PEDOT-N_3

The efficiency of applying post-stamping DMSO/water washes for removing over-oxidized PEDOT and PEDOT-N_3 was tested for various substrates. Different DMSO concentrations were tested. Higher DMSO concentration removed over-oxidized PEDOT and PEDOT-N_3, more efficiently. This is fits well with the strong swelling of PEDOT and PEDOT-N_3 observed in DMSO.[1] Pure DMSO was not investigated, since DMSO dissolves many relevant polystyrene based polymers such as PS-N_3. Over-oxidized PEDOT-N_3 was in general found in larger amount than over-oxidized PEDOT, perhaps due to a slower oxidation. More leftover over-oxidized material was generally observed for PS-N_3 than for the COC and especially the PMOXA substrates. No detergent was applied in this study.

Experimental				XPS atomic comp.			
Substrate	Coating	film	Stamped?	C	O	S	N
PS-N_3	PEG	-	No	81.94	10.95		7.11
PS-N_3	PEG	-	Yes	81.05	11.24		7.71
PS-N_3	PMOXA-COOH	-	No	75.04	8.84		16.12
PS-N_3	PMOXA-COOH	-	Yes	76.76	8.13		15.12
PS-N_3	PMOXA-OH	-	No	81.31	5.91		12.78
PS-N_3	PMOXA-OH	-	Yes	81.85	5.19		13.23
PS-N_3	PMOXA-OH	PEDOT	Yes	82.44	5.44	0.36	11.76

Table 11 Probing the influence of the stamp oxidant (hypochlorite) when stamping directly on PS-N_3 surfaces reacted with PEG or PMOXA

The XPS results show only minor changes in surface elemental composition after being contacted by the hypochlorite loaded stamp. After the stamping the samples were rinsed in Milli-Q water. The PEDOT sample was washed as described in experimental section.

For the experiments displayed in Figure 33-Figure 37, the reducing agent NaAsc was added to the detergent washing solution that was used in the washing step following the agarose stamping. The addition of NaAsc keeps PEDOT films in a reduced state during the wash, similar to in the CuAAC reactions. This additive was found to aid the dissolution of the over-oxidized PEDOT on some substrates. Following such a reduced state wash, the un-stamped PEDOT film could easily be re-oxidized to restore the native p-doped state, as described in Chapter 2-3.[10, 126, 127, 153] The effect of adding either this reducing agent or the oxidizing agent Fe(III)tosylate to the washing step was examined in a series of experiments. In these experiments, DMSO/water mixture washes and Triton-X100 washes were performed with or without these additives, on stamped PEDOT and PEDOT-N_3 samples. The results are displayed in Figure 39. The addition of the reducing agent in most cases only had a minor effect. However, it was observed to have a significant impact on the removal of over-oxidized PEDOT-N_3 from COC, see Figure 39E-F.

In the studies of the removal of over-oxidized PEDOT from COC displayed above in Figure 33, the data suggests that it is of little importance in which step the detergent is added. This could imply that the detergent is simply aiding the dissolution of the over-oxidized product, rather than directly influencing the oxidation mechanism. However, when we compared the effect of adding detergent to the stamp and to the washing step when patterning PEDOT on PS-N_3 substrates, we found that the addition of detergent to the stamp was needed for removing over-oxidized PEDOT effectively, as can be seen in Figure 39C-D. This might suggest that the Triton-X100 plays a role in aiding the oxidation of the PEDOT at the PS-N_3 interphase, possibly by solvating the over-oxidized products during the etching process. Also, for the removal of PEDOT-N_3 from COC the data in Figure 39E-F show a clear effect of adding the detergent directly to the stamp, especially when not using NaAsc in the washing step. Interestingly, although the addition of Triton-X100 to the stamp thus aids the removal of PEDOT-N_3 from COC substrates, it did not appear to accelerate the stamping procedure on these films. In fact, when patterning PEDOT-N_3 films, the addition of detergent to the stamp appeared to decelerate the process, judged from the speed of the color change of the film. Therefore, the effect of adding detergent to the stamp might mainly

be arising from an improved oxidation at the interphase with the substrate, while the oxidization process taking place on the surface or the bulk of the film, might not be improved.

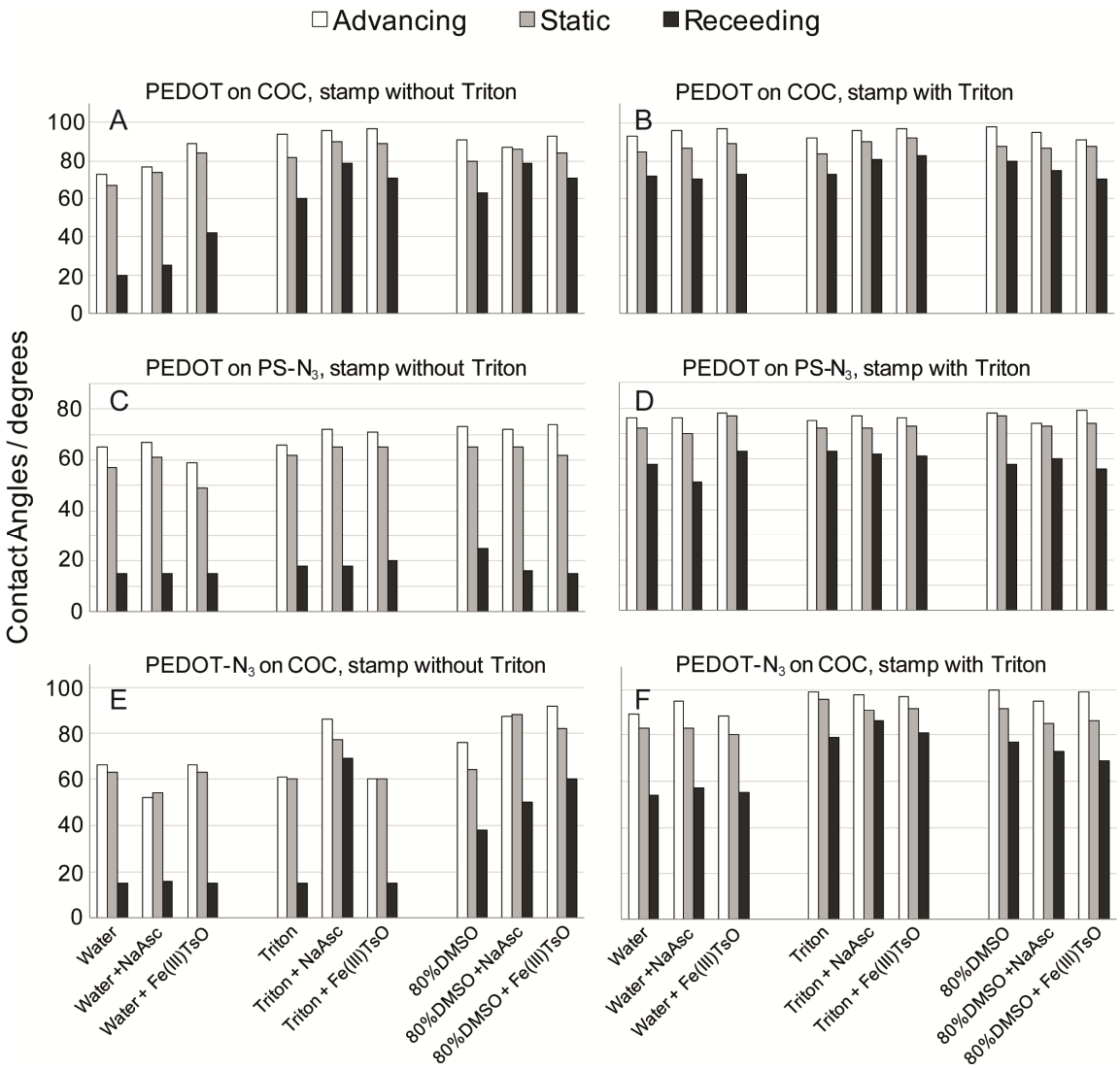

Figure 39 The effect of adding a mildy reducing or oxidizing agent to the washing step following the stamping
The efficiency of the removal of PEDOT and PEDOT-N_3 from COC and PS-N_3, when adding an oxidizing or reducing agent to the post-stamping washing step. Both stamping with Triton-X100 and without were tested. **A:** Stamping PEDOT on COC, without detergent in the agarose stamp solution. The addition of the reducing agent sodium ascorbate (NaAsc) to the washing solutions had some effect. **B:** Stamping PEDOT on COC, with detergent in the agarose stamp solution. Here, the conditions in the washing step were of minor importance, since removal was good in all cases. **C:** Stamping PEDOT on PS-N_3 without detergent in the agarose stamp solution. The over-oxidized PEDOT was difficult to remove in all cases. **D:** Stamping PEDOT on PS-N_3 with detergent in the agarose stamp solution. The conditions in the washing step had little significance as long as detergent was added to the stamp. **E:** Stamping PEDOT-N_3 on COC, without detergent in the agarose stamp solution. The addition of sodium NaAsc was effective, and the Triton-X100 wash was found to be superior to washes with 80/20 vol/vol DMSO/H_2O. **F:** Stamping PEDOT-N_3 on COC, with detergent in the agarose stamp solution. The washing conditions were of minor importance. The best removal of PEDOT-N_3 was obtained when applying detergent both in the stamp and in the subsequent wash.

There are a number of potential improvements and additions to the printed dissolution scheme that we did not investigate. One appealing addition would be to perform detailed studies on non-polymeric functional substrates. The studies on azide modified glass substrates indicate that the process should be applicable for such substrates as well, however the experiments remain preliminary. On such non-polymeric substrates, and for polymers with great resistance to organic solvents such as DMSO or DMF, it might additionally be possible to avoid detergents entirely. However, we did not investigate this in detail. Another interesting addition would be to investigate re-exposure of functional substrates containing other chemical anchoring groups than the azide and PMOXA groups presented above, and the alkyne groups which will be presented in Chapter 8. The major concern should be if the groups undergo oxidation when exposed to hypochlorite during the stamping. This should not be the case e.g. for carboxylate groups. Another concern might be if the substrate has a strong interaction with the (over-oxidized) PEDOT, making the removal of PEDOT difficult. Our failure to hide and re-expose PEG functionalized PS-N_3 might be an example of such a problem.

There are also a number of potential limitations to our methodology. An important potential limitation is the risk of partial integration of the PEDOT polymer in the substrate. It has been reported numerous times that PEDOT can be integrated into various polymeric substrates by washing with appropriate solvents.[120, 121] In this study, all PEDOT films were made by *in situ* polymerization from an n-butanol precursor solution. Accordingly, one should expect that when applying polymeric substrates that undergo significant swelling in n-butanol, PEDOT will be partially integrated into the substrate, making it difficult to remove the PEDOT upon patterning. Polystyrene has been reported to take up 10 wt% n-butanol at 65°C.[159] In correspondence with this, we observed that when spin coating polystyrene substrates with Fe(III)tosylate in n-butanol without any EDOT present, the surfaces became notably more hydrophilic, even after rinsing with water. This suggests that partial integration of PEDOT into the outermost part of polystyrene surfaces might in principle take place during the polymerization. Such integration could be the cause for the observation that it generally appeared to be more difficult to remove PEDOT from PS-N_3 than from COC. From a practical point of view PEDOT was however removed from the polystyrene surfaces well enough to the allow introduction of covalently attached surface chemistries. In Chapter 8, this will be supported further, as additional alkyne reactants are attached to re-exposed functional polystyrene substrates. For other types of substrates, PEDOT integration might however become a more serious problem. Should such cases occur, we suggest that they might be evaded by polymerizing PEDOT from other solvents, at lower temperatures or by polymerization from vapor phase.[160]

Conclusion

The printed dissolution patterning of PEDOT was shown to be a facile method for fabricating microelectrodes with controlled chemistries between the electrodes. The method is in-expensive as it largely avoids clean-room processing. The novelty of the method lies in the use of non-ionic detergents to remove the film, rather than only removing the conductance of the film, upon over-oxidation. The role of the non-ionic detergent when being added directly to a NaOCl soaked agarose stamp appears to be related to the oxidation of the PEDOT at the interphase with the substrate, whereas it is unclear if the detergent aids the general oxidation of in the bulk of the film. When the detergent is applied in a subsequent washing step the addition of the reducing agent NaAsc improve the effect of the washing procedure, for some substrates. The general concept of locally over-oxidizing and dissolving a conducting polymer thin films to expose an underlying functional substrate, should in principle not be limited to PEDOT type polymers, but could be equally applicable for other conducting polymers.

Experimental

Cyclic Olefin Copolymer supports
COC supports were fabricated as described in Chapter 2.

PS-N_3 Substrates
5 mg/ml 4-dioxan solutions of the polymers were spin coated onto COC supports at 1000 rpm. The samples were heated briefly on a hotplate at 60°C to remove residual solvent.

Azide-modified glass Substrates
Microscope glass slides were rinsed briefly in acetone, iso-propanol, ethanol, and Milli-Q water and blown dry. Subsequently they were cleaned in a Piranha solution of 2/3 concentrated H_2SO_4 and 1/3 concentrated H_2O_2 for 15 min. The glasses were subsequently rinsed in copious amounts of Milli-Q water. The glasses were blown dry and placed in an excicator. The excicator was evacuated for >1 h. A small glass bottle containing 300 µl 3-bromopropyl-tri-chloro-silane (from Sigma-Aldrich) was then placed in the excicator. The excicator was then evacuated for 5 min, before sealing the chamber, and leaving it over-night. XPS could confirm the presence of a stable bromine coating of the glass substrates after this reaction. The following day the samples were placed in a glass container suspended in a 200 mL DMF solution with ~0.5 g NaN_3. The bath was placed on a hot plate set to 70°C, and left overnight under lid. The next day the samples were rinsed in large amounts of Milli-Q water. XPS analysis could confirm the complete substitution of bromine with azide, as no bromine could be found on the surface, and nitrogen was now present instead. To confirm the presence of azide groups click-reactions with PEG-alkyne and PMOXA-

alkynes, as described below, were performed. As expected this lead to a significant drop in the contact angles on the surfaces.

PEDOT and PEDOT-N_3 thin film preparation

PEDOT and PEDOT-N_3 thin films were generally fabricated as described in Chapter 2, 4, generally using 1000 rpm for spin-coating the precursor solution. For the PEDOT-N_3 films in Figure 39 2000 rpm was used.

Alkyne reactants

Alkyne modified PMOXAs were synthesized and characterized by Dr. C. Acikgöz as described in the Appendix 1, combining earlier reported schemes [161-16]. PEG-alkyne (PEG2840) was obtained from IRIS Biotech GmbH (Germany). 5-iodo-pentyne was obtained from Sigma-Aldrich.

PEG and PMOXA film formation by CuAAC click-reaction

PMOXA and PEG films were made by coupling a PS-N_3 substrate with 1.5 mM alkyne-PMOXA (4000 Da) or PEG-alkyne overnight in 50/50 vol/vol DMSO/H_2O using 7.5 mM sodium ascorbate and 0.75 mM $CuSO_4$ as catalyst.

Agarose stamp preparation

For the micro-patterned agarose stamp, a silicon mold was fabricated by standard photolithography and deep reactive ion etching. The mold fabricated in this manner proved more stable over time than the earlier reported method using SU-8 [110]. For the flat agarose stamps, a pure Si-wafer was used. Prior to each use the mold was rinsed in ethanol, and occasionally rinsed in air plasma to remove any residual organic material. The silicon mold was placed on a hotplate set to 65°C. A 10 wt% solution of agarose in Milli-Q water was mixed thoroughly. The solution was heated in a microwave oven to remove air bubbles from the solution. To prevent the solution from boiling, this was done by using multiple short heating steps. The hot agarose solution was poured directly onto the silicon mold, using a Ø 5 cm polystyrene Petri dish where the bottom had been removed to contain the agarose. The container was covered with a lid and kept on the hot plate for 10 min. The mold was then transferred to a fridge and left for minimum 10 min to cool down. After the fabrication the agarose stamp was usually cut with a scalpel to a smaller size for improved handling. See Figure 40 for pictures of tools and samples.

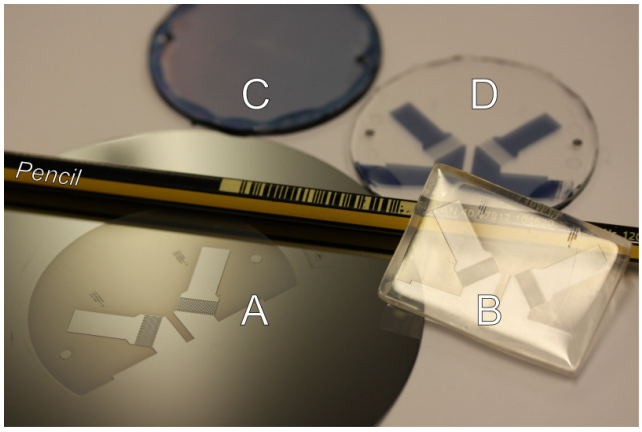

Figure 40 Tools and samples used for printed dissolution patterning of PEDOT films.
A: Silicon wafer patterned using deep reactive ion etching. The wafer serves as a master for making multiple agarose stamps. **B:** An agarose hydrogel stamp, replicating the pattern on the wafer. One stamp can be used for patterning multiple PEDOT thin films. C**:** A PEDOT film on a COC substrate prior to stamping. **D:** A PEDOT film on a COC substrate patterned by stamping with an agarose stamp soaked in a solution of 1.5 wt% NaOCl and 0.1 vol% Triton-X100 for 4 min, followed by washing. A pencil is included as scale.

Agarose stamping procedure

The agarose stamp was soaked for 15 min in a stamping solution, and excess solution was blown off using an air gun. The stamp was gently pressed onto the sample surface to establish contact, and left for 4 min (unless stated otherwise) before removing the stamp, and immediately rinsing the sample in Milli-Q water. Between each stamping cycle, the stamp was soaked for 5 min in the stamping solution. A 1/10 solution of a 10-15 wt% NaOCl (Sigma-Alldrich) stock was generally used leading to a 1-1.5 wt% solution. In Table 9, Figure 39 and Figure 37 a 1/6 solution of the NaOCl stock was used, leading to a 1.7-2.5 wt% solution. Other concentrations were used where noted. Stamping solutions also included 0.1 vol% Triton-X100 where indicated. In Table 9 5% Triton-X100 was used. Studies which were not included here, showed that no difference was seen between 0.1% Triton and 5% Triton.

Post-stamping washing procedure

Generally, following the stamping, the samples were washed for 10 min in an aqueous solution of 0.1 vol% Triton-X100 and 1 wt% sodium ascorbate at 50°C (except where stated otherwise). The samples were then washed twice for 10 min in Milli-Q water at 50°C and 10 min in 80/20 vol/vol DMSO/H_2O at room temperature, before rinsing in ethanol, Milli-Q water, and re-oxidization of the PEDOT by rinsing in 10/90 vol/vol Clevios C-B40/H_2O, and rinsing in Milli-Q water. In Table 9, a 5 vol% Triton-X100 solution, and no DMSO wash was used. In Table 10 no Triton washing and DMSO solution washes were performed as noted. In Figure 39 2 wt% NaAsc or 10 vol% Clevios Cb40 (Fe(III)tosylate in n-butanol) were added to the washes where indicated. The Triton-X100 washes included 5 vol% Triton.

Iodine XPS marker CuAAC click-reaction conditions:
Post stamping click-reactions were all done overnight in water-DMSO mixtures, and stopped by rinsing in de-ionized water followed by re-oxidizing the PEDOT by rinsing in a 10 vol% aqueous solution of Clevios C-B40, and rinsing in de-ionized water again.
PEDOT on PS-N_3 clicked with 5-iodo-pentyne: 65 vol% DMSO, 5 mM $CuSO_4$, 20 mM sodium ascorbate, 25 mM 5-iodo-pentyne.
PEDOT on Azide modified-glass clicked with 5-iodo-pentyne: 65 vol% DMSO, 1 mM $CuSO_4$, 10 mM sodium ascorbate, 5 mM 5-iodo-pentyne.

XPS experimental investigations
XPS experiments were conducted as described in Chapter 3. For line-scan investigations a 40 µm spot and a step-size 30 µm was used. This means that on each single 100 µm electrode, as well as in each spacing area, there will be at least one measurement point where the atomic composition will originate entirely from that electrode/spacing area. For all samples, flood-gun charge compensation was used.

XPS data analysis
Data analyses of the XPS spectra obtained were performed using the Avantage software package supplied by the manufacturer. For the line-scan measurements, the elemental composition of each spot was determined from the high resolution spectra, using the build-in add-peak function with a linear background. In the following atomic content determination, a standard of 0.9 signal to noise threshold was used for all samples. For the glass substrates a 0.7 threshold was used, due to the very low iodine signal.

Contact angle measurements
All contact angles were measured using a Data Physics OCA20 contact angle system, and dedicated software. Prior to all measurements, the samples were blow with inert gas to remove dust.

Chapter 8

All-Polymer Microsystems with Multiple In-Register Surface Chemistries

Introduction

In Chapter 7 we showed that printed dissolution is a versatile procedure for fabricating micro-electrodes of PEDOT-type polymers. The major benefit of the method, compared to conventional photolithographic procedures, was the low price and the ability to re-expose an unperturbed surface chemistry of the underlying substrate in the areas between the electrodes. This made it possible to covalently modify the gaps between the electrodes. Such covalent control allows the surface chemistry to be conveniently chosen in accordance with a specific application. In this Chapter we expand on this finding. We show how the application of functional PEDOT type polymers enables the introduction of covalently attached surface chemistries, also to the electrodes. These studies consequently illustrate a further benefit of the printed dissolution technique, namely that it facilitates the introduction of multiple surface chemistries in register. These in-register chemical modifications are done without the need of any alignment step, and in general avoiding clean-room processing. This makes the method ideal for fabricating advanced all-polymeric microsystems in a simple and in-expensive manner.

In this Chapter we initially apply XPS investigations to show how the commercially available PEDOT-OH can be combined with PS-N_3 to allow the introduction of two distinct types of surface chemistry in an all polymer micro-system. As a further example, we show how another PEDOT-N_3, in combination with an alkyne-modified polystyrene substrate, can give up to three types of locally directed surface chemistries. This is achieved by using electro-click reactions similar to those presented in Chapter 6.[125-127] We further show how the biologically active surface chemistries that were introduced in Chapter 2, can be combined with the printed dissolution technique for achieving all-polymeric microsystems, with localized bio-specific surface chemistries, *on* and *between* conducting polymer electrodes. In addition to the functional molecules presented in Chapter 2, we also show how entire preformed coatings of PMOXA can be hidden below the conducting polymer, and re-exposed upon printed dissolution patterning to allow the fabrication of cell capturing microelectrodes on a cell non-adhesive background, in a few simple steps. Finally, we show how localized electro-polymerization of PEDOT-N_3 onto PEDOT electrodes, can serve as an additional tool for fabricating conducting polymer electrodes with controlled surface chemical properties.

The central findings of this Chapter are presented in the newly submitted manuscript: “Facile micropatterning of functional conductive polymers with multiple surface chemistries in register” and the following Chapter contains entire continuous sections taken from this manuscript.

Functional polymers of orthogonal reactivity direct localized surface modifications

As mentioned in Chapter 1, one of the major advantages of PEDOT-type conducting polymers is that small chemical groups can easily be introduced in the monomer without disrupting the conductance of the polymer. Consequently there are numerous functional PEDOT alternatives to PEDOT-N_3 which has been the main focus of this thesis. One such alternative is the commercially available 3,4-(1-hydroxymethylethylene)-dioxythiophene (EDOT-OH). The printed dissolution procedure was found to be equally effective for PEDOT-OH films as for PEDOT. By combining PEDOT-OH thin films with PS-N_3 substrates, microelectrodes and substrates with individual covalently attached surface chemistries can easily be fabricated. This is illustrated in Figure 41. Here, a PEDOT-OH thin film spin-coated on top of a PEDOT film (PEDOT-OH/PEDOT) placed on a PS-N_3 substrate, was first coupled to a 5-bromo-pentanoic acid using ester coupling reactants. After this reaction, the film was patterned using printed dissolution and the underlying PS-N_3 was reacted with 5-iodo-pentyne. When examining the sample in XPS, bromine was observed to be localized on the electrodes exclusively, whereas iodine was found in the PS-N_3 areas.

Functionalizing the conducting polymer film before patterning it into micro-electrodes, as done in Figure 41, has some advantages and some draw-backs. The major advantages are the simplicity of the scheme and the fact that there is practically no risk of a molecule intended for adding functionality specifically to the electrodes being attached un-specifically to the area between the electrodes. Another advantage is that the same reaction chemistry can be used in series to functionalize both the electrodes and the underlying substrate. We have for example used this approach to give PEDOT-N_3 electrodes on a PS-N_3 background two different types of functionality, as we will illustrate further below. The major disadvantage of adding a surface functionality to the thin films prior to patterning is that addition of some functionalities might influence the stamping procedure, especially if an in-depth functionalization, similar to those described in Chapter 5, is conducted.[153] Deep reaction with hydrophilic molecules such as the PEG-alkyne was thus observed to make the oxidizing solution diffuse much faster from the stamp into the film, making the over-oxidization process faster and difficult to control. Conversely, the addition of some hydrophobic molecules appeared to slow down the process and could hinder the agarose stamp from adsorbing properly onto the film (data not shown). As an alternative, the conducting polymer can be functionalized after being patterned into microelectrodes. To avoid cross-reactions, this approach naturally demands that the anchoring groups of the electrodes and those of the substrate are chemically orthogonal.

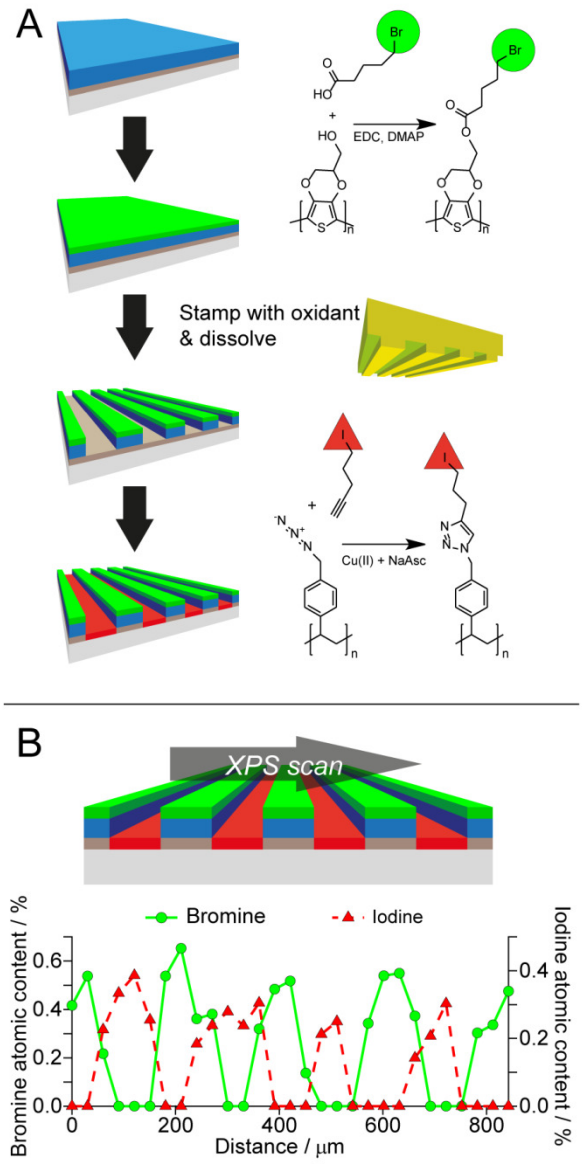

Figure 41 All-polymer micro-system with two types of localized covalently attached surface chemistries
PEDOT-OH on PEDOT micro-electrodes functionalized with 5-bromo pentanoic acid patterned into 100 µm electrodes on a PS-N_3 substrate, functionalized with 5-iodo-pentyne. **A**: The sample was ester-coupled with 5-bromo-pentanoic acid, and afterwards patterned using the printed dissolution procedure, before finally reacting PS-N_3 with 5-iodo-pentyne. **B**: XPS line-scan across five electrodes, showing the local atomic content of bromine and iodine, the iodine being placed specifically at the PS-N_3 between the functionalized electrodes (indicated by bromine). See experimental section for details.

An example of adding the functionality to both the electrodes and substrate after the patterning is shown in Figure 42. Here, a PEDOT-N_3 thin film was spin-coated on top of a PEDOT film placed on an alkyne-functional polystyrene co-polymer substrate; Poly-[(4-prop-2-yn-1-yloxy)-styrene-ran-styrene] (PS-alkyne). After patterning into electrodes, the PS-alkyne substrate was specifically functionalized a with fluorine-containing azide reactants. Following this, electro-click reactions,[126, 127] similar to those used in Chapter 6, was applied to attach bromine-containing alkyne molecules onto one set of electrodes, and iodine-containing molecules onto the other set of electrodes. Thus, in total, three types of localized surface chemistry were introduced.

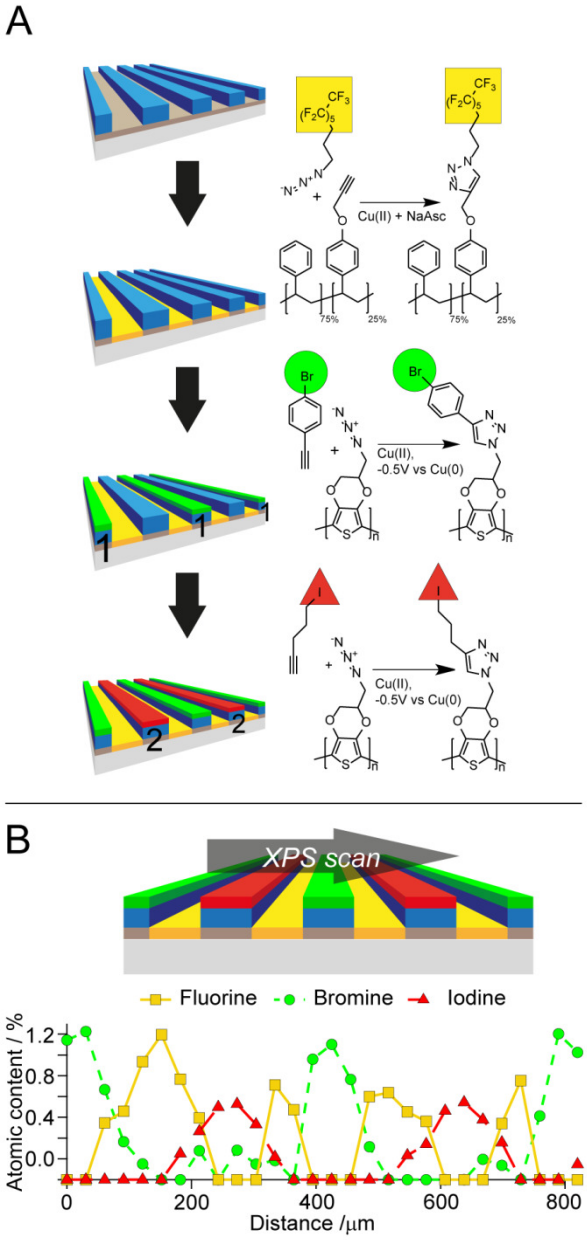

Figure 42 All-polymer micro-system with three types of localized covalently attached surface chemistries

PEDOT-N_3/PEDOT micro-electrodes on a substrate were fabricated using printed dissolution, as described in experimental section. **A**: The patterned sample was first functionalized at the PS-alkyne with 4,4,5,5,6,6,7,7,8,8,9,9,9-Tridecafluorononyl azide as indicated. One set of electrodes "1" was then electro-clicked with 1-bromo-4-ethynylbenzene using a procedure similar to that used in Chapter 6. The other set of electrodes "2" was then electro-clicked with 5-iodo-pentyne. **B**: XPS line-scan across five electrodes, showing the local atomic content of bromine, iodine and fluorine, showing the presence of three different types of localized surface chemistry.

Multiple micro-patterned cell-affecting chemistries can spatially control cell adhesion

In addition to the small XPS-marker molecules used above, macromolecules could similarly be attached to the different surface areas, adding, for example, specific biological functions to the individual areas. Similar to in Chapter 2, we applied alkyne-PEG-GRGDS to induced cellular binding, and PEG-alkyne, to limit cellular attachment. In Figure 43, a PEDOT-N_3/PEDOT thin film on a PS-N_3 substrate was functionalized with alkyne-PEG-GRGDS prior to patterning. After the patterning of the films, PEG-alkyne was coupled to the substrate in order to fabricate a PEG coating of the re-exposed PS-N_3 substrate, and to cover potential un-reacted azide groups found on the PEDOT-N_3 electrodes. 3T3 fibroblast cells were seeded onto the substrate and were found to adhere specifically to the electrodes, and not to the gaps between the electrodes.

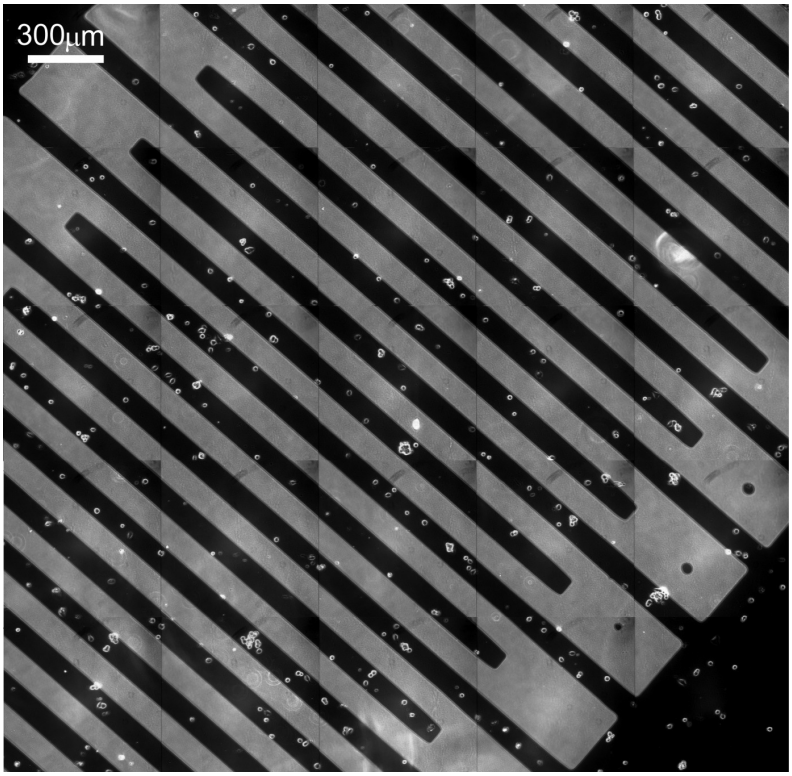

Figure 43 Cell adhesion onto RGD functional PEDOT-N_3 microelectrodes on a PEG covered PS-N_3 background
A mosaic of phase contrast microscope images of the adhesion of 3T3 Fibroblast cells (bright spots) onto PEDOT-N_3/PEDOT electrodes on a PS-N_3 substrate. The electrodes were functionalized with cell-binding alkyne-PEG-GRGDS and the PS-N_3 between the electrodes was coupled to PEG-alkyne after printed dissolution patterning. See experimental section for details. The cell adhesion experiment was performed similar to those described in Chapter 2. The cells were allowed to adhere for 1 h and unattached cells were washed away at a shear rate of 20 Pa

Concurrently with investigating cell adhesion to the functionalized electrode area displayed in Figure 43, the cell adhesion onto a control area, which was neither functionalized with PEG-alkyne nor alkyne-PEG-GRGDS, was investigated. This is displayed in Figure 44. Here it can be

seen that the cells adhere both to the electrodes and to the gaps between the electrodes. This confirms that the induced adhesion onto the electrodes seen in Figure 43 was indeed caused by the covalent attachment of the functional alkyne reactants.

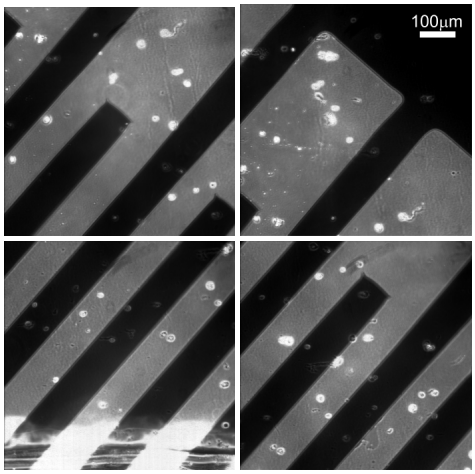

Figure 44 Cell adhesion onto PEDOT-N_3 microelectrodes on a PS-N_3 background without added functionalities
Phase contrast microscope images of the adhesion of 3T3 Fibroblast cells (bright spots) onto PEDOT-N_3/PEDOT electrodes on a PS-N_3 substrate. The substrate was not functionalized with any alkyne reactants. The cell adhesion experiment was performed similar to those described in Chapter 2. The cells were allowed to adhere for 1 h and unattached cells were washed away at a shear rate of 20 Pa. The experiment was conducted on the same sample as that used in Figure 43, investigating an un-functionalized control area. Therefore, the experiment confirms that functionalization of the spacing between the electrodes, as well as of the electrodes is required for the specific cell capture presented in Figure 43.

We found in Chapter 7 that coatings of PMOXA made by functionalizing PS-N_3 with alkyne modified PMOXA molecules were prone to be re-exposed upon printed dissolution patterning of PEDOT films. We consequently fabricated PEDOT/PEDOT-N_3 electrodes on such a background, using printed dissolution patterning. After the patterning, the contact angles in the re-exposed PMOXA functionalized areas were found to be similar to those obtained for the same areas prior to the spin-coating of PEDOT onto the substrate. We then subsequently coupled alkyne-PEG-GRGDS onto the PEDOT-N_3 electrodes, using a standard CuAAC click-reaction, and probed the adhesion of 3T3 fibroblasts. The results are displayed in Figure 45. As expected, we found that the cells adhere with great preference to the electrodes, while negligible cell adhesion was observed onto the PMOXA background. This confirmed that the PMOXA coating had been re-exposed and displayed the anticipated cell resistant properties.

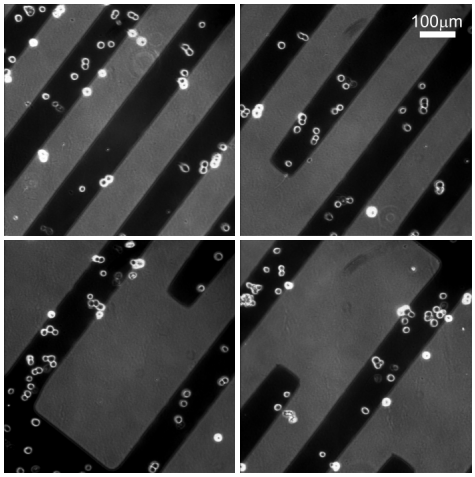

Figure 45 adhesion onto RGD functional PEDOT-N_3 microelectrodes on a PMOXA covered PS-N_3 background Phase contrast microscope images of the adhesion of 3T3 cells. 3T3 cellular adhesion to alkyne-PEG-GRGDS modified PEDOT-N_3/PEDOT electrodes on a PMOXA-functionalized PS-N_3 substrate. The cell adhesion experiment was performed similar to those described in Chapter 2. The cells were allowed to adhere for 1 h and unattached cells were washed away at a shear rate of 20 Pa.

Figure 46A displays an all-polymer micro-system with three types of bio-functional surfaces chemistries in register. To limit cellular adhesion between the electrodes, a PMOXA functionalized PS-N_3 film was hidden below a PEDOT/PEDOT-N_3 thin film re-exposed upon patterning. Using electro-click chemistry, one set of electrodes was functionalized with the active alkyne-PEG-G**RGD**S peptide, and the other set with the inactive scrambled alkyne-PEG-G***RDG***S peptide. When 3T3 fibroblast cells were allowed to adhere for 1 h onto this substrate, they attached specifically to the GRGDS coated electrodes, while showing no adhesion to the other functionalized areas of the sample. The localization of the peptides was confirmed by performing XPS analysis of duplicates of the sample examined in Figure 46A. The XPS data is presented Figure 46B. The same observables as those outlined in Chapter 3 were used: The iodine signal, the nitrogen azide signal, and the sulfur signal, all indicate that the scrambled peptide is found on alternating electrodes after the first electro-click reaction, while after the second electro-clcik reaction, bound peptides were found on both sets of electrodes, confirming that the G**RGD**S peptides was coupled to the other set of electrodes.

Printed dissolution compared to other patterning techniques

Photolithography based patterning techniques were mentioned in the Introduction as one example of the numerous methods to pattern conductive polymers that are available, as recently reviewed by Feng *et al.* [149]. We will only discuss a few approaches of particular interest to the fabrication of all-polymer micro-systems with spatially defined surface chemistries. Various

printing techniques are available for locally adding the conductive polymer to a surface, as opposed to removing it. Pre-polymerized conductive polymers or precursors for initiating polymerization have been transferred to various substrates by additive printing, e.g. using micro-contact printing.[149, 167] Additive printing requires that the substrate surface has a high affinity for the printed material, being either an initiator or a conductive polymer. Polymer substrates are typically hydrophobic and non-polar, which generally results in low affinity for polar conductive polymer materials and associated problems in printing the latter class of materials. In contrast, our approach only requires that the surface allows wetting by the PEDOT precursor solution during spin coating and polymerization. Wetting is possible on most substrate materials as the solvent can be chosen in accordance with the surface chemistry of a particular material. Additive printing has a further challenge in achieving high accuracy overlay alignment, i.e. to deposit multiple areas of different types of chemistry in register with sharply defined boundaries between neighboring chemistries. Printed dissolution meets this challenge by actively removing chemically poorly defined boundary zones between neighboring areas during the dissolution step. The benefits of additive printing techniques and of printed dissolution could possibly be combined, for example by using high-resolution ink-jet printing of an oxidant and a detergent to perform subtractive rather than additive ink-jet printing of conductive polymers. [168]

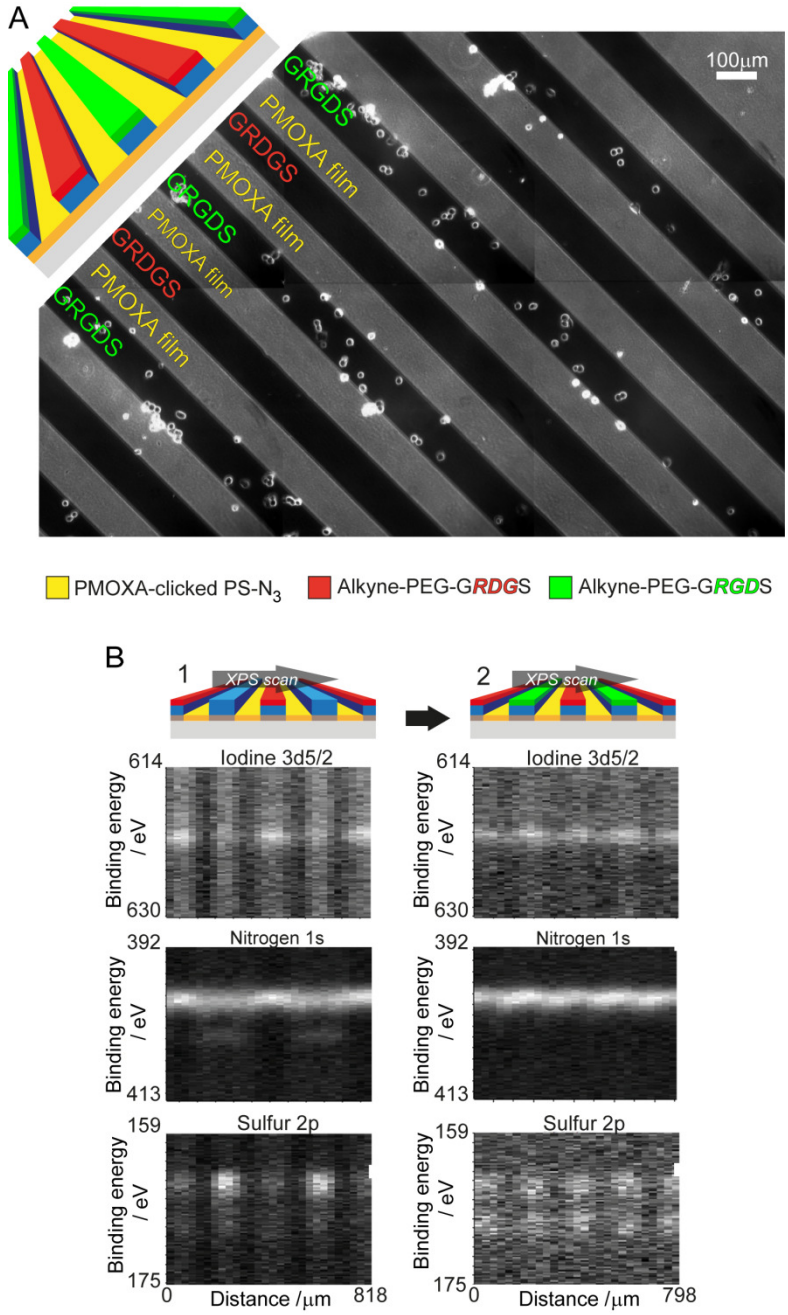

Figure 46 All-polymer micro-system with three types of localized bio-functional surface chemistries

A: Specific adhesion of 3T3 fibroblasts was seen to PEDOT-N_3/PEDOT microelectrodes electro-clicked with alkyne-PEG-G**RGD**S versus corresponding PEDOT-N_3/PEDOT microelectrodes electro-clicked with alkyne-PEG-G***RDG***S and the PMOXA-alkyne surface re-exposed between the electrodes. The PMOXA-alkyne was reacted onto an underlying PS-N_3 substrate before coating with the PEDOT-N_3/PEDOT thin film. The cell adhesion experiment was performed similar to those described in Chapter 2. The cells were allowed to adhere for 1 h and unattached cells were washed away at a shear rate of 20 Pa. **B**: Samples similar to that used for cellular studies in "A" were investigated using XPS. 1: After the first electro-click reaction, 2: After both electro-click reactions. The results confirm that scrambled and functional peptides are placed on alternating electrodes, as the residual azide signal found on every second electrode after the first electro-click coupling, is removed after the second coupling. Also iodine is initially majorly found to every second electrodes, while after the second coupling iodine is found both electrode sets. Finally the sulfur signal show only reaction on every second electrodes after the first electro-click coupling.

Electro-polymerization of PEDOT-N_3 on micro-electrodes

In Chapter 7 we found that the adhesion of the over-oxidized PEDOT-N_3 onto various substrates was stronger than that of over-oxidized PEDOT. In order to fabricate multi-functional all-polymer microsystems based on PEDOT-N_3 we circumvented this problem by placing a PEDOT thin film below the PEDOT-N_3, throughout this Chapter. Although this procedure could be used for fabricating multifunctional microsystems, there are other useful approaches, to the simple fabrication all-polymer microsystems with multiple surface chemistries in register. One potentially useful tool is electro-polymerization. For instance, we applied electro-polymerization to locally polymerize PEDOT-N_3 onto prefabricated microelectrodes. We found that this could be done in a number of different solvents, including aqueous suspensions, and on various electrode materials. Figure 47 displays some examples. Figure 47B demonstrates polymerization of PEDOT-N_3 onto 20 µm wide gold thin film electrodes. The image was acquired on a transparent COC sample illuminated from the back therefore the gold thin film electrodes appear blue in the micrograph. Using galvanostatic polymerization conditions, PEDOT-N_3 was electro-polymerized onto one set of the electrodes from an EDOT-N_3 solution in 75/25 vol/vol water/acetonitrile. After polymerization these electrodes appear darker in the micrograph. Figure 47C-D display XPS investigations of a sample of 100 µm wide PEDOT electrodes on a COC support. Again using a galvanostatic procedure, PEDOT-N_3 had been polymerized onto one set of electrodes. In the XPS measurements this could be observed through the emergence of a signal nitrogen one set of the electrodes, whereas no nitrogen was observed on the other electrode set in Figure 47C. The nitrogen signal was lower than expected, but the high resolution nitrogen spectrum could confirm the presence of intact azide functionalities, see Figure 47D. Similar electro-polymerization schemes in DMSO/water mixtures were also effective. Polymerization in pure water suspensions could also be performed. Here the addition of SDS detergent proved useful, following the procedure of Sakmeche.[169, 170] The PEDOT electrodes used in this study were fabricated by applying an agarose stamp soaked in NaOCl, but applying no detergent or washes in the process. Therefore, residual over-oxidized PEDOT material can be observed in the gaps between the electrodes.

There are a number of potential advantages to applying electro-polymerization of PEDOT-N_3. As mentioned above, the slower oxidation of PEDOT-N_3 observed when performing printed dissolution patterning can be avoided. This should lead to a better removal of the conducting polymer film, and thus an improved surface chemical contrast between the different compartments of the fabricated micro-system. Another major benefit is that different types of functional PEDOT derivates can be electro-polymerized locally, adding distinct chemical properties to individual electrodes. We envision that this could be a useful supplement to the localized electro-click reactions for fabricating all-polymer microsystems with even more types of

well defined localized surface chemistries. The challenges we encountered for performing electro-click reactions in water, might be entirely avoided by performing sequential water-based electro-polymerizations.[169-171] Also, although we did not experience any issues with residual copper and concurrent toxicity towards the cells, localized electro-polymerizations would allow the use of copper-free click chemistry[172] for functionalizing the PEDOT-N_3, while still maintaining the localization of the surface chemistries. Yet an advantage of the electro-polymerization approach is that the amount of material consumed when fabricating functional microelectrodes can be lowered e.g. by performing the polymerization inside a microfluidic channel, and adding only a very thin coating of the functional PEDOT type onto regular PEDOT electrodes. This approach further takes advantage of the higher conductance of the native PEDOT.

In most of the reports on electro-polymerizing PEDOT-type polymers, metal or ITO electrodes have been used as starting point. [11, 21, 173, 174]However, as we have shown here, PEDOT itself can also serve as a convenient starting material such electro-polymerization, enabling the fabrication of all-polymeric devices. There are naturally situations where the high conductance of metal is demanded. As PEDOT-N_3 could also be electro-polymerized onto gold electrodes, we suggest that the efficient covalent surface chemical derivation schemes which we have developed for PEDOT-N_3 in this thesis can easily be transferred to metal based devices.

Conclusion

It has been shown that the application of printed dissolution for micro-patterning PEDOT-type thin films, enable a straightforward route to introducing multiple types of surface chemistries in register. Importantly, this is done without any alignment step, and limiting the use of clean room processes. This limits the time consumption and expenses of fabricating the microsystems significantly. Various surface chemistries could be added to PEDOT-OH and PEDOT-N_3 micro-electrodes as well as to PS-alkyne and PS-N_3 substrates in the gaps between the electrodes, either before or after the patterning step. The method could be used for making an all-polymeric microfluidic system in which fibroblast cells could be specifically captured onto designated electrodes. As the process, in addition to being versatile, is in-expensive, it is especially well-suited for fabricating all-polymeric microsystems. Localized electro-polymerization of PEDOT-N_3 onto PEDOT and gold microelectrodes was introduced as a further extension of the available tools for designing and fabricating advanced microsystems. The polymerization onto prefabricated PEDOT electrodes should be useful for the fabrication of advanced all-polymeric devices. The polymerization of PEDOT-N_3 onto metal electrodes is however equally interesting. This illustrates that the processes for controlling the (bio)-functional surface chemistries of PEDOT-N_3, which have been developed in the work presented in this thesis, can be transferred to other types of material surfaces. This expands the applicability of our findings significantly.

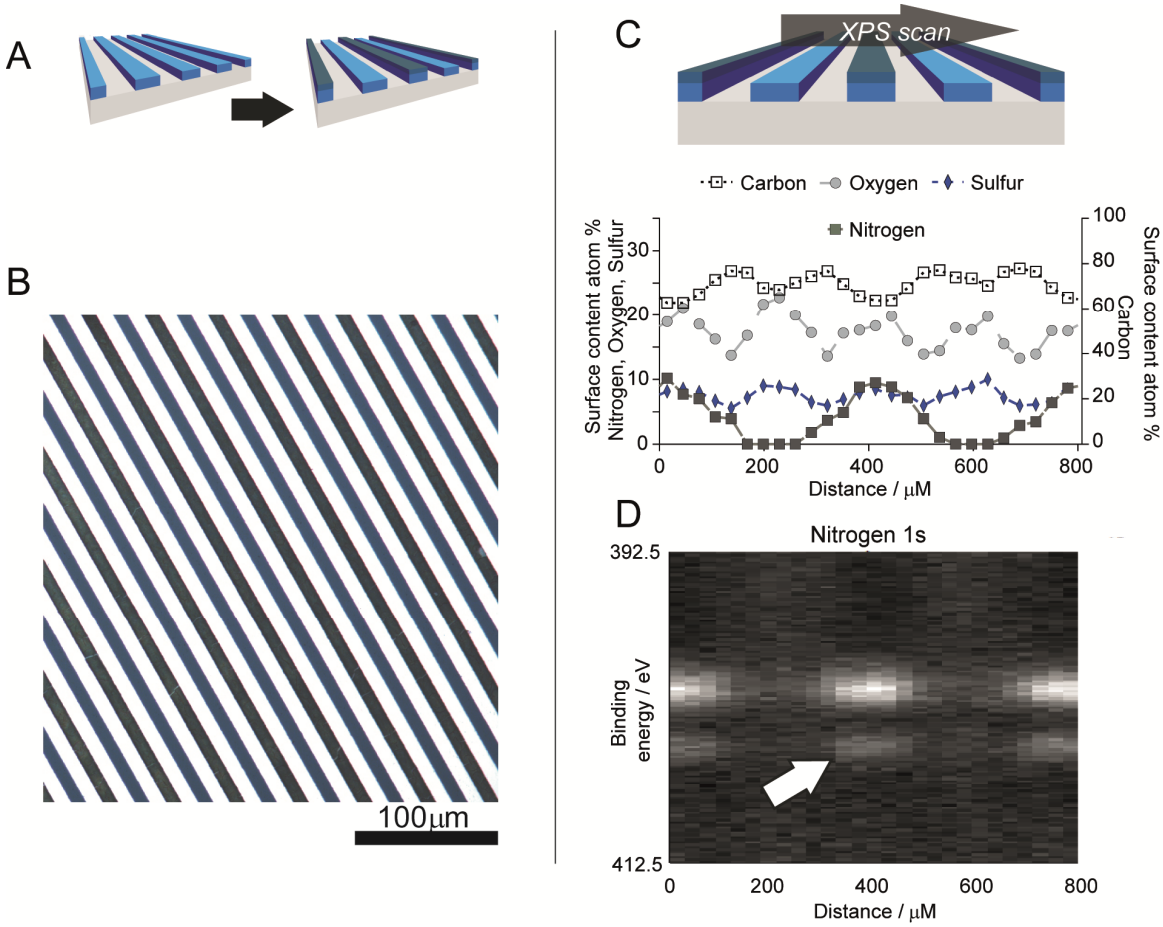

Figure 47 Electro-polymerization of PEDOT-N_3 onto microelectrodes

A: Principle sketch showing the local electro-polymerization of PEDOT-N_3 polymer onto a non-functional microelectrode **B:** Optical micrograph of 20 µm wide gold electrodes on a COC substrate, with PEDOT-N_3 electro-polymerized onto one set of electrodes. These electrodes appear darker in the micrograph. **C**: XPS line-scan analysis of the atomic composition of a sample of 100 µm wide PEDOT electrodes on a COC support, where PEDOT-N_3 has been electro-polymerized onto every second electrode. This can be seen as an increase in the nitrogen signal from 0 to ~10%. Note that the PEDOT electrodes in this example were fabricated using an agarose stamping procedure without any detergent in the stamp or in the subsequent washing procedure, thus residual over-oxidized PEDOT can be observed between the electrodes, for example as a high quantity of sulfur. **D**: High resolution nitrogen XPS line-scan confirming that the nitrogen found in the elemental composition arises from the introduction of azide functional groups. The inserted arrow marks the characteristic high binding energy peak of the partially positively charged nitrogen atom in the Azide group. See experimental section for details on the electro-polymerization conditions.

Experimental

Cyclic Olefin Copolymer supports
COC substrates were fabricated as described in Chapter 2.

Syntheses
Alkyne-PEG-(GRGDS) and alkyne-PEG-(GRDGS) were synthesized and characterized as described in Appendix 1. PS-alkyne and PS-N_3, were synthesized and characterized by Dr. A.E. Daugaard, as described in Appendix 2. Alkyne-PMOXAs were synthesized and characterized by Dr. C. Acikgöz as described in Appendix 1, combining earlier reported schemes.[161-166]

PS-alkyne and PS-N_3 Substrates
5 mg/ml 4-dioxan solutions of the polymers were spin-coated onto clean COC supports at 1000rpm. The samples were heated briefly on a hotplate at 60°C to remove residual solvent.

PEDOT, PEDOT-OH and PEDOT-N_3 thin film preparation
PEDOT and PEDOT-N_3 thin films were fabricated as described in Chapter 2 and 4, the precursor solution was spin-coated at 1000rpm. PEDOT-OH thin films were fabricated using the same procedure as that used for regular PEDOT, described in Chapter 2. All PEDOT-N_3 and PEDOT-OH films in this Chapter were fabricated on top of a premade PEDOT film.

Agarose stamp preparation
Micro-structured agarose stamps were fabricated as described in Chapter 7.

Agarose stamping procedure
Agarose stamping was performed as described in Chapter 7, applying 1.7-2.5wt% NaOCl and 0.1 vol% Triton-X100 in the stamping solution. For samples with PEDOT-N_3 no Triton-X100 was applied in the stamp.

Post-Stamping washing procedure:
The same general washing procedure as that described in Chapter 7, was used.

Additional surface chemical reactants
PEG-alkyne (750 Da, art. no. PEG2840) was obtained from IRIS Biotech GmbH (Germany). Hydroxymethyl EDOT, 5-iodo-pentyne, 5-bromo-pentanoic acid, 4,4,5,5,6,6,7,7,8,8,9,9,9-Tridecafluorononyl azide, 1-bromo-4-ethynylbenzene, were all obtained from Sigma-Aldrich.

PMOXA film formation
For the PMOXA films used for the cellular studies in this Chapter, A PS-N_3 substrate was reacted overnight with a CuAAC reaction solution containing: 1 mM $CuSO_4$, 15 mM sodium ascorbate, 2 mM PMOXA(4000)-alkyne, in 64 vol% DMSO. The following day the substrate was exposed to a

CuAAC reaction solution with a PMOXA(2000)-alkyne, to ensure complete surface coverage: 1 mM $CuSO_4$, 15 mM sodium ascorbate, 2 mM PMOXA-alkyne, in 64 vol% DMSO. 4 h reaction time was used. Following the reaction the sample was rinsed with de-ionized water.

Surface chemical reactions

Ester coupling of 5-bromo-pentanoic acid on PEDOT-OH: 180 mM 5-bromo-pentanoic acid, 150 mM 1-Ethyl-3-(3-dimethylaminopropyl)carbodiimide (EDC), 150 mM 4-Dimethylaminopyridine (DMAP) was mixed in dry DMSO and added to the surface of the PEDOT-OH film. Reaction time was 45 min. After reaction the sample was rinsed in de-ionized water followed by re-oxidizing the PEDOT by rinsing in a 10 vol% aqueous solution of Clevios C-B40 (Fe(III)tosylate in n-butanol), and rinsing in de-ionized water again.

CuAAC click-reaction conditions: Post stamping click-reactions were all done overnight in water-DMSO mixtures, and stopped by rinsing in de-ionized water followed by re-oxidizing the PEDOT by rinsing in a 10 vol% aqueous solution of Clevios C-B40 (Fe(III)tosylate in n-butanol), and rinsing in de-ionized water again.

PEDOT-OH (ester coupled to bromo-pentanoic acid)/PEDOT on PS-N_3 clicked with 5-iodo pentyne: 65 vol% DMSO, 1 mM $CuSO_4$, 10 mM sodium ascorbate, 5 mM 5-iodo-pentyne.

PEDOT-N_3/PEDOT on PS-alkyne clicked with 4,4,5,5,6,6,7,7,8,8,9,9,9-Tridecafluorononyl azide: 70 vol% DMSO, 1 mM $CuSO_4$, 10 mM sodium ascorbate, 5 mM 4,4,5,5,6,6,7,7,8,8,9,9,9-Tridecafluorononyl azide.

Electro-click reaction conditions: Electro-click reactions were conducted using a copper plate top electrode, in a setup similar to our earlier report,[127] presented in Chapter 6. A Cu top electrode was used to ensure a uniform functionalization of the electrodes. The spacing to the top electrode was ~330 µm. one set of PEDOT-N_3/PEDOT electrodes was set to 0.5 V potential and the other to -0.5 V vs. the copper top electrode. For the second reaction the potentials were swapped. 90 vol% DMSO reaction mixtures were used. 1 mM alkyne-reactant concentration and 1 mM $CuSO_4$ was used. Reaction time of 5 min was used for the halogen-alkyne marker reactions, and 20 min was used for the alkyne-PEG-G***RDG***S and alkyne-PEG-G**RGD**S. Reactions were stopped by rinsing in de-ionized water followed by re-oxidizing the PEDOT by rinsing in a 10 vol% aqueous solution of Clevios C-B40 (Fe(III)tosylate in n-butanol), and rinsing in de-ionized water.

XPS experimental investigations and data analysis

XPS experiments and analysis were conducted as described in Chapter 3 and Chapter 7.

Fibroblast attachment studies

The fibroblast adhesion studies were generally performed as described in Chapter 2.

However, for these studies, a homemade flow chamber with channel dimensions of 0.140 mm x 2 mm x 10 mm (*h,w,l*) was used. The components are displayed in Figure 48. The chamber was assembled by connecting two homemade COC substrates, the bottom containing the functionalized electrode / PMOXA sample, and the top defining inlets and outlets, with a strip of transfer adhesive (ARcare 90106, Adhesive Research, Glen Rock, PA, USA). The adhesive was cut

using a CO_2-laser to define the lateral geometry of the channel. The thickness of the adhesive defined the height of the channel.

Electro-polymerization of PEDOT-N_3

The polymerization of PEDOT-N_3 onto micro-electrodes was performed inside a microfluidic channel identical to that used for the fibroblast adhesion studies. For the electro-polymerizations, the regular COC top part of the channel was exchanged for a COC foil sputtered with a continuous gold thin film. This sheet was used as counter electrode during the electro-polymerizations.

Electro-polymerizations of PEDOT-N_3 on 20 µm wide gold electrodes: A 25/75 vol/vol acetonitril/water solution of 9 mM EDOT-N_3 monomer, and 90 mM sodium tosylate was added to the chamber. A Galvanostatic polymerization was performed, applying a current of 0.04 mA. The total electrode area should be ~0.4 cm^2 giving a current density of ~1 A /m^2. 5 min polymerization time was used.

Electro-polymerizations of PEDOT-N_3 on 100 µm wide PEDOT electrodes:

A 25/75 vol/vol acetonitril/water solution of 10 mM EDOT-N_3 monomer, and 100 mM sodium tosylate was added to the chamber. A Galvanostatic polymerization was performed, applying a current of 2 µA. The total electrode area should be ~0.4 cm^2 giving a current density of ~50 mA /m^2. 25 min polymerization time was used. This lower current density was used, as larger current densities lead to over-oxidation of the PEDOT electrodes, and concurrent loss of conductivity.

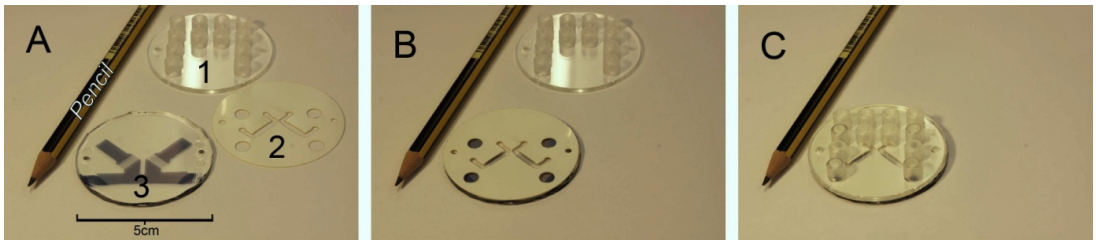

Figure 48 Components of the homemade micro-fluidic chamber. 1: A COC top part containing luer inlet parts 2: A laser-cut CO_2 transfer adhesive tape defining channels and inlets 3: Stamped PEDOT electrodes on a flat COC substrate. **A-C**: The components positioned on top of each other. A pencil is included as scale.

Chapter 9

Conclusion

The studies presented in this thesis, together suggests that post-polymerization covalent functionalizations of PEDOT-type conducting polymers can serve as a valuable approach to modifying the surface chemistry of these materials, in order to facilitate their use in advanced cell handling bio-medical systems. The use of CuAAC to modify PEDOT-N_3 served to show that substrates with highly bio-specific surface chemistries can be made using a covalent approach and that these surface chemistries can be patterned into, for example, gradient patterns. Furthermore, we developed simple schemes for micropatterning the conducting polymers and for combining them with other functional polymeric materials. These findings highlight that, largely due to the covalent nature of the surface chemistries, the conducting polymer material can be processed in numerous manners, without sacrificing the possibility for specifically and locally controlling the (bio)-chemical surface characteristics. Also, the electronic properties of the material remain largely un-perturbed by the presented covalent modifications and processing schemes.

Although the major focus of this thesis has been to tailor PEDOT type polymers to bio-medical cell handling systems, we propose that a number our findings should be of general interest to the conducting polymers research field. We hope to have contributed to the general understanding of PEDOT-type conducting polymers, and that some of our findings will also be useful for adapting PEDOT polymers to other applications such as opto-electronic devices.

Prior to the studies presented in this thesis, the vast majority of successful studies considering modification of the surface chemical properties of conducting polymers toward living cell applications were based on non-covalent methods. Post-polymerization covalent modifications can however also be of great value for addressing this topic, as the presented work demonstrates. Still, it should be stressed that we did not conduct long term studies of long term cellular responses to covalently engineered conducting polymer surfaces. The findings presented in this thesis are therefore rather to be looked at as tools. These tools can be applied for fabricating conducting polymer substrates and all-polymer microsystems that contain numerous types of well defined and localized biologically active surface chemistries. Depending on how these tools are combined, the biological activity of a system can be changed to accommodate particular bio-medical application. The protocols which we have developed can aid the fabrication of advanced cell handling polymeric devices by addressing different important issues for the fabrication of such devices.

One central issue when tuning the surface chemistry of advanced materials for bio-medical devices is *specificity*. Carefully presenting selected bio-functional molecules on a material surface, albeit not being a trivial process, will not necessarily grant biological specificity to a substrate. The unspecific adsorption of bio-molecules, particularly proteins, can change the biochemical properties of a substrate drastically. This problem is particularly apparent when a substrate is being subjected to long-term exposure to solutions containing such bio-molecules. This is, for example, the case when culturing cells. Our approach to this important issue was to engineer surfaces that resist unspecific adsorption of bio-molecules, while at the same time presenting selected bio-functional motives. We fabricated such conducting polymer substrates by covering

the substrates with a coating of highly hydrophilic PEG-molecules, which served as a background, and present specific bio-molecules motives on this background. This common scheme was found to be well suited for conducting polymers, mainly after we realized that PEDOT-N_3 substrate could be swelled by choosing appropriate solvents. Since the swelling could be exploited for fabricating dense protein resistant PEG coatings. Such covalently attached PEG coatings of PEDOT type substrates have, to our knowledge, not been produced before. To show that the PEG-coatings could facilitate the production of substrates displaying biological specificity, we presented RGD peptides on PEG-coated substrates. This modification was found to induce attachment of 3T3 fibroblast onto the PEG-covered substrates, which was otherwise repellant to the cells and proteins. Most importantly, we found that the equivalent presentation of scrambled, biologically inert, RDG peptides did not induce any cellular attachment. Evidently, a high degree of biological specificity was achieved. Also, our investigations showed that the ratio between different bio-functional reactants attached to a substrate, could easily be varied, due to the covalent nature of our approach. Importantly, such stoichiometric variations were found to translate directly to the observed biological function. Although we only tested few bio-functional molecules, we propose that this approach should be generally applicable. By presenting other bio-functional molecules and general anchoring groups, such as NTA or biotin, on a similar conducting polymer substrate resistant to protein adsorption, it should be possible to tailor surface chemistries specifically for a particular bio-medical application.

Another important issue of modifying the surface chemical properties of advanced materials for bio-medical devices is *localization*. Localization of specific surface chemistries is needed, for instance, in order to compartmentalize a microsystem. Such compartmentalization can be useful for capturing specific bio-molecules or cell phenotypes at specific sites, thereby for example enabling specific sensing of biologic entities or controlled co-culturing of two distinct cell types. In or studies we showed that electro-click chemistry can serve as a convenient tool for localizing the developed covalently attached bio-active surface chemistries. By using this technique, we were able to directly functionalize specific conducting polymer electrodes, and more so, to fabricate highly diverse surface gradient patterns of covalently attached bio-molecules on PEDOT-N_3 substrates. As gradient patterns of bio-molecules are commonly found in tissue, this "stenciled electro-click chemistry" technique, serves as an additional valuable tool for engineering advanced bio-mimetic conducting polymer devices. Similarly, our finding that the swelling of the polymer can be used for controlling the reaction depth and density illustrates, that not only lateral localization of functional chemistries are possible, but also vertical direction is possible when applying a post-polymerization modification scheme.

An additional key issue is *integration*. In order to be applicable in advanced cell-handling polymeric devices, it is essential that the conducting polymers can be processed and combined with other functional materials. If such devices are to be of practical use in the clinic, it is further imperative, that the processing techniques, in addition to being effective, are scalable and in-expensive. Ideally, such processing techniques should also enable the facile introduction of

additional functionalities to the microsystems, supplementing those provided by the conducting polymer. Specifically controlled surface chemistry of the material adjacent to the conducting polymers is one example of such an additional functionality. In this thesis we have contributed to the collection of inexpensive yet effective methods that are available for processing PEDOT-type conducting polymers. We have thus presented a novel method for patterning thin films of PEDOT-type polymers into microelectrodes, which allow the convenient combination with other functional polymeric materials by "hiding" these materials below the PEDOT thin films. This "printed dissolution" scheme is unique in that it is sufficiently harsh, that it does not only remove the conductance of the thin film, but entirely removes the film, and sufficiently mild, that underlying functional surface chemistries are re-exposed in an unperturbed form. We combined this patterning technique with the methods which we have developed for achieving bio-specific surface chemistries, to achieve bio-functional coatings of the conducting polymers and of the re-exposed functional polymers. Doing so, we were able to fabricate all-polymeric microfluidic systems containing conducting polymer micro-electrodes and multiple, in-register, bio-functional surface chemistries. The printed dissolution concept should, in principle, not be limited to PEDOT-type polymers, and may therefore serve as a common tool for pattering conducting polymer thin films, to expose underlying functional features.

In our efforts to expand the toolbox available for engineering the interaction between PEDOT-type polymers and living cells, there are many important issues and approaches that we did not investigate. For example, although obviously being an important parameter, we did not attempt to control the surface roughness of the substrates, and explore how this affects the activity of the fabricated surface chemistries. We find that this would be a highly relevant topic for future studies. Also, the combination of our covalent modifications with non-covalent approaches, such as the entrapment of bio-molecules during electro-polymerization, could be a highly rewarding study. Our few studies on electro-polymerization highlighted another potential application of our findings, namely that the specific surface chemistries which can be achieved for PEDOT-N_3, can be transferred directly to other conducting substrates, by electro-polymerizing thin films of PEDOT-N_3 onto a substrate surface. This would also be an interesting topic for future studies. Future studies should also be conducted to improve our understanding of the interaction between the covalently modified conducting polymers and living cells. Especially long term studies of the interaction with living cells are demanded.

In addition to such studies on issues closely related to the themes of this thesis, there are a number of further challenges that must be overcome in order to fabricate automated polymer-based cell-handling devices relying on conducting polymers. For instance, detailed studies on the application of conducting polymers for sensing and stimulating specific cell developments must be improved. Also, studies on the assembly and automation of entire cell-handling devices based on these polymers are highly needed. The tools which we have developed in this thesis should therefore not only be optimized, but more so, they must be combined with such complementing studies, in order to enable the fabrication of advanced automated polymer-based cell handling devices.

However, as the surface chemical solutions that we have developed here can be transferred and engineered to fit numerous applications, we find it likely that they can find practical use. Thus, the surface chemistries presented in this thesis, are not only “smart” in that they are capable of specifically recognizing and capturing living cells onto localized areas. They are also “smart” in the sense that the underlying principles are sufficiently generic that they can adapt to various biological tasks.

References

[1] C. Liu, *Advanced Materials* **2007**, *19*, pp. 3783-3790.

[2] J. El-Ali, P. K. Sorger, K. F. Jensen, *Nature* **2006**, *442*, pp. 403-411.

[3] J. Voldman, *Annu. Rev. Biomed. Eng.* **2006**, *8*, pp. 425-454.

[4] H. Kaji, G. Camci-Unal, R. Langer, A. Khademhosseini, *Biochimica Et Biophysica Acta-General Subjects* **2011**, *1810*, pp. 239-250.

[5] S. Kirchmeyer, K. Reuter, *J. Mater. Chem.* **2005**, *15*, pp. 2077-2088.

[6] M. Asplund, T. Nyberg, O. Inganas, *Polymer Chemistry* **2010**, *1*, pp. 1374-1391.

[7] A. Kumar, D. Welsh, M. Morvant, F. Piroux, K. Abboud, J. Reynolds, *Chemistry of Materials* **1998**, *10*, pp. 896-902.

[8] F. Cataldo, P. Maltese, *European Polymer Journal* **2002**, *38*, pp. 1791-1803.

[9] H. Bu, G. Goetz, E. Reinold, A. Vogt, S. Schmid, R. Blanco, J. L. Segura, P. Baeuerle, *Chemical Communications* **2008**, pp. 1320-1322.

[10] A. E. Daugaard, S. Hvilsted, T. S. Hansen, N. B. Larsen, *Macromolecules* **2008**, *41*, pp. 4321-4327.

[11] S. C. Luo, E. Mohamed Ali, N. C. Tansil, H. H. Yu, S. Gao, E. A. Kantchev, J. Y. Ying, *Langmuir* **2008**, *24*, pp. 8071-8077.

[12] P. M. George, D. A. LaVan, J. A. Burdick, C. Y. Chen, E. Liang, R. Langer, *Advanced Materials* **2006**, *18*, pp. 577-581.

[13] D. Kim, S. M. Richardson-Burns, J. L. Hendricks, C. Sequera, D. C. Martin, *Advanced Functional Materials* **2007**, *17*, pp. 79-86.

[14] C. Salto, E. Saindon, M. Bolin, A. Kanciurzewska, M. Fahlman, E. W. H. Jager, P. Tengvall, E. Arenas, M. Berggren, *Langmuir* **2008**, *24*, pp. 14133-14138.

[15] K. Svennersten, M. H. Bolin, E. W. H. Jager, M. Berggren, A. Richter-Dahlfors, *Biomaterials* **2009**, *30*, pp. 6257-6264.

[16] K. M. Persson, R. Karlsson, K. Svennersten, S. Loffler, E. W. H. Jager, A. Richter-Dahlfors, P. Konradsson, M. Berggren, *Advanced Materials* **2011**, *23*, pp. 4403-4408.

[17] B. Winther-Jensen, D. W. Breiby, K. West, *Synth. Met.* **2005**, *152*, pp. 1-4.

[18] M. Marimuthu, S. Kim, *Anal. Biochem.* **2011**, *413*, pp. 81-89.

[19] M. Wu, S. Huang, G. Lee, *Lab on a Chip* **2010**, *10*, pp. 939-956.

[20] H. Xie, S. C. Luo, H. Yu, *Small* **2009**, *5*, pp. 2611-2617.

[21] S. C. Luo, H. Xie, N. Chen, H. Yu, *ACS Applied Materials & Interfaces* **2009**, *1*, pp. 1414-1419.

[22] J. Sekine, S. Luo, S. Wang, B. Zhu, H. Tseng, H. Yu, *Advanced Materials* **2011**, *23*, pp. 4788-4792.

[23] H. C. Kolb, M. Finn, K. B. Sharpless, *Angewandte Chemie International Edition* **2001**, *40*, pp. 2004-2021.

[24] M. Meldal, C. W. Tornoe, *Chem. Rev.* **2008**, *108*, pp. 2952-3015.

[25] W. H. Binder, R. Sachsenhofer, *Macromolecular rapid communications* **2008**, *29*, pp. 952-981.

[26] S. Fleischmann, K. Hinrichs, U. Oertel, S. Reichelt, K. J. Eichhorn, B. Voit, *Macromolecular rapid communications* **2008**, *29*, pp. 1177-1185.

[27] R. T. Chen, B. W. Muir, G. K. Such, A. Postma, R. A. Evans, S. M. Pereira, K. M. McLean, F. Caruso, *Langmuir* **2010**, *26*, pp. 3388-3393.

[28] M. A. Gauthier, M. I. Gibson, H. A. Klok, *Angewandte Chemie International Edition* **2009**, *48*, pp. 48-58.

[29] S. G. Im, B. S. Kim, W. E. Tenhaeff, P. T. Hammond, K. K. Gleason, *Thin Solid Films* **2009**, *517*, pp. 3606-3611.

[30] J. Sinha, R. Sahoo, A. Kumar, *Macromolecules* **2009**, *42*, pp. 2015-2022.

[31] J. Xu, Y. Tian, R. Peng, Y. Xian, Q. Ran, L. Jin, *Electrochemical Communications* **2009**, *11*, pp. 1972-1975.

[32] H. Bu, G. Goetz, E. Reinold, A. Vogt, S. Schmid, J. L. Segura, R. Blanco, R. Gomez, P. Baeuerle, *Tetrahedron* **2011**, *67*, pp. 1114-1125.

[33] T. A. Skotheim, R. L. Elsenbaumer, J. R. Reynolds, *Handbook of conducting polymers*, Second edn., Marcel Dekker inc.**1998**.

[34] F. C. Krebs, S. A. Gevorgyan, J. Alstrup, *J. Mater. Chem.* **2009**, *19*, pp. 5442-5451.

[35] S. Sakurai, H. Jiang, M. Takahashi, K. Kobayashi, *Electrochim. Acta* **2009**, *54*, pp. 5463-5469.

[36] N. R. Armstrong, W. Wang, D. M. Alloway, D. Placencia, E. Ratcliff, M. Brumbach, *Macromolecular rapid communications* **2009**, *30*, pp. 717-731.

[37] B. Winther-Jensen, K. Fraser, C. Ong, M. Forsyth, D. R. MacFarlane, *Advanced Materials* **2010**, *22*, pp. 1727-1730.

[38] B. Winther-Jensen, O. Winther-Jensen, M. Forsyth, D. R. MacFarlane, *Science* **2008**, *321*, pp. 671.

[39] F. Vidal, C. Plesse, G. Palaprat, A. Kheddar, J. Citerin, D. Teyssié, C. Chevrot, *Synth. Met.* **2006**, *156*, pp. 1299-1304.

[40] H. Okuzaki, H. Suzuki, T. Ito, *Synth. Met.* **2009**, *159*, pp. 2233-2236.

[41] K. Krishnamoorthy, R. S. Gokhale, A. Q. Contractor, A. Kumar, *Chemical Communications* **2004**, pp. 820-821.

[42] F. Mouffouk, S. J. Higgins, *Electrochemistry Communications* **2006**, *8*, pp. 317-322.

[43] E. M. Ali, E. A. B. Kantchev, H. Yu, J. Y. Ying, *Macromolecules* **2007**, *40*, pp. 6025-6027.

[44] J. Park, H. K. Kim, Y. Son, *Sensor. Actuat. B-Chem.* **2008**, *133*, pp. 244-250.

[45] C. H. Weng, W. M. Yeh, K. C. Ho, G. B. Lee, *Sensor. Actuat. B-Chem.* **2007**, *121*, pp. 576-582.

[46] L. J. del Valle, D. Aradilla, R. Oliver, F. Sepulcre, A. Gamez, E. Armelin, C. Alemán, F. Estrany, *European Polymer Journal* **2007**, *43*, pp. 2342-2349.

[47] L. J. del Valle, F. Estrany, E. Armelin, R. Oliver, C. Aleman, *Macromolecular Bioscience* **2008**, *8*, pp. 1144-1151.

[48] S. M. Richardson-Burns, J. L. Hendricks, B. Foster, L. K. Povlich, D. H. Kim, D. C. Martin, *Biomaterials* **2007**, *28*, pp. 1539-1552.

[49] R. A. Green, N. H. Lovell, L. A. Poole-Warren, *Biomaterials* **2009**, *30*, pp. 3637-3644.

[50] R. A. Green, S. Baek, L. A. Poole-Warren, P. J. Martens, *Science and Technology of Advanced Materials* **2010**, *11*, pp. 14107.

[51] S. Sekine, Y. Ido, T. Miyake, K. Nagamine, M. Nishizawa, *J. Am. Chem. Soc.* **2010**, *123*, pp. 13174-13175.

[52] K. Svennersten, M. Berggren, A. Richter-Dahlfors, E. W. H. Jager, *Lab on a Chip* **2011**, *11*, pp. 3287-3293.

[53] M. R. Abidian, J. M. Corey, D. R. Kipke, D. C. Martin, *Small* **2010**, *6*, pp. 421-429.

[54] Y. Hsiao, C. Lin, H. Hsieh, S. Tsai, C. Kuo, C. Chu, P. Chen, *Lab on a Chip* **2011**, *11*, pp. 3674-3680.

[55] J. Yang, D. H. Kim, J. L. Hendricks, M. Leach, R. Northey, D. C. Martin, *Acta Biomaterialia* **2005**, *1*, pp. 125-136.

[56] A. S. Widge, M. Jeffries-El, X. Cui, C. F. Lagenaur, Y. Matsuoka, *Biosensors and Bioelectronics* **2007**, *22*, pp.1723-1732.

[57] D. D. Ateh, A. Waterworth, D. Walker, B. H. Brown, H. Navsaria, P. Vadgama, *Journal of Biomedical Materials Research Part a* **2007**, *83A*, pp. 391-400.

[58] T. S. Hansen, D. Selmeczi, N. B. Larsen, *J. Micromech. Microengineering* **2010**, *20*, pp. 15020-15020.

[59] K. Kiilerich-Pedersen, C. R. Poulsen, T. Jain, N. Rozlosnik, *Biosens. Bioelectron.* **2011**, *28*, pp. 386-392.

[60] K. Ø. Andresen, M. Hansen, M. Matschuk, S. T. Jepsen, H. S. Sørensen, P. Utko, D. Selmeczi, T. S. Hansen, N. B. Larsen, N. Rozlosnik, *J. Micromech. Microengineering* **2010**, *20*, pp. 55010-55019.

[61] M. Balog, H. Rayah, F. L. Derf, M. Sallé, *New J. Chem.* **2008**, *32*, pp. 1183-1188.

[62] R. B. Bazaco, R. Gómez, C. Seoane, P. Bäuerle, J. L. Segura, *Tetrahedron Lett.* **2009**, *50*, pp. 4154-4157.

[63] J. Arias-Pardilla, T. F. Otero, R. Blanco, J. L. Segura, *Electrochim. Acta* **2009**, *55*, pp. 1535–1542.

[64] C. A. Cutler, M. Bouguettaya, T. S. Kang, J. R. Reynolds, *Macromolecules* **2005**, *38*, pp. 3068-3074.

[65] T. Darmanin, M. Nicolas, F. Guittard, *Langmuir* **2008**, *24*, pp. 9739-9746.

[66] M. Döbbelin, C. Pozo-Gonzalo, R. Marcilla, R. Blanco, J. L. Segura, J. A. Pomposo, D. Mecerreyes, *J. Polym. Sci. , Part A: Polym. Chem.* **2009**, *47*, pp. 3010-3021.

[67] J. L. Segura, R. Gómez, R. Blanco, E. Reinold, P. Bäuerle, *Chem.Mater.* **2006**, *18*, pp. 2834-2847.

[68] F. Mouffouk, S. J. Higgins, *Electrochemistry Communications* **2006**, *8*, pp. 15-20.

[69] A. Benedetto, M. Balog, H. Rayah, F. Le Derf, P. Viel, S. Palacin, M. Sallé, *Electrochim. Acta* **2007**, *53*, pp. 3779-3788.

[70] F. L. E. Jakobsson, X. Crispin, L. Lindell, A. Kanciurzewska, M. Fahlman, W. R. Salaneck, M. Berggren, *Chem. Phys. Lett.* **2006**, *433*, pp. 110-114.

[71] A. Menaker, V. Syritski, J. Reut, A. Öpik, V. Horváth, R. E. Gyurcsányi, *Advanced Materials* **2009**, *21*, pp. 2271-2275.

[72] Y. Xiao, C. M. Li, S. Wang, J. Shi, C. P. Ooi, *J. Biomed. Mater. Res. A.* **2010**, *92*, pp. 766-772.

[73] T. Dai, X. Qing, H. Zhou, C. Shen, J. Wang, Y. Lu, *Synth. Met.* **2010**, *160*, pp. 791–796.

[74] L. Lindell, A. Burquel, F. L. E. Jakobsson, V. Lemaur, M. Berggren, R. Lazzaroni, J. Cornil, W. R. Salaneck, X. Crispin, *Chem. Mater.* **2006**, *18*, pp. 4246-4252.

[75] H. Wang, L. Ji, D. Li, J. Wang, *J. Phys. Chem. B* **2008**, *112*, pp. 2671-2677.

[76] X. Cui, V. Lee, Y. Raphael, J. Wiler, J. Hetke, D. Anderson, D. Martin, *J. Biomed. Mater. Res.* **2001**, *56*, pp. 261-272.

[77] A. Akkouch, G. Shi, Z. Zhang, M. Rouabhia, *Journal of Biomedical Materials Research Part A* **2010**, *92A*, pp. 221-231.

[78] K. J. Gilmore, M. Kita, Y. Han, A. Gelmi, M. J. Higgins, S. E. Moulton, G. M. Clark, R. Kapsa, G. G. Wallace, *Biomaterials* **2009**, *30*, pp. 5292-5304.

[79] M. R. Abidian, D. H. Kim, D. C. Martin, *Advanced Materials* **2006**, *18*, pp. 405-409.

[80] S. Sirivisoot, R. Pareta, T. J. Webster, *Nanotechnology* **2011**, *22*, pp. 85101.

[81] R. A. Green, N. H. Lovell, L. A. Poole-Warren, *Acta Biomaterialia* **2010**, *6*, pp. 63-71.

[82] M. Asplund, H. von Holst, O. Inganäs, *Biointerphases* **2008**, *3*, pp. 83.

[83] M. Asplund, E. Thaning, J. Lundberg, A. C. Sandberg-Nordqvist, B. Kostyszyn, O. Inganas, H. von Holst, *Biomedical Materials* **2009**, *4*, pp. 45009.

[84] Y. Xiao, C. Li, M. L. Toh, R. Xue, *J. Appl. Electrochem.* **2008**, *38*, pp. 1735-1741.

[85] Y. Xiao, D. Martin, X. Cui, M. Shenai, *Appl. Biochem. Biotechnol.* **2006**, *128*, pp. 117-129.

[86] J. Che, Y. Xiao, X. Zhu, X. Sun, *Polym. Int.* **2008**, *57*, pp. 750-755.

[87] A. Herland, K. M. Persson, V. Lundin, M. Fahlman, M. Berggren, E. W. H. Jager, A. I. Teixeira, *Angewandte Chemie International Edition* **2011**, *50*, pp. 12529 –12533.

[88] V. Lundin, A. Herland, M. Berggren, E. W. H. Jager, A. I. Teixeira, *PloS one* **2011**, *6*, pp. 18624.

[89] A. Gumus, J. P. Califano, A. M. D. Wan, J. Huynh, C. A. Reinhart-King, G. G. Malliaras, *Soft Matter* **2010**, *6*, pp. 5138-5142.

[90] J. E. Collazos-Castro, J. L. Polo, G. R. Hernández-Labrado, V. Padial-Cañete, C. García-Rama, *Biomaterials* **2010**, *31*, pp. 9244-9255.

[91] U. Hersel, C. Dahmen, H. Kessler, *Biomaterials* **2003**, *24*, pp. 4385-4415.

[92] A. Sanghvi, K. Miller, A. Belcher, C. Schmidt, *Nature Materials* **2005**, *4*, pp. 496-502.

[93] J. Lee, F. Serna, C. E. Schmidt, *Langmuir* **2006**, *22*, pp. 9816-9819.

[94] R. Flemming, C. Murphy, G. Abrams, S. Goodman, P. Nealey, *Biomaterials* **1999**, *20*, pp. 573-588.

[95] C. Wilkinson, M. Riehle, M. Wood, J. Gallagher, A. Curtis, *Materials Science and Engineering: C* **2002**, *19*, pp. 263-269.

[96] A. S. Andersson, F. Bäckhed, A. Von Euler, A. Richter-Dahlfors, D. Sutherland, B. Kasemo, *Biomaterials* **2003**, *24*, pp. 3427-3436.

[97] M. H. Bolin, K. Svennersten, X. Wang, I. S. Chronakis, A. Richter-Dahlfors, E. W. H. Jager, M. Berggren, *Sensors and Actuators B-Chemical* **2009**, *142*, pp. 451-456.

[98] S. I. Jeong, I. D. Jun, M. J. Choi, Y. C. Nho, Y. M. Lee, H. Shin, *Macromolecular Bioscience* **2008**, *8*, pp. 627-637.

[99] H. Lodish, A. Berk, P. Matsudaira, C. A. Kaiser, M. Krieger, M. P. Scott, L. Zipursky, J. Darnell, *Molecular Cell Biology*, Fourth edn., W. H. Freeman and Company **2000**.

[100] B. Ratner, S. Bryant, *Annu. Rev. Biomed. Eng.* **2004**, *6*, pp. 41-75.

[101] P. Kingshott, H. J. Griesser, *Current Opinion in Solid State & Materials Science* **1999**, *4*, pp. 403-412.

[102] V. V. Rostovtsev, L. G. Green, V. V. Fokin, K. B. Sharpless, *Angewandte Chemie International Edition* **2002**, *41*, pp.2596-2599.

[103] X. Crispin, S. Marciniak, W. Osikowicz, G. Zotti, A. W. D. van der Gon, F. Louwet, M. Fahlman, L. Groenendaal, F. De Schryver, W. R. Salaneck, *J. Polym. Sci. Pol. Phys.* **2003**, *41*, pp. 2561-2583.

[104] G. Zotti, S. Zecchin, G. Schiavon, F. Louwet, L. Groenendaal, X. Crispin, W. Osikowicz, W. Salaneck, M. Fahlman, *Macromolecules* **2003**, *36*, pp. 3337-3344.

[105] D. Briggs, *Surface Analysis of Polymers by XPS and Static SIMS*, Cambridge University Press **1998**.

[106] R. K. Schulze, D. C. Boyd, J. F. Evans, W. L. Gladfelter, *J. Vac. Sci. Technol. A.* **1990**, *8*, pp. 2338-2343.

[107] D. B. Wang, B. H. Chen, B. Zhang, Y. X. Ma, *Polyhedron* **1997**, *16*, pp. 2625-2629.

[108] T. Y. Kim, J. E. Kim, K. S. Suh, *Polym. Int.* **2006**, *55*, pp. 80-86.

[109] T. Y. Kim, C. M. Park, J. E. Kim, K. S. Suh, *Synth. Met.* **2005**, *149*, pp. 169-174.

[110] T. S. Hansen, K. West, O. Hassager, N. B. Larsen, *Advanced Materials* **2007**, *19*, pp. 3261-3265.

[111] K. E. Aasmundtveit, E. J. Samuelsen, L. A. A. Pettersson, O. Inganas, T. Johansson, R. Feidenhans'l, *Synth. Met.* **1999**, *101*, pp. 561-564.

[112] J. Ouyang, Q. Xu, C. W. Chu, Y. Yang, G. Li, J. Shinar, *Polymer* **2004**, *45*, pp. 8443-8450.

[113] D. Bagchi, R. Menon, *Chem. Phys. Lett.* **2006**, *425*, pp. 114-117.

[114] O. P. Dimitriev, D. A. Grinko, Y. V. Noskov, N. A. Ogurtsov, A. A. Pud, *Synth. Met.* **2009**, *159*, pp. 2237-2239.

[115] J. Huang, P. F. Miller, J. C. De Mello, A. J. De Mello, D. D. C. Bradley, *Synth. Met.* **2003**, *139*, pp. 569-572.

[116] S. K. M. Jönsson, J. Birgerson, X. Crispin, G. Greczynski, W. Osikowicz, Denier van der Gon, A.W., W. R. Salaneck, M. Fahlman, *Synth. Met.* **2003**, *139*, pp. 1-10.

[117] J. Y. Kim, J. H. Jung, D. E. Lee, J. Joo, *Synth. Met.* **2002**, *126*, pp. 311-316.

[118] G. M. Sando, K. Dahl, J. C. Owrutsky, *J. Phys. Chem. B* **2007**, *111*, pp. 4901-4909.

[119] P. Kingshott, H. Thissen, H. J. Griesser, *Biomaterials* **2002**, *23*, pp. 2043-2056.

[120] B. Winther-Jensen, J. Chen, K. West, G. Wallace, *Polymer* **2005**, *46*, pp. 4664-4669.

[121] T. S. Hansen, K. West, O. Hassager, N. B. Larsen, *Synth. Met.* **2006**, *156*, pp. 1203-1207.

[122] J. Malyszko, M. Scendo, *Mon. Chem.* **1987**, *118*, pp. 435-443.

[123] W. H. Binder, R. Sachsenhofer, *Macromolecular rapid communications* **2007**, *28*, pp. 15-54.

[124] P. M. Habib, B. Rama Raju, V. Kavala, C. W. Kuo, C. F. Yao, *Tetrahedron* **2009**, *65*, pp. 5799-5804.

[125] N. K. Devaraj, P. H. Dinolfo, C. E. D. Chidsey, J. P. Collman, *J. Am. Chem. Soc.* **2006**, *128*, pp. 1794-1795.

[126] T. S. Hansen, A. E. Daugaard, S. Hvilsted, N. B. Larsen, *Advanced Materials* **2009**, *21*, pp. 4483-4486.

[127] T. S. Hansen, J. U. Lind, A. E. Daugaard, S. Hvilsted, T. L. Andresen, N. B. Larsen, *Langmuir* **2010**, *26*, pp. 16171-16177.

[128] A. C. von Philipsborn, S. Lang, J. Loeschinger, A. Bernard, C. David, D. Lehnert, F. Bonhoeffer, M. Bastmeyer, *Development* **2006**, *133*, pp. 2487-2495.

[129] A. D. Luster, R. Alon, U. H. von Andrian, *Nat. Immunol.* **2005**, *6*, pp. 1182-1190.

[130] J. Genzer, R. R. Bhat, *Langmuir* **2008**, *24*, pp. 2294-2317.

[131] N. L. Jeon, H. Baskaran, S. K. W. Dertinger, G. M. Whitesides, L. Van de Water, M. Toner, *Nat. Biotechnol.* **2002**, *20*, pp. 826-830.

[132] M. K. Chaudhury, G. M. Whitesides, *Science* **1992**, *256*, pp. 1539-1541.

[133] J. Thome, M. Himmelhaus, M. Zharnikov, M. Grunze, *Langmuir* **1998**, *14*, pp. 7435-7449.

[134] N. D. Gallant, K. A. Lavery, E. J. Amis, M. L. Becker, *Advanced Materials* **2007**, *19*, pp. 965.

[135] R. H. Terrill, K. M. Balss, Y. M. Zhang, P. W. Bohn, *J. Am. Chem. Soc.* **2000**, *122*, pp. 988-989.

[136] A. Buxboim, M. Bar-Dagan, V. Frydman, D. Zbaida, M. Morpurgo, R. Bar-Ziv, *Small* **2007**, *3*, pp. 500-510.

[137] J. M. Belisle, J. P. Correia, P. W. Wiseman, T. E. Kennedy, S. Costantino, *Lab on a Chip* **2008**, *8*, pp. 2164-2167.

[138] J. Malyszko, M. Scendo, *J. Electroanal. Chem.* **1988**, *250*, pp.61-72.

[139] J. Malyszko, M. Scendo, *J. Electroanal. Chem.* **1989**, *269*, pp.113-128.

[140] B. Stepnikswiatek, J. Malyszko, *J. Electroanal. Chem.* **1990**, *292*, pp.175-185.

[141] A. Foll, M. Le Démezet, J. Courtot-Coupez, *J. Electroanal. Chem.* **1972**, *35*, pp.41-54

[142] O. Duschek, V. Gutmann, *Z. Anorg. Allg. Chem.* **1972**, *394*, pp. 243-253

[143] E. Hochuli, W. Bannwarth, H. Döbeli, R. Gentz, D. Stüber, *Nat. Biotechnol.* **1988**, *6*, pp. 1321-1325.

[144] G. M. Whitesides, *Lab on a Chip* **2010**, *10*, pp. 2317-2318.

[145] J. Porath, *Protein Expr. Purif.* **1992**, *3*, pp. 263-281.

[146] T. Lämmermann, B. L. Bader, S. J. Monkley, T. Worbs, R. Wedlich-Söldner, K. Hirsch, M. Keller, R. Förster, D. R. Critchley, R. Fässler, *Nature* **2008**, *453*, pp. 51-55.

[147] R. M. Steinman, J. Banchereau, *Nature* **2007**, *449*, pp. 419-426.

[148] A. K. Palucka, H. Ueno, J. W. Fay, J. Banchereau, *Immunol. Rev.* **2007**, *220*, pp.129-150.

[149] Y. Xu, F. Zhang, X. Feng, *Small* **2011**, *7*, pp. 1338-1360.

[150] L. Jiang, X. Wang, L. Chi, *Small* **2011**, *7*, pp. 1309-1321.

[151] P. Tehrani, N. Robinson, T. Kugler, T. Remonen, L. Hennerdal, J. Hall, A. Malmstrom, L. Leenders, M. Berggren, *Smart Materials & Structures* **2005**, *14*, pp. N21-N25.

[152] S. Sekine, S. Nakanishi, T. Miyake, K. Nagamine, H. Kaji, M. Nishizawa, *Langmuir* **2010**, *26*, pp. 11526-11529.

[153] J. U. Lind, T. S. Hansen, A. E. Daugaard, S. Hvilsted, T. L. Andresen, N. B. Larsen, *Macromolecules* **2011**, *44*, pp. 495-501.

[154] R. Konradi, B. Pidhatika, A. Mühlebach, M. Textor, *Langmuir* **2008**, *24*, pp. 613-616.

[155] R. Hoogenboom, *Angewandte Chemie International Edition* **2009**, *48*, pp. 7978-7994.

[156] B. Pidhatika, J. Moller, V. Vogel, R. Konradi, *CHIMIA International Journal for Chemistry* **2008**, *62*, pp. 264-269.

[157] B. Pidhatika, J. Möller, E. M. Benetti, R. Konradi, E. Rakhmatullina, A. Mühlebach, R. Zimmermann, C. Werner, V. Vogel, M. Textor, *Biomaterials* **2010**, *31*, pp. 9462-9472.

[158] D. W. Branch, B. C. Wheeler, G. J. Brewer, D. E. Leckband, *Biomaterials* **2001**, *22*, pp. 1035-1047.

[159] G. Bernardo, D. Vesely, *European Polymer Journal* **2007**, *43*, pp. 938-948.

[160] B. Winther-Jensen, K. West, *Macromolecules* **2004**, *37*, pp. 4538-4543.

[161] R. Luxenhofer, R. Jordan, *Macromolecules* **2006**, *39*, pp. 3509-3516.

[162] M. W. M. Fijten, C. Haensch, B. M. van Lankvelt, R. Hoogenboom, U. S. Schubert, *Macromolecular Chemistry and Physics* **2008**, *209*, pp. 1887-1895.

[163] C. Weber, R. C. Becer, A. Baumgaertel, R. Hoogenboom, U. S. Schubert, *Polymers* **2009**, *12*, pp. 149-165.

[164] T. Kagiya, S. Narisawa, T. Maeda, K. Fukui, *Journal of Polymer Science Part B: Polymer Letters* **1966**, *4*, pp. 441-445.

[165] F. Wiesbrock, R. Hoogenboom, M. A. M. Leenen, M. A. R. Meier, U. S. Schubert, *Macromolecules* **2005**, *38*, pp. 5025-5034.

[166] F. Wiesbrock, R. Hoogenboom, C. H. Abeln, U. S. Schubert, *Macromolecular rapid communications* **2004**, *25*, pp. 1895-1899.

[167] B. Weng, R. L. Shepherd, K. Crowley, A. J. Killard, G. G. Wallace, *Analyst* **2010**, *135*, pp. 2779-2789.

[168] T. S. Hansen, O. Hassager, N. B. Larsen, N. B. Clark, *Synth. Met.* **2007**, *157*, pp. 961-967.

[169] N. Sakmeche, S. Aeiyach, J. J. Aaron, M. Jouini, J. C. Lacroix, P. C. Lacaze, *Langmuir* **1999**, *15*, pp. 2566-2574.

[170] C. Zhou, Z. Liu, X. Du, S. P. Ringer, *Synth. Met.* **2010**, *160*, pp. 1636-1641.

[171] Y. Wen, J. Xu, H. He, B. Lu, Y. Li, B. Dong, *J. Electroanal. Chem.* **2009**, *634*, pp. 49-58.

[172] J. M. Baskin, J. A. Prescher, S. T. Laughlin, N. J. Agard, P. V. Chang, I. A. Miller, A. Lo, J. A. Codelli, C. R. Bertozzi, *Proc. Natl. Acad. Sci. U. S. A.* **2007**, *104*, pp. 16793-16797.

[173] S. Akoudad, J. Roncali, *Electrochemistry communications* **2000**, *2*, pp. 72-76.

[174] W. J. Doherty III, R. J. Wysocki, N. R. Armstrong, S. S. Saavedra, *Macromolecules* **2006**, *39*, pp. 4418-4424.

[175] A. E. Daugaard, S. Hvilsted, *Macromolecular Rapid Communications* **2008**, *29*, pp. 1119-1125.

[176] A. D. Thomsen, E. Malmström, S. Hvilsted, *Journal of Polymer Science Part A: Polymer Chemistry* **2006**, *44*, pp. 6360-6377.

Acknowledgements

I would like to express my gratitude to everyone who contributed to this thesis. Especially, I would like to thank:

My main supervisor Niels B. Larsen: For being a great mentor throughout the process.

My co-supervisor Thomas L. Andresen: For the many helpful discussions and advices.

Thomas S. Hansen: For being my everyday discussion partner and advisor in the first years.

My additional major collaborators Anders E. Daugaard and Søren Hvilsted: For the fruitful research discussions and collaborations.

Janet Acikgöz and Marcus Textor: For making my external stay at ETH Zürich rewarding both on the personal and scientific level.

Ina Blom, Lene Hubert, Lotte Nielsen and Ole Kristoffersen: For the everyday technical assistance and for being the most positive and helpful colleagues.

Steen Skaarup: For the helpful advice on electro-chemistry.

Additionally, I would like to thank *all* my present and former colleagues in Poly-Cell and at DTU Nanotech in general, especially:

David Selmeczi, Maria Matchuk, Jan Kafka, Gertrud Hjortø, Maria Holmberg, Morten Hansen, Mark Olsen, Claus Nielsen, Pawel Utko, Rasmus Jølck, Noemi Rozlosnik and Katrine Kiilerich-Pedersen.

Finally, thanks to: Anine, Esben, Peter, Sophie, Stig, Thor and Troels, for sharing the burden of proof-reading this manuscript.

External Communication Activities

Peer-reviewed journal papers included in this thesis

COMPLEX SURFACE CONCENTRATION GRADIENTS BY STENCILED "ELECTRO-CLICK CHEMISTRY"
T.S. Hansen*, J.U. Lind*, A.E. Daugaard, S. Hvilsted, T.L. Andresen, N.B. Larsen
*these authors contributed equally
Langmuir **2010**, *26*, pp. 16171-16177

SOLVENT COMPOSITION DIRECTING CLICK-FUNCTIONALIZATION AT THE SURFACE OR IN THE BULK OF AZIDE-MODIFIED PEDOT
J.U. Lind, T.S. Hansen, A.E. Daugaard, S. Hvilsted, T.L. Andresen, N.B. Larsen
Macromolecules **2011**, *44* (3), pp. 495–501

FACILE MICROPATTERNING OF FUNCTIONAL CONDUCTIVE POLYMERS WITH MULTIPLE SURFACE CHEMISTRIES IN REGISTER
J.U. Lind, C. Acikgöz, A.E. Daugaard, S. Hvilsted, T.L. Andresen, M. Textor, N.B. Larsen
Manuscript submitted to Langmuir **2012**

Peer-reviewed journal papers not included in this thesis

ENHANCED TRANSDUCTION OF PHOTONIC CRYSTAL DYE LASERS FOR GAS SENSING VIA SWELLING POLYMER FILM
C.L.C. Smith, J.U. Lind, C.H. Nielsen, M.B. Christiansen, T. Buss, N.B. Larsen, A. Kristensen.
Optics Letters **2011**, *36*, pp. 1392-1394

INCREASED ADSORPTION OF HISTIDINE-TAGGED PROTEINS ONTO TISSUE CULTURE POLYSTYRENE
M. Holmberg, T.S. Hansen, J.U. Lind, G.M. Hjortø
Colloids and Surfaces B: Biointerfaces **2012** *92*, pp. 286–292

Conference contributions (presenter underlined)

Poster:
CELL CAPTURING CONDUCTING POLYMER MICROELECTRODES
J.U. Lind, T.L. Andresen, N.B. Larsen
GRC on the Science of Adhesion
New London, NH, USA, **2009**

Poster:
PREPARING BIO-MOLECULE GRADIENTS ON PEDOT-N_3 USING ELECTRO-CLICK REACTIONS
J.U. Lind, T.S. Hansen, T.L. Andresen and N. B. Larsen
International Conference on science and technology of Syntetic Metals (ICSM)
Kyoto, Japan, **2010**
*Awarded with the "2010 Synthetic Metals Young Scientist Award"

Oral presentation:
ELECTRO-CLICK ON CONDUCTING POLYMER FILMS
T.S. Hansen, J.U. Lind, A.E. Daugaard, S. Hvilsted, N.B. Larsen
International Conference on science and technology of Syntetic Metals (ICSM)
Kyoto, Japan, **2010**

Poster and abstract in Conference proceeding in *European Cells & Material* **2010**, Vol. 20. Suppl. 3, pp. 161
PREPARING BIO-MOLECULE GRADIENTS ON PEDOT-N_3 USING ELECTRO-CLICK REACTIONS
J.U. Lind, T.S. Hansen, T.L. Andresen, N. B.Larsen
International NanoBio Conference,
Zurich, Switzerland, **2010**

Poster and Conference Proceedings from *IEEE*:
SELECTIVE GAS SENSING FOR PHOTONIC CRYSTAL LASERS
C.L.C Smith, M.B. Christiansen, T. Buss, A. Kristensen, C.H. Nielsen, J.U. Lind, N.B. Larsen
Conference: Conference on Lasers and Electro-Optics (CLEO):
Baltimore, USA, **2011**

Poster and abstract in Conference Proceeding in *European Cells & Material* **2011**, 21, Suppl. 2, pp. 39
IMPLANT INFECTION (IMPLANT INFECTION (ANTIFOULING AND ANTIMICROBIAL SURFACE COATINGS THROUGH POLY(2-METHYL-2-OXAZOLINE))
C. Acikgoz, J. U. Lind, J. Nowakowska, M. Charnley, N. Khanna, R. Landmann, M. Textor
eCM XII: Implant Infection
Davos, Switzerland, **2011**

Poster:

ANTIFOULING AND ANTIMICROBIAL SURFACE COATINGS THROUGH POLY(2-METHYL-2-OXAZOLINE)

C. Acikgoz, J.U. Lind, M. Charnley, M. Textor

7th International Symposium "Molecular Mobility and Order in Polymer Systems"

St. Petersburg, Russia, **2011**

Poster:

DIRECTING FUNCTIONAL CHEMISTRIES ON MICROPATTERNED CONDUCTING POLYMERS FOR ALL-POLYMER CELL ANALYSIS MICROSYSTEMS

J.U. Lind, A.E. Daugaard, T.L. Andresen, C. Acikgöz, M. Textor, N. B. Larsen

MicroTAS

Seattle, WA, USA, **2011**

Appendices

Smart Surface Chemistries of Conducting Polymers

-for Guiding Cell Behavior in Polymeric Microsystems

Johan Ulrik Lind

Ph.D. Thesis

DTU Nanotech
Department of Micro- and Nanotechnology

· Ph.D. Thesis · Johan Ulrik Lind ·

· Technical University of Denmark · Department of Micro- and Nanotechnology ·

· February 2012 ·

Appendix 1

Syntheses of Alkyne Reactants

Syntheses of alkyne-PEG-GRDGS and alkyne-PEG-GRGDS

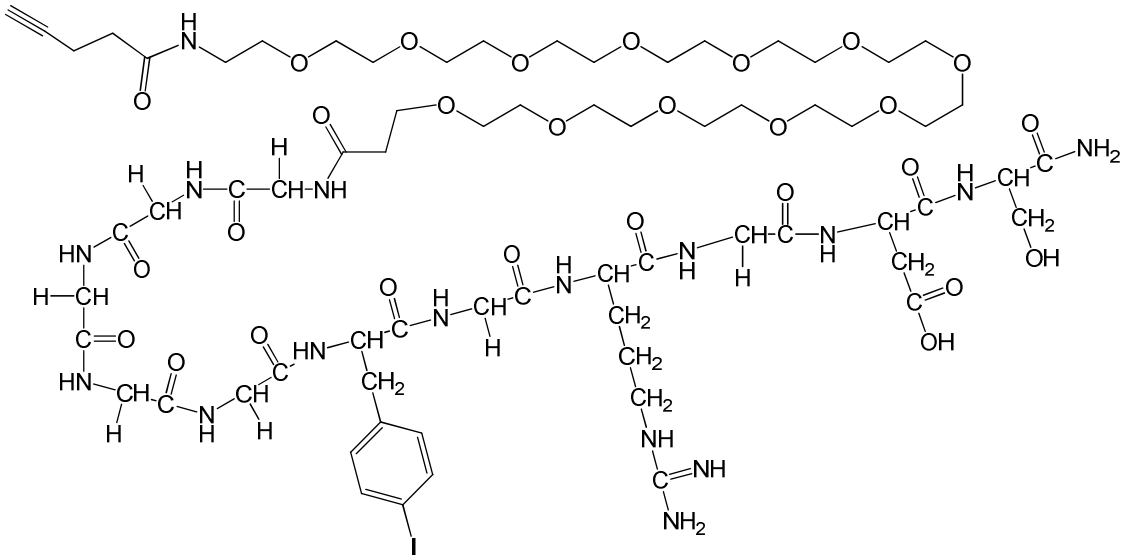

Figure 1 The structure of the alkyne-PEG-GRGDS (similar for "scrambled" alkyne-PEG-GRDGS, except for interchange of the glycine and aspartate moieties). Note the presence for a phenylalanine derivative containing iodine for XPS identification of the molecule(s).

Pentyne-PEG$_{11}$-G$_5$-F(4-iodo)-GRGDS (alkyne-PEG-GRGDS) was made using solid phase synthesis. Base labile Fmoc was used for protecting groups for the amines, and the employed resin was acid labile rink-amide. 2-(1H-7-Azabenzotriazol-1-yl)-1,1,3,3-tetramethyl-uronium-hexafluorophosphate-Methanaminium (HATU), Fmoc-Ser(tBu)-OH, Fmoc-Asp(OtBu)-OH, Fmoc-Arg(Pbf)-OH, Fmoc-4-Iodo-Phe-OH, Fmoc-Gly-OH and Rink Amide-AM Resin were bought from GL Biochem, Shanghai, China. Fmoc-NH-PEG$_{11}$-COOH, PEG1080, was acquired from IRIS biotech, Marktredwitz, Germany. 4-Pentynoic acid, (EDC), 2,4,6-Collidine, tri-fluoro-acetic-acid (TFA), Tri-isopropyl silane (TIPS), ninhydrin, piperidine, and all solvents, were acquired from Sigma-Aldrich.

Before reaction, the resin was swelled in Dichloromethane (DCM) for 1½hr. In each coupling step four equivalents of the new amino acid was used. The amino acid was first mixed with 3.9 equivalent HATU coupling reagent and 8 eq. 2,4,6-Collidine in Dimethyl-formamide (DMF), then added to the peptide, and allowed to react for 30 min. The beads were washed 4 times in DMF and 2 times in DCM, each washing step lasting 30 s. De-protection of the Fmoc group was done by washing twice for 2 min with a 20 vol% solution of piperidine in DMF.

Kaiser tests were performed to test the presence of free amino groups, between each reaction/de-protection step. The coupling of the PEG segment was done by performing two 1

hour long consecutive coupling reactions to ensure a successful binding of the PEG segment. The following pentynoic acid step was also allowed to react for 1h.

The peptide was cleaved from the resin using a solution of 2.5 vol% TIPS, 2.5 vol% milli-Q water and 95 vol% TFA. A cleaving time of 3 h was used. The cleaving solution containing the peptides was then dried on a rotary evaporator. The material remaining was then gently decanted five times using 5 ml diethyl ether.

The product was purified using preparative reverse phase High Performance Liquid Chromatography (RP-HPLC). The RP-HPLC was conducted on a 250 mm x 20 mm C18 column with a bead size of 5um and a pore size of 100 Å. Solvent A: 95/5 vol% / vol% H_20/Methanol 0.1vol% TFA. Solvent B: 99.9% Methanol/0.1% TFA. The solvents were degassed using a glass filter, prior to their use on the RP-HPLC. Solutions of the peptides were made in 50% Solvent A/Solvent B. In the RP-HPLC procedure, a linear gradient from 52 vol% to 54 vol% of Solvent A over 16 min were used. UV detection was set to 206 nm (carbonyl) and 257 nm (phenylalanine). An equivalent procedure was used for the fabrication and purification of the scrambled sequence peptide, Pentyne-PEG_{11}-G_5-F(4-iodo)-GRDGS (alkyne-PEG-GRDGS).

Outputs after RP-HPLC purification and freeze drying:

Pentyne-PEG_{11}-G_5-F(4-iodo)-GRGDS, (alkyne-PEG-GRGDS): 41.3 mg (16%)

Scrambled Pentyne-PEG_{11}-G_5-F(4-iodo)-GRDGS, (alkyne-PEG-GRDGS): 48.8 mg (19%)

The purity of the products was confirmed by MALDI-TOF MS using a Bruker Reflex IV MALDI-TOF, matrix 50 mg/ml 2,5-dihydroxy benzoic acid (DHB) in ethanol, and 0.1-1 mg/ml solutions.

Synthesis of PEG-alkyne

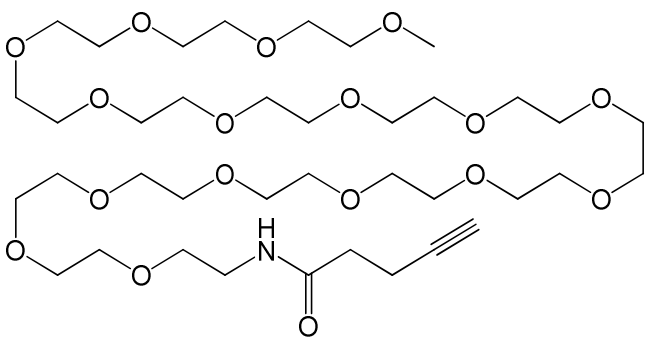

Figure 2 Structure of PEG-alkyne

α-Methoxy-poly(ethylene glycol)-ω-pent-4-ynamide, (PEG-alkyne) was made by coupling 2.0173 g MeO-PEG-NH_2 (PEG1155, 750 Da, PDI 1.2, Iris biotech, Marktredwitz, Germany) and 237.3 mg

(0.9 eq.) 4-Pentynoic acid (Sigma-Aldrich) in 60 mL dichloromethane using 155.24 mg (1 eq.) N-(3-Dimethylaminopropyl)-N´-ethyl-carbodiimide (EDC) (Sigma-Aldrich) overnight.

The reaction mixture was concentrated to dryness using a rotary evaporator and the product was hereafter purified by flash chromatography packed with silica gel (eluent: methanol/DCM 5:95). The product fractions were concentrated on a rotary evaporator and dried overnight on an oil pump. The yield was 916 mg (45.6%) output.

The purity of the products was confirmed by MALDI-TOF MS using a Bruker Reflex IV MALDI-TOF, matrix 50 mg/ml 2,5-dihydroxy benzoic acid (DHB) in ethanol, and using compound concentrations of 0.1-1 mg/ml. TLC (eluent: methanol/DCM 5:95) showed no presence of the starting materials. This was confirmed by ^{1}H- and ^{13}C-NMR.

^{13}C-NMR (63 MHz): (δ_C, ppm) 170.9(N-C=O), 83.08(C≡C-H) 71.9(CH_3-O-CH2) 70.6-69.7(O-C-C), 69.2(C-C≡C), 58.9(CH_3-O-CH2) 39.3(C-C-NH-C=O), 35.2(O=C-C-C) 14.8(C-C-C≡C)

^{1}H-NMR (250 MHz): (δ_H, ppm) 6.35(s, HN-C=O), 3.4-3.7(m, O-CH_2-CH_2-O), 3.35(s,O-CH_3) 2.4-2.6(m,O=C-CH_2-CH_2-C≡C), 1.95(H-C≡C).

MS (m/z, MALDI-TOF): 816.0 $\{M+H\}^+$.

Synthesis of NTA-alkyne

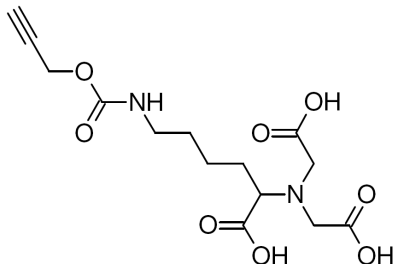

Figure 3 Structure of the NTA-alkyne

The NTA-alkyne molecule was synthesized and characterized by Dr. A.E. Daugaard.

N,N-Bis(carboxymethyl)-L-lysine hydrate (NTA, 0.100 g, 0.4 mmol) and $NaHCO_3$ (0.128 g, 1.5 mmol) was dissolved in H_2O (3.5 mL). Propargylchloroformate (0.05 g, 0.4 mmol) in toluene (2 mL) was added slowly at 0°C. The reaction mixture was stirred overnight at room temperature. Toluene was removed in vacuo and the residue was acidified with DOWEX. The product was isolated after lyophilization as a white solid (79.0 %, T_m= 135°C).

IR (cm^{-1}): 3405 (N-H); 3280 (C≡C-H); 3100-2800 (C-H); 2120 (C≡C); 1705 (COOH); 1615 OC(O)N); 1395 (C-N); 1255, 1135 (C-O).

^{1}H-NMR (300 MHz) D_2O, δ_H, (ppm): 1.2-1.7 (m, 6 H, CH_2-CH_2); 2.92 (t, ^{4}J = 2.2 Hz, 1 H, C≡C-H); 3.18 (t, ^{3}J =5.9 Hz, 2 H, OC(O)N-CH_2); 3.82 (m, 5 H, N-CH_2-COOH, N-CH-COOH); 4.69 (m, 2 H, OCH_2-C≡CH).

^{13}C-NMR (75 MHz) D_2O, δ_C, (ppm): 23.6, 26.5, 28.6 (3 C, CH_2-CH_2); 40.1 (1 C, OC(O)N-CH_2); 52.7 (1 C, C≡C-CH_2); 55.5 (2 C, N-CH_2-COO); 68.3 (1 C, N-CH-COOH); 75.7 (1 C, HC≡C); 78.8 (1 C, HC≡C-CH_2); 157.6 (1 C, OC(O)N); 170.5 (2 C, CH_2-COOH); 172.8 (1 C, CH-COOH).

MS (m/z, ESI): 367 $\{M+Na\}^+$.

NMR spectroscopy was performed on a 300 MHz Cryomagnet from Spectrospin & Bruker (^{1}H-NMR at 300 MHz, ^{13}C-NMR at 75 MHz), at room temperature.

IR was performed on a PerkinElmer Spectrum One model 2000 Fourier transform infrared system with a universal attenuated total reflection sampling accessory on a ZnSe/diamond composite.

Synthesis of hydroxyl-terminated Poly(2-methyl-2-Oxazoline)s

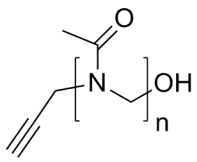

Figure 4 Structure of Propargyl-Poly(2-methyl-2-Oxazoline) (alkyne-PMOXA-OH)

The PMOXA molecules were synthesized and characterized by Dr. C. Acikgöz

Hydroxyl-terminated propargyl-PMOXA (alkyne-PMOXA-OH) was prepared by living cationic ring opening polymerization as previously described [154, 156, 157, 161, 162, 164]. The cationic ring opening polymerization of 2-methyl-2-oxazoline was initiated with addition of propargyl p-toluenesulfonate at initiator ratios of 1:20, 1:50 and 1:100. The polymerization was terminated with Na_2CO_3/water to obtain hydroxyl-terminated PMOXA. The polymers were purified by dialysis (2 times 24 h; Spectrum Laboratories Inc., Spectra/Por 7). PMOXA-OH was collected as a white solid after lyophilization and characterized by proton nuclear magnetic resonance (^{1}H NMR) spectroscopy (500 MHz, Bruker). By comparison the integrals from the methylene group adjacent to the acetylene group and the methylene groups in the backbone, the degree of polymerizations were found to be approximately 16, 60 and 109, close to the expected values of 20, 50, 100 respectively.

^{1}H NMR (D_2O): δ 4.0 - 4.2 (CH-C-C**H2**-N-), 3.3 - 3.7 (-C**H2**-N(CH_3-C=O)), 1.8 - 2.2 ppm (-(C=O)-C**H3**).

Synthesis of carboxy-terminated Poly(2-methyl-2-Oxazoline)s

The PMOXA molecules were synthesized and characterized by Dr. C. Acikgöz

Carboxy-terminated alkyne-PMOXA was prepared by living cationic ring opening polymerization with an initial monomer:initiator ratio of 50. The 2-methyl-2-oxazoline (MeOx) was dissolved in acetonitrile under argon and propargyl p-toluenesulfonate was added at 0˚C under argon. The mixture was then heated to 70˚C for 20 h. Subsequently, the reaction mixture was cooled to room temperature and the reaction was quenched by addition of ethyl piperidine-4-carboxylate for 12 h. The solvent was removed under reduced pressure to yield clear colorless oil. After addition of water, the polymers were purified by dialysis. (2 times 24 h; Spectrum Laboratories Inc., Spectra/Por 7). PMOXA-$COOC_2H_5$ was collected as a white solid after lyophilization. The carboxy ethyl ester (-$COOC_2H_5$) functionalized PMOXA was further reacted with sodium hydroxide solution at pH = 14 and room temperature for 24 h, resulting in alkyne-PMOXA-COOH. The polymers were purified and lyophilized using the same procedure as described above. Proton (^{1}H NMR) spectroscopy was performed to confirm the chemical structure of the synthesized polymers. By comparison the integrals from the methylene group adjacent to the acetylene group and the methylene groups in the backbone, the degree of polymerizations were found to be approximately 55.

^{1}H NMR (D_2O): δ 4.0 - 4.2 (CH-C-C**H**$_2$-N-), 3.3 - 3.7 (-C**H**$_2$-N(CH_3-C=O)), 1.8 - 2.2 ppm (-(C=O)-C**H**$_3$).

Synthesis of hydroxyl-terminated 2-methyl-2-Oxazoline in a Microwave Synthesizer

The PMOXA molecules were synthesized and characterized by Dr. C. Acikgöz

PMOXA synthesis assisted by microwave, was conducted in a similar manner to earlier reports [163, 165, 166]. Propargyl p-toluenesulfonate, MeOx and acetonitrile were prepared in a pre-dried microwave vial under inert conditions. The monomer to initiator ratio was 50 and the volume was 20 ml. The vial was capped and heated to 140˚C for 2 min. After the reaction, Na_2CO_3/water was added to terminate the polymerization. The polymers were purified by dialysis (2 times 24 h; Spectrum Laboratories Inc., Spectra/Por 7). Alkyne-PMOXA-OH was collected as a white solid after lyophilization and characterized by proton nuclear magnetic resonance (^{1}H NMR) spectroscopy (500 MHz, Bruker) similar to above.

Appendix 2

Syntheses of Modified Polystyrene Polymers

Synthesis of Poly-[(4-prop-2-yn-1-yloxy)-styrene-ran-styrene] (PS-alkyne)

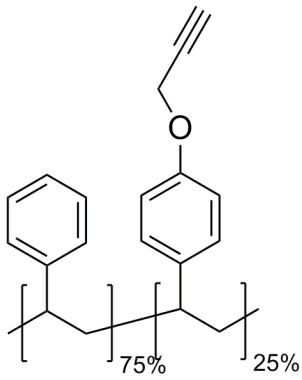

Figure 5 Poly[(4-prop-2-yn-1-yloxy)-styrene-ran-styrene] (PS-alkyne)

PS-alkyne was synthesized and characterized by Dr. A.E. Daugaard

A randomized co-polymer of styrene and an alkyne-functionalized styrene was fabricated in accordance with former reports.[175, 176] The polymer was based on 25% alkyne functional monomer and 75% standard styrene monomer.

Synthesis of 4-(azidomethyl)styrene (PS-N_3)

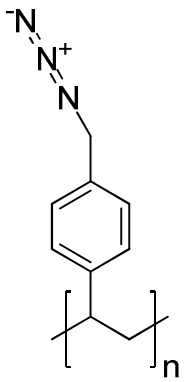

Figure S6. Structure of poly(4-(azidomethyl)styrene (PS-N_3)

PS-N_3 was synthesized and characterized by Dr. A.E. Daugaard.

2,2'-Azobisisobutyrylnitrile (AIBN, 71.2 mg, 0.4 mmol), 4-(chloromethyl)styrene (10 mL, 71.0 mmol and xylene were mixed in a Schlenk tube and the solution was bubbled through with

nitrogen for 30 min. The polymerization was run under a positive nitrogen pressure at 65°C for 18 h. The polymer was precipitated in methanol, filtered and dried in vacuo. The isolated intermediate (poly(4-(chloromethyl)styrene)) was a white powder and was used for the following step without further purification (6.4 g, Mn= 30000 g/mol, PDI= 1.7).

FT-ATR-IR (cm-1): 3100-2800 (C-H stretch); 1612+1510 (aromatic ring stretch); 672 (C-Cl stretch).

^{1}H-NMR($CDCl_3$, 300 MHz, δH, ppm): 1.39 (m, 2H, CH_2-CH); 1.70 (m, 1H, CH-CH_2); 4.52 (s, 2H, CH_2-N_3); 6.49, 7.05 (2xm, 4H, aromatic H).

HSQC confirmed the following proton/carbon correlations (δH/δC (ppm)): 1.39/41.6 (CH-CH_2); 1.70/38.7 (CH-CH_2-ph); 4.52/44.9 (CH_2-N_3); 6.49/126.4 (aromatic CH); 7.05/127.0 (aromatic CH).

Poly(4-(chloromethyl)styrene) (5.18 g, 34.0 mmol functional group) was dissolved in DMF (100 mL) and NaN_3 (2.75 g, 42.4 mmol) was added to the solution. The reaction mixture was stirred at 40°C for 18 h under nitrogen. After reaction the excess of reagent was removed by precipitation into H_2O. The precipitate was isolated by filtration and rinsed with copious amounts of H_2O and methanol. The solid was dissolved in THF and precipitated in methanol to afford poly(4-(azidomethyl)styrene) as a white powder (4.62 g, 86%).

FT-ATR-IR(cm^{-1}): 3100-2800 (C-H stretch); 2090 (C-N_3 stretch); 1612+1510 (aromatic ring stretch).

^{1}H-NMR($CDCl_3$, 300 MHz, δ_H, ppm): 1.39 (m, 2H, CH_2-CH); 1.69 (m, 1H, CH-CH_2); 4.24 (s, 2H, CH_2-N_3); 6.48, 6.97 (2xm, 4H, aromatic H).

HSQC confirmed the following proton/carbon correlations (δ_H/δ_C (ppm)): 1.39/44.9 (CH-CH_2); 1.69/40.4 (CH-CH_2-ph); 4.24/54.0 (CH_2-N_3); 6.48/127.7 (aromatic CH); 6.97/127.7 (aromatic CH).

NMR spectroscopy was performed on a 300 MHz Cryomagnet from Spectrospin & Bruker (^{1}H-NMR at 300 MHz, ^{13}C-NMR at 75 MHz), at room temperature.

IR was performed on a PerkinElmer Spectrum One model 2000 Fourier transform infrared system with a universal attenuated total reflection sampling accessory on a ZnSe/diamond composite.

Appendix 3

Complex Surface Concentration Gradients by Stenciled "Electro Click Chemistry"

Langmuir **2010**, *26*, pp. 16171-16177

Langmuir
Article
pubs.acs.org/Langmuir
© 2010 American Chemical Society

Complex Surface Concentration Gradients by Stenciled "Electro Click Chemistry"

Thomas S. Hansen,[†,§] Johan U. Lind,[†,§] Anders E. Daugaard,[‡] Søren Hvilsted,[‡] Thomas L. Andresen,[†] and Niels B. Larsen*,[†]

[†]*Department of Micro- and Nanotechnology, Technical University of Denmark, DTU Nanotech, Frederiksborgvej 399, 4000 Roskilde, Denmark, and* [‡]*Department of Chemical and Biochemical Engineering, Technical University of Denmark, Søltofts Plads, Building 227, 2800 Kgs. Lyngby, Denmark.*
[§]*These authors contributed equally*

Received July 1, 2010. Revised Manuscript Received September 7, 2010

Complex one- or two-dimensional concentration gradients of alkynated molecules are produced on azidized conducting polymer substrates by stenciled "electro click chemistry". The latter describes the local electrochemical generation of catalytically active Cu(I) required to complete a "click reaction" between alkynes and azides at room temperature. A stencil on the counter electrode defines the shape and multiplicity of the gradient(s) on the conducting polymer substrate, while the specific reaction conditions control gradient steepness and the maximum concentration deposited. Biologically active ligands including cell binding peptides are patterned in gradients by this method without losing their biological function or the conductivity of the polymer.

Introduction

Chemical concentration gradients in one or more dimensions are essential to numerous biological processes, for example, during development of animal organisms[1] and for the proper function of the mammalian immune system.[2] In vitro models to study these processes have been pursued extensively through the generation of concentration gradients in solution, in gels, or at surfaces to mimic the appropriate in vivo cell environment. Gradients of surface-immobilized (bio)chemistry are particularly relevant for exploring directed cell migration (haptotaxis). This will typically require a gradient steepness sufficient for a mammalian cell to sense a surface concentration difference between its anterior and posterior ends (tens of micrometers), therefore calling for gradients of lengths from several tens of micrometers to millimeter range.[3]

Stable, covalently bound, and well-defined surface gradients in complex patterns are not easily established by existing procedures. Gold is probably the most widely employed surface gradient substrate based on the versatile reversible chemisorption process of thiols and due to its excellent properties for many types of electrochemical analysis. However, material and processing costs are high, and gold itself may not be well suited for many biological applications, for example, involving the culture of cells. Inexpensive and easily processed chemically functionalizable conducting polymers may be used for a range of electrochemical processes, as substitute for gold electrodes. In addition, they may be used as a passive chemically patterned substrate after their electrical properties have been employed to generate chemical patterns of interest. Here, we present a method for generating gradients of covalently bound molecules in arbitrary two-dimensional (2D) shapes on reactive electrically conducting polymers, based on "electro click chemistry".[4,5] We demonstrate that proteins and biologically active peptides can be attached while retaining the functionality of the attached compounds and the conductivity of the polymer. Furthermore, we explore the experimental parameters governing gradient shape and steepness using easily traceable small molecules.

A number of other methods for making surface gradients have been reported in literature, as excellently reviewed by Genzer and Bhat.[6] A common approach for creating a gradient of adsorbed proteins is via diffusion between parallel streams of differing concentrations in a microsystem.[7] Gradients based on self-assembled monolayers (SAMs) on gold using diffusion,[8,9] using controlled ozone exposure,[10] and in-plane voltage drop[11] have also been described. Both the parallel stream setup and diffusion based gradients are limited to simple linear gradients and unspecific binding. Bipolar gold electrodes have recently been used

*To whom correspondence should be addressed. E-mail: niels.b.larsen@nanotech.dtu.dk.

(1) von Philipsborn, A. C.; Lang, S.; Loeschinger, J.; Bernard, A.; David, C.; Lehnert, D.; Bonhoeffer, F.; Bastmeyer, M. Growth Cone Navigation in Substrate-Bound Ephrin Gradients. *Development* **2006**, *133*, 2487–2495.
(2) Luster, A. D.; Alon, R.; von Andrian, U. H. Immune Cell Migration in Inflammation: Present and Future Therapeutic Targets. *Nat. Immunol.* **2005**, *6*, 1182–1190.
(3) Rhoads, D. S.; Guan, J. L. Analysis of Directional Cell Migration on Defined FN Gradients: Role of Intracellular Signaling Molecules. *Exp. Cell Res.* **2007**, *313*, 3859–3867.
(4) Devaraj, N. K.; Dinolfo, P. H.; Chidsey, C. E. D.; Collman, J. P. Selective Functionalization of Independently Addressed Microelectrodes by Electrochemical Activation and Deactivation of a Coupling Catalyst. *J. Am. Chem. Soc.* **2006**, *128*, 1794–1795.
(5) Hansen, T. S.; Daugaard, A. E.; Hvilsted, S.; Larsen, N. B. Spatially Selective Functionalization of Conducting Polymers by "Electroclick" Chemistry. *Adv. Mater.* **2009**, *21*, 4483–4486.
(6) Genzer, J.; Bhat, R. R. Surface-Bound Soft Matter Gradients. *Langmuir* **2008**, *24*, 2294–2317.
(7) Jeon, N. L.; Baskaran, H.; Dertinger, S. K. W.; Whitesides, G. M.; Van de Water, L.; Toner, M. Neutrophil Chemotaxis in Linear and Complex Gradients of Interleukin-8 Formed in a Microfabricated Device. *Nat. Biotechnol.* **2002**, *20*, 826–830.
(8) Chaudhury, M. K.; Whitesides, G. M. How to make Water Run Uphill. *Science* **1992**, *256*, 1539–1541.
(9) Thome, J.; Himmelhaus, M.; Zharnikov, M.; Grunze, M. Increased Lateral Density in Alkanethiolate Films on Gold by Mercury Adsorption. *Langmuir* **1998**, *14*, 7435–7449.
(10) Gallant, N. D.; Lavery, K. A.; Amis, E. J.; Becker, M. L. Universal Gradient Substrates for "Click" Biofunctionalization. *Adv. Mater.* **2007**, *19*, 965.
(11) Terrill, R. H.; Balss, K. M.; Zhang, Y. M.; Bohn, P. W. Dynamic Monolayer Gradients: Active Spatiotemporal Control of Alkanethiol Coatings on Thin Gold Films. *J. Am. Chem. Soc.* **2000**, *122*, 988–989.

for patterned desorption of SAMs to form line gradients[12] or simple radial gradients.[13] Light assisted photocoupling has been demonstrated for generating complex surface gradients.[14,15] The main advantage of light controlled gradients is direct access to produce complex structures with high resolution. The drawbacks are expensive and advanced equipment and the requirement for special chemicals that are not commercially available.

We suggest five main advantages of our stenciled electro click chemistry approach: (i) The principle is based upon the well-known "click chemistry" offering a high degree of versatility and a high number of reagents available; (ii) very complex gradients can be established with multiple functionalities, for example, overlapping gradients of orthogonal ligand chemistry on the same substrate; (iii) the species are covalently bound to support long-term stability; (iv) the substrate is conducting and can therefore be combined with electrical analysis tools such as impedance spectrometry; and (v) the conducting polymer substrate can easily be micropatterned before or after the gradient functionalization.[16−18]

The reaction between azide groups and terminal alkynes by copper(i)-catalyzed azide−alkyne cycloaddition (CuAAC)[19,20] is one of the most widely applied types of "click chemistry".[21] Electro click chemistry was introduced by Devaraj et al.[4] and differs from the standard reaction in that the Cu(I) catalyst is generated electrochemically. Since the catalyst can be generated locally through electrochemical reduction of Cu(II) to Cu(I), the areas of reaction can be controlled. We and others have recently shown that microscopic interdigitated electrode arrays of the electrically conductive polymer poly-3,4-(1-azidomethylethylene)-dioxythiophene (PEDOT-N_3)[22,23] can be selectively functionalized by this method.[5]

Here, we show that the amount of catalyst generated is determined by the spatial confinement of the active electrodes. The further the distance between the counter electrode and the reactive surface, the slower the catalyst generation. We demonstrate how this condition can be used for creating surface gradients of alkynated biologically active molecules on PEDOT-N_3 substrates. Gradients of two classes of biologically relevant molecules are presented: The first is an alkynated peptide containing the RGD tripeptide motif (alkyne-PEG-GRGDS, see Supporting Information Figure S1). This motif is well-known as a cellular adhesion ligand for cells expressing appropriate integrins.[24] The second molecule investigated is an alkynated nitrilotriacetic acid (NTA-alkyne, see Supporting Information Figure S2) capable of capturing proteins with an oligohistidine tag through Ni coordination.[25] The general influence of experimental parameters on the gradient shape is explored by reaction with a small alkynated fluorocarbon (EBTB[5]) for which the degree of reaction across the reaction zone is easily quantified by imaging X-ray photoelectron spectroscopy (XPS).

Experimental Section

PEDOT-N_3 was synthesized according to our reported procedure.[22] Syntheses of the alkyne reactants are described in the Supporting Information. For all samples, PEDOT-N_3 was spin-coated and polymerized into a thin film in situ on a cyclic olefin copolymer (COC) support as described briefly in the Supporting Information and in greater detail in our former work.[22]

Alkyne-PEG-GRGDS-PEG and EBTB Gradient Sample Fabrication. A copper plate was partially covered with a transfer adhesive (ARcare 90106, Adhesive Research, Glen Rock, PA) in which a 0.5 mm wide slit was cut using a CO_2 laser (48-5S Carbon Dioxide laser, Synrad Inc. USA) to form the pattern stencil. The copper electrode was placed above a PEDOT-N_3 film using a 190 μm thick spacer (see Supporting Information Figure S4), and clamps to keep the sample in place. The functionalization was done using a dimethyl sulfoxide (DMSO) solution of 1 mM alkyne-PEG-GRGDS and 1 mM $CuSO_4$, and application of a potential of −0.5 V on the PEDOT-N_3 versus the copper electrode for 5 min. After functionalization, the PEDOT-N_3 part could be removed. It was then reoxidized in ∼4 wt % Fe(III) tosylate in 90:10 water/butanol and then rinsed in Milli-Q water. The remaining azide groups were reacted for 6 h in a second click reaction in a 0.05 M NaCl aqueous solution containing 20 mM PEG-alkyne (see Supporting Information Figure S3), 0.67 mM $CuSO_4$, and 27 mM sodium ascorbate. The 1-ethynyl-3,5-bis-(trifluoromethyl)benzene (EBTB, see Figure 2A inset) gradient was fabricated by an equivalent procedure, only replacing the alkyne-PEG-GRGDS with EBTB and varying the reaction parameters as described in the Supporting Information.

NTA/eGFP Gradient Fabrication. The micropatterned stencil was produced by photolithography and subsequent reactive ion etching in a thin film of COC deposited on an evaporated copper electrode, as detailed in the Supporting Information ("Fabrication of mask for complex NTA gradients"). The PEDOT-N_3 surface was functionalized using a spacer thickness of 25 μm and a reaction time of only 2 min to produce steep gradients. A solution of 1 mM $CuSO_4$ and 1 mM NTA-alkyne was used. After functionalization, the sample was reoxidized in ∼4 wt % Fe(III) tosylate in 90:10 water/butanol and placed in 50 mM EDTA/50 mM TRIS pH 7.5 for 30 min. The sample was then immersed in 100 mM $NiSO_4$ for 30 min, washed with a solution of 150 mM NaCl and 10 mM TRIS pH 7.5, and blocked with a block buffer containing 150 mM NaCl, 10 mM TRIS pH 7.5, and 2 wt % bovine serum albumin (BSA). Reaction with 5 μg/mL His-tagged enhanced green fluorescent protein (eGFP, Cell Sciences, Canton, MA) in 150 mM NaCl and 10 mM TRIS occurred overnight at 4 °C. The sample was finally thoroughly washed with 1 M NaCl and 0.1 wt % Tween 20 in Milli-Q water.

Flow Chamber 3T3 Fibroblast Adhesion Studies. A homemade flow chamber with rectangular channel dimensions of 0.140 mm × 5 mm × 32 mm (h,w,l) was used. The chamber is assembled by connecting two homemade COC substrates, one

(12) Ulrich, C.; Andersson, O.; Nyholm, L.; Björefors, F. Formation of Molecular Gradients on Bipolar Electrodes. *Angew. Chem., Int. Ed.* **2008**, *47*, 3034–3036.
(13) Ulrich, C.; Andersson, O.; Nyholm, L.; Bjorefors, F. Potential and Current Density Distributions at Electrodes Intended for Bipolar Patterning. *Anal. Chem.* **2009**, *81*, 453–459.
(14) Buxboim, A.; Bar-Dagan, M.; Frydman, V.; Zbaida, D.; Morpurgo, M.; Bar-Ziv, R. A Single-Step Photolithographic Interface for Cell-Free Gene Expression and Active Biochips. *Small* **2007**, *3*, 500–510.
(15) Belisle, J. M.; Correia, J. P.; Wiseman, P. W.; Kennedy, T. E.; Costantino, S. Patterning Protein Concentration using Laser-Assisted Adsorption by Photobleaching, LAPAP. *Lab Chip* **2008**, *8*, 2164–2167.
(16) Hansen, T. S.; Hassager, O.; Larsen, N. B.; Clark, N. B. Micropatterning of a Stretchable Conductive Polymer using Inkjet Printing and Agarose Stamping. *Synth. Met.* **2007**, *157*, 961–967.
(17) Hansen, T. S.; West, K.; Hassager, O.; Larsen, N. B. Direct Fast Patterning of Conductive Polymers using Agarose Stamping. *Adv. Mater.* **2007**, *19*, 3261–3265.
(18) Hansen, T. S.; West, K.; Hassager, O.; Larsen, N. B. An all-Polymer Micropump Based on the Conductive Polymer Poly(3,4-Ethylenedioxythiophene) and a Polyurethane Channel System. *J. Micromech. Microeng.* **2007**, *17*, 860–866.
(19) Tornoe, C. W.; Christensen, C.; Meldal, M. Peptidotriazoles on Solid Phase: [1,2,3]-Triazoles by Regiospecific Copper(I)-Catalyzed 1,3-Dipolar Cycloadditions of Terminal Alkynes to Azides. *J. Org. Chem.* **2002**, *67*, 3057–3064.
(20) Rostovtsev, V. V.; Green, L. G.; Fokin, V. V.; Sharpless, K. B. A Stepwise Huisgen Cycloaddition Process: Copper(I)-Catalyzed Regioselective "Ligation" of Azides and Terminal Alkynes. *Angew. Chem., Int. Ed.* **2002**, *41*, 2596–2599.
(21) Kolb, H. C.; Finn, M. G.; Sharpless, K. B. Click Chemistry: Diverse Chemical Function from a Few Good Reactions. *Angew. Chem., Int. Ed.* **2001**, *40*, 2004–2021.
(22) Daugaard, A. E.; Hvilsted, S.; Hansen, T. S.; Larsen, N. B. Conductive Polymer Functionalization by Click Chemistry. *Macromolecules* **2008**, *41*, 4321–4327.
(23) Bu, H. B.; Götz, G.; Reinold, E.; Vogt, A.; Schmid, S.; Blanco, R.; Segura, J. L.; Bäuerle, P. Click"-Functionalization of Conducting Poly (3, 4-Ethylenedioxythiophene)(PEDOT). *Chem. Commun.* **2008**, *2008*, 1320–1322.
(24) Hersel, U.; Dahmen, C.; Kessler, H. RGD Modified Polymers: Biomaterials for Stimulated Cell Adhesion and Beyond. *Biomaterials* **2003**, *24*, 4385–4415.
(25) Sigal, G. B.; Bamdad, C.; Barberis, A.; Strominger, J.; Whitesides, G. M. A Self-Assembled Monolayer for the Binding and Study of Histidine Tagged Proteins by Surface Plasmon Resonance. *Anal. Chem.* **1996**, *68*, 490–497.

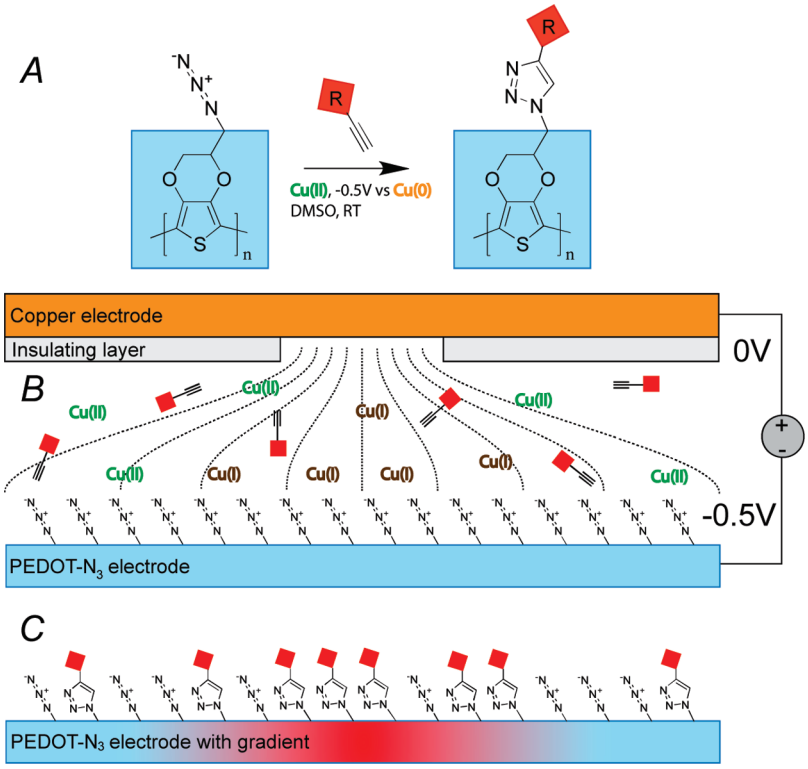

Figure 1. Schematic of the stenciled electro click chemistry process. (A) The Azide/alkyne click chemistry reaction depends on electrochemically generated Cu(I) from dissolved Cu(II). (B) A copper counter electrode with a patterned insulating coating forms a "stencil" for the fan-out of electrical field lines to the click reactive PEDOT-N_3 electrode. Application of a negative bias to the PEDOT-N_3 will lead to local generation of Cu(I) in a current dependent manner. (C) The local current and thus the rate of formation of Cu(I) depend on the distance to the exposed copper electrode, resulting in a gradual change in areal density of alkynes clicked onto the azides.

containing the gradient and the other defining inlets and outlets, with a strip of transfer adhesive. The adhesive was cut using a CO_2-laser to define the lateral geometry of the channel. The thickness of the adhesive sets the height of the channel. The flow experiments were conducted in HBSS buffer (Lonza) containing Mg^{2+} and Ca^{2+} to permit integrin binding to RGD moieties. A total of 250 μL of a 5 mio cells/mL suspension of 3T3 fibroblasts was injected into the flow chamber. The cells were allowed to adhere for 1 h. The flow rate was gradually increased to a flow corresponding to a surface shear stress of 0.1 Pa for 2 min. Flow through the chamber was controlled using a NE-1000 syringe pump (New Era Pump Systems, Wantagh, NY). Images were recorded on a Zeiss Axiovert S100 microscope (Carl Zeiss, Oberkochen, Germany), equipped with a LD Plan-NEOFLUAR 20×/0.4 objective and an iXon camera (Andor Technology, Belfast, Northern Ireland). The pump and the image acquisition were controlled by dedicated software running under LabView. The blue color of the PEDOT-N_3 did not adversely affect visualization of the cells by bright field microscopy.

X-ray Photoelectron Spectroscopy (XPS) Studies. Experiments were conducted using a K Alpha X-ray photoelectron spectrometer (Thermo Fisher Scientific, East Grinstead, U.K.). Monochromatized Al Kα radiation and charge compensation were employed. Line scan studies were performed using step sizes from 40 to 100 μm and employing an X-ray spot size equal to the step size. Spectra of the relevant elements were collected at each spot using data collection times varied from 10 to 80 s per spectrum depending on the element being sampled. Binding energies ranges were as follows: nitrogen, 392−413 eV; carbon, 278−299 eV; sulfur, 158−179 eV; oxygen, 524−545 eV; iodine, 613−634 eV; iron, 700−721 eV; copper, 926−947 eV; fluorine, 682−703 eV. The peak-fitting and analyses of the XPS spectra obtained were performed using the Avantage software package (Thermo Fisher Scientific, East Grinstead, U.K.). For XPS investigations of the alkyne-PEG-GRGDS gradient used for cell studies, two gradients were made using identical conditions. One was used for the XPS analysis and the other was used for the cellular experiments.

Results and Discussion

The general principle of the stenciled electro click process is illustrated in Figure 1. A PEDOT-N_3 coated surface is placed at a defined distance from a copper electrode partially covered with an insulator. A DMSO solution of 1 mM alkyne species and 1 mM $CuSO_4$ is injected, and a potential of −0.5 V versus the copper electrode is applied to the PEDOT-N_3 film. The applied potential reduces Cu(II) to the catalytically active Cu(I) on the PEDOT-N_3 surface, producing most Cu(I) in the areas with low resistance between the two electrodes, that is, in closest proximity. PEDOT-N_3 areas further away from the exposed parts of the copper electrode thus experience smaller degrees of reaction than the area just below the uncovered electrode.

Evidently a wide range of gradient patterns can be formed by altering the geometry of the exposed counter electrode. However the shape of the gradient produced is also strongly influenced by factors such as concentration, geometry of the setup, electrical potential, and reaction time. The influence of these properties was investigated to identify the dominant factors in gradient design. A model system with the fluorine-containing alkyne EBTB, see Figure 2A inset, was employed in these studies. EBTB contains six fluorine atoms per molecule and can be detected with high sensitivity and specificity using XPS. The findings based on the increasing fluorine signal were confirmed by a concomitant decrease in the characteristic signal of the unreacted azide groups.[5,22] Experiments were performed using varying reaction times, electrode spacings, electrical potential, EBTB (alkyne reactant) concentrations, and $CuSO_4$ (catalyst precursor) concentrations.

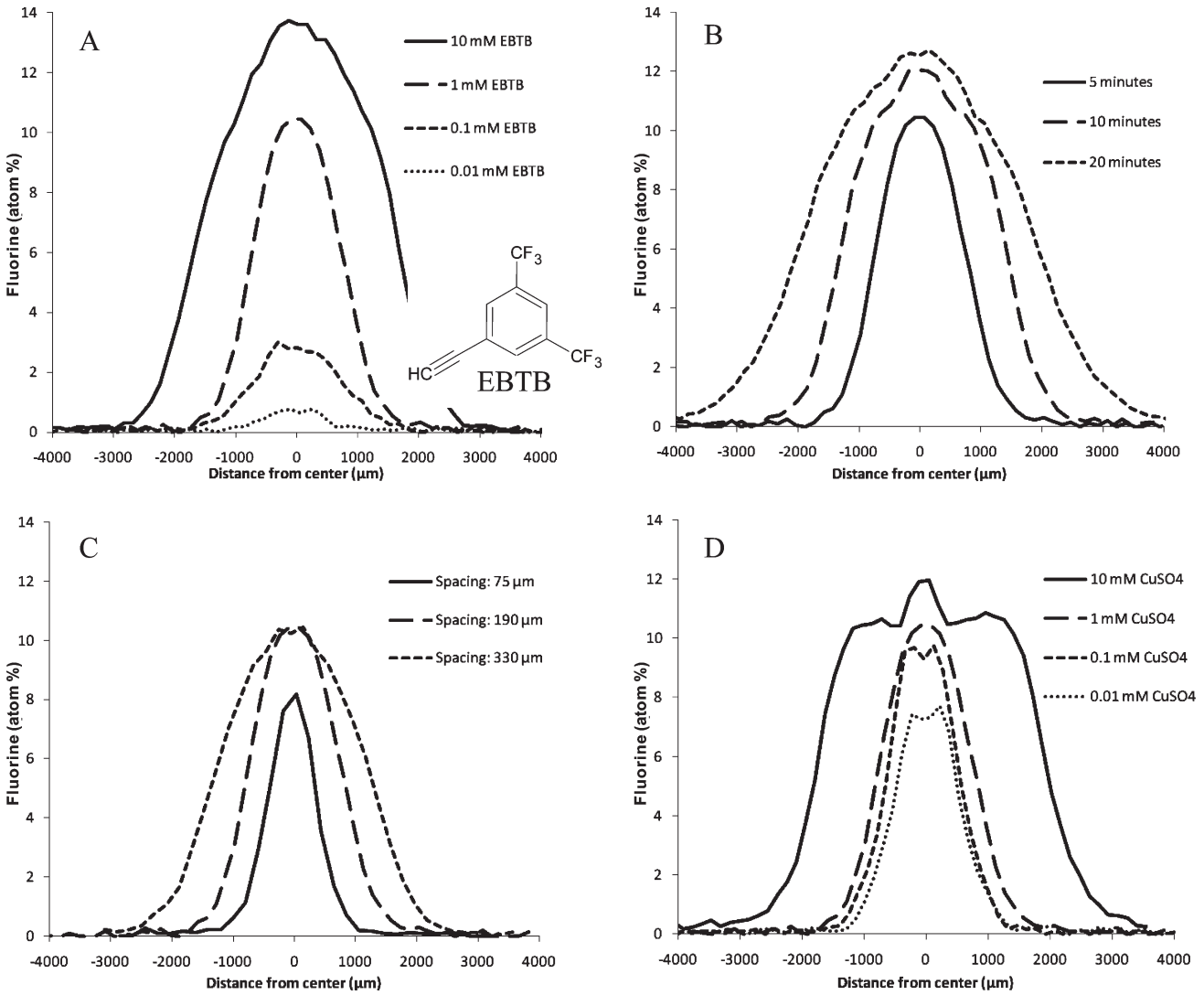

Figure 2. XPS line scan data on gradients reacted with EBTB (inset in A) with varying parameters. Varying the EBTB concentration (A) has a high impact on the amplitude of the gradient and, for the highest concentration used, also on the width. Reaction time (B) and electrode spacing (C) mainly affect the width of the gradient. The $CuSO_4$ concentration (D) has little overall influence except for the highest concentration employed. Reaction conditions except for the varied parameter were 1 mM $CuSO_4$, a potential of −0.5 V on the PEDOT-N_3 electrode, a reaction time of 5 min, and a spacing of 190 μm. All concentrations are given as the percentage of fluorine atoms.

The resulting gradients were analyzed using XPS line scans (Figure 2 and Supporting Information Figures S5 and S6). Figure 2A shows that the alkyne concentration mainly influences the maximum concentration (amplitude) of the gradient without affecting its width, except at very high concentrations. The alkyne concentration is therefore the best parameter for controlling the steepness and height of the gradient. Reaction time and electrode spacing primarily control the width of the gradient, as can be deduced from Figure 2B and C, suggesting that small electrode separations and low reaction times should be used for the generation of multiple gradients with submillimeter separations. Thus, multiple gradient designs can be made fast and reproducibly by varying these easily controlled parameters. The influence of the Cu(II) concentration is more complex (figure 2D). In the lower end of the range investigated, only small changes in the amplitude are observed. However, when increasing the concentration, a limiting amplitude appears to be reached and a distinctive broadening is observed.

The relative low influence of the $CuSO_4$ at low concentrations may arise from Cu(II) generation at the counter electrode, ensuring some degree of available Cu(II) although only small amounts are added. The origin of the odd gradient shape at 10 mM $CuSO_4$ might be related to the role of Cu(II) as catalyst precursor or due to its contribution to the solvent conductivity. This aspect was examined by substituting 90% of the $CuSO_4$ by $NiSO_4$, with the latter having no potential catalyst effect. The resulting shape of the gradient largely resembles that from using 10 mM $CuSO_4$ (Supporting Information Figure S5), suggesting that the shape is unrelated to catalyst generation. We further traced the origin of the odd shape by finite element modeling of the stenciled electro click chemistry system, as will be discussed in the next section. Experimentally, the effect of varying applying potentials was also investigated. Application of zero potential difference did not lead to any reaction, as expected, while more negative potentials led to slight overall broadening of the gradient profiles (Supporting Information Figure S6).

To validate and clarify the experimental findings using EBTB, a theoretical approach based on numerical simulations of the reaction using the commercial finite element modeling software package COMSOL was pursued (Supporting Information

Figures S7−S10). COMSOL can perform numerical simulations of diffusing species and electrical conduction simultaneous. The simulations were performed qualitatively as several physical constants of the system are unknown, in particular the reaction rate constant but also the diffusion constant of the species in DMSO and the electron transfer resistance between the polymer backbone and Cu(II). It is however possible to simulate a dimensionless system with the same characteristics and compare to the results observed using XPS analysis.

Equations 1−3 were used for calculating the concentration of Cu(I) as it was assumed that all the current passing through the liquid was used to reduce Cu(II) to Cu(I) at the interface between PEDOT-N_3 and the electrolyte.

$$\sigma \nabla^2 V = Q \tag{1}$$

$$j = \frac{Q_{\mathrm{PEDOTN_3}}}{F} \tag{2}$$

$$\sigma = \Lambda_{\mathrm{m}} C_{\mathrm{CuSO4}} \tag{3}$$

σ is the conductivity, V is the electrical potential, and Q is the charge flow. j is the flux of Cu(I) from the electrode, F is Faraday's constant, $Q_{\mathrm{PEDOTN_3}}$ is the current passing through the interface between the electrolyte and the PEDOT-N_3 film, and Λ_{m} is the molar conductivity. The reaction at the counter electrode was not considered in the simulation. The diffusion of the formed Cu(I) and the alkyne was simulated using Fick's second law of diffusion including a reaction rate term, r, for the alkyne (eq 4).

$$\frac{\partial C}{\partial t} = D\left(\frac{\partial^2 C}{\partial x^2} + \frac{\partial^2 C}{\partial y^2}\right) + r \tag{4}$$

The azide and triazole compounds were simulated as bound to a subdomain with a thickness mimicking the PEDOT-N_3 film. We have previously demonstrated that bulk reaction occurs[22] and it is therefore not possible to limit the reaction to a monolayer. The reaction of the alkyne and azide was assumed to be of second order for Cu(I) and alkyne, and first order for azide[26] (eq 5).

$$r_{\mathrm{triazole}} = k[\mathrm{Cu(I)}]^2[\mathrm{alkyne}]^2[\mathrm{azide}] \tag{5}$$

The system was made dimensionless using the height (h), the applied potential (V_0), the start concentration of alkyne ($c_{\mathrm{alk},0}$), time (t), and the molar conductivity (Λ_{m}) and then solved for the potential and the concentrations of alkyne, Cu(I), azide, and triazole. The variables and constants used are shown in Supporting Information Scheme S1.

The simulations did only reproduce the trends observed in the experiments if a complete simulation was conducted where diffusion and reaction rate terms were included. If only the current field or the generation of catalytic Cu(I) was considered, the simulation could not describe the experimental data to an acceptable degree (Figure 3). The simulations showed, as the experimental data, that the gradient amplitude is best controlled via the alkyne concentration. According to the simulations, this is caused by depletion of the alkyne (Supporting Information Figure S8B) in the volume proximal to the exposed copper counter electrode, thus making the alkyne the limiting reactant. The characteristic gradient shape at high $CuSO_4$ concentrations (see Figure 2D, 10 mM $CuSO_4$), consisting of a plateau with a small protrusion in the center, can also be explained by alkyne depletion. The plateau is reached because all alkyne in the solution has reacted. The small protrusion results from the slightly higher volume over the center of the sample, due to the two-layered fabrication method (Supporting Information Figures S4 and S7). Diffusion of Cu(I) also plays a significant role in determining the width of gradient, thus explaining the widening of the gradient over time. From the simulations, it can be concluded that parameters should be chosen so that the alkyne is not depleted, as this leads to complex gradients.

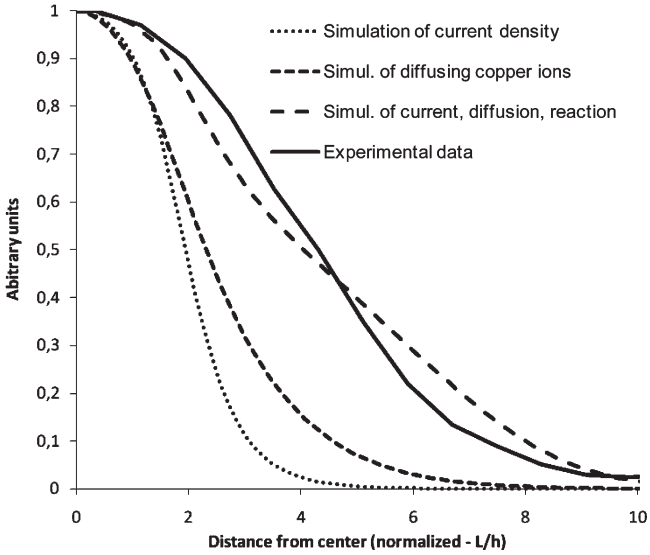

Figure 3. Degree of surface reaction as a function of distance to a center slit electrode as predicted by different simulation methods (simulation parameters in Supporting Information Scheme S1) or measured experimentally using an applied potential of −0.5 V, 1 mM $CuSO_4$, 1 mM EBTB, electrode spacing 190 μm, and 5 min reaction time. Neither a model including only the current density ("Simulation of current density") nor a model including only the generation and diffusion of Cu(I) ("Simulation of copper ion diffusion") gives a valid description of the experimental results. A simulation including current density, generation and diffusion of Cu(I), and removal of dissolved alkyne by reaction with azides in the surface film can approximately account for the shape of the experimental data. See the Supporting Information for details of the length scale normalization.

The applicability of stenciled electro click chemistry to form biologically active gradients was explored by forming surface gradients of alkyne-PEG-GRGDS, an RGD-containing peptide promoting cell adhesion. Azides remaining on the PEDOT-N_3 substrate after the gradient fabrication were reacted with a PEG-alkyne (see Supporting Information Figure S3) using a standard aqueous click reaction to reduce nonspecific cell adhesion. The alkyne-PEG-GRGDS-PEG includes a PEG spacer segment that serves to present the RGD motif to the cells on a PEG background, thus further limiting nonspecific interaction between cells and substrate.

A microfluidic channel was produced with the bottom surface being the gradient-modified PEDOT-N_3, and 3T3 fibroblast cells were allowed to adhere to the surface. Nonadherent cells were removed by flowing buffer through the chamber after 1 h of incubation. Figure 4B shows a mosaic of phase contrast images of the central channel parts with the remaining cells appearing

(26) Meldal, M.; Tornoe, C. W. Cu-Catalyzed Azide-Alkyne Cycloaddition. *Chem. Rev.* **2008**, *108*, 2952–3015.

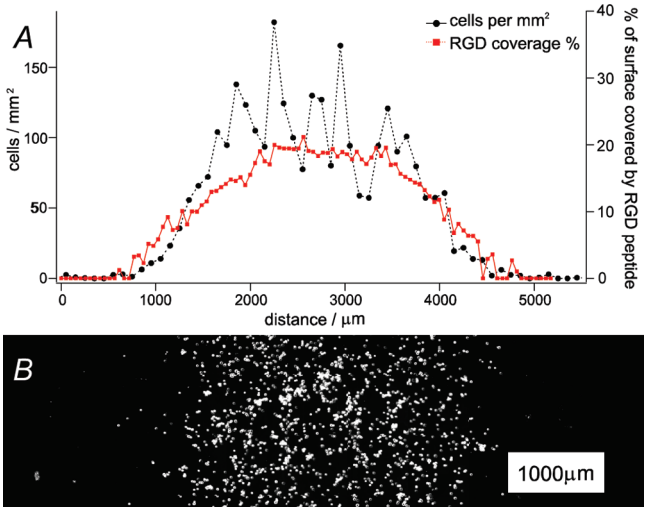

Figure 4. Surface gradient of cell-adhesive RGD-containing alkyne-PEG-GRGDS on PEDOT-N_3 and its cell-adhesive properties. (A) Comparison of the fractional alkyne-PEG-GRGDS coverage, calculated from XPS investigation of the substrate, to the adherent cell density observed in a flow chamber experiment on this surface. (B) Mosaic of phase contrast microscopy images of 3T3 fibroblast cells adhered to the alkyne-PEG-GRGDS gradient. Unreacted azides on the PEDOT-N_3 were postfunctionalized with a PEG-alkyne. The cells were allowed to adhere for 1 h, and nonadhered cells were washed off at a surface shear stress of 0.1 Pa.

bright. Control experiments using alkyne-PEG-GRDGS, that is, having a scrambled peptide sequence, showed no ability to induce cellular adhesion (data not shown), verifying that the cellular adhesion observed for the RGD peptides is biologically specific.

A phenylalanine residue labeled with iodine had been incorporated into the peptides, giving a unique and highly sensitive marker for the density of RGD peptides on the surface using XPS. The peak height ratio of the characteristic double nitrogen peak of azides was used as an additional tracer of the degree of reaction (data not shown),[5,22] although the nitrogens present in both the alkyne-PEG and the alkyne-PEG-GRDGS reagents complicated quantitative interpretation at intermediate degrees of reaction. After the second reaction with PEG, all azide signals were removed, signifying a complete surface coverage.

An overlay of cell count and RGD concentration is shown in Figure 4A. The figure shows a clear correlation between RGD density and the ability of the cells to adhere to the surface. This confirms that the cellular adhesion is induced by the peptides. This study shows that, above ~15% coverage of the surface with RGD peptides, the cellular adhesion varies within the same range, whereas markedly lower cellular adhesion is seen below 10% RGD.

Surface gradients of larger biomolecules, in particular proteins, may be formed in a two-step process through initial generation of a gradient of protein-capturing moieties. Here, we fabricate a gradient of an NTA-alkyne, (prop-2-ynyl 5-(*N*,*N*-bis(carboxymethyl)amino)-5-(*S*)carboxypentanecarbamate), that will capture His-tagged proteins via chelated Ni^{2+}. The widespread use of His-tagged proteins expands the applicability of our approach significantly. Figure 5A shows a schematic of the stencil used: A 2D array of 100 μm diameter holes is fabricated in the insulating layer on the copper counter electrode. This stencil is employed to form NTA-alkyne gradients on the PEDOT-N_3 surface, followed by immersion of the gradient surface in a Ni^{2+} containing solution, and final exposure to His-tagged eGFP (enhanced green fluorescent protein). The resulting gradients of

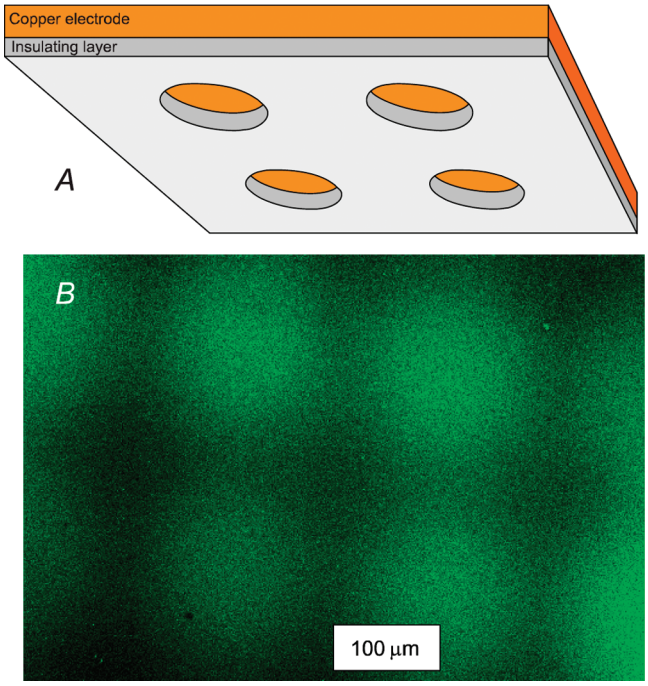

Figure 5. (A) Schematic of a stenciled copper counter electrode designed to establish separate microscopic surface gradients in a regular 2D array. The hole diameters are 100 μm, and the holes are laid out in a square grid with a center-to-center distance of 200 μm. (B) Fluorescence microscopy image of 2D gradients of NTA-alkyne formed on a PEDOT-N_3 surface, visualized by subsequent capture of His-tagged eGFP.

His-tagged eGFP were visualized by fluorescence microscopy (Figure 5B). Individual gradients emerge radially in registry with the stencil openings. It should be noted that an electrode spacing of only 25 μm and a reaction time of 2 min were used to limit the lateral extent of the individual gradients, in agreement with the mechanistic investigations using EBTB (cf. Figure 2B and C). This further exemplifies how the geometry of the gradient can be adjusted by the accessibility of the solution to the electrode.

Conclusion

We have demonstrated a method for fast production of gradients on an electrically conductive surface using stenciled electro click chemistry. The method can be used to make linear and complex 2D gradients of covalently bound molecules. The characteristics of the gradient fabrication technique have been examined using XPS and numerical simulations, and these studies confirm that a range of gradient patterns can be formed by varying simple parameters of the setup. Surface gradients of cell-binding or selective protein-binding moieties have been formed without adversely affecting their targeted interactions with biological entities. The method is thus well suited for making fast, reproducible, and complex gradients for investigations and manipulations of biological systems The method is not only of interest to biological research and cell handling systems based on conducting polymers: The generality of the electro click reaction should make it applicable to any conducting substrate presenting click-reactive moieties, for example, azidated or alkynated self-assembled monolayers.

Acknowledgment. The Danish Council for Technology and Innovation is acknowledged for financial support through the Innovation Consortium CEMIK, Grant 07-015463. The Danish

Council for Independent Research is also acknowledged for support through Grant 274-09-0101. David Selmeczi is thanked for his technical assistance with the microscope setup.

Supporting Information Available: Detailed description of the synthesis of alkynes; chemical structure of the alkynes; detailed description of the setup used for gradient formation; XPS analysis results of selected EBTB-clicked samples; detailed description and selected results of the COMSOL simulation. This material is available free of charge via the Internet at http://pubs.acs.org.

Complex surface concentration gradients by stencilled ”Electro click chemistry”

Thomas S. Hansen[1,†], Johan U. Lind[1 †], Anders E. Daugaard[2], Søren Hvilsted[2], Thomas L. Andresen[1], and Niels B. Larsen[1,*]

Supporting Information

Synthesis of alkyne-PEG-GRGDS and alkyne-PEG-GRDGS (see Figure S1):

Pentyne-PEG$_{11}$-Gly$_5$-(4-iodo-Phe)-Gly-Arg-Gly-Asp-Ser-NH$_2$ (alkyne-PEG-GRGDS) was made using solid phase synthesis. Base labile Fmoc was used for protecting groups for the amines, and the employed resin was acid labile rink-amide. 2-(1H-7-Azabenzotriazol-1-yl)-1,1,3,3-tetramethyl-uronium-hexafluorophosphate-Methanaminium (HATU), Fmoc-Ser(tBu)-OH, Fmoc-Asp(OtBu)-OH, Fmoc-Arg(Pbf)-OH, Fmoc-4-Iodo-Phe-OH, Fmoc-Gly-OH and Rink Amide-AM Resin were bought from *GL Biochem*, Shanghai, China. Fmoc-NH-PEG$_{11}$-COOH, *PEG1080,* was acquired from IRIS biotech, Marktredwitz, Germany. 4-Pentynoic acid, (EDC), 2,4,6-Collidine, tri-fluoro-acetic-acid (TFA), Tri-isopropyl silane (TIPS), ninhydrin, piperidine, and all solvents, were acquired from Sigma-Aldrich.

Before reaction, the resin was swelled in dichloromethane (DCM) for 1½hr. In each coupling step four equivalents of the new amino acid was used. The amino acid was first mixed with 3.9 equivalent (eq.)

HATU coupling reagent and 8 eq. 2,4,6-collidine in dimethylformamide (DMF), then added to the peptide, and allowed to react for 30min. The beads were washed 4 times in DMF and 2 times in DCM, each washing step lasting 30sec. De-protection of the Fmoc group was done by washing twice for 2 min with a 20% solution of piperidine in DMF.

Kaiser tests were performed to test the presence of free amino groups, between each reaction/de-protection step. The coupling of the PEG segment was done by performing two consecutive 1 hr coupling reactions to ensure a successful binding of the PEG segment. The following pentynoic acid step was also allowed to react for 1 hr.

The peptide was cleaved from the resin using a solution of 2.5%vol TIPS, 2.5%vol milli-Q water and 95% TFA. A cleaving time of 3 hrs was used. The cleaving solution containing the peptides was then dried on a rotary evaporator. The material remaining was then gently decanted five times using 5ml diethyl ether.

The product was purified using preparative reverse phase High Performance Liquid Chromatography (RP-HPLC). The RP-HPLC was conducted on a 250mm x 20mm C18 column with a bead size of 5um and a pore size of 100Å. Solvent A: 95/5 % H_20/MeOH 0.1% TFA. Solvent B: 99.9% MeOH/0.1% TFA. The solvents were degassed using a glass filter, prior to their use on the RP-HPLC.

Solutions of the peptides were made in 50% Solvent A/Solvent B. In the RP-HPLC procedure, a linear gradient from 52% to 54% of Solvent A over 16mins were used. UV detection was set to 206 nm (carbonyl) and 257 nm (phenylalanine).

An equivalent procedure was used for the fabrication and purification of the scrambled sequence peptide, *Pentyne-PEG$_{11}$-Gly$_5$-(4-iodo-Phe)-Gly-Arg-Asp-Gly-Ser-NH$_2$ (alkyne-PEG-GRDGS).*

Yields after RP-HPLC purification and freeze drying were:

Alkyne-PEG-GRGDS: 41.3mg (16%)

Alkyne-PEG-GRDGS: 48.8mg (19%)

The purity of the products was confirmed by MALDI-TOF MS using a Bruker Reflex IV MALDI-TOF, matrix 50mg/ml 2,5-dihydroxy benzoic acid (DHB) in ethanol, and 0.1-1mg/ml solutions.

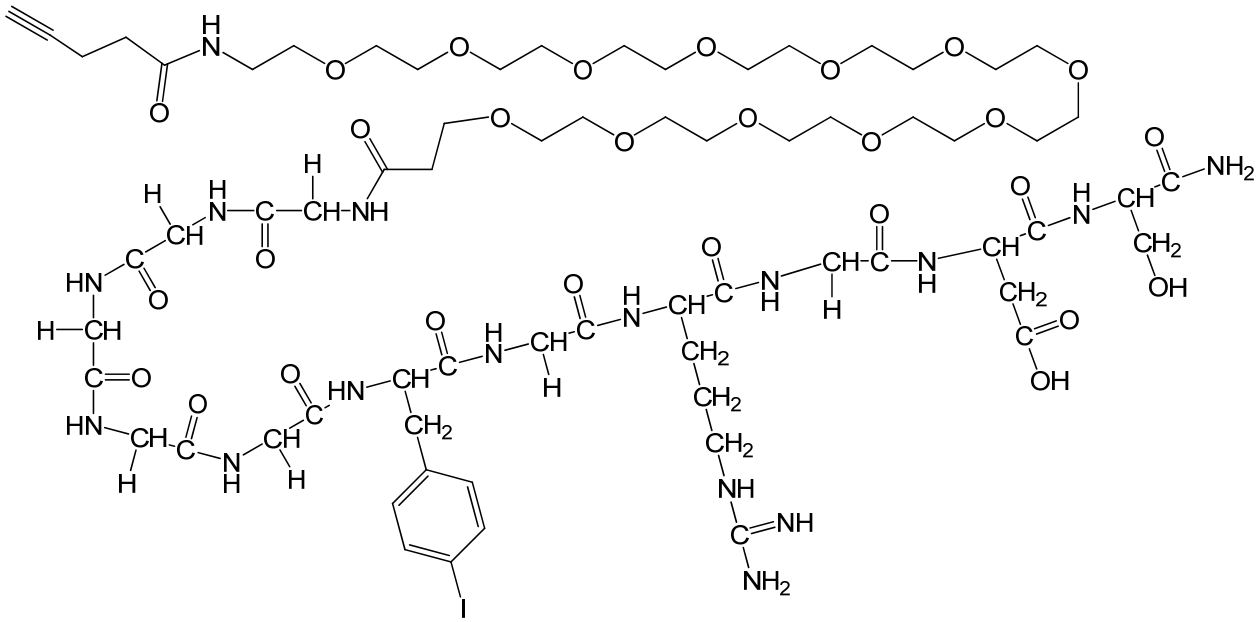

Figure S1: The structure of the alkyne-PEG-GRGDS (similar for "scrambled" alkyne-PEG-GRDGS, except for exchange of the last glycine and aspartate moeities).

Synthesis of NTA-alkyne (Prop-2-ynyl 5-(N,N-bis(carboxymethyl)amino)-5-(*S*)carboxypentanecarbamate) (see Figure S2):

N,N-Bis(carboxymethyl)-L-lysine hydrate (NTA, 0.100 g, 0.4 mmol) and $NaHCO_3$ (0.128 g, 1.5 mmol) was dissolved in H_2O (3.5 mL). Propargylchloroformate (0.05 g, 0.4 mmol) in toluene (2 mL) was added slowly at 0 ^oC. The reaction mixture was stirred overnight at room temperature. Toluene was removed *in vacuo* and the residue was acidified with DOWEX. The product was isolated after lyophilization as a white solid (79.0 %, T_m= 135 ^oC).

IR (cm^{-1}): 3405 (N-H); 3280 (C≡C-H); 3100-2800 (C-H); 2120 (C≡C); 1705 (COOH); 1615 OC(O)N); 1395 (C-N); 1255, 1135 (C-O).

^{1}H-NMR (300 MHz) D_2O, δ_H (ppm): 1.2-1.7 (m, 6 H, C*H*$_2$-CH$_2$); 2.92 (t, ^4J = 2.2 Hz, 1 H, C≡C-*H*); 3.18 (t, ^{3}J =5.9 Hz, 2 H, OC(O)NH-C*H*$_2$); 3.82 (m, 5 H, N-C*H*$_2$-COOH, N-C*H*-COOH); 4.69 (m, 2 H, OC*H*$_2$-C≡CH).

^{13}C-NMR (75 MHz) D_2O, δ_C (ppm): 23.6, 26.5, 28.6 (3 C, *C*H$_2$-CH$_2$); 40.1 (1 C, OC(O)N-*C*H$_2$); 52.7 (1 C, C≡C-*C*H$_2$); 55.5 (2 C, N-*C*H$_2$-COO); 68.3 (1 C, N-*C*H-COOH); 75.7 (1 C, H*C*≡C); 78.8 (1 C, HC≡*C*-CH$_2$); 157.6 (1 C, O*C*(O)N); 170.5 (2 C, CH$_2$-*C*OOH); 172.8 (1 C, CH-*C*OOH).

MS (m/z, ESI): 367 $\{M+Na\}^+$.

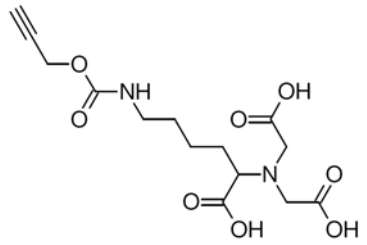

Figure S2: Structure of the NTA-alkyne

Synthesis of PEG-alkyne (see Figure S3):

α-Methoxy-poly(ethylene glycol)-ω-pent-4-ynamide, was made by coupling 2.0173g MeO-PEG-NH$_2$ (*PEG1155*, 750Da, PDI 1.2, Iris biotech, Marktredwitz, Germany) and 237.3mg (0.9 eq.) 4-Pentynoic acid (Sigma-Aldrich) in 60mL dichloromethane using 155.24mg (1.eq.) N-(3-Dimethylaminopropyl)-N´-ethyl-carbodiimide (EDC) (Sigma-Aldrich) overnight.

The reaction mixture was concentrated to dryness using a rotary evaporator and the product was hereafter purified by flash chromatography packed with silica gel (eluent: methanol/DCM 5:95). The product fractions were concentrated on a rotary evaporator and dried overnight on an oil pump. The yield was 916mg (45.6%) output.

MALDI-TOF MS confirmed the successful coupling had taken place. A Bruker Reflex IV MALDI-TOF, matrix 50mg/ml 2,5-dihydroxy benzoic acid (DHB) in ethanol, and 0,1-1mg/ml solutions of the product were applied.TLC (eluent: methanol/DCM 5:95) indicated no presence of the starting materials. This was confirmed by ^{1}H- and ^{13}C-NMR.

^{13}C-NMR(63 MHz): (δ_C, ppm) 170.9(N-C=O), 83.08(C≡C-H) 71.9(CH_3-O-CH2) 70.6-69.7(O-C-C), 69.2(C-C≡C), 58.9(CH_3-O-CH2) 39.3(C-C-NH-C=O), 35.2(O=C-C-C) 14.8(C-C-C≡C)

^{1}H-NMR (250 MHz): (δ_H, ppm) 6.35(s, HN-C=O), 3.4-3.7(m, O-CH_2-CH_2-O), 3.35(s,O-CH_3) 2.4-2.6(m,O=C-CH_2-CH_2-C≡C), 1.95(H-C≡C),

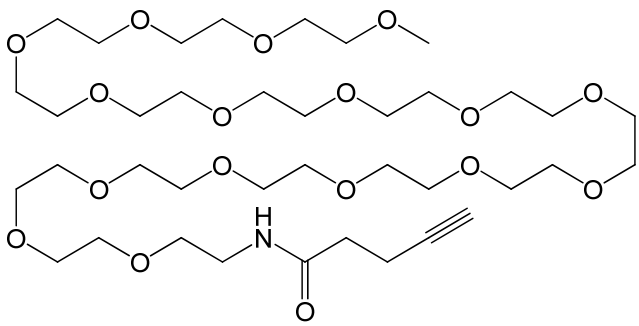

Figure S3: Structure of PEG-alkyne

Polymerization of thin films of PEDOT-N_3 onto COC supports:

PEDOT-N_3 electrodes were prepared by in situ polymerization of EDOT-N_3 on injection molded COC (TOPAS 5013, TOPAS Advanced Polymers, Frankfurt, Germany) discs. The discs were cleaned with acetone, IPA, ethanol and water. EDOT-N_3 (see Figure 1A in main paper) (20 mg,0.15 mmol), Baytron C (0.48 mL, ~40 wt % Fe(III)Tosylate in butanol), and butanol (0.48 mL) were mixed and spin-coated on the COC-discs (20 s at 700 rpm). The samples were placed on a hot plate at 65 °C for 5 min and subsequently washed with water and blown dry in a nitrogen flow, yielding films with a thickness of approximately 150 nm.

Potentiostat and Microscope

The fabrication of the gradient was performed using a VMP multichannel potentiostat (Biologic Science Instruments, Claix, France). The fluorescence of the eGFP treated areas were measured using a Zeiss LSM 5 confocal laser scanning microscope (Carl Zeiss, Oberkochen, Germany) using exciting light at 488 nm and collecting emitted light of wavelength longer than 505 nm.

Nuclear magnetic resonance

NMR spectroscopy of the NTA-alkyne was performed on a 300 MHz Cryomagnet from Spectrospin & Bruker (^{1}H-NMR at 300MHz, ^{13}C-NMR at 75MHz), while the PEG-alkyne was analyzed on a Bruker Avance 250MHz spectrometer (^{1}H-NMR at 250MHz, ^{13}C-NMR at 63MHz). All analyses were performed at room temperature.

Infrared spectroscopy (IR)

IR was performed on a PerkinElmer Spectrum One model 2000 Fourier transform infrared system with a universal attenuated total reflection sampling accessory on a ZnSe/diamond composite.

Fabrication of mask for complex NTA gradients:

A 4 inch silicon wafer was coated by 500 nm copper using electron beam evaporation, before spin coating with COC mr-I T85 (Micro Resist Technology, Berlin, Germany) at 3000 rpm for 30 seconds to yield a 4.5 µm thick layer, as measured with an Ambios XP-2 (Ambios Technology, Inc., Santa Cruz, US) profilometer using a stylus force of 1 mg. After baking at 80°C for 10 minutes a layer of ma-P 1275 (Micro Resist Technology, Berlin, Germany) was spin coated on top at 3000 rpm for 30 seconds, and the sample was rebaked at 80°C for 10 minutes. The photoresist was exposed through a chrome mask in a Karl Süss MA4 mask aligner (Munich, Germany) with a dose of 400 mJ/cm^2. The chrome mask motif consisted of a square grid of 100 µm diameter holes with a center-to-center distance of 200 µm in both lateral dimensions (see Fig. 5A of the main text for a schematic). The photoresist was developed using ma D 331 (Micro Resist Technology, Berlin, Germany) for 60 seconds. The wafer was then etched in a Reactive Ion Etcher (Plasmatherm 740, Unaxis, St Petersburg, FL) for 15 minutes at 300 W and 7 Pa O_2. Finally the remaining photoresist was removed by washing in acetone, isopropanol, ethanol, and MilliQ water.

The gradient fabrication setup:

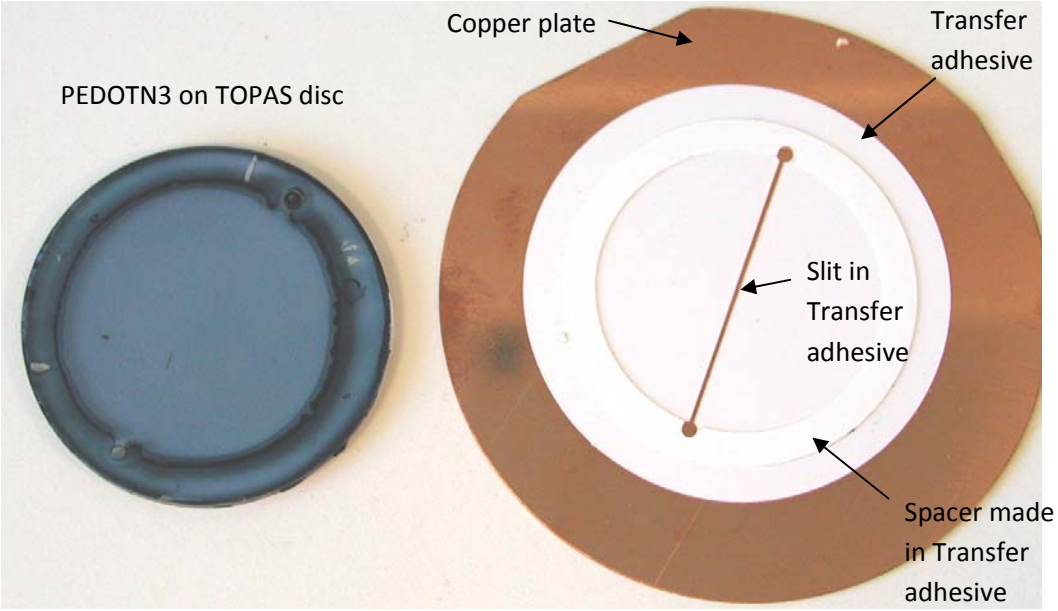

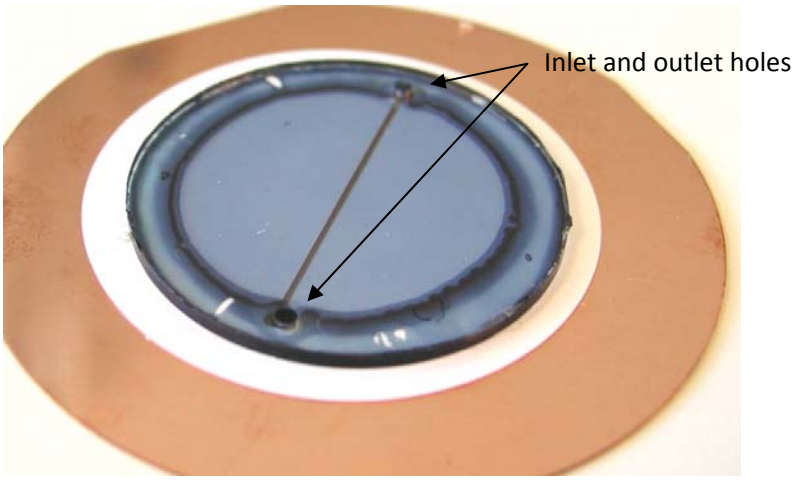

Figure S4: Top: The PEDOT-N_3 coated TOPAS disc (left) and the copper plate with transfer adhesive (right). A slit has been cut in the transfer adhesive using a CO_2 laser. The rim is also made of transfer adhesive and is used for defining the spacing between the PEDOT-N_3 surface and the copper electrode. Bottom: the assembled setup without clamps and connectors. The TOPAS disc has two holes for inlet and outlet of the alkyne/$CuSO_4$ solution.

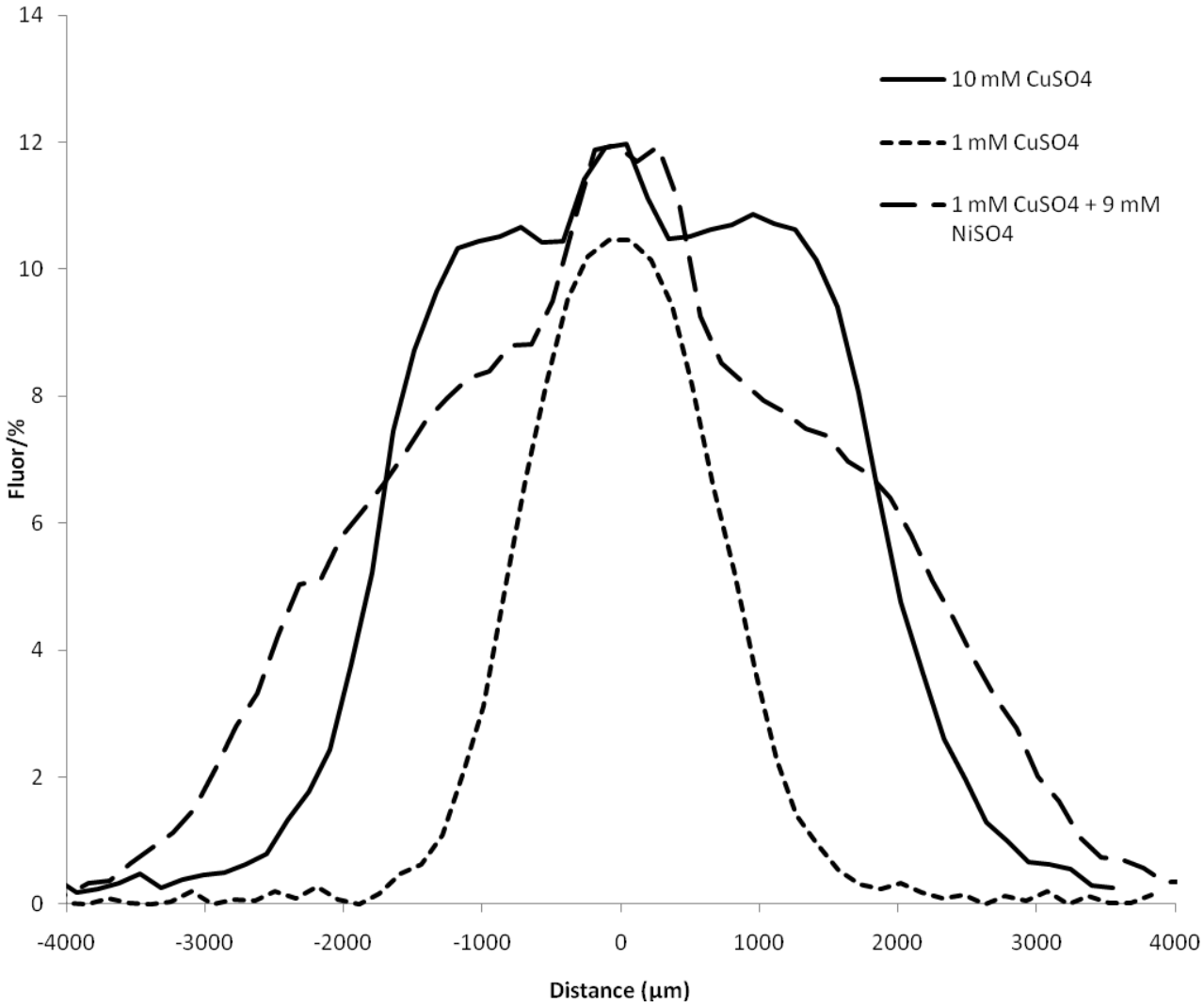

Figure S5: XPS linescan data on gradients made using a concentration of 1 mM EBTB, a potential of -0.5V, a reaction time of 5 minutes and a spacing of 190 µm. A test sample was made where the solution contained 9 mM of the inert $NiSO_4$ to test the influence on electrolyte conductivity on the gradient profile. The profile of the 1 mM $CuSO_4$ + 9 mM $NiSO_4$ compared to 10 mM $CuSO_4$ indicates that the shape of the 10 mM $CuSO_4$ is most likely linked to conductivity of the electrolyte.

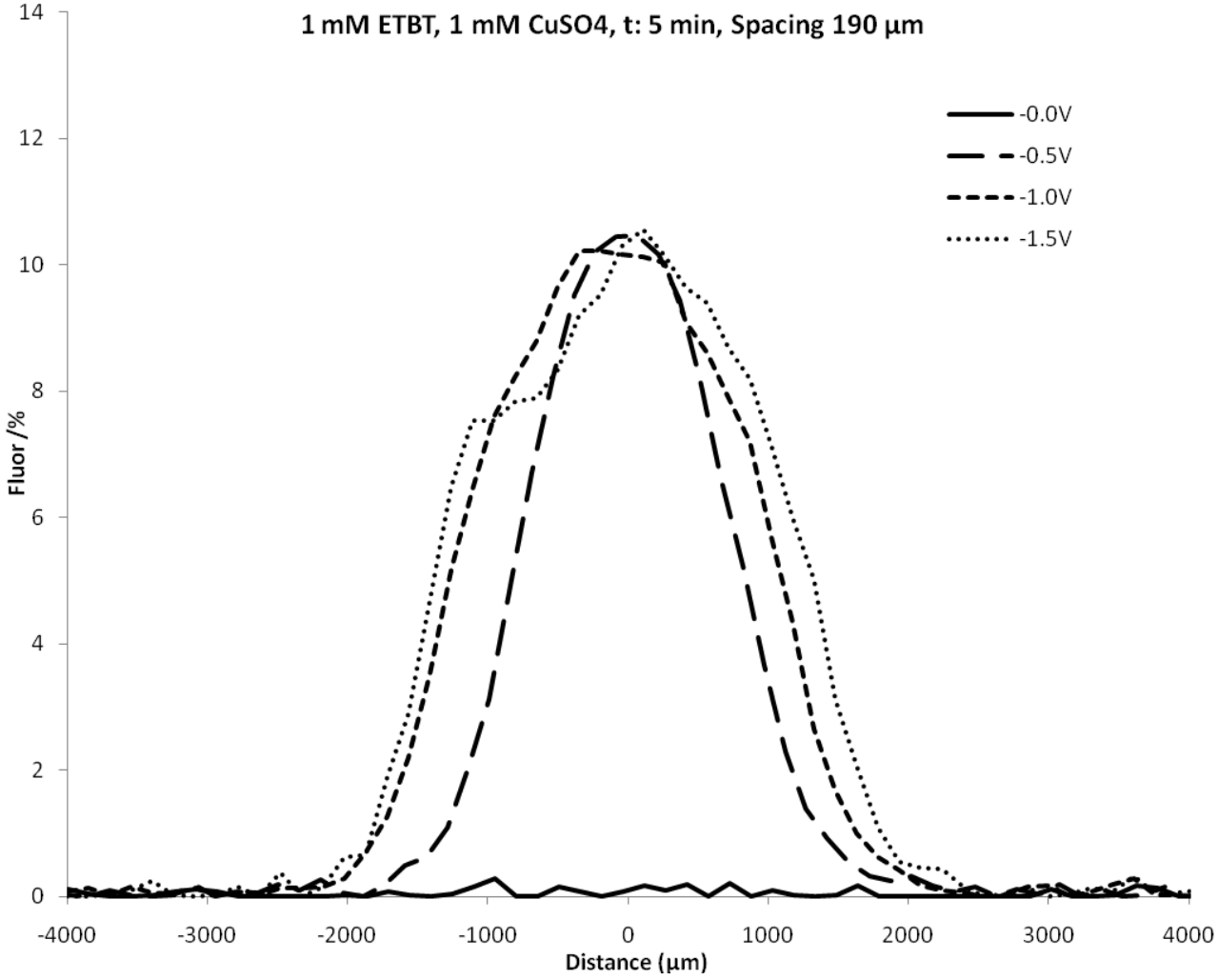

Figure S6: XPS linescan data on gradients made using a concentration of 1 mM EBTB, 1 mM $CuSO_4$, a reaction time of 5 minutes, a spacing of 190 µm and various potentials. The figure shows that only little effect is gained by increasing the potential from -0.5V to -1.5V. The control with 0.0V shows that no chemical modification is observed when no potential is applied.

COMSOL simulation

The setup was simulated using COMSOL Multiphysics 3.5 (COMSOL AB, Stockholm, Sweden) using the packages "Conductive media DC" and "Diffusion".

Scheme S1: The Values used for the COMSOL simulation. The diffusion coefficients and the molar conductivity of $CuSO_4$ in DMSO were assessed from similar values in water. The reaction rate constant was determined from figure S9.

Variable	Symbol	Estimated value/Units	Dimensionless variable	Dimensionless values used in the simulations
Spacing Height	h	190 µm	$\hat{h} = \frac{h}{h} = 1$	1
Length	L	m	$\hat{L} = \frac{L}{h}$	20
Film thickness	d	150 nm	$\hat{d} = \frac{d}{h}$	10^{-4}
Slit width	W	500 µm		3
Applied potential	V	-0.5 V	$\hat{V} = \frac{V}{V_0} = 1$	1
Time	t	300 s	$\hat{t} = \frac{t}{t} = 1$	1
Molar Conductivity	Λ_m	0.01 Sm^2/mol	$\hat{\Lambda}_m = \frac{\Lambda_m}{\Lambda_m} = 1$	1
Concentration of alkyne	c_{alk}	1 mol/m^3	$\hat{c}_{alk} = \frac{c_{alk}}{c_{alk,0}} = 1$	
Concentration of azide	c_{azi}	4000 mol/m^3	$\hat{c}_{azi} = \frac{c_{azi}}{c_{alk,0}}$	4000
Concentration of Cu(II)	$c_{Cu(II)}$	1 mol/m^3	$\hat{c}_{Cu(II)} = \frac{c_{Cu(II)}}{c_{alk,0}}$	1
Concentration of Triazole	c_{tri}	mol/m^3	$\hat{c}_{tri} = \frac{c_{tri}}{c_{alk,0}}$	
Diffusion coefficients	$D_{Cu(I)}, D_{Alkyne}$	$\sim 1 \cdot 10^{-9}$ m^2/s	$\hat{D} = \frac{Dt}{h^2}$	10
Current	I	A	$\hat{I} = \frac{Ih}{A_m V_0 c_{alk,0}}$	
Reaction Rate Constant	k	3333 $M^{-4}s^{-1}$	$\hat{k} = k c_{alk,0}{}^4 t$	10^4

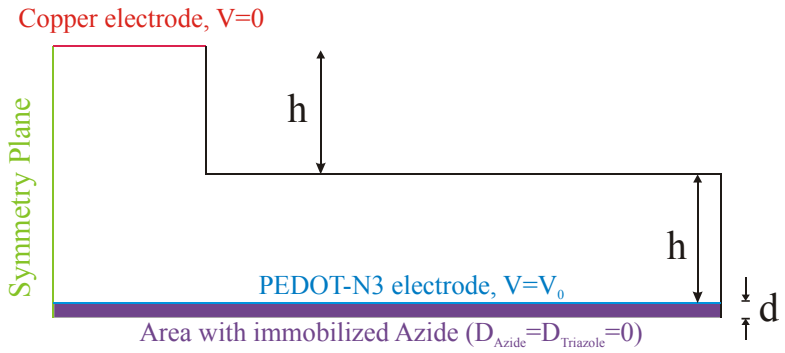

Figure S7: The geometry used in the COMSOL simulation. The azides and triazoles are bound to a thin area in the bottom resembling the PEDOT-N_3 layer. The symmetry plane makes is possible to simulate only one half of the geometry.

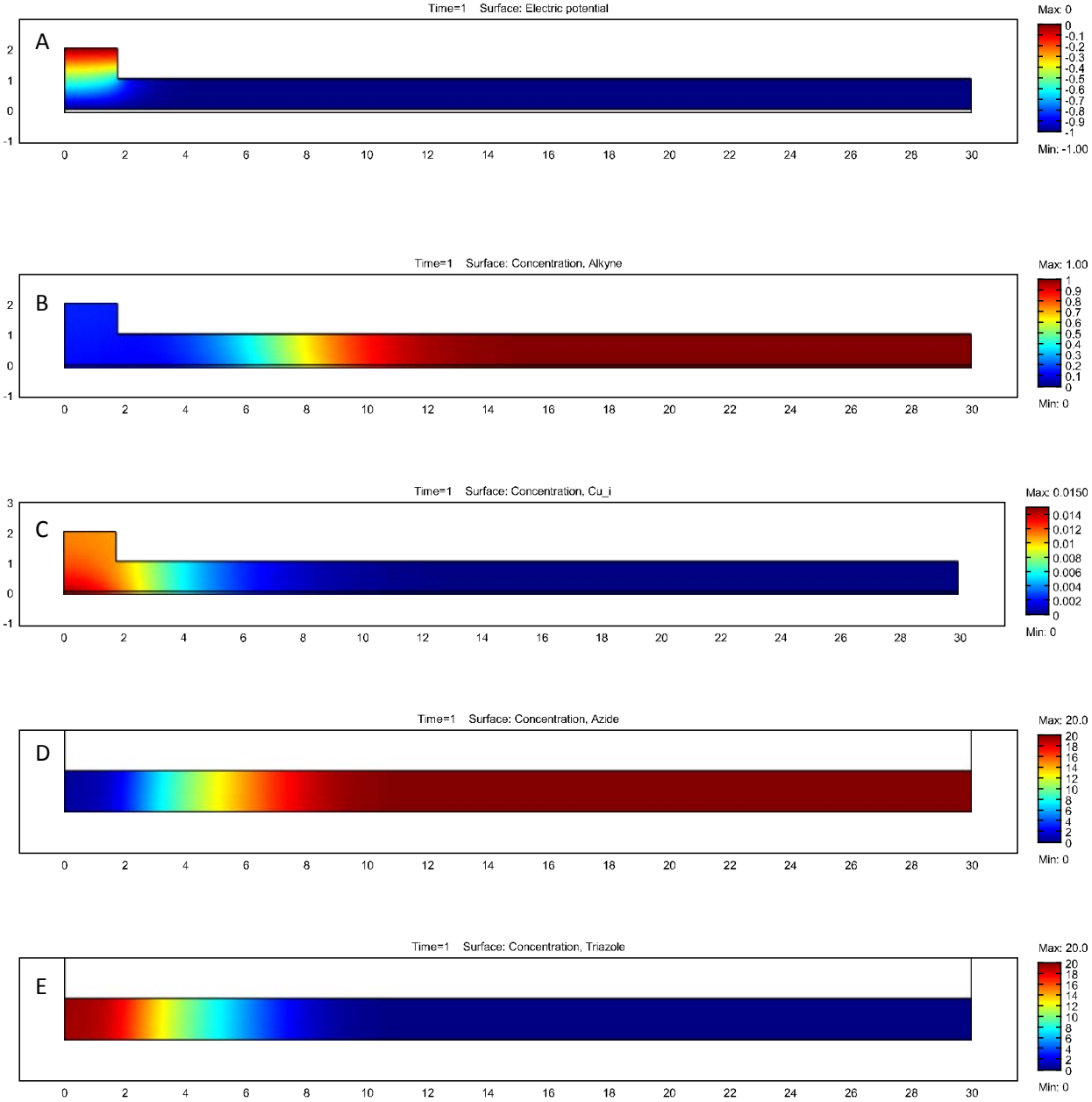

Figure S8: Example of the dimensionless output from a COMSOL simulation using the values in scheme S1. A) is the electric potential, B) is the alkyne concentration, showing signs of depletion in the volume below and next to the stencil opening, C) is the Cu(I) concentration, D) and E) are the Triazole and Azide concentrations, respectively, bound in the PEDOT-N_3-mimicking subdomain.

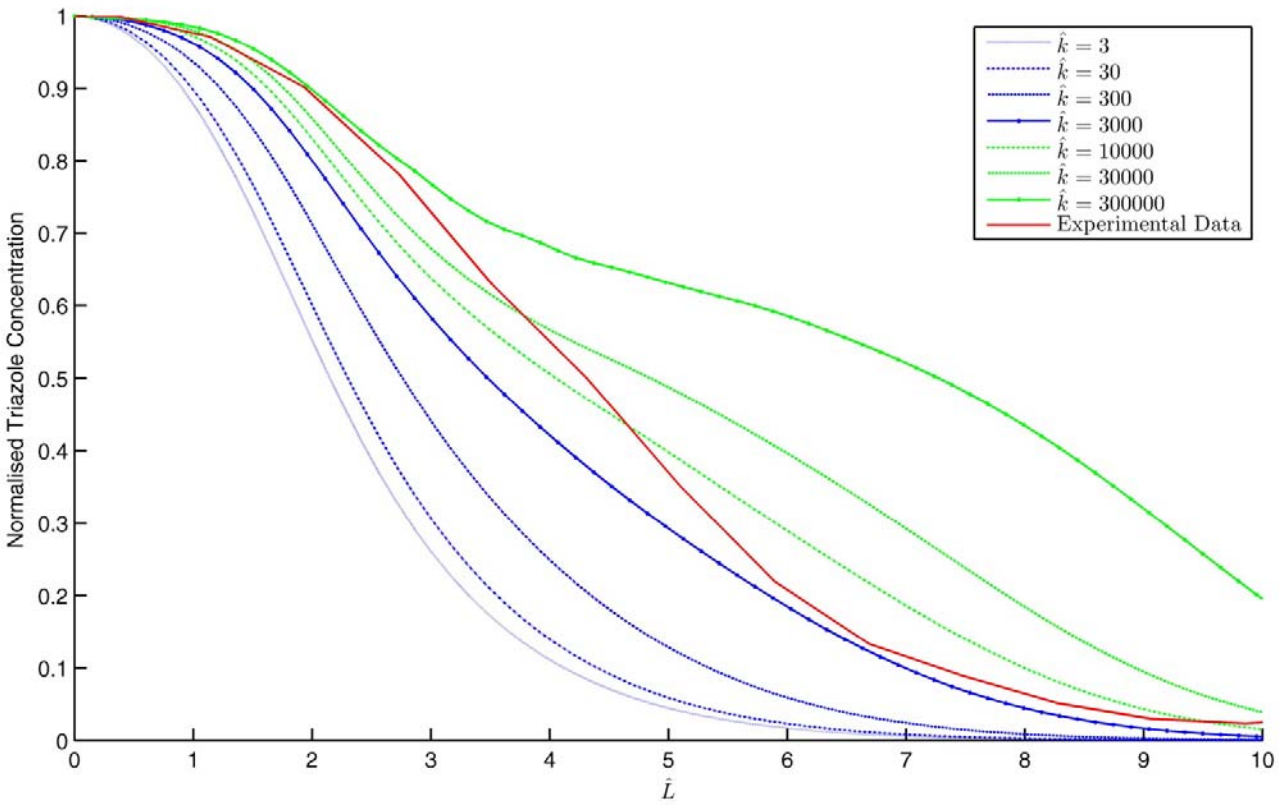

Figure S9: COMSOL simulation of the resulting triazole surface concentration for a range of values of the dimensionless reaction rate $\hat{k}$ compared to experimental data produced at -0.5V, 1 mM $CuSO_4$, 1 mM EBTB, electrode spacing 190 µm and 5 minutes reaction time. The optimal value of the reaction rate constant is found to be $\hat{k}$=10000 for the current setup.

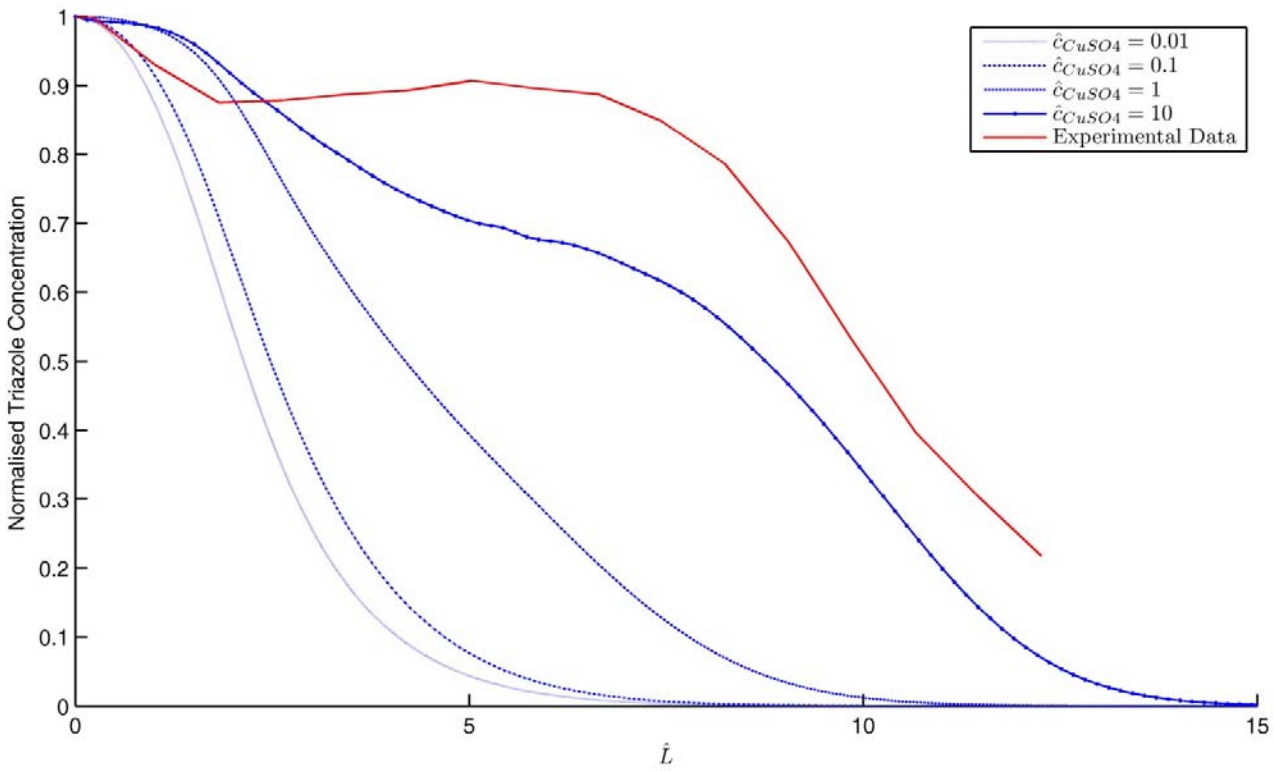

Figure S10: Numerical simulation of the triazole concentration as a function of distance for varying values of $\hat{c}_{CuSO4}$ compared to experimental data using an applied potential of -0.5V, 10 mM $CuSO_4$, 1mM EBTB, electrode spacing 190 µm, and 5 minutes reaction time. The shoulder observed in the experimental data at large $CuSO_4$ values can partly be reproduced using the numerical simulations. The simulations reveal that the distinct shape with the shoulder is caused by depletion of the alkyne.

Appendix 4

Solvent Composition Directing Click-Functionalization at the Surface or in the Bulk of Azide-Modified PEDOT

Macromolecules **2011**, *44* (3), pp. 495–501

Macromolecules
ARTICLE

Macromolecules **2011**, *44*, 495–501 **495**
DOI: 10.1021/ma102149u

Solvent Composition Directing Click-Functionalization at the Surface or in the Bulk of Azide-Modified PEDOT

Johan U. Lind,[†] Thomas S. Hansen,[†] Anders E. Daugaard,[‡] Søren Hvilsted,[‡] Thomas L. Andresen,[†] and Niels B. Larsen*,[†]

[†]*Department of Micro- and Nanotechnology, Technical University of Denmark, DTU Nanotech, Ørsteds Plads 345ø, 2800 Kgs. Lyngby, Denmark, and* [‡]*Department of Chemical and Biochemical Engineering, Technical University of Denmark, Søltofts Plads, Building 227, 2800 Kgs. Lyngby, Denmark*

Received September 15, 2010; Revised Manuscript Received December 22, 2010

ABSTRACT: Thin films of the conducting polymer poly(3,4-(1-azidomethylethylene)dioxythiophene) tosylate (PEDOT−N_3) can be functionalized by reaction with alkynated reagents in aqueous solutions. Reaction in pure water resulted in surface specific modification of PEDOT−N_3 films, whereas both surface and bulk reaction was achieved in solvent mixtures of water and DMSO. These reaction patterns were confirmed by a combination of AFM and XPS measurements on the front- and back-side of the film. The phenomenon is attributed to a strong dependence of the swelling of PEDOT−N_3 on the solvent mixture used. Liquid AFM studies showed increasing film thickness with increasing DMSO content, with the measured thickness in pure DMSO being >250% of the thickness in pure water. A similar, but less pronounced, behavior was observed for unmodified poly(3,4-ethylenedioxythiophene) tosylate (PEDOT). High-density grafting of a number of alkynated compounds onto PEDOT−N_3 was achieved via controlled swelling of the polymer. In particular, grafting of alkynated poly(ethylene glycol) (PEG) was optimized to minimize protein adsorption to the conductive polymer surface. Intermediate swelling of PEDOT−N_3 during the reaction, using ~50% DMSO, resulted in the formation of a dense PEG surface layer with low protein adhesiveness without adversely affecting the conductive properties of the film.

Introduction

The conductive polymer poly(3,4-ethylenedioxythiophene) (PEDOT) is employed for a wide range of applications, including solar cells,[1,2] organic light emitting electrodes,[3] photographic films,[4] biosensors,[5] fuel cells,[6,7] and actuators.[8,9] PEDOT is often chemically modified to facilitate a specific application. Various chemical entities have been incorporated, commonly through covalent bonding to the ethylene part of the PEDOT molecule, which is not part of the π-conjugated backbone,[10−18] but also noncovalently by adsorption or incorporation into the PEDOT matrix.[19−23] Such modifications can e.g. serve to change the electronic properties of the polymer,[10,14,20] or to add a biological functionality.[11,15,19] The "click"-type reaction between an azide group and a terminal alkyne, the copper(I)-catalyzed azide−alkyne Huisgen 1,3-dipolar cycloaddition (CuAAC) is a popular method for postpolymerization modification of polymers.[24−28] Recently, a number of studies have focused on the fabrication of PEDOT-type polymers containing alkyne and azide groups and functionalization of these using CuAAC.[29−32] We have previously developed a 3,4-(1-azidomethylethylene)-dioxythiophene (EDOT−N_3) monomer that can be chemically oxidized to yield PEDOT−N_3 films containing tosylate as counterions for the p-doped polymer. The films are stable, insoluble, highly conductive, and can be functionalized by a range of alkynated reagents.[30] We have also demonstrated localized functionalization under electrochemical control ("electro click") for individual modification of PEDOT−N_3 microelectrodes[33] or creation of complex chemical surface gradient patterns.[34]

*Corresponding author. E-mail: niels.b.larsen@nanotech.dtu.dk.

Here, we present a simple method for controlling the degree of reaction and the depth of modification of PEDOT−N_3 thin films by varying the solvent composition of aqueous solvents for a number of alkynated reagents (see Scheme 1). The methodology is based on our finding that the polymer undergoes significant, reversible and gradually increasing swelling in DMSO/water mixtures of increasing DMSO concentration. We further demonstrate the usefulness of the method to produce high-density poly(ethylene glycol) (PEG) coatings with low nonspecific protein adhesiveness on PEDOT−N_3 while retaining most of the thin film's electrical conductivity. This ability is central to many advanced biological uses, since the reduction of nonspecific interactions is a requirement for utilizing specific interactions between the substrate and, e.g., a living cell.[35,36] Formation of a high-density surface layer of PEG molecules by grafting from solution is difficult due to steric hindrance by initially bound PEG molecules.[37] We find that addition of DMSO to the aqueous solution results in a much denser PEG film and reduces its protein adhesiveness, probably due to the swelling of the PEDOT−N_3, which increases the number of accessible reactive azide groups. Such a dense PEG coverage can be achieved at intermediate DMSO concentrations without compromising the conductivity of the PEDOT−N_3, whereas the use of very high DMSO concentrations leads to a substantial bulk modification and concomitant reduction of the film conductivity.

Experimental Section

Solvents. Ultrapure water of resistivity > 18.2 MΩ cm (Milli-Q water) was produced on a Millipore Quantum system (Millipore, MA). DMSO (>99% purity) was obtained from Merck (Darmstadt, Germany). DMSO concentrations in DMSO/water solutions are given in volume percent throughout the text.

© 2011 American Chemical Society

Scheme 1. (Top) Cu(I)-Catalyzed Click Reaction between the Azide of PEDOT−N_3 and an Alkynated Reagent and (Bottom) Illustration of the Swelling of PEDOT−N_3 Thin Films (White) in Water, in Water/DMSO Mixtures, and in Pure DMSO, Respectively, and the Resulting Degrees of Reaction (Gray) at the Surface and in the Bulk of the Film in Its Swelled State after Reaction or after Washing with Water and Drying

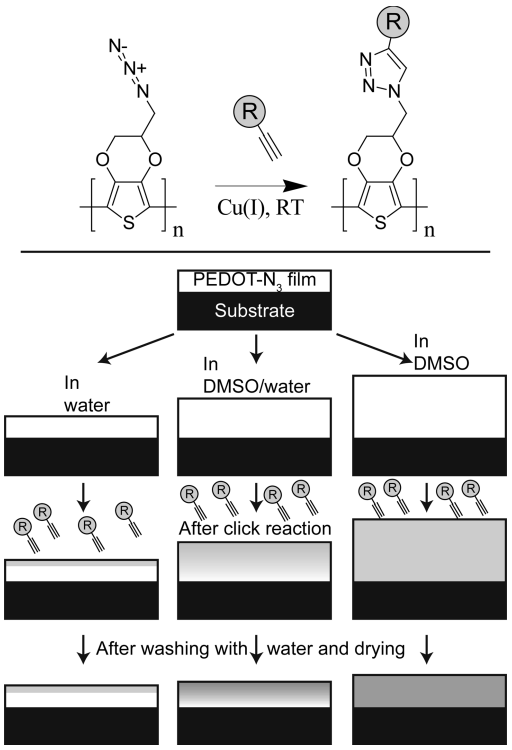

Conducting Polymer Samples Fabrication. EDOT-N_3 was synthesized in accordance with our earlier reported procedure.[30] PEDOT:TsO and PEDOT−N_3:TsO thin films were fabricated by spin-coating and polymerizing on cyclic olefin copolymer (COC) supports as described previously[30,38] and as summarized in the Supporting Information. AFM studies used octadecyltrichlorosilane (OTS) treated glass microscope slides as substrates for PEDOT:TsO films or (3-aminopropyl)trimethoxysilane (APTMS) treated glass microscope slides as substrates for PEDOT:PSS film, instead of COC supports, to minimize the risk of film delamination. OTS treatment proceeded by immersion of the glass slides in a 0.5% solution of OTS (Sigma-Aldrich) in toluene for at least 15 min. After treatment the slides were rinsed in toluene, ethanol, and Milli-Q water. APTMS treatment was done by placing the microscope slide for 2 h in a 0.1 M solution of APTMS (Sigma-Aldrich) in 2-propanol containing 1.5 M water, and rinsing in 2-propanol, ethanol and Milli-Q water. PEDOT:PSS films for AFM investigation were made by spin-coating a 1.2−1.4% PEDOT:PSS aqueous solution (483095, Sigma-Aldrich) at 1000 rpm onto a glass microscope slide. Following spin-coating the film was annealed on a hot plate at 200 °C for 30 min.

Alkyne Reagents. The syntheses of the alkyne reagents are described in the Supporting Information. Propargyl alcohol and 4-pentynoic acid were purchased from Sigma-Aldrich.

Postpolymerization Click-Reactions on PEDOT−N_3 Substrates. All reactions were performed in a homemade reaction well system. The wells were defined by circular holes of 5−7 mm in diameter in a 2 mm thick silicone rubber film (Leewood Elastomer, Skogaas, Sweden) that was attached to the substrates via double-sided adhesive tape (ARcare 90106, Adhesive Research, Glen Rock, PA). Holes of 4−6 mm in diameter were punched in the adhesive tape and placed in registry with the holes of the silicone rubber film. This system allowed for the exchange of the well sidewalls in later protein adsorption studies, thus eliminating the influence of nonspecific protein adsorption to the sidewalls. In each reaction well, 70−75 μL of reaction solution was added. Unless otherwise noted, 10 mM alkyne reagent, 2 mM $CuSO_4$, and 40 mM sodium ascorbate were used. The reaction time and the DMSO content of the reaction solution were varied. During reaction each well was covered by a piece of PET foil to limit the access of air. After reaction the wells were rinsed in Milli-Q water.

AFM Measurements. AFM measurements were performed on a PSIA XE-150 (Park Systems, Suwon, Korea) operating in intermittent contact mode and using Tap300Al and Tap75Al cantilevers (Budget Sensors, Sofia, Bulgaria). Liquid measurements used a liquid probe hand (Park Systems) and a homemade sample chamber permitting complete immersion of the substrate. Film thicknesses were determined by measuring the step height of a step produced either by cutting a narrow line with a scalpel or through masked oxygen plasma etching of part of the film (Plasmatherm 740, Unaxis, St Petersburg, FL). The step heights of at least three points on each sample were measured. For measurement series using a sequence of solvent mixtures, the same measurement areas were probed in each step of the series. Exchange of DMSO/water mixtures proceeded by washing the sample chamber twice with the new mixture and a waiting period at least 30 min before analysis to allow the film to respond. The DMSO content was increased in each step of the measurement series, except for the final reimmersion in pure water.

XPS Investigations. XPS experiments were conducted using a Thermo Fisher Scientific K Alpha (East Grinstead, U.K.). A 400 μm spot on each sample was irradiated using monochromatized aluminum Kα radiation, and survey (pass energy 200 eV) and high resolution (pass energy 25 eV) spectra of relevant elements were acquired. Flood-gun charge compensation was used for all samples. Data analyses of the XPS spectra were performed using the Avantage software package supplied by the manufacturer. The elemental composition was obtained and a peak fit of the nitrogen high resolution data was conducted: The azide group gives rise to a nitrogen doublet peak with a peak area ratio of 1:2. The smaller peak at higher binding energy disappears upon click reaction as the azide reacts to form a triazole. For an unreacted surface a ratio of $^1/_2$ is expected, and smaller ratios correspond to increasing degrees of reaction. The back side of the PEDOT−N_3 films was made available for analysis by stripping the entire film off its OTS-coated glass substrate after reaction, using a piece of double-sided adhesive tape.

Conductivity Measurements. Conductivity measurements were done using a four-point probe (Jandel Engineering, Linsdale, U.K.) connected to a Keithly 2400 source-meter (Cleveland, OH). Two measurements in perpendicular orientations were performed on each sample. Measurements in water or DMSO were performed by immersing the contact pins of the four-point probe into a droplet of the solvent placed on top of the substrate. Control experiments were conducted on a nonconducting substrate with Milli-Q water and DMSO droplets, respectively. The control experiments verified that the conductivity of DMSO and of Milli-Q water did not significantly contribute to the values measured on the polymer films.

Protein Adsorption Studies. PEDOT−N_3 films reacted with alkyne-PEG were tested for their protein adhesiveness. The click reaction proceeded in a chemically reducing environment, and the samples were subsequently reoxidized by immersion in ~4% iron(III) tosylate in 10% 1-butanol/90% Milli-Q water for 10 min. The surface was then immersed in DMSO for 10 min and finally rinsed in Milli-Q. PBS (25 μL) was added to each well for 5 min, followed by addition of 25 μL of 7.5 μg/mL HRP-rabbit anti-goat IgG (611620 Invitrogen, Camarillo, CA) in PBS solution that was left to adsorb for 15 min. The protein solution was removed and the samples were washed twice with 0.1%

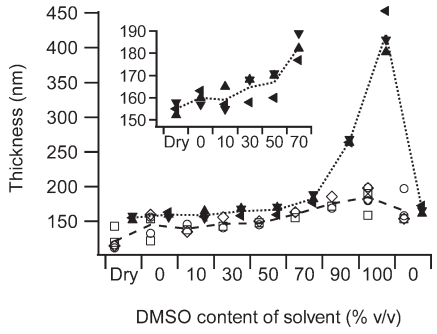

Figure 1. Thicknesses of PEDOT (open symbols) and PEDOT−N_3 (solid symbols) thin films were measured by AFM for gradually increasing DMSO content. The thickness was first measured under dry conditions and then in mixtures of water and DMSO, starting from pure water and increasing the DMSO content until reaching pure DMSO. The films were then reimmersed in pure water. For each film at least three different areas were measured with each symbol corresponding to one of the areas. The lines show average thickness of these points. Insert: The thickness of PEDOT−N_3 films at low DMSO contents shown at larger magnification.

Tween-20 in PBS for 5 min. As final procedure step, the samples were washed with Milli-Q water and blown dry in a stream of nitrogen. The wells were then removed and replaced with a new set of silicone wells. Quantification of the adsorbed HRP-containing protein was performed by adding 100 μL of 3,3′,5,5′-tetramethylbenzidine solution (TMB, Sigma-Aldrich) to each well and letting the enzymatic reaction run for 4 min on a rocking table. The solutions were then transferred to a 96-well plate and the light absorption at 450 nm was evaluated using a Wallac Victor 1420 plate reader (Perkin-Elmer).

Results and Discussion

Thin films of PEDOT−N_3 undergo substantial swelling in DMSO as compared to in water. The swelling of PEDOT−N_3 tosylate and of PEDOT tosylate films were investigated in a series of AFM measurements (see Figure 1). The changes in film thickness were measured in a series starting with pure water, followed by mixtures with gradually increasing amounts of DMSO in water, and ending with pure water to probe reversibility of the swelling process. The thickness of both PEDOT-type polymers increase with increasing DMSO content. For PEDOT−N_3 in mixtures with ≤50% DMSO in water, the effect is weak with an average relative increase of < 5% compared to the thickness in pure water. For > 50% DMSO in water, the thickness increases strongly with DMSO content up a maximum in pure DMSO of ∼260% of the film thickness found in water. Importantly, immersion in water of the maximally swelled film results in the thickness returning to its original value in water. The corresponding effect on PEDOT tosylate films is less pronounced with a measured thickness in pure DMSO of ∼150% of that in pure water. The thickness of PEDOT also decreases upon re-exposure to water, although is cannot be determined with certainty from these measurements if it returns to its original value in water.

PEDOT is usually employed in a p-doped state with counter-anions ensuring charge neutrality. Tosylate (TsO) or polymeric poly(styrenesulfonate) (PSS) counterions are commonly used (see Figure 2).[4] The investigated PEDOT and PEDOT−N_3 films contain tosylate counterions that lead to highly conducting films.[4,38] The generality of the observed swelling pattern was investigated by including PEDOT with polymeric PSS counterions (PEDOT:PSS) in the AFM and conductivity analysis series. Table 1 compares thickness and sheet resistance of PEDOT:PSS in the dry state, in water, and in DMSO, respectively, to the

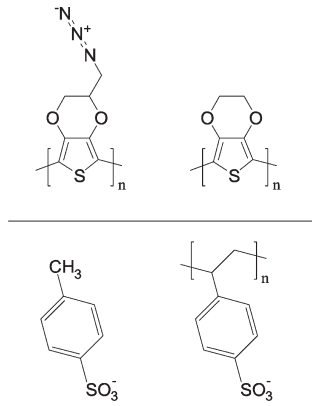

Figure 2. Structure of PEDOT-type polymers and counterions. Top left: PEDOT−N_3. Top right: PEDOT. Bottom left: Tosylate counterion. Bottom right: Poly(styrenesulfonate) counterion.

corresponding values found for PEDOT−N_3 tosylate (PEDOT−N_3:TsO) or PEDOT tosylate (PEDOT:TsO).

Our AFM studies revealed very large swelling of PEDOT:PSS with measured thicknesses in both DMSO and in water of > 700% of the dry state thickness. This finding is not surprising as it is well established that PEDOT:PSS is both hygroscopic and capable of absorbing large amounts of DMSO.[39,40] The interaction between DMSO and PEDOT:PSS has recently attracted considerable attention, as DMSO and a number of other polar organic solvents can be used to drastically increase PEDOT:PSS conductance.[40−42] Addition of these solvents to aqueous suspensions of PEDOT:PSS during or after spin-casting of films improves the conductance by orders of magnitude.[40,42,43] We similarly observe a ∼500 times lower sheet resistance of a preformed PEDOT:PSS film after immersion in DMSO followed by washing in water and drying (see Table 1, columns "dry" vs "dry after DMSO"). It is worth noting that even the heavily swelled state of PEDOT:PSS during DMSO treatment exhibit ∼200 times lower sheet resistance (columns "dry" vs "DMSO"). In contrast, PEDOT−N_3:TsO and PEDOT:TsO films show small increases in sheet resistance of ∼1.75 times and ∼1.1 times, respectively, upon DMSO treatment. In this comparison, it should be noted that the initial and final sheet resistance of the latter films are actually both close to the resistance for PEDOT:PSS after solvent treatment.

We also investigated if the swelling of PEDOT−N_3:TsO thin films and, to lesser extent, PEDOT:TsO thin films was associated with changes in light absorption or in changes of their surface morphology. Absorption spectroscopy revealed small variations in a broad absorption peak centered at 530 nm after exposure of PEDOT−N_3 films to different liquid environments (see Figure S4A), while no changes in visible and near-infrared absorption were found for PEDOT films exposed to the same treatments (see Figure S4B). AFM analysis of the film surface morphology after repeated exchange of the immersion liquids showed very little dependence on the degree of swelling, with mean and rms roughness values of less than 10 nm for all the conditions explored (see Figure S5 and Table S1).

We observe much stronger swelling of PEDOT:PSS than of PEDOT:TsO in both water and DMSO. The large volume fraction of hygroscopic PSS in PEDOT:PSS compared to the volume fraction of tosylate in PEDOT:TsO[44] likely accounts for most of this difference. We therefore considered if the larger swelling of PEDOT−N_3:TsO than of PEDOT:TsO in DMSO could reflect differences in the doping levels and tosylate content of the two polymers. However, estimation of the tosylate content from XPS analysis of the sulfur peak[44,45] does not indicate markedly different levels in PEDOT:TsO and in PEDOT−N_3:TsO. Another

Table 1. Thickness and Sheet Resistance of PEDOT−N_3 Tosylate, PEDOT Tosylate, and PEDOT:PSS Thin Films Prior to Immersion in Liquid, for Immersion in Liquid, and after Drying, Respectively

	film thickness in nm[a]			film sheet resistance in KΩ/square[b]					
	dry[c]	water[d]	DMSO[e]	dry[c]	water[d]	dry after water[f]	dry[c]	DMSO[e]	dry after DMSO[g]
PEDOT−N_3:TsO	155	160	420	0.71	1.15	1.00	0.77	1.33	1.34
PEDOT:TsO	121	145	185	0.08	0.11	0.11	0.09	0.10	0.10
PEDOT:PSS	266	2087	1879	267	h	241	218	1.10	0.45

[a] Average value of at least three different areas on each film measured by AFM after ≥30 min exposure. [b] Average of two four-point probe measurements of perpendicular orientations obtained after ≥10 min exposure. [c] Film in dry state before immersion in liquids. [d] Film immersed in water. [e] Film immersed in DMSO. [f] Film dried in a stream of nitrogen after immersion in water. [g] Film washed in water and dried in a stream of nitrogen after immersion in DMSO. [h] The PEDOT:PSS film immersed in water did not produce stable sheet resistance values.

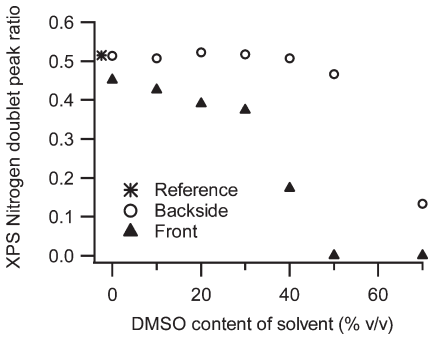

Figure 3. XPS analysis of the degree of reaction on PEDOT−N_3 films modified by PEG−alkyne as a function of DMSO concentration. All reactions used 10 mM PEG−alkyne, 2 mM $CuSO_4$, 40 mM sodium ascorbate, and a fixed reaction time of 4 h. A nitrogen peak intensity ratio of $^1/_2$ corresponds to zero degree of reaction, while full conversion of the azides yields a peak ratio of 0. Nitrogen peak analysis was performed both on the front side (facing the reaction solution; solid triangles) and on the back side (facing the substrate; open squares) of the film, with the reference (asterisk) being a freshly prepared PEDOT−N_3 film.

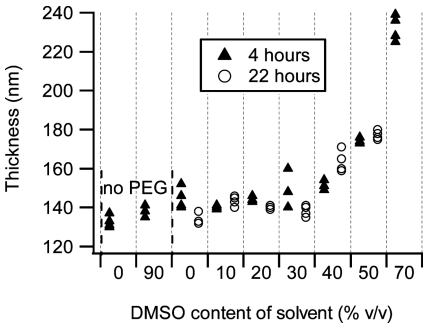

Figure 4. AFM analysis of the PEDOT−N_3 film thickness after reaction with PEG−alkyne at varying DMSO concentrations and reaction times (4 h, solid triangles; 22 h, open circles), followed by washing with water and drying the samples. All reactions used 10 mM PEG−alkyne, 2 mM $CuSO_4$, and 40 mM sodium ascorbate. The two controls to the left in the graph underwent all process steps except for the addition of PEG−alkyne.

explanation for their different swelling properties might be the presence or absence of the azide functionality. In a recent study by Sando et al. on the vibrational behavior of the inorganic azide ion in DMSO and water, no preferential solvation of the azide toward water or DMSO was reported.[46] We can therefore only suggest that the azide group in organic polymers may have a favorable interaction with DMSO, perhaps in synergy with other interactions such as those suggested by Ouyang.[41]

Our finding of a correlation of PEDOT−N_3 film swelling to the concentration of DMSO in water made us consider if the DMSO concentration in the click-reaction solution could be employed to control (a) the reaction depth into the PEDOT−N_3 film, and (b) the degree of reaction at its surface due to accessibility of a larger number of reactive groups in the swollen state. This was explored by functionalization of PEDOT−N_3 films with a PEG−alkyne (~815 Da). The DMSO concentration and the reaction time were varied in a series of experiments with fixed concentrations of PEG−alkyne, $CuSO_4$, and sodium ascorbate. XPS analysis was employed to quantify the degree of reaction via measurement of the nitrogen doublet peak characteristic of azide groups: The intensity ratio of the higher binding energy peak to the lower binding peak is 1:2 for azide groups. The higher binding energy peak disappears upon conversion of the azide to a triazole group, thus leading to a ratio of less than 1:2. Figure 3 presents the determined nitrogen peak intensity ratios for both the front side and the back side of the prepared films.

The analysis shows that some reaction occurs on the front side of the film in pure water after 4 h reaction time. However, the resulting PEG layer is of low density. Given a typical XPS mean-free-path-length in organic materials of ~2.5 nm,[47] the nitrogen peak ratio found for the reaction in pure water corresponds to a surface PEG layer thickness of <0.5 nm in the vacuum conditions of the XPS. Addition of DMSO to the aqueous solvent leads to gradually increasing degrees of reaction until no azides can be found on the front side within the XPS sampling depth. On the back side of the film, no reaction is seen for the pure water samples or for DMSO concentrations below 50%. For DMSO concentrations ≥50%, reaction occurs even on the back side of the film. Thus, the increased swelling at high DMSO concentrations does indeed allow reaction to occur deep into the film.

Figure 3 shows that smaller DMSO concentrations also have an effect, either by increasing the surface density of reacted groups or by permitting reaction deeper into the film. The degree of reaction in the film interior cannot easily be determined by XPS analysis, since the obvious option of performing XPS depth profiling may adversely affect the azide functionality. Stable coupling of PEG−alkyne to azides in the bulk of the film will result in a larger film volume, so measurement of the film thickness after reaction, washing with water, and drying the film is an indirect measure of the average degree of reaction. The PEDOT−N_3 film thickness in dry condition after reaction with PEG−alkyne was measured by AFM for a range of DMSO concentrations and reaction times of 4 and 22 h, respectively (see Figure 4). Some minor inhomogeneities in the film structure could be observed during the AFM measurements. Still, a correlation between the thickness of the film and the DMSO content of the reaction solvent is evident for both the 4 h and the 22 h series. For the 4 h reaction at 50% DMSO, the thickness was ~175 nm and at 70% DMSO it was 230 nm, equivalent to respectively 130% and 175% of the thickness of the reference areas without PEG. This clearly shows that bulk reaction does indeed take place for higher DMSO concentrations. We observed similar bulk reaction of a PEDOT−N_3 film in an earlier study on modifying PEDOT−N_3 with an alkynated fluorescein in dimethylformamide.[30] Notably for the low DMSO concentrations and for pure water, no significant thickness increase is

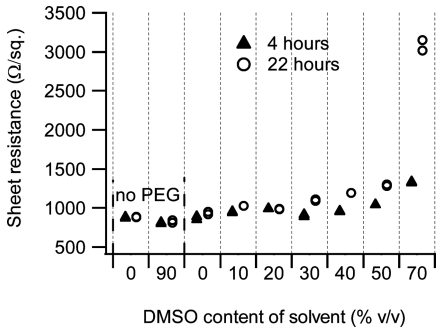

Figure 5. Sheet resistance of the PEDOT−N_3 film after reaction with PEG−alkyne at varying DMSO concentrations and reaction times (4 h, solid triangles; 22 h, open circles). All reactions used 10 mM PEG−alkyne, 2 mM $CuSO_4$, and 40 mM sodium ascorbate. Prior to the resistance measurement all films had been rinsed and reoxidized as described in the Experimental Section, since the click reactions are performed in a chemically reducing environment. The two controls to the left in the graph underwent all process steps except that no PEG−alkyne was added to the reaction solution.

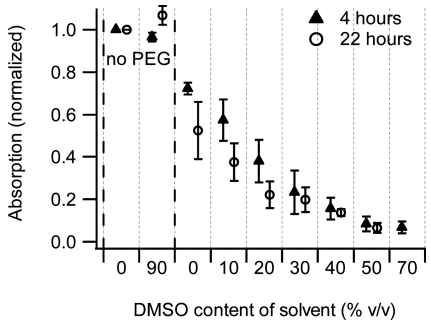

Figure 6. Protein adsorption to PEDOT−N_3 functionalized with PEG at varying DMSO concentration and reaction times (4 h, solid triangles; 22 h, open circles). The ability of the films to resist protein adsorption was tested using IgG-HRP. The relative adsorption of IgG-HRP was determined via the turnover of the HRP-substrate TMB and measured by light absorption at 450 nm. Four independent experiments were conducted. All results are normalized to the highest protein adsorption measured, i.e., for the reference point at 0% DMSO with no added PEG−alkyne. Error bars show the standard error of the mean (n = 4).

observed even for the 22 h reaction time, indicating the absence of bulk reaction. The importance of the reaction time for bulk reaction at high DMSO concentrations is stressed by the missing point at 70% DMSO for the 22 h series: This experiment was in fact performed, but the film was not sufficiently mechanically stable after the PEG−alkyne reaction to perform the height analysis procedure. In general the films often became unstable for reactions conducted in ≥70% DMSO. We take this as an indication that upon heavy PEG functionalization the material loses its cohesive strength and fractures during the rinsing steps. The swelling process itself is not responsible for the loss of mechanical stability, since the control sample of immersed in 90% DMSO without adding PEG−alkyne (see left side of Figure 4) remained perfectly stable after washing with water and drying.

Global and local volumetric expansion of the PEDOT−N_3 film upon covalent coupling of alkynes in the film interior may adversely affect its conductive properties in addition to its mechanical properties. The sheet resistance of the films after PEG modification is displayed in Figure 5. The conductivity is only weakly influenced by the reaction steps up to reaction conditions affecting the overall film stability (≥70% DMSO, cf. Figure 4). Interestingly, the AFM measurements in Figure 4 indicate incorporation of significant amounts of material in the

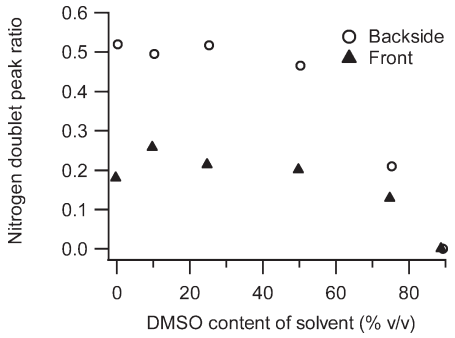

Figure 7. XPS analysis of the degree of reaction on PEDOT−N_3 films modified by pentynoic acid as a function of DMSO concentration. All reactions used 10 mM pentynoic acid, 2 mM $CuSO_4$, 40 mM sodium ascorbate, and a reaction time of 18 h. A nitrogen peak intensity ratio of 1/2 corresponds to zero degree of reaction, while full conversion of the azides yields a peak ratio of 0. Nitrogen peak analysis was performed both on the front side (solid triangles) and back side (open circles) of the film.

film using 40−50% DMSO in the reaction solution and yet only small increases in the sheet resistance are observed in Figure 5, in particular for the shorter reaction time of 4 h. These findings are in good agreement with earlier reports that large amounts of a second molecular (PEG) or polymeric (poly(methyl methacrylate)) material can be incorporated into PEDOT without compromising its conductivity.[48,49]

The XPS data (Figure 3) indicates that PEG−alkyne can be grafted at higher density in solvents with larger DMSO concentrations. Increased PEG coverage is expected to reduce the protein adhesiveness of the PEDOT−N_3 film surface[37] and thereby approach an ideal "non-fouling" surface. We tested this concept by means of adsorption of horseradish peroxidase conjugated to IgG (HRP-IgG) as test protein. The enzymatic HRP part allows for easy detection of the amount of adsorbed protein by following the formation of a colored product of the enzymatic process, similar to direct ELISA experiments. The results are displayed in Figure 6. Only a small reduction in protein adsorption was found for the PEDOT−N_3 film modified by PEG−alkyne in water, whereas increasing the DMSO content leads to decreasing protein adsorption. The minimum adsorption is found for film surfaces reacted in ≥50% DMSO. This is a very good agreement with the XPS analysis presented in Figure 3, which showed complete reaction of the azide groups within the XPS sampling depth for ≥50% DMSO in the reaction solution. An intermediate DMSO concentration of 40%-50% in the reaction solution may consequently be employed to form a dense PEG surface layer that strongly reduces protein adsorption without adversely affecting the conductive properties of the PEDOT−N_3 (cf. Figure 5).

The observed dependence on DMSO content might be particular to the PEG−alkyne, e.g. by influencing the solubility of the PEG-domain.[37] We tested the generality of our approach by reacting PEDOT−N_3 films with several other alkynated reagents. Figure 7 shows the results of reacting PEDOT−N_3 with pentynoic acid, a reagent being negatively charged and containing a short hydrophobic segment in contrast to the neutral hydrophilic domain of the PEG−alkyne. Reaction in solvent mixtures containing ≤50% DMSO results in intermediate reaction on the front side and no reaction on the back side of the film. Higher DMSO content leads to increasing degrees of reaction on the back side of the film, in full agreement with the results obtained for PEG−alkyne (cf. Figure 3). Three other alkynes spanning a range of molecular weights, propargyl alcohol (MW 42 Da), a Ni(II)-chelating nitrilotriacetic acid (NTA, MW 344 Da), and a PEG-modified undeca-peptide (MW 1727 Da), were reacted with

the PEDOT−N_3 using different DMSO concentrations, and evaluated using XPS analysis of the nitrogen doublet peak. These reagents all showed an increasing degree of reaction with increasing DMSO concentration (see Figures S6−S8, Supporting Information), confirming that the method is applicable to a wide range of reactants. The modification by the NTA and by the peptide was further independently probed by quantitative XPS analysis of heteroatoms specific to the two reagents (nickel and iodine, respectively; see Figures S7 and S8, Supporting Information). Reaction trends observed by the two analysis approaches were in agreement for both reagents tested.

An important final consideration is that DMSO could have a general accelerating effect on the click-reaction, independent of the type of alkyne. DMSO is often employed as solvent or cosolvent for click reactions, it is a good solvent for the catalytic Cu(I) ion,[24,50] and it has served to accelerate a number of reactions.[51] However, even when increasing the reaction time to 80 h for the smallest of the reactants (propargyl alcohol) we did not see any noticeable change in the degree of reaction for low DMSO concentrations, compared to a much shorter reaction time of 16 h (see Figure S6, Supporting Information). Thus, we maintain that film swelling is of key importance for the increased reaction depth observed upon adding DMSO, although changes in the reaction kinetics may play a secondary role.

We speculated earlier that the introduction of the azide functionality might be important to the observed swelling behavior of PEDOT−N_3 and the associated high accessibility of the azides for click reactions with alkynes. If so, other polymers containing azide groups should exhibit a similar behavior. As a simple test case, we performed preliminary tests of a click-reaction between an azide-modified polystyrene (PS−N_3, see Figure S9, Supporting Information) and PEG−alkyne at varying DMSO content in the reaction solution (see Figure S10, Supporting Information). The results show a strong dependence on the DMSO content with complete conversion of azides at the surface occurring for ≥40% DMSO and a 2-fold increase in the surface density of PEG chains over the reaction performed in pure water. Thus, our approach may be useful for achieving high grafting densities on a wider range of azide-modified polymers than only PEDOT−N_3.

Conclusion

We have observed a distinctive swelling behavior for the recently developed conducting polymer PEDOT−N_3. In water, the polymer film swelled only a few percent, whereas in DMSO the thickness increased to >250% of its thickness in water. PEDOT containing tosylate as counterions displayed a similar but less pronounced effect, while PEDOT with polymeric PSS counterions swelled to more than seven times its original thickness. We further showed how this swelling behavior could be exploited for directing a postpolymerization functionalization of PEDOT−N_3 thin films. In pure water and in water with low DMSO content, reaction only took place on the surface. Increasing DMSO content resulted in gradually larger swelling that lead to higher degree of bulk reaction. Such controlled reaction depth was demonstrated for a number of alkynated reactants. The modification with PEG−alkyne served to illustrate how such control of the degree of reaction via the swelling of the film can be employed to fabricate a conducting polymer film surface with minimal protein adhesiveness without adversely affecting the film conductivity.

Acknowledgment. The Danish Council for Technology and Innovation is acknowledged for financial support through the Innovation Consortium CEMIK, Grant 07-015463.

Supporting Information Available: XPS data for the reaction of additional alkynes on PEDOT−N_3 and PS−N_3 as well as details on the syntheses of the alkynated reactants, structures, optical data, AFM micrographs, and additional conductivity measurements. This material is available free of charge via the Internet at http://pubs.acs.org.

References and Notes

(1) Krebs, F. C.; Gevorgyan, S. A.; Alstrup, J. *J. Mater. Chem.* **2009**, *30*, 5442–5451.
(2) Sakurai, S.; Jiang, H.; Takahashi, M.; Kobayashi, K. *Electrochim. Acta* **2009**, *23*, 5463–5469.
(3) Armstrong, N. R.; Wang, W.; Alloway, D. M.; Placencia, D.; Ratcliff, E.; Brumbach, M. *Macromol. Rapid Commun.* **2009**, *9−10*, 717–731.
(4) Kirchmeyer, S.; Reuter, K. *J. Mater. Chem.* **2005**, *21*, 2077–2088.
(5) Park, J.; Kim, H. K.; Son, Y. *Sensor. Actuat. B—Chem.* **2008**, *1*, 244–250.
(6) Winther-Jensen, B.; Fraser, K.; Ong, C.; Forsyth, M.; MacFarlane, D. R. *Adv. Mater.* **2010**, *15*, 1727–1730.
(7) Winther-Jensen, B.; Winther-Jensen, O.; Forsyth, M.; MacFarlane, D. R. *Science* **2008**, *5889*, 671.
(8) Vidal, F.; Plesse, C.; Palaprat, G.; Kheddar, A.; Citerin, J.; Teyssié, D.; Chevrot, C. *Synth. Met.* **2006**, *21−24*, 1299–1304.
(9) Okuzaki, H.; Suzuki, H.; Ito, T. *Synth. Met.* **2009**, *21−22*, 2233–2236.
(10) Segura, J. L.; Gómez, R.; Blanco, R.; Reinold, E.; Bäuerle, P. *Chem. Mater.* **2006**, *12*, 2834–2847.
(11) Xie, H.; Luo, S. C.; Yu, H. *Small* **2009**, *22*, 2611–2617.
(12) Döbbelin, M.; Pozo-Gonzalo, C.; Marcilla, R.; Blanco, R.; Segura, J. L.; Pomposo, J. A.; Mecerreyes, D. *J. Polym. Sci., Part A: Polym. Chem.* **2009**, *12*, 3010–3021.
(13) Darmanin, T.; Nicolas, M.; Guittard, F. *Langmuir* **2008**, *17*, 9739–9746.
(14) Cutler, C. A.; Bouguettaya, M.; Kang, T. S.; Reynolds, J. R. *Macromolecules* **2005**, *8*, 3068–3074.
(15) Bazaco, R. B.; Gómez, R.; Seoane, C.; Bäuerle, P.; Segura, J. L. *Tetrahedron Lett.* **2009**, *28*, 4154–4157.
(16) Balog, M.; Rayah, H.; Derf, F. L.; Sallé, M. *New J. Chem.* **2008**, *7*, 1183–1188.
(17) Arias-Pardilla, J.; Otero, T. F.; Blanco, R.; Segura, J. L. *Electrochim. Acta* **2010**, *55*, 1535−1542.
(18) Xiao, Y.; Martin, D. C.; Cui, X.; Shenai, M. *Appl. Biochem. Biotechnol.* **2006**, *2*, 117–129.
(19) Menaker, A.; Syritski, V.; Reut, J.; Öpik, A.; Horváth, V.; Gyurcsányi, R. E. *Adv. Mater.* **2009**, *22*, 2271–2275.
(20) Jakobsson, F. L. E.; Crispin, X.; Lindell, L.; Kanciurzewska, A.; Fahlman, M.; Salaneck, W. R.; Berggren, M. *Chem. Phys. Lett.* **2006**, *1−3*, 110–114.
(21) Xiao, Y.; Li, C. M.; Wang, S.; Shi, J.; Ooi, C. P. *J. Biomed. Mater. Res. A.* **2010**, *2*, 766–772.
(22) Dai, T.; Qing, X.; Zhou, H.; Shen, C.; Wang, J.; Lu, Y. *Synth. Met.* **2010**, *160*, 791−796.
(23) Weng, C. H.; Yeh, W. M.; Ho, K. C.; Lee, G. B. *Sensor. Actuat. B—Chem.* **2007**, *2*, 576–582.
(24) Binder, W. H.; Sachsenhofer, R. *Macromol. Rapid Commun.* **2008**, *12−13*, 952–981.
(25) Fleischmann, S.; Hinrichs, K.; Oertel, U.; Reichelt, S.; Eichhorn, K. J.; Voit, B. *Macromol. Rapid Commun.* **2008**, *12−13*, 1177–1185.
(26) Chen, R. T.; Muir, B. W.; Such, G. K.; Postma, A.; Evans, R. A.; Pereira, S. M.; McLean, K. M.; Caruso, F. *Langmuir* **2010**, *5*, 3388–3393.
(27) Gauthier, M. A.; Gibson, M. I.; Klok, H. A. *Angew. Chem., Int. Ed.* **2009**, *1*, 48–58.
(28) Im, S. G.; Kim, B. S.; Tenhaeff, W. E.; Hammond, P. T.; Gleason, K. K. *Thin Solid Films* **2009**, *12*, 3606–3611.
(29) Sinha, J.; Sahoo, R.; Kumar, A. *Macromolecules* **2009**, *6*, 2015–2022.
(30) Daugaard, A. E.; Hvilsted, S.; Hansen, T. S.; Larsen, N. B. *Macromolecules* **2008**, *12*, 4321–4327.
(31) Bu, H. B.; Götz, G.; Reinold, E.; Vogt, A.; Schmid, S.; Blanco, R.; Segura, J. L.; Bäuerle, P. *Chem. Commun.* **2008**, *11*, 1320–1322.
(32) Xu, J.; Tian, Y.; Peng, R.; Xian, Y.; Ran, Q.; Jin, L. *Electrochem. Commun.* **2009**, *10*, 1972–1975.
(33) Hansen, T. S.; Daugaard, A. E.; Hvilsted, S.; Larsen, N. B. *Adv. Mater.* **2009**, *44*, 4483–4486.
(34) Hansen, T. S.; Lind, J. U.; Daugaard, A. E.; Hvilsted, S.; Andresen, T. L.; Larsen, N. B. *Langmuir* **2010**, *26*, 16171−16177.

(35) Goddard, J. M.; Hotchkiss, J. H. *Prog. Polym. Sci.* **2007**, *7*, 698–725.
(36) Heyes, C. D.; Groll, J.; Moller, M.; Nienhaus, G. U. *Mol. Biosyst* **2007**, *6*, 419–430.
(37) Kingshott, P.; Thissen, H.; Griesser, H. J. *Biomaterials* **2002**, *9*, 2043–2056.
(38) Winther-Jensen, B.; Breiby, D. W.; West, K. *Synth. Met.* **2005**, *1−3*, 1–4.
(39) Huang, J.; Miller, P. F.; De Mello, J. C.; De Mello, A. J.; Bradley, D. D. C. *Synth. Met.* **2003**, *3*, 569–572.
(40) Dimitriev, O. P.; Grinko, D. A.; Noskov, Y. V.; Ogurtsov, N. A.; Pud, A. A. *Synth. Met.* **2009**, *21−22*, 2237–2239.
(41) Ouyang, J.; Xu, Q.; Chu, C. W.; Yang, Y.; Li, G.; Shinar, J. *Polymer* **2004**, *25*, 8443–8450.
(42) Jönsson, S. K. M.; Birgerson, J.; Crispin, X.; Greczynski, G.; Osikowicz, W.; Denier van der Gon, A. W.; Salaneck, W. R.; Fahlman, M. *Synth. Met.* **2003**, *1*, 1–10.
(43) Kim, J. Y.; Jung, J. H.; Lee, D. E.; Joo, J. *Synth. Met.* **2002**, *2−3*, 311–316.
(44) Crispin, X.; Marciniak, S.; Osikowicz, W.; Zotti, G.; van der Gon, A. W. D.; Louwet, F.; Fahlman, M.; Groenendaal, L.; De Schryver, F.; Salaneck, W. R. *J. Polym. Sci., Polym. Phys.* **2003**, *21*, 2561–2583.
(45) Zotti, G.; Zecchin, S.; Schiavon, G.; Louwet, F.; Groenendaal, L.; Crispin, X.; Osikowicz, W.; Salaneck, W.; Fahlman, M. *Macromolecules* **2003**, *9*, 3337–3344.
(46) Sando, G. M.; Dahl, K.; Owrutsky, J. C. *J. Phys. Chem. B* **2007**, *18*, 4901–4909.
(47) Briggs, D. *Surface Analysis of Polymers by XPS and Static SIMS*; Cambridge University Press: Cambridge, U.K., 1998; .
(48) Winther-Jensen, B.; Chen, J.; West, K.; Wallace, G. *Polymer* **2005**, *13*, 4664–4669.
(49) Hansen, T. S.; West, K.; Hassager, O.; Larsen, N. B. *Synth. Met.* **2006**, *18−20*, 1203–1207.
(50) Meldal, M.; Tornoe, C. W. *Chem. Rev.* **2008**, *8*, 2952–3015.
(51) Habib, P. M.; Rama Raju, B.; Kavala, V.; Kuo, C. W.; Yao, C. F. *Tetrahedron* **2009**, *29−30*, 5799–5804.

Supporting information for:

Solvent Composition Directing Click-functionalization at the Surface or in the Bulk of Azide-Modified PEDOT

Johan U. Lind,[†] Thomas S. Hansen,[†] Anders E. Daugaard,[‡] Søren Hvilsted,[‡] Thomas L. Andresen,[†] and Niels B. Larsen[*,†]

[†] *Department of Micro- and Nanotechnology, Technical University of Denmark, DTU Nanotech, Ørsteds Plads 345ø, 2800 Kgs. Lyngby, Denmark, and* [‡] *Department of Chemical and Biochemical Engineering, Technical University of Denmark, Søltofts Plads, Building 227, 2800 Kgs. Lyngby Denmark*

*Corresponding author. E-mail: niels.b.larsen@nanotech.dtu.dk

Polymerization of thin films PEDOT-N_3 onto COC supports

PEDOT-N_3 electrodes were prepared by in situ polymerization of EDOT-N_3 on injection molded COC (TOPAS 5013, TOPAS Advanced Polymers, Frankfurt, Germany) discs. The discs were cleaned with acetone, isopropanol, ethanol, and water. EDOT-N_3 (see Figure 1A in main text) (20 mg, 0.15 mmol), CLEVIOS C (0.48 mL, ~40 wt % Fe(III)tosylate in 1-butanol, H.C. Starck, Goslar, Germany), and 1-butanol (0.48 mL) were mixed and spin-coated on the COC discs (20 s at 700 rpm). The samples were placed in an oven at 70 °C for 2 min and subsequently washed with water and blown dry in a nitrogen flow, yielding films with a thickness of approximately 150 nm.

Polymerization of thin films of PEDOT onto COC or glass supports

PEDOT electrodes were prepared by in situ polymerization of EDOT on injection molded COC (TOPAS 5013, TOPAS Advanced Polymers, Frankfurt, Germany) discs, or microscope glass slides substrates, cleaned with acetone, isopropanol, ethanol and water. 6.5 mL CLEVIOS C-B40 (H.C. Starck, Goslar, Germany), 2 mL 1-butanol, 0.15 mL pyridine, and 0.22 ml CLEVIOS M (H.C. Starck), were mixed in the stated order and spin-coated on the COC-discs (20 s at 700 rpm). The samples were placed in an oven at 70 °C for 2 min and subsequently washed with water and blown dry in a nitrogen flow, yielding films with a thickness of approximately 140 nm.

Synthesis of Alkyne-PEG-G_5-F(I)-GRGDS (see Figure S1)

Pentyne-EG_{11}-G_5-F(4-iodo)-GRGDS was made using solid phase synthesis. Base labile Fmoc was used for protecting groups for the amines, and the employed resin was acid labile rink-amide. 2-(1H-7-Azabenzotriazol-1-yl)-1,1,3,3-tetramethyl-uronium-hexafluorophosphate-Methanaminium (HATU), Fmoc-Ser(tBu)-OH, Fmoc-Asp(OtBu)-OH, Fmoc-Arg(Pbf)-OH, Fmoc-4-Iodo-Phe-OH, Fmoc-Gly-OH and Rink Amide-AM Resin were from GL Biochem (Shanghai, China). Fmoc-NH-PEG_{11}-COOH, *PEG1080,* was acquired from IRIS biotech (Marktredwitz, Germany). 4-Pentynoic acid, (EDC), 2,4,6-Collidine, trifluoro acetic acid (TFA), Tri-isopropyl silane (TIPS), ninhydrin, piperidine, and all solvents, were acquired from Sigma-Aldrich.

Before reaction, the resin was swelled in dichloromethane (DCM) for 1½ hours. In each coupling step four equivalents of the new amino acid was used. The amino acid was first mixed with 3.9 equivalents (eq.) HATU coupling reagent and 8 eq. 2,4,6-Collidine in dimethylformamide (DMF), then added to the peptide, and allowed to react for 30 minutes. The beads were washed 4 times in DMF and 2 times in DCM, each washing step lasting 30 seconds. De-protection of the Fmoc group was done by washing twice for 2 minutes with a 20% solution of piperidine in DMF.

Kaiser tests were performed to test the presence of free amino groups between each reaction/de-protection step. The coupling of the PEG segment was done by performing two consecutive coupling reactions, each lasting 1 hour, to ensure a successful binding of the PEG segment. The following pentynoic acid step was also allowed to react for 1 hour.

The peptide was cleaved from the resin using a solution of 2.5%v/v TIPS, 2.5%v/v Milli-Q water and 95%v/v TFA. A cleaving time of 3 hours was used. The cleaving solution containing the peptides was then dried on a rotary evaporator. The material remaining was then gently decanted five times using 5 ml diethyl ether.

The product was purified using preparative reverse phase High Performance Liquid Chromatography (RP-HPLC). The RP-HPLC was conducted on a 250 mm x 20 mm C18 column with a bead size of 5 um and a pore size of 100Å. Solvent A: 95%v/v H_2O / 5%v/v MeOH / 0.1%v/v TFA. Solvent B: 99.9%v/v MeOH / 0.1%v/v TFA. The solvents were degassed using a glass filter prior to their use on the RP-HPLC.

Solutions of the peptides were made in 50%v/v Solvent A/Solvent B. In the RP-HPLC procedure, a linear gradient from 52% to 54% of Solvent A over 16 minutes was used. UV detection was set to 206 nm (carbonyl) and 257 nm (phenylalanine).

An equivalent procedure was used for the fabrication and purification of the scrambled sequence peptide, *Pentyne-EG_{11}-G_5-F(4-iodo)-GRDGS*.

The yields after RP-HPLC purification and freeze drying were:

Pentyne-EG_{11}-G_5-F(4-iodo)-GRGDS: 41.3mg (16%)

Pentyne-EG_{11}-G_5-F(4-iodo)-GRDGS: 48.8mg (19%)

The purity of the products was confirmed by MALDI-TOF MS using a Bruker Reflex IV MALDI-TOF, matrix 50 mg/ml 2,5-dihydroxy benzoic acid (DHB) in ethanol, and using compound concentrations of 0.1-1 mg/mL.

MS (m/z, MALDI-TOF): 1727.3 $\{M+H\}^+$.

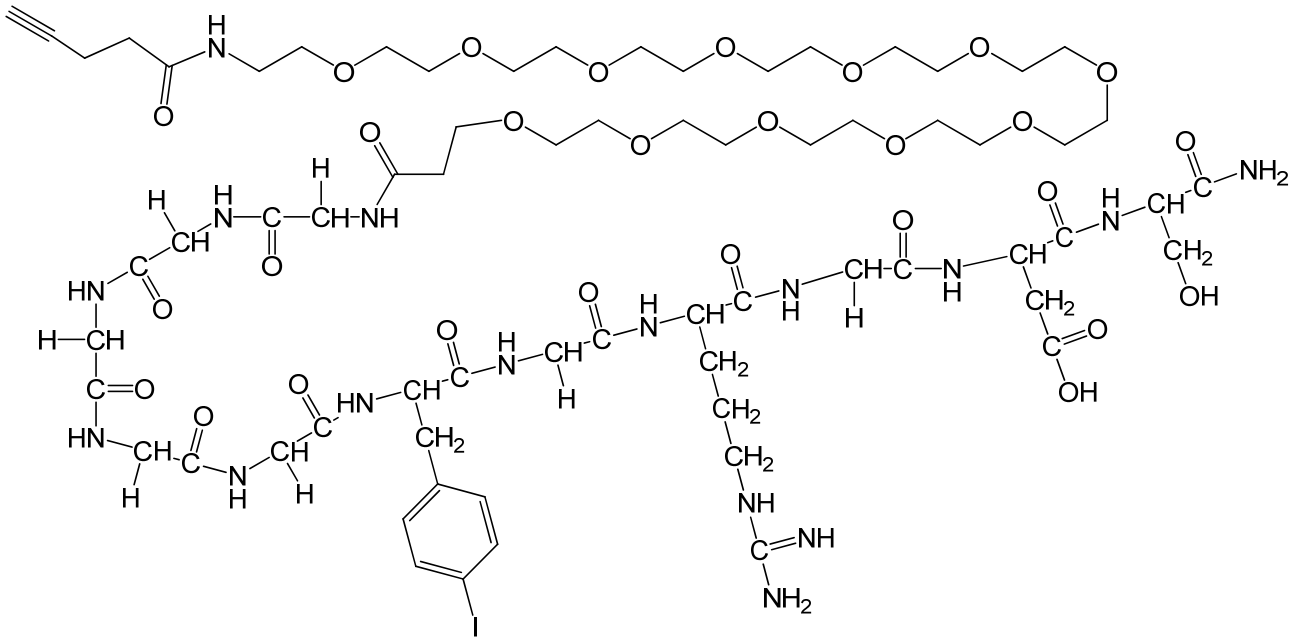

Figure S1. The structure of the Alkyne-PEG-G_5-F(I)-GRGDS (similar for "scrambled" alkyne-PEG-G5-F(I)-GRDGS, except for exchange of the last glycine and aspartate moieties).

Synthesis of Prop-2-ynyl 5-(N,N-bis(carboxymethyl)amino)-5-(*S*)carboxypentanecarbamate (NTA-alkyne, Figure S2)

N,*N*-Bis(carboxymethyl)-L-lysine hydrate (NTA, 0.100 g, 0.4 mmol) and $NaHCO_3$ (0.128 g, 1.5 mmol) was dissolved in H_2O (3.5 mL). Propargylchloroformate (0.05 g, 0.4 mmol) in toluene (2 mL) was added slowly at 0 ^oC. The reaction mixture was stirred overnight at room temperature. Toluene was removed *in vacuo* and the residue was acidified with DOWEX. The product was isolated after lyophilization as a white solid (79.0 %, T_m= 135 ^oC).

IR (cm^{-1}): 3405 (N-H); 3280 (C≡C-H); 3100-2800 (C-H); 2120 (C≡C); 1705 (COOH); 1615 OC(O)N); 1395 (C-N); 1255, 1135 (C-O).

^{1}H-NMR (300 MHz) D_2O, δ_H (ppm): 1.2-1.7 (m, 6 H, CH_2-CH_2); 2.92 (t, ^4J = 2.2 Hz, 1 H, C≡C-*H*); 3.18 (t, ^3J =5.9 Hz, 2 H, OC(O)N-CH_2); 3.82 (m, 5 H, N-CH_2-COOH, N-C*H*-COOH); 4.69 (m, 2 H, OCH_2-C≡CH).

^{13}C-NMR (75 MHz) D_2O, δ_C (ppm): 23.6, 26.5, 28.6 (3 C, *C*H_2-CH_2); 40.1 (1 C, OC(O)N-*C*H_2); 52.7 (1 C, C≡C-*C*H_2); 55.5 (2 C, N-*C*H_2-COO); 68.3 (1 C, N-*C*H-COOH); 75.7 (1 C, H*C*≡C); 78.8 (1 C, HC≡*C*-CH_2); 157.6 (1 C, O*C*(O)N); 170.5 (2 C, CH_2-*C*OOH); 172.8 (1 C, CH-*C*OOH).

MS (m/z, ESI): 367 $\{M+Na\}^+$.

NMR spectroscopy was performed on a 300 MHz Cryomagnet from Spectrospin & Bruker (^{1}H-NMR at 300MHz, ^{13}C-NMR at 75MHz), at room temperature.

IR was performed on a PerkinElmer Spectrum One model 2000 Fourier transform infrared system with a universal attenuated total reflection sampling accessory on a ZnSe/diamond composite.

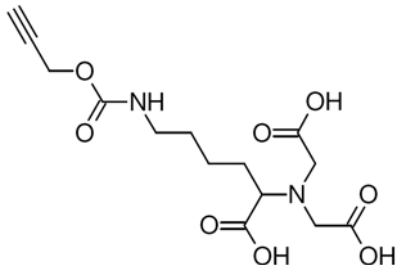

Figure S2. Structure of the NTA-alkyne

Synthesis of PEG-alkyne (see Figure S3)

α-Methoxy-poly(ethylene glycol)-ω-pent-4-ynamide, was made by coupling 2.0173 g MeO-PEG-NH_2 (*PEG1155*, 750 Da, PDI 1.2, Iris biotech, Marktredwitz, Germany) and 237.3 mg (0.9 eq.) 4-Pentynoic acid (Sigma-Aldrich) in 60 mL dichloromethane using 155.24 mg (1 eq.) N-(3-Dimethylaminopropyl)-N´-ethyl-carbodiimide (EDC) (Sigma-Aldrich) overnight.

The reaction mixture was concentrated to dryness using a rotary evaporator and the product was hereafter purified by flash chromatography packed with silica gel (eluent: methanol/DCM 5:95). The product fractions were concentrated on a rotary evaporator and dried overnight on an oil pump. The yield was 916 mg (45.6%) output.

The purity of the products was confirmed by MALDI-TOF MS using a Bruker Reflex IV MALDI-TOF, matrix 50 mg/ml 2,5-dihydroxy benzoic acid (DHB) in ethanol, and using compound concentrations of 0.1-1 mg/ml. TLC (eluent: methanol/DCM 5:95) showed no presence of the starting materials. This was confirmed by ^{1}H- and ^{13}C-NMR.

^{13}C-NMR (63 MHz): (δ_C, ppm) 170.9(N-C=O), 83.08(C≡C-H) 71.9(CH_3-O-CH2) 70.6-69.7(O-C-C), 69.2(C-C≡C), 58.9(CH_3-O-CH2) 39.3(C-C-NH-C=O), 35.2(O=C-C-C) 14.8(C-C-C≡C)

^{1}H-NMR (250 MHz): (δ_H, ppm) 6.35(s, HN-C=O), 3.4-3.7(m, O-CH_2-CH_2-O), 3.35(s,O-CH_3) 2.4-2.6(m,O=C-CH_2-CH_2-C≡C), 1.95(H-C≡C).

MS (m/z, MALDI-TOF): 816.0 $\{M+H\}^+$.

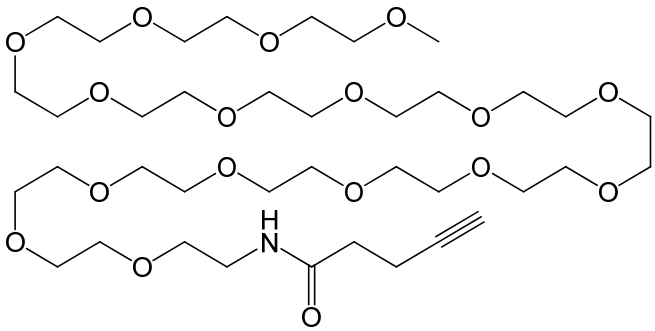

Figure S3. Structure of PEG-alkyne

Optical absorption of PEDOT-N_3 and PEDOT films in liquid environments

PEDOT:TsO or PEDOT-N_3:TsO films on COC supports were immersed for 10 minutes in MilliQ water or DMSO, respectively, before measuring their absorbance spectra. Reoxidation of the films were performed by brief immersion in 10% Fe(III) tosylate (CLEVIOS C, Heraeus, Germany) in MilliQ water followed by thorough washing with MilliQ water. Absorbance spectra were recorded on a Shimadzu UV-1700 spectrophotometer. The results are presented in Figure S4.

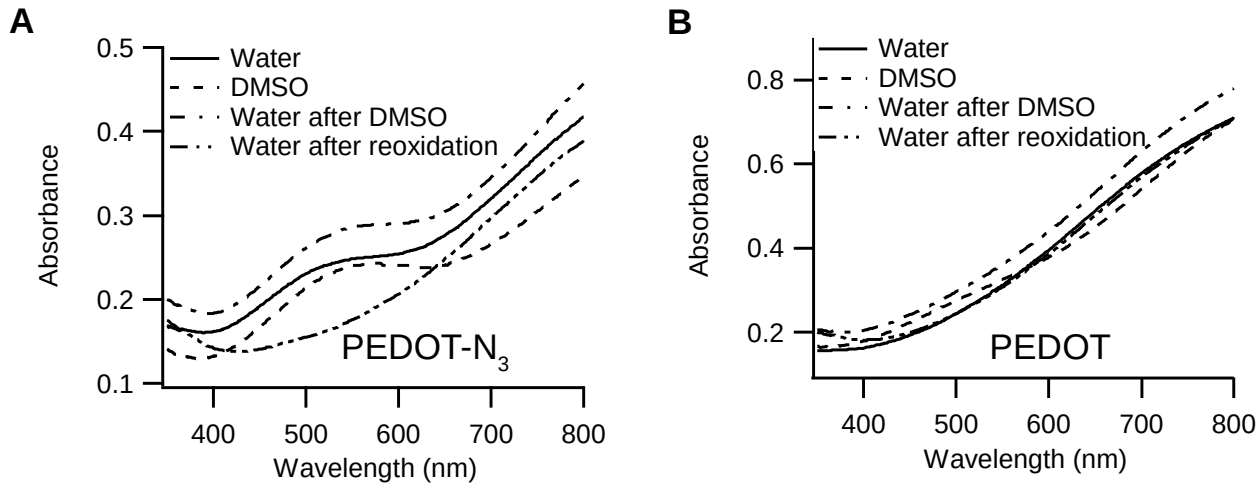

Figure S4. Optical absorbance of (A) PEDOT-N_3:TsO or (B) PEDOT:TsO film after immersion in water, immersion in DMSO, immersion in DMSO followed by washing in water, or reoxidation in Fe(III) tosylate followed by washing in water, respectively.

Surface morphology of PEDOT-N_3 and PEDOT films in liquid environments

AFM micrographs were acquired on films of PEDOT-N_3:TsO or PEDOT:TsO, respectively, according to the procedure presented in the "AFM measurements" section of the main text. Figure S5 displays selected images of films in the dry state, immersed in MilliQ water, immersed in DMSO, and immersed in DMSO followed by exchange to MilliQ water, respectively.

Figure S5. AFM micrographs of (A) PEDOT-N_3:TsO or (B) PEDOT:TsO films immersed in liquid environments and measured across a mechanically induced surface defect. The color legend corresponds to the measured heights with all images being presented using the same height-to-color scaling, and with each image vertically shifted to have zero height at the substrate surface (black areas). Scale bars: 10 µm.

The film surface morphology was analyzed using the open source software package Gwyddion (gwyddion.net): A surface area of 8 μm by 30 μm was extracted from each AFM image, background corrected using a first-order plane fit, and analyzed by the "Statistical quantities" function. The results are summarized in Table S1.

Table S1. Surface roughness of PEDOT-N_3 tosylate and PEDOT tosylate films prior to immersion in liquid, immersed in water, then immersed in DMSO, and finally after drying, respectively. Analysis proceeded using the roughness analysis routine of the Gwyddion software package on an area of the images presented in Figure S4 visually estimated to be part of the conducting polymer film.

	Roughness R_a				Roughness R_{rms}			
	Dry	Water	DMSO	Water after DMSO	Dry	Water	DMSO	Water after DMSO
PEDOT-N_3:TsO	2.1	5.7	3.1	2.8	2.9	8.6	3.9	3.6
PEDOT:TsO	1.5	2.7	4.3	4.5	1.9	4.1	4.9	6.1

Modification of PEDOT-N_3 substrates with propargyl alcohol, NTA-alkyne, or alkyne-peptide, as a function of DMSO content in the solvent

The reactions were overall conducted as described in the *Experimental Section* of the main text, using varying DMSO content in the reaction solution. The figure captions of Figures S6-S8 presents the specific concentrations and reaction times used for the three different compounds (Figure S6: propargyl alcohol; Figure S7: NTA-alkyne; Figure S8: alkyne-peptide). The modified PEDOT-N_3 films were analyzed by XPS as described in the *Experimental Section*.

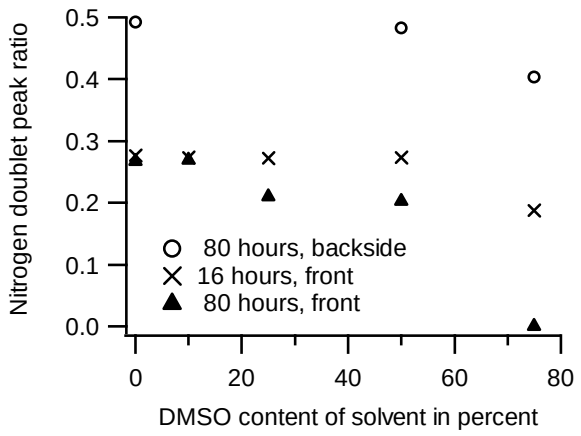

Figure S6. XPS analysis of the degree of reaction on PEDOT-N_3 films modified by propargyl alcohol as a function of DMSO concentration. The longer reaction time of 80 hours used 12.5 mM propargyl alcohol, 1.25 mM $CuSO_4$, and 50 mM sodium ascorbate (front side: closed triangles; backside: open circles). The shorter reaction time of 16 hours (crosses) used 10 mM propargyl alcohol, 1 mM $CuSO_4$, and 40 mM sodium ascorbate. A nitrogen peak intensity ratio of ½ corresponds to zero degree of reaction, while full conversion of the azides yields a peak ratio of 0. Nitrogen peak analysis was performed both on the front side and backside of the film. The signal from the backside suggest some degree of reaction throughout the film thickness for the highest DMSO concentration.

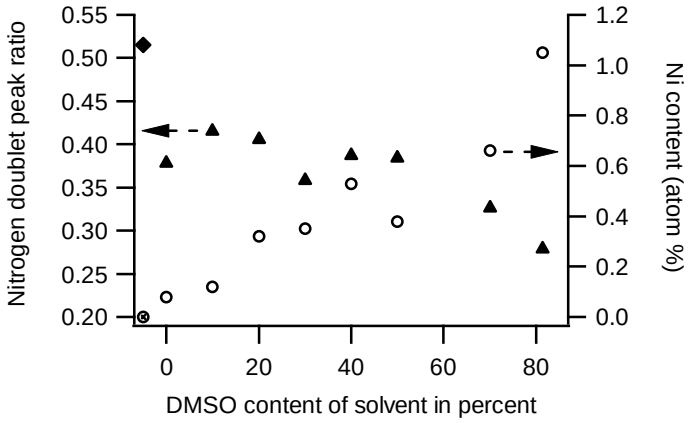

Figure S7. XPS analysis of the degree of reaction on PEDOT-N_3 films modified by NTA-alkyne as a function of DMSO concentration, determined by the nitrogen doublet peak ratio (solid triangles; reference: solid diamond) and the surface concentration of nickel (open circles; reference: cross in circle). All reactions used 10 mM NTA-alkyne, 2 mM $CuSO_4$, 40 mM sodium ascorbate, and a reaction time of 4 hours. The NTA moiety can chelate transition row metals such as Ni(II), which was used as an independent XPS assay of the degree of reaction in addition to the nitrogen peak ratio analysis. For the Ni(II) assay, the samples were immersed in 50 mM EDTA in 50 mM Tris buffer for 30 minutes, reacted with 100 mM Ni(II)SO_4 in Milli-Q water for 30 minutes, and rinsed with Milli-Q water before drying in a stream of nitrogen. *Left axis:* A nitrogen peak intensity ratio of ½ corresponds to zero degree of reaction, while full conversion of the azides yields a peak ratio of 0. *Right axis:* Increasing nickel content corresponds to higher degrees of reaction. The reference is a freshly prepared PEDOT-N_3 film.

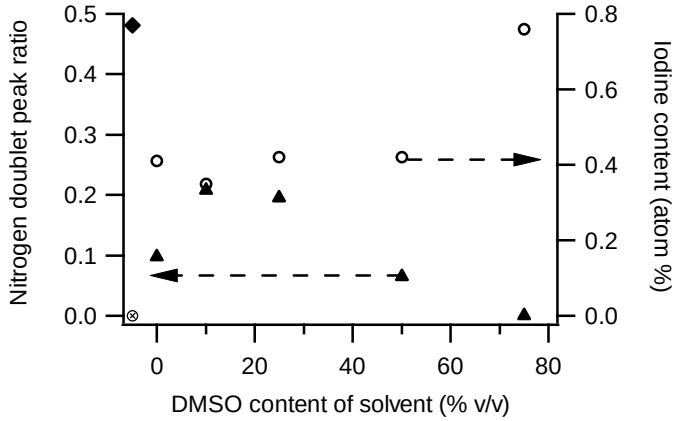

Figure S8. XPS analysis of the degree of reaction on PEDOT-N_3 films modified by alkyne-PEG-G_5-F(I)-GRGDS as a function of DMSO concentration, determined by the nitrogen doublet peak ratio (solid triangles; reference: solid diamond) and the surface concentration of iodine (open circles; reference: cross in circle). All reactions used 5 mM alkyne-peptide, 1 mM $CuSO_4$, 20 mM sodium ascorbate, and overnight reaction time. *Left axis:* A nitrogen peak intensity ratio of ½ corresponds to zero degree of reaction, while full conversion of the azides yields a peak ratio of 0. The nitrogen peak ratio will also be influenced by coupling of the nitrogen-rich peptide fragment, and is therefore less straight-forward to interpret for this molecule. *Right axis:* Increasing iodine content reliably corresponds to higher degrees of reaction as only the alkyne-peptide contains iodine as hetero-atom. The reference is a freshly prepared PEDOT-N_3 film.

Synthesis of poly(4-(azidomethyl)styrene) (PS-N_3) (see Figure S9)

2,2'-Azobisisobutyrylnitrile (AIBN, 71.2 mg, 0.4 mmol), 4-(chloromethyl)styrene (10 mL, 71.0 mmol and xylene was mixed in a Schlenk tube and the solution was bubbled through with nitrogen for 30 min. The polymerization was run under a positive nitrogen pressure at 65°C for 18 h. The polymer was precipitated in methanol, filtered and dried in vacuo. The isolated intermediate (poly(4-(chloromethyl)styrene)) was a white powder and was used for the following step without further purification (6.4 g, M_n= $30 \cdot 10^3$ g/mol, PDI= 1.7).

FT-ATR-IR (cm^{-1}): 3100-2800 (C-H stretch); 1612+1510 (aromatic ring stretch); 672 (C-Cl stretch).

^{1}H-NMR (300 MHz) $CDCl_3$, δH (ppm): 1.39 (m, 2H, CH_2-CH); 1.70 (m, 1H, CH-CH_2); 4.52 (s, 2H, CH_2-N_3); 6.49, 7.05 (2xm, 4H, aromatic H).

HSQC confirmed the following proton/carbon correlations (δH/δC (ppm)): 1.39/41.6 (CH-CH_2); 1.70/38.7 (CH-CH_2-ph); 4.52/44.9 (CH_2-N_3); 6.49/126.4 (aromatic CH); 7.05/127.0 (aromatic CH).

Poly(4-(chloromethyl)styrene) (5.18 g, 34.0 mmol functional group) was dissolved in DMF (100 mL) and NaN_3 (2.75 g, 42.4 mmol) was added to the solution. The reaction mixture was stirred at 40°C for 18 h under nitrogen. After reaction the excess of reagent was removed by precipitation into H_2O. The precipitate was isolated by filtration and rinsed with copious amounts of H2O and methanol. The solid was dissolved in THF and precipitated in methanol to afford poly(4-(azidomethyl)styrene) as a white powder (4.62 g, 86 %).

FT-ATR-IR(cm^{-1}): 3100-2800 (C-H stretch); 2090 (C-N_3 stretch); 1612+1510 (aromatic ring stretch).

^{1}H-NMR (300 MHz) $CDCl_3$, δH (ppm): 1.39 (m, 2H, CH_2-CH); 1.69 (m, 1H, CH-CH_2); 4.24 (s, 2H, CH_2-N_3); 6.48, 6.97 (2xm, 4H, aromatic H).

HSQC confirmed the following proton/carbon correlations (δH/δC (ppm)): 1.39/44.9 (CH-CH_2); 1.69/40.4 (CH-CH_2-ph); 4.24/54.0 (CH_2-N_3); 6.48/127.7 (aromatic CH); 6.97/127.7 (aromatic CH).

NMR spectroscopy was performed on a 300 MHz Cryomagnet from Spectrospin & Bruker (^{1}H-NMR at 300MHz, ^{13}C-NMR at 75MHz), at room temperature.

IR was performed on a PerkinElmer Spectrum One model 2000 Fourier transform infrared system with a universal attenuated total reflection sampling accessory on a ZnSe/diamond composite.

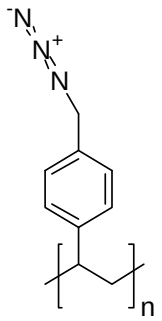

Figure S9. Structure of poly(4-(azidomethyl)styrene) (PS-N_3)

Spin-coating of PS-N_3 onto COC substrates.

A 10 mg/mL solution of PS-N_3 in dioxane was made. 500 µL of the solution was spin-coated onto a COC substrate a 1000 rpm.

Modification of PS-N_3 with PEG-alkyne

The reactions were overall conducted as described in the *Experimental Section* of the main text, using varying DMSO content in the reaction solution. Figure S10 shows the results from XPS analysis of the modified samples.

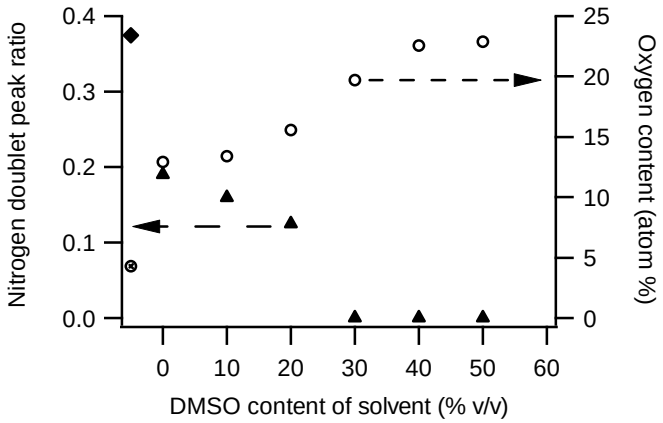

Figure S10. XPS analysis of the degree of reaction on PS-N_3 films modified by PEG-alkyne as a function of DMSO concentration, determined by the nitrogen doublet peak ratio (solid triangles; reference: solid diamond) and the surface concentration of oxygen (open circles; reference: cross in circle). All reactions used 5 mM PEG-alkyne, 1 mM $CuSO_4$, 20 mM sodium ascorbate, and overnight reaction time. *Left axis:* A nitrogen peak intensity ratio of ½ corresponds to zero degree of reaction, while full conversion of the azides yields a peak ratio of 0. *Right axis:* Increasing oxygen content corresponds to higher degrees of reaction as only the alkyne-peptide contains oxygen as hetero-atom. A dense surface layer of reacted PEG-alkyne in a largely stretched conformation would approach an oxygen content of ~30 atom%. The reference is a freshly prepared PS-N_3 film.

Appendix 5

Facile Micropatterning of Functional Conductive Polymers with Multiple Surface Chemistries in Register

Manuscript submitted to *Langmuir* **2012**

Micropatterning of functional conductive polymers with multiple surface chemistries in register

Journal:	*Langmuir*
Manuscript ID:	la-2012-00503p
Manuscript Type:	Article
Date Submitted by the Author:	02-Feb-2012
Complete List of Authors:	Lind, Johan; DTU, Nanotech Acikgoz, Canet; ETH Zürich, Department of Materials Daugaard, Anders; Technical University of Denmark, Chemical Engineering Andresen, Thomas; Technical University of Denmark, Department of Micro- and Nanotechnology Hvilsted, Soeren; Technical University of Denmark, Chemical Engineering Textor, Marcus; ETH Zurich, Department of Materials Larsen, Niels; DTU-Nanotech,

SCHOLARONE™
Manuscripts

Micropatterning of functional conductive polymers with multiple surface chemistries in register

Johan U. Lind [†], Canet Acikgöz [‡], Anders E. Daugaard [§], Thomas L. Andresen [†], Søren Hvilsted [§], Marcus Textor [‡], and Niels B. Larsen *[,†]

† Department of Micro- and Nanotechnology, Technical University of Denmark, DTU Nanotech, Ørsteds Plads 345B, 2800 Kgs. Lyngby, Denmark

‡ Laboratory for Surface Science and Technology, Department of Materials, ETH Zürich, Wolfgang-Pauli-Strasse 10, CH-8093 Zürich, Switzerland

§ Department of Chemical Engineering, Technical University of Denmark, Søltofts Plads Building 227, 2800 Kgs. Lyngby, Denmark

* To whom correspondance should be addressed. E-mail: niels.b.larsen@nanotech.dtu.dk

RECEIVED DATE (to be automatically inserted after your manuscript is accepted if required according to the journal that you are submitting your paper to)

ABSTRACT

A versatile procedure is presented for fast and efficient micropatterning of multiple types of covalently bound surface chemistry in perfect register on and between conductive polymer microcircuits. The micropatterning principle is applied to several types of native and functionalized PEDOT (poly(3,4-ethylenedioxythiophene)) thin films. The method is based on contacting PEDOT-type thin films with a micropatterned agarose stamp containing an oxidant (aqueous hypochlorite) and applying a non-ionic detergent. Where contacted, PEDOT not only loses its conductance, but is entirely removed, thereby locally revealing the underlying substrate. Surface analysis showed that the substrate surface chemistry was fully exposed and not affected by the treatment. Click chemistry could thus be applied to selectively modify re-exposed alkyne and azide functional groups of functionalized polystyrene substrates. The versatility of the method is illustrated by micropatterning cell-binding RGD-functionalized PEDOT on low cell-binding PMOXA (poly(2-methyl-2-oxazoline)) to produce cell capturing microelectrodes on a cell non-adhesive background in a few simple steps. The method should be applicable to a wide range of native and chemically functionalized conjugated polymer systems.

KEYWORDS

Conducting polymers, patterning, surface modification, functional coatings

1. Introduction

Micropatterned conductive polymers are exciting active materials for low-cost microsystems with a number of attractive unique characteristics. These include their ability to act both as an ionic and an electronic conductor, and the potential for altering the chemical appearance of the polymers by simply altering the monomer unit.[1-6] For biomedical applications, conductive polymers have further valuable features such as the ability to capture biomolecules on or within the polymer and specifically release these molecules upon electrical stimuli,[7, 8] and as a vehicle for electrochemically controlled cellular adhesion.[9, 10] These applications rely on the ability to engineer the surface chemistry of the conductive polymer as well as its surroundings to control biomolecule and cell adhesive properties. PEDOT (poly(3,4-ethylenedioxythiophene)) is a particularly interesting conductive polymer due to its ease of handling, high conductivity, chemical stability, and cellular compatibility.[1, 11, 12]

Conductive polymers are conventionally micropatterned using photolithography and other clean room processes.[13, 14] Such processes are versatile but expensive, and may additionally use harsh chemical conditions that adversely affect the surface chemistry of the final product. Alternative inexpensive micropatterning methods are therefore in demand. Such methods should ideally preserve the surface chemical properties and even permit engineering of the surface chemistry. We address this need by demonstrating a simple method for producing defined functionalized PEDOT microelectrodes on functionalized polymer substrates. The method allows the introduction of multiple types of patterned surface chemistries, both onto the electrodes and to the gaps in between. These in-register surface chemistries are covalently bound, and local functionalities can thus be chosen to fit a given task. Notably, no alignment steps are required and the presented “printed dissolution” method is inexpensive, since it largely avoids clean room processes.

The central concept of the method is to locally remove the conductive polymer film to expose a chemically unaffected underlying functional substrate (Fig.1). The local removal is initiated by physically contacting a PEDOT thin film with a bas-relief structured agarose stamp containing an oxidizing agent, e.g. aqueous sodium hypochlorite (NaOCl) (Fig.1A). We have earlier reported that such stamping, without the use of detergent, can be used for locally making the thin film electrically insulating, since oxidization degrades the conjugated system of the PEDOT backbone.[15] In the absence of detergent, a stable film of oxidized PEDOT will however be left in the gaps between the electrodes (Fig.1B). Here, we report that the remaining oxidized PEDOT can be removed from the supporting substrate by applying a non-ionic detergent either directly in the agarose stamp, or in a subsequent washing step (Fig. 1C). Equally important, we have found that various functional chemical groups are not influenced by the oxidative environment used in the patterning procedure. These findings open a simple route to fabricate polymeric microsystems with controlled surface chemistries both on and between PEDOT electrodes by "hiding" polymer thin films containing specific functional groups below the PEDOT film. This aspect distinguishes our method from standard micropatterning techniques such as reactive ion etching (RIE) that normally destroys any predefined organic chemistry below the etched film. Our procedure is shown to be applicable for patterning several functionalized PEDOT types, poly-(3,4-(1-azidomethylethylene)-dioxythiophene) (PEDOT-N_3) and poly-(3,4-(1-hydroxymethylethylene)-dioxythiophene) (PEDOT-OH), in addition to regular PEDOT. Consequently, multiple types of localized chemistries can easily be introduced into an all-polymer micro-system by combining functional substrates with functional PEDOT films of orthogonal chemical reactivity.

We first show how PEDOT thin films can be locally removed from injection molded cyclic-olefin-copolymer (COC) substrates by applying detergents either directly in the stamp or in a subsequent washing step. This serves to demonstrate the general principles and the degrees of freedom in the methodology. We then proceed to the removal of PEDOT from, and ensuing click-reaction onto, a click-reactive substrate (PS-N_3, poly(4-azidomethylstyrene)). We illustrate how this can be combined with the

chemically orthogonal PEDOT-OH to introduce two distinct types of surface chemistry in the system. As a further example, we show how another type of chemically reactive PEDOT, click-reactive PEDOT-N_3, in combination with an alkyne-modified polystyrene substrate can provide three types of locally directed surface chemistries in register. This is achieved using electro-click reactions.[16-18] Finally we show that a high degree of biological specificity can be achieved by first introducing coatings of poly(2-methyl-2-oxazoline) (PMOXA) or poly(ethylene glycol) (PEG), both having low cell-binding properties, below click-functionalizable PEDOT-N_3 microelectrodes. The microelectrodes are then sequentially reacted with high cell-binding RGD-containing peptides to enable local cellular attachment onto selected sets of microelectrodes in an all-polymer microfluidic system.

2. Experimental section

Chemicals and materials: EDOT-OH, 10-15 wt% aqueous NaOCl (sodium hypochlorite), Triton-X100, agarose, and all small halogenated marker molecules were purchased from Sigma-Aldrich. Clevios M (EDOT monomer) and Clevios C-B 40 (40 wt% iron(III)tosylate in n-butanol) were acquired from Heraeus Clevios GmbH (Germany). PEG-alkyne (750 Da, art. no. PEG2840) was obtained from IRIS Biotech GmbH (Germany). EDOT-N_3 was synthesized as described in our previous report.[5] Alkyne modified polystyrene (PS-alkyne) was synthesized as outlined in the Supporting Information, following an earlier established route.[19] Azide modified polystyrene (PS-N_3), alkyne-PEG-GRGDS and alkyne-PEG-GRDGS were synthesized and characterized as described in the Supporting Information. Alkyne-PMOXAs were synthesized and characterized as described in the Supporting Information, combining earlier reported schemes.[20-25] Disc-shaped (Ø 50 mm; thickness 2 mm) cyclic olefin copolymer (COC) substrates were injection molded on an Engel Victory 80/45 (Schwertberg, Austria) using TOPAS 5013 (TOPAS Advanced Polymers, Frankfurt-Höchst, Germany).

Thin film preparations: PS-N_3 and PS-alkyne thin films were prepared by spin coating a solution of 5 mg/mL polymer in 1,4-dioxane onto COC substrates at 1000 rpm. The samples were heated briefly on a

hotplate at 60ºC to remove residual solvent. PMOXA films used for the cellular studies of Fig. 7 resulted from overnight reaction of a PS-N_3 covered COC substrate with a PMOXA(4000)-alkyne solution of 1 mM $CuSO_4$, 15 mM sodium ascorbate, 2 mM PMOXA-alkyne dissolved in 64/36 v/v DMSO/H_2O. The following day the substrate was backfilled by reaction for 4 h with a PMOXA(2000)-alkyne reactant solution of 1 mM $CuSO_4$, 15 mM sodium ascorbate, 2 mM PMOXA-alkyne dissolved in 64/36 v/v DMSO/H_2O. Following the reaction, the sample was rinsed in MilliQ water. PEDOT, PEDOT-N_3, and PEDOT-OH thin films with tosylate counter-ions were prepared by in situ polymerization on their respective substrate surfaces.[5, 12] PEDOT films were prepared by spin coating a solution of 6.5 mL Clevios C-B40, 2 mL n-butanol, 220 µL EDOT monomer, and 150 µl pyridine, at 700-1000 rpm followed by >2 mins baking on a hotplate at 65ºC. Following polymerization the film was rinsed in Milli-Q water and ethanol. PEDOT-OH films were fabricated on top of a premade PEDOT film using the same methodology (PEDOT-OH/PEDOT). PEDOT-N_3 was likewise spin coated onto PEDOT (PEDOT-N_3/PEDOT) by using 45 mg EDOT-N_3, 700 µL n-butanol, and 700 µL Clevios C-B40 as precursor solution. Both PEDOT-OH and PEDOT-N_3 solutions were spin coated at 1000 rpm. The resulting conducting polymer films had a thickness of ~150 nm.[26]

Agarose stamp preparation: A silicon mold was fabricated by standard photolithography and deep reactive ion etching. The mold fabricated in this manner proved more stable over time than our earlier reported method using SU-8.[15] Also, this method allowed deeper featured to be produced in the stamp, which facilitated the patterning of large areas. Prior to each use the mold was rinsed in ethanol, and occasionally rinsed in air plasma to remove any residual organic material. The silicon mold was placed on a hotplate set to 65ºC. A 10 wt% solution of agarose in MilliQ water was mixed thoroughly. The solution was heated in a microwave oven to remove air bubbles from the solution. To prevent the solution from boiling, this was done using a series of multiple short heating cycles. The hot agarose solution was poured directly onto the silicon mold, contained inside a Ø 5 cm polystyrene Petri dish with its bottom removed. The container was covered with a lid and kept on the hot plate for 10 min. The

mold was then transferred to a fridge and left for minimum 10 min to cool down. After the fabrication the agarose stamp was usually cut with a scalpel to a smaller size for improved handling.

Agarose stamping procedure: The agarose stamp was soaked for 15 min in a stamping solution, and excess solution was blown off using an air gun. The stamp was gently pressed onto the sample surface to establish contact, left for 4 min (unless stated otherwise) before removing the stamp, and then immediate rinsing of the sample in MilliQ water. Between each stamping cycle, the stamp was soaked for 5 min in the stamping solution. For stamping PEDOT films, a solution of 1:10 solution of NaOCl stock in MilliQ water was used leading to a 1-1.5 wt% solution while for the samples containing PEDOT-OH on PEDOT or PEDOT-N_3 on PEDOT 1/6 of the NaOCl stock was used leading to a 1.7-2.5 wt% solution. Stamping solutions also included 0.1 vol% Triton-X100 where indicated.

Post-stamping washing procedure: Following the stamping, the samples were washed for 10 min in an aqueous solution of 0.1 vol% Triton-X100 and 1 wt% sodium ascorbate at 50ºC (except where stated otherwise). All samples were washed twice for 10 min in MilliQ water at 50ºC and 10 min in 80/20 v/v DMSO/H_2O at room temperature, before rinsing in ethanol, MilliQ water, and re-oxidization of the PEDOT by rinsing in 10/90 v/v Clevios C-B40/H_2O, and rinsing in MilliQ water.

Ester coupling of 5-bromopentanoic acid on PEDOT-OH: PEDOT-OH was reacted for 45 mins using 180 mM 5-bromopentanoic acid, 150 mM 1-ethyl-3-(3-dimethylaminopropyl)carbodiimide (EDC), 150 mM 4-dimethylaminopyridine (DMAP) in dry DMSO. The sample was rinsed in MilliQ water followed by re-oxidization of the PEDOT by rinsing in 10/90 v/v Clevios C-B40/H_2O, and rinsing in MilliQ water.

Click-reaction conditions: Post stamping click-reactions were all done overnight in water-DMSO mixtures, and stopped by rinsing in de-ionized water followed by re-oxidizing the PEDOT by rinsing in

10/90 v/v Clevios C-B40/H_2O, and rinsing in MilliQ water. Clicking of 5-iodopentyne to a substrate of PEDOT on PS-N_3: 65/35 v/v DMSO/H_2O, 5 mM $CuSO_4$, 20 mM sodium ascorbate, 25 mM 5-iodopentyne. Clicking of 5-iodopentyne to a substrate of PEDOT-OH (ester coupled to bromopentanoic acid)/PEDOT on PS-N_3: 65/35 v/v DMSO/H_2O, 1 mM $CuSO_4$, 10 mM sodium ascorbate, 5 mM 5-iodopentyne. Clicking of perfluoro-nonyl-azide to a substrate of PEDOT-N_3/PEDOT on PS-alkyne: 70/30 v/v DMSO/H_2O, 1 mM $CuSO_4$, 10 mM sodium ascorbate, 5 mM 4,4,5,5,6,6,7,7,8,8,9,9,9-tridecafluorononyl azide.

Electro-click reaction conditions: Electro-click reactions were conducted using a copper plate top electrode, in a setup similar to that of our earlier report.[18] The top electrode was used to ensure a uniform functionalization of the electrodes. The spacing to the top electrode was ~330 µm. One set of PEDOT-N_3/PEDOT electrodes was set to 0.5 V potential and the other to -0.5 V vs. the copper top electrode. For the second reaction the potentials were swapped. 1 mM alkyne-reactant and 1 mM $CuSO_4$ in 90/10 v/v DMSO/H_2O were used. The reactions proceeded for 5 min using halogen-alkyne marker reactions, and for 20 min using alkyne-PEG-(GRDGS) and alkyne-PEG-(GRGDS). Reactions were stopped by rinsing in MilliQ water followed by re-oxidization of the PEDOT by rinsing in a 10/90 Clevios C-B40/H_2O, and rinsing in MilliQ water.

XPS analysis: XPS experiments were conducted on a Thermo Fisher Scientific K-Alpha (East Grinstead, UK). Large area surface analysis used a 400 µm spot of monochromatized aluminum Kα radiation, and survey (pass energy 200 eV) and high resolution (pass energy 50 eV) spectra of relevant elements were acquired. Line-scan investigations proceeded using a nearly circular x-ray spot of 40 µm diameter and a step-size of 30 µm with acquisition of high resolution (pass energy 50 eV) spectra of relevant elements. This implies that on each 100 µm wide electrode, as well as in each 100 µm wide space between electrodes, there will be at least one measurement point where the detected elemental composition originates entirely from the electrode or the space between electrodes, respectively. Charge

compensation was used on all samples. Data analyses of the XPS spectra obtained were performed using the Avantage software package supplied by the manufacturer. For the line-scan measurements, the elemental composition of each spot was determined from the high resolution spectra using a fitted peak with a linear background and a signal-to-noise threshold of 0.9.

Contact angle measurements: All contact angles were measured using a Data Physics OCA20 contact angle system, and dedicated software. Contact angles were measured on at least 3 different areas of each sample using MilliQ water as probe liquid. Prior to all measurements, any dust on the samples was blown off by inert gas.

Fibroblast attachment studies: A homemade all-polymer flow chamber with channel dimensions of 0.140 mm x 2 mm x 10 mm (h, w, l) was used. The chamber was assembled by connecting two disc-shaped COC substrates, the bottom containing the functionalized electrode / PMOXA sample, and the top defining inlets and outlets, with a layer of patterned transfer adhesive (ARcare 90106, Adhesive Research, Glen Rock, PA, USA). The adhesive was cut using a CO_2-laser system (FH Flyer, Synrad, Mukilteo, WA, USA) to define the lateral geometry of the channel. The thickness of the adhesive (140 µm) defined the height of the channel. The flow experiments were conducted in HBSS buffer containing Mg^{2+} and Ca^{2+}. Approximately 150 µL of a suspension of 3T3 fibroblasts (10^6 cells/mL) in RPMI was injected into the flow chamber. The cells were allowed to adhere for 1 h. HBSS buffer was then flowed through the chamber at a gradually increasing flow rate to reach a surface shear stress of 20 Pa that was maintained for 1 min. The flow rate was controlled by an NE-1000 syringe pump (New Era Pump Systems, Farmingdale, NY, USA). Images were acquired by an iXon camera (Andor Technology, Belfast, Northern Ireland) mounted on a Zeiss Axiovert S100 microscope (Carl Zeiss, Oberkochen, Germany) using an LD Plan-NeoFluar 20x/0.4NA objective. The pump flow and the image acquisition were controlled by dedicated software running under LabView.

3. Printed dissolution can locally re-expose unperturbed substrate chemistry

Exposure of PEDOT films to an agarose stamp containing aqueous hypochlorite (NaOCl) results in the formation of a chemically stable, transparent, and non-conducting material. We reported earlier how this can be used for making micrometer sized patterns of PEDOT and non-conductive PEDOT.[15] Here, we show that the over-oxidized material can be dissolved when a non-ionic detergent was added to the stamp or to a subsequent washing step, thereby exposing the chemistry of the underlying substrate. Figure 2 presents the efficiency in removing PEDOT on COC hydrocarbon substrates using unstructured stamps. The effect of applying the detergent Triton-X100 was examined using X-ray photoelectron spectroscopy (XPS) and contact angle analysis. PEDOT-on-COC samples stamped without the use of detergent were found to be hydrophilic and to contain significant amounts of oxygen and sulfur. These properties were observed to be largely invariable over macroscopic length scales (centimeters). The addition of detergent either in the stamp and/or in a subsequent wash resulted in the dissolution and removal of the stamped films. The surface chemical characteristics of the samples then closely resembled those of the underlying COC.

Various solvents were also assessed for their ability to dissolve the oxidized PEDOT-type films. The films were observed to be resistant to a number of commonly used polar solvents such as water, ethanol, isopropanol, n-butanol, acetone, acetonitrile, and 1,4-dioxane. Over-oxidized PEDOT-N_3 films, being light-brown in visual appearance, could be thinned by immersion in DMF or DMSO as evidenced by a gradual decrease in light absorption. XPS confirmed that a majority of the oxidized film was indeed removed. This corresponds well to our earlier finding that PEDOT and especially PEDOT-N_3 undergoes strong swelling in DMSO.[26] The fabrication of all-polymer microsystems requires a dissolution system that dissolves the oxidized material without affecting other polymer components. Since DMF and DMSO dissolve a wide range of polymers, including the functionalized polystyrenes used later in this work, their generic applicability for removing the oxidized PEDOT material is limited. Addition of just small amounts of water to the DMSO prevented the modified polystyrenes from dissolving. This

possible solution was investigated by measuring the ability of DMSO/water mixtures with up to 90 vol% DMSO to remove the oxidized PEDOT and PEDOT-N_3 material (see Supporting Information Table S1). Higher DMSO concentrations dissolved the oxidized PEDOT more effectively, but measurable amounts of oxidized PEDOT remained on the substrates even at 90/10 v/v DMSO/water. In addition, the use of DMSO/water mixtures may not be applicable to other polymer materials with higher solubility in DMSO.

The mild reducing agent sodium ascorbate was added to the Triton-X100 wash to maintain the PEDOT films in an undoped state, and was additionally found to aid the dissolution of oxidized PEDOT on some substrates. Following this reductive wash, the non-contacted PEDOT film was easily re-oxidized to restore the conductive state by immersion in an aqueous solution of Fe(III)tosylate also used for preparing the conductive polymer films.[5, 17, 26] Triton-X100 washing solutions without this reducing agent, or even containing an oxidizing agent, in most cases had an equivalent effect. The reducing agent was found mainly to be of importance for removing oxidized PEDOT-N_3 (see Supporting Information Figs. S4+S5) but for analytical consistency the same washing procedure was used for all samples. An additional 80/20 v/v DMSO/water wash was also applied to all samples for consistency in comparing the results, although this step was generally only required in the absence of detergent (see Supporting Information Tables S1+S2 and Figs. S4+S5). Figure 2 shows that the detergent may be introduced with equal success during stamping or during washing for the PEDOT-on-COC system. This indicates that the detergent is simply aiding the dissolution of the oxidized product, rather than directly influencing the oxidation process. For other polymer substrates such as PS-N_3 (poly(4-(azidomethyl)styrene)), the addition of Triton-X100 in the stamp was found to be superior to applying it in a subsequent wash (see Supporting Information Fig. S5). This might suggest that the Triton-X100 plays a role in aiding the oxidation of the PEDOT at the PEDOT/PS-N_3 interface, possibly by solvating the oxidized products during the etching process. In the remainder of this work Triton-X100 was used both in the stamp as well as in a subsequent washing step, unless noted.

The optimized printed dissolution method was subsequently employed for producing conductive polymer microelectrode arrays by locally removing PEDOT using a microstructured agarose stamp. The targeted microelectrode design consisted of dual sets of interdigitated 100 µm wide and 3.5 mm long PEDOT electrodes with 100 µm spacing on a COC substrate. The same structural motif was used for all microstructuring in this work. The resulting PEDOT pattern in displayed in Fig. 1D, while Figs. S1 and S2 in the Supporting Information show photographs of the tools and samples used, respectively. XPS line scans were performed across the electrodes to analyze their elemental composition, using an analysis spot of nominally 40 µm in diameter. The elemental composition in the middle of each electrode (Fig. 3A, positions with highest oxygen and sulfur content) corresponds closely to the elemental composition measured on untreated PEDOT (Fig. 2A, "PEDOT"), indicating that the PEDOT electrodes are not influenced by the stamping process. Correspondingly, the elemental compositions measured in the points between the electrodes match that of pure COC (Fig. 2A, "COC"). The XPS results confirm that printed dissolution can also be used for locally removing PEDOT on microscopic length scales. PEDOT structures much smaller than 100 µm in width can be made using hypochlorite-loaded agarose stamps as demonstrated for line widths down to 2 µm in our previous work without the use of detergent.[15] Reproducible fabrication of similarly sized features using our current approach may require shorter stamping times and lower NaOCl concentrations than presented here. The studies presented in tables S3 and S4 in the Supporting Information show that a stamp contact time of 1 min is equally effective for the detergent aided removal of over-oxidized PEDOT on COC as the 4 min generally used in this work. For a stamping time of 4 min, equally good PEDOT removal can be achieved for a 10 times lower NaOCl concentration, while the concentration can be reduced by at least 4 times for a stamping time of 1 min.

Polymer substrates with functional chemical groups can also be locally re-exposed using printed dissolution and subsequently covalently functionalized. Figure 4A shows schematically how the re-

exposed azide groups of a PS-N_3 substrate beneath a micropatterned PEDOT film can be coupled to an organic alkyne (5-iodopentyne containing iodine as heteroatom for selective detection by XPS), through click chemistry. XPS line scan analysis of the variation in elemental composition across a number of microelectrodes (Fig. 4B) confirmed the successful confinement of the click reaction to the re-exposed areas between PEDOT electrodes by showing spatially alternating peaks from iodine (reacted 5-iodopentyne) and sulfur (PEDOT electrodes). The azide groups of exposed PS-N_3 give rise to a characteristic doublet peak (intensity ratio 1:2) in the high resolution XPS nitrogen 1s spectra. XPS line scans of the micropatterned PEDOT showed the presence of this doublet between the PEDOT electrodes (Fig. 4C, left), which strongly indicates that the PS-N_3 was exposed without damaging the functional chemical groups. After subsequent reaction with the 5-iodopentyne, the high binding energy peak was observed to decrease in intensity (Fig. 4C, right) as expected for the successful click reaction of an azide and an alkyne to form a triazole.

4. Micropatterned orthogonal surface chemistries can spatially direct chemical reactivity

One of the major advantages of PEDOT-type conductive polymers is that small chemical groups can easily be introduced in the monomer unit without disrupting the conductance of the polymer.[4-6, 17, 26, 27] One example is the commercially available 3,4-(1-hydroxymethylethylene)-dioxythiophene (EDOT-OH). We tested the patterning procedure on PEDOT-OH films and found that it was equally effective as for PEDOT. This opens the possibility for covalently attaching chemical functionalities directly to the electrodes as well as to the spaces between the electrodes. Figure 5A illustrates this concept, where a thin film of PEDOT-OH on PEDOT was deposited on a PS-N_3 substrate and then coupled to 5-bromo-pentanoic acid using standard ester coupling conditions. The modified PEDOT-OH/PEDOT film was subsequently micropatterned using patterned dissolution to locally expose the underlying PS-N_3 that was further coupled to 5-iodopentyne by click chemistry. XPS line scans on the resulting surfaces showed spatially alternating signals from bromine (modified PEDOT-OH electrodes) and iodine (modified PS-N_3 substrate) (Fig. 5B).

Functionalizing the conductive polymer film before micropatterning has advantages and disadvantages. The major advantages are the simplicity of this scheme and the very low risk of molecules designated for the electrodes to bind unspecifically to the areas between the electrodes. Another advantage is that the same reaction chemistry can be used in series to functionalize both the electrodes and the underlying substrate. Figure S8 in the Supporting Information shows an example of this approach to provide two different types of chemical functionality to PEDOT-N_3 electrodes on a PS-N_3 background, i.e. two materials with equal surface reactivity. In Figure S8, cell-binding electrodes on a cell non-binding background resulted from coupling a cell-binding oligopeptide-alkyne onto the unstructured PEDOT-N_3, patterning the film into microelectrodes using patterned dissolution, and final grafting PEG-alkyne to the areas between the electrodes. The major disadvantage of the approach is that the functionalization of the film with certain types of molecules may influence the stamping procedure, especially if a bulk functionalization is performed.[26] Bulk modification of PEDOT-N_3 with hydrophilic molecules such as PEG-alkynes appeared to significantly increase the rate of oxidant diffusion from the stamp into the film. The increase in diffusion rate made the process faster and more difficult to control. Conversely, prior reaction with hydrophobic molecules (a fluorocarbon alkyne) slowed the diffusive process and could prevent the agarose stamp from adsorbing properly onto the film (data not shown).

The use of orthogonal reactive chemistries to add separate surface chemistry on the electrodes and on the substrate was illustrated in Figure 5A. Figure 6A shows a schematic of how to add separate covalently bound functionalities to the substrate and to *either* set of microelectrodes: A thin film of PEDOT-N_3 on PEDOT was deposited on an alkyne-containing polystyrene co-polymer substrate (PS-alkyne). The PEDOT-N_3/PEDOT film was micropatterned by patterned dissolution, and the re-exposed alkynes of the PS-alkyne substrate were reacted with perfluoro-nonyl-azide to provide fluorine as heteroatom for XPS analysis. Next, electro-click chemistry[17, 18] was sequentially employed to couple 1-bromo-4-ethynylbenzene (bromine as heteroatom) onto one set of electrodes and couple 5-iodopentyne

(iodine as heteroatom) onto the other set of electrodes. Thus, in total, three types of localized surface chemistry were introduced. XPS line scans on the resulting surfaces showed spatially alternating signals from fluorine (modified PS-alkyne substrate) and either bromine (modified PEDOT-N_3 electrode set 1) or iodine (modified PEDOT-N_3 electrode set 2) (Fig. 6B).

5. Multiple micropatterned cell-affecting chemistries can spatially control cell adhesion

Macromolecules can also be covalently attached and used for introducing e.g. biological specificity to the systems. We illustrate this by showing how cellular adhesion can be locally and specifically controlled in an all-polymer microsystem. Many cells have been shown to adhere and proliferate on PEDOT-type polymers, and the adhesion is known to be influenced by the redox state of the PEDOT.[1, 9, 10] Our aim was to minimize such unspecific adhesion on and between the PEDOT electrodes while presenting specific cell anchoring motifs on designated PEDOT electrodes only.

PEG coatings are widely applied to reduce protein adsorption and cellular adhesion to surfaces. Nevertheless, there are alternatives to PEG and recently (poly(2-methyl-2-oxazoline)) (PMOXA) has received a lot of attention as a promising candidate.[28-31] Some benefits of PMOXA compared to PEG are greater hydrophilicity and better resistance to oxidative degradation and chain cleavage, thus offering higher resistance to long-term non-specific protein adsorption.[28-32] We anticipated that the stability of PMOXA in oxidative environments would be sufficient to allow a preformed PMOXA film present below a PEDOT film to be exposed and remain functional after stamping. First, the oxidative environment of the printed dissolution process was tested on PMOXA coatings made by reacting PS-N_3 films with an alkyne-terminated PMOXA. XPS analysis showed almost identical elemental compositions of the films before and after stamping (see Supporting Information Table S7). Second, such PMOXA films were coated by PEDOT films and re-exposed upon patterning. The PMOXA films were found to be intact and to contain only small amounts of oxidized PEDOT, based on contact angle and XPS analysis (see Fig. S9 and Table S7 in the Supporting Information). Importantly, the resulting

PMOXA films exhibited low binding of cells compared to unmodified PS-N_3 (Fig. 7A, top). We also investigated if a similar approach of coupling PEG-alkynes to PS-N_3 followed by PEDOT coating and re-exposure could be employed, but this was not possible. Notably, the failure of PEG coatings apparently did not originate in oxidation of the PEG upon contact with NaOCl: Table S7 in the Supporting Information shows that the elemental compositions of the PEG films before and after stamping are identical. This suggests that PMOXA and PEG may interact differently with PEDOT either during PEDOT polymerization or during the stamping procedure, which apparently prevents re-exposure of PEG. Useful low cell-binding PEG coatings were instead obtained by coupling a re-exposed PS-N_3 surface with PEG-alkyne after the patterning procedure (see Fig.7A, bottom and Supporting Information Fig. S7).

We used peptides containing the amino acid sequence Arg-Gly-Asp (RGD) that is known to induce specific cellular attachment through the appropriate type(s) of integrin membrane proteins.[33] The amino acid sequence Gly-Arg-Gly-Asp-Ser (G**RGD**S) has been reported to be effective when the RGD motif is placed at the C-terminal of a peptide.[33] We synthesized molecules containing this amino acid sequence connected via a short PEG spacer to an alkyne group, the latter being used for coupling the molecule to azide-containing surfaces. Additionally, we synthesized equivalent molecules containing the scrambled amino acid sequence G***RDG***S. This scrambled sequence is not expected to induce specific cell attachment. The cell binding efficiency of the modified surfaces was evaluated by allowing 3T3 fibroblast cells to adhere for 1 h under stationary flow conditions in a microfluidic setup followed by applying a defined flow for a specified time to detach and remove weakly bound cells. Coupling of the GRGDS-containing peptide to PEDOT-N_3 resulted in a larger number of 3T3 fibroblasts adhering to the surface compared to native PEDOT-N_3 (Fig. 7B top). In contrast, coupling of the scrambled GRDGS-containing peptide resulted in much fewer cells adhering than on native PEDOT-N_3 (Fig. 7B bottom).

We employed the outlined processes to produce an all-polymer microsystem with three types of bio-functional surface chemistries in register, i.e. one electrode set with high cell-binding peptide chemistry, a second electrode set with low cell-binding peptide chemistry, and low cell-binding PMOXA chemistry between the electrode sets. A PMOXA-alkyne functionalized PS-N_3 substrate was coated by a PEDOT-N_3/PEDOT film. The latter film was then microstructured by patterned dissolution to re-expose PMOXA between the resulting microelectrodes. Electro-click chemistry was used to functionalize one set of electrodes with the active G**RGD**S peptide followed by functionalizing of the other set with the inactive scrambled G***RDG***S peptide. Figure 7C shows that 3T3 fibroblast cells attached specifically to the GRGDS peptide coated electrodes while showing no adhesion to the other functionalized sample areas, when the cells were allowed to adhere for 1 h before washing. Control experiments were also performed with G**RGD**S peptides on both electrodes on a PMOXA background (Supporting Information Fig. S6) and on samples without any added functionalities (Supporting Information Fig. S8).

6. Discussion

The printed dissolution PEDOT patterning scheme is a simple but versatile tool that enables fabrication of all-polymer microsystems systems with incorporated electrically conductive circuits and various types of in-register localized (bio)-chemistry. The method should also applicable for patterning PEDOT films on non-polymer substrates. Preliminary tests showed that it can be used, for instance, for patterning PEDOT and re-exposing azide groups on glass substrates that had initially been covered with azides using silane chemistry. On such non-polymer substrates, and for polymers with high resistance to organic solvents such as DMSO or DMF, our early investigations suggest that the use of detergent can be avoided by washing away the oxidized material using organic solvents. Substrates presenting other functional chemical groups than the click-reactive azide and alkyne groups used in this work should also have the potential to be “hidden” below PEDOT films and re-exposed upon stamping. The main requirement is that the groups do not oxidize when exposed to hypochlorite during stamping. This should not be the case for e.g. carboxylate groups. Another concern can be strong interactions between

the substrate and the (oxidized) PEDOT, which makes the removal of PEDOT more difficult. Our failure to hide and re-expose PEG-functionalized PS-N_3 may be caused by such strong interfacial interactions.

Patterned dissolution may have other limitations. Previous reports showed that PEDOT can be integrated into a range of polymer substrates by washing with appropriate solvents to induce swelling of the substrate.[34, 35] In our work, all PEDOT-type films resulted from in situ polymerization of an n-butanol containing solution of the respective PEDOT precursor. Accordingly, PEDOT is expected to be partially integrated into polymer substrates that undergo significant swelling in n-butanol, thereby making it more difficult to remove the PEDOT by patterned dissolution. Polystyrene has been reported to take up 10 wt% n-butanol at 65ºC.[36] In agreement with this, we observed that spin coating of polystyrene substrates with Fe(III)tosylate in n-butanol (the EDOT oxidant solution) resulted in notably more hydrophilic surfaces, even after rinsing with water. This suggests that partial integration of PEDOT into the outermost part of polystyrene surfaces may occur during EDOT polymerization. Such integration could explain why it was generally more difficult to remove PEDOT from polystyrenes than from COC, this being reflected in the requirement for using detergent directly in the stamp (see Supporting Information Figs. S4 and S5). From a practical point of view PEDOT can be removed from the polystyrene surfaces sufficient well to allow introduction of a range of complex surface chemistries, as exemplified in this work. For other types of polymer substrates, PEDOT integration could be a larger problem. We suggest to circumvent this by polymerizing PEDOT from other solvents or at lower temperatures, or by polymerizing PEDOT from the vapor phase.[37]

The conjugated backbone of PEDOT is a universal feature of (intrinsically) conductive polymers. Correspondingly, over-oxidation of the conductive backbone has been used in numerous other patterning / local deactivation schemes of a variety of conductive polymers.[13, 14, 38, 39] Our printed dissolution concept essentially exploits that the over-oxidation changes the solubility parameters of the

conductive polymer, thus likely making the approach applicable for locally removing other conductive polymers and other PEDOT type polymers than those tested here.

Photolithography based patterning techniques were mentioned in the Introduction as one example of a multitude of other methods to pattern conductive polymers, as recently reviewed by Feng et al.[13] We will only discuss a few approaches of particular interest to polymer systems with spatially defined surface chemistries. Numerous printing techniques are available for locally adding the conductive polymer to a surface, as opposed to removing it. Pre-polymerized conductive polymers or precursors for initiating polymerization have been transferred to various substrates by additive printing, e.g. using microcontact printing.[13, 40] Additive printing requires a substrate surface with high affinity for the printed material, being either an initiator or a conductive polymer. Polymer substrates are typically hydrophobic and non-polar, which generally results in low affinity for polar conductive polymer materials and associated problems in printing the latter class of materials. In contrast, our approach only requires wetting of the substrate surface by the PEDOT precursor solution during spin coating and polymerization, and wetting is possible on most substrate materials given an appropriate choice of solvent. Additive printing has a further challenge in achieving high accuracy overlay alignment, i.e. to deposit multiple areas of different types of chemistry in register with sharply defined boundaries between neighboring chemistries. Printed dissolution meets this challenge by actively removing chemically poorly defined boundary zones between neighboring areas during the dissolution step. The benefits of additive printing techniques and of printed dissolution could possibly be combined, for example by using high-resolution ink-jet printing of an oxidant and a detergent to perform subtractive rather than additive printing of the conductive polymer.[41]

7. Conclusions

Printed dissolution is an easy and versatile method for making microelectrodes of PEDOT-type polymers that can be used as a vehicle for in-register micropatterning of multiple types of covalently

bound surface chemistry. The method was shown to be applicable for diverse reaction schemes through the introduction of various defined surface chemistries on PEDOT-OH and PEDOT-N_3 electrodes as well as on PS-alkyne and PS-N3 substrates, either before or after the patterning step. The method was further used as an enabling technology in the fabrication of an all-polymer microfluidic demonstrator system, in which fibroblast cells could be specifically captured onto designated electrodes. We suggest that the general concept of oxidizing PEDOT and dissolving the oxidized material is not limited to polymer substrates, and that the concept is likely applicable to patterning of other conjugated organic materials than PEDOT-type materials.

Acknowledgement.

This work was financially supported by the Danish Council for Independent Research, Technology and Production Sciences, grant# 09-070021.

Supporting Information Available.

Quantification by contact angle analysis and XPS of the removal of PEDOT-type films by patterned dissolution on different substrates and for varying process conditions, including different solvents, detergents, stamping times, and oxidant concentrations. XPS analysis of low cell-binding coatings exposed to stamping. Optical micrographs of the parts used for electrode fabrication and for the homemade microfluidic chamber. Optical micrographs of cell adhesion to other combinations of surface modified materials. Experimental details for synthesis of the compounds used. This material is available free of charge via the Internet at http://pubs.acs.org.

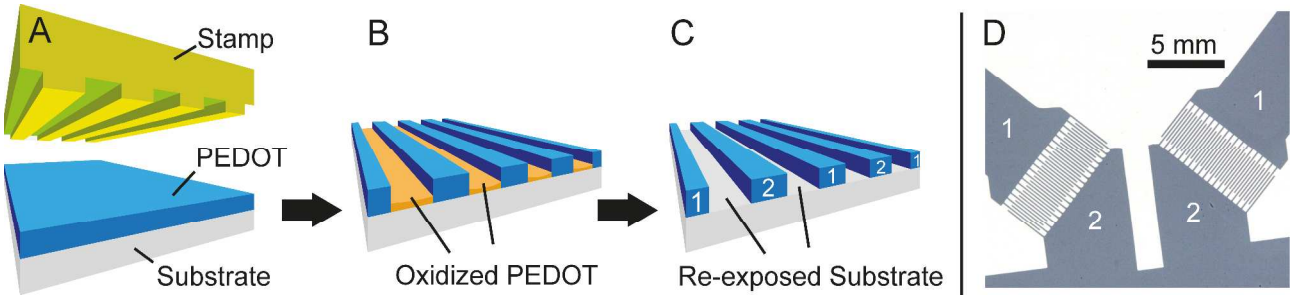

Figure 1. Schematic of conductive polymer micropatterning by printed dissolution. (A) An agarose hydrogel stamp with a predefined microstructure in bas-relief is soaked in an oxidant-containing solution (aqueous NaOCl) and brought into contact with a conductive polymer (PEDOT) thin film on a substrate. (B) Oxidized and non-conducting PEDOT remains in the contacted areas after stamping. (C) The oxidized PEDOT is removed by washing in aqueous detergent (Triton X-100) or by adding detergent directly to the aqueous oxidant. (D) Optical micrograph of a PEDOT thin film on a polymer (COC) substrate patterned into two sets of interdigitated arrays of 100 µm wide electrodes (digits "1" and "2" mark connectors for independently addressable electrodes, as shown in (C)).

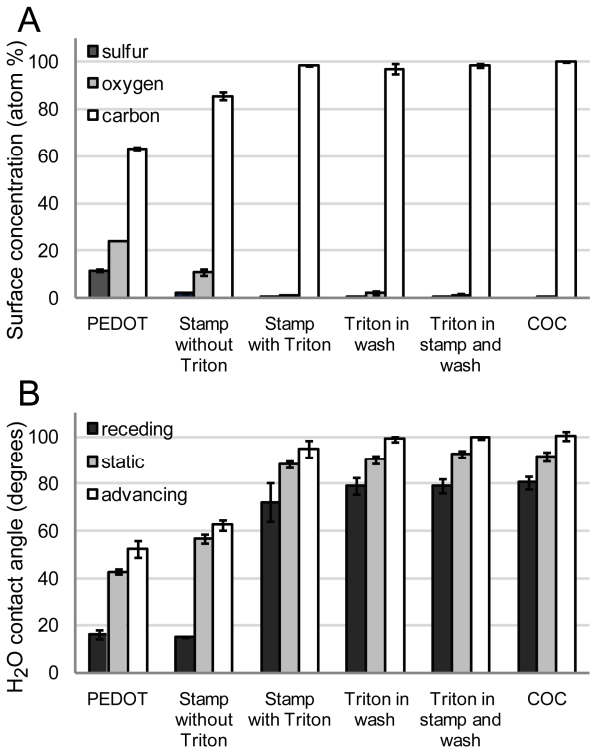

Figure 2. Efficiency in removing PEDOT from polymer (COC) substrates by printed dissolution using planar (unstructured) agarose stamps with or without added detergent (Triton X100) in the oxidant-containing stamping solution or/and in the washing step. (A) Surface elemental composition determined by XPS analysis. (B) Advancing, receding, and static water contact angle analysis. Error bars show the standard deviation of three independent experiments. The left-most and right-most data points represent analysis performed on untreated PEDOT films or on uncoated COC, respectively.

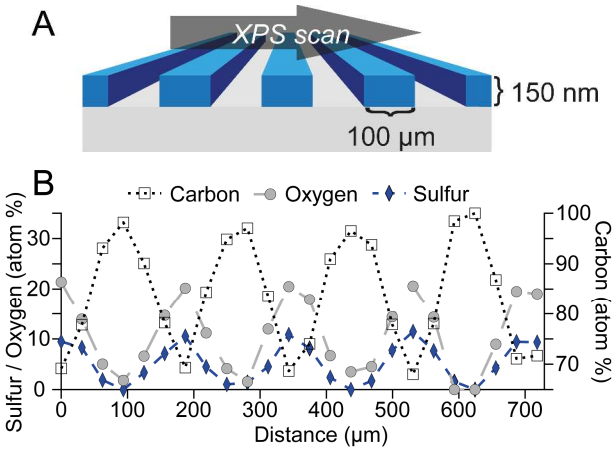

Figure 3. (A) Sketch of PEDOT on polymer (COC) substrates micropatterned by printed dissolution to fabricate 100 µm wide and 150 nm high electrodes (blue) with 100 µm spacing exposing the underlying substrate (gray). (B) Elemental composition across five PEDOT microelectrodes and the exposed substrate between electrodes, as determined by an XPS linescan. Note that the aspect ratio of the sketched microelectrodes is not to scale.

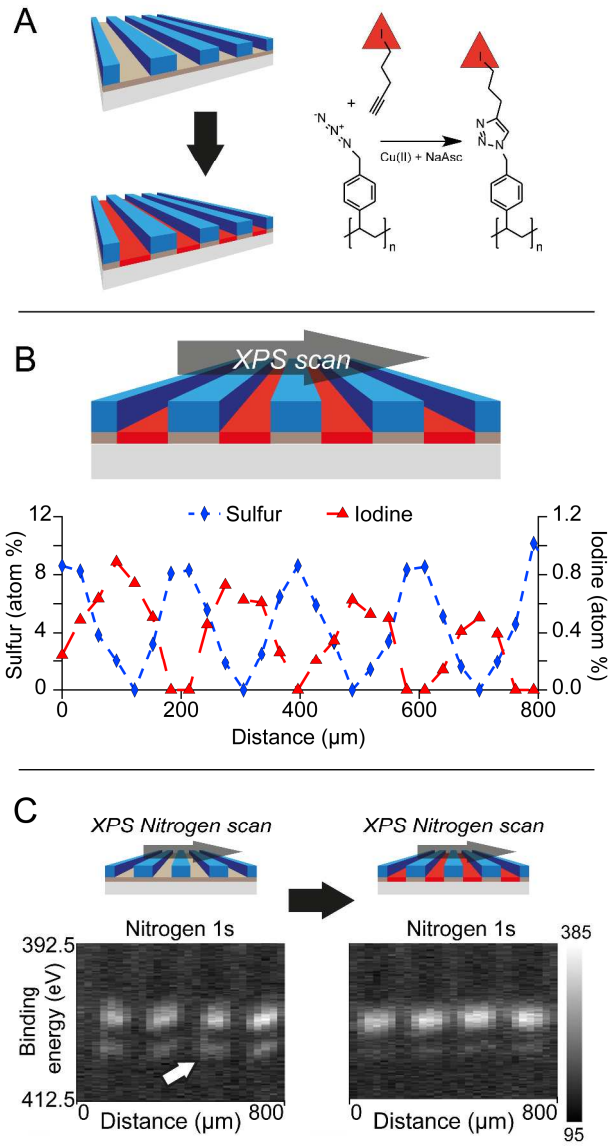

Figure 4. Chemical modification of a re-exposed functional polymer substrate. (A) Re-exposed poly(azido styrene) (PS-N_3) is covalent modified by 5-iodopentyne using click chemistry after patterning a PEDOT film on PS-N_3 into 100 µm wide electrodes. (B) XPS linescan of the elemental composition across five electrodes (for clarity, only the surface concentrations of sulfur from PEDOT and iodine from 5-iodopentyne are presented). (C) High resolution XPS linescans of the nitrogen peak before (left) and after (right) the click reaction. The initial presence of azides (left) and subsequent reaction into triazoles (right) is revealed by the reduction in intensity of the high binding energy doublet peak (404 eV, white arrow).

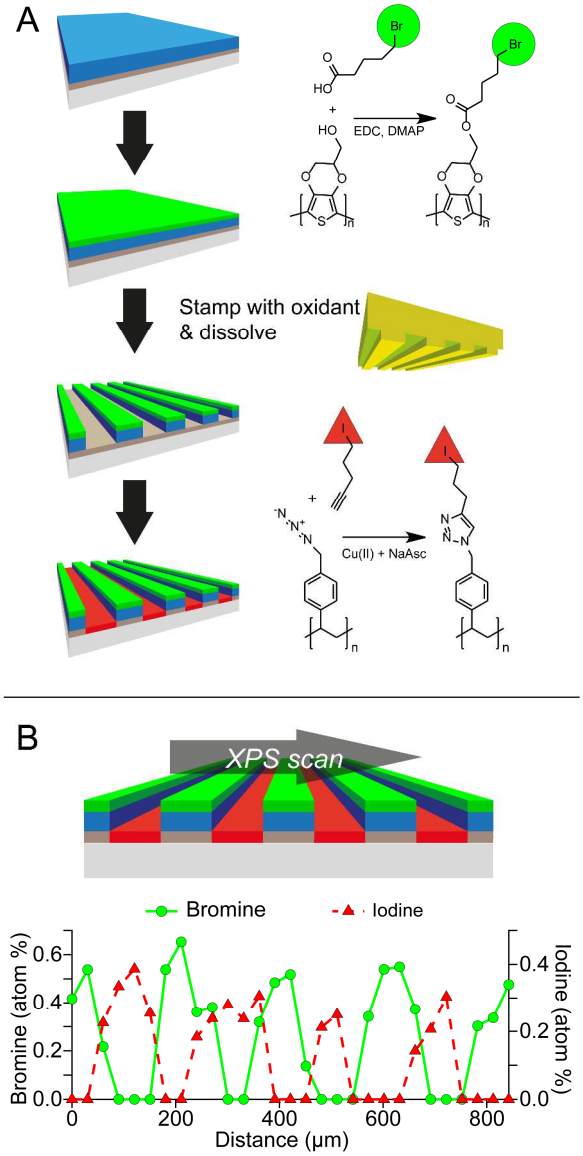

Figure 5. Chemical micropatterning of 2 types of covalently bound surface chemistry in register. (A) PEDOT-OH/PEDOT on PS-N_3 is modified with 5-bromopentanoic acid (bromine as tracer) using standard ester coupling chemistry. Subsequent micropatterning of the PEDOT-OH/PEDOT film into 100 μm wide electrodes exposes the underlying PS-N_3 substrate for click chemistry coupling of 5-iodopentyne (iodine as tracer) between the electrodes. (B) XPS linescan of the elemental composition across five electrodes (for clarity, only bromine and iodine concentrations are presented).

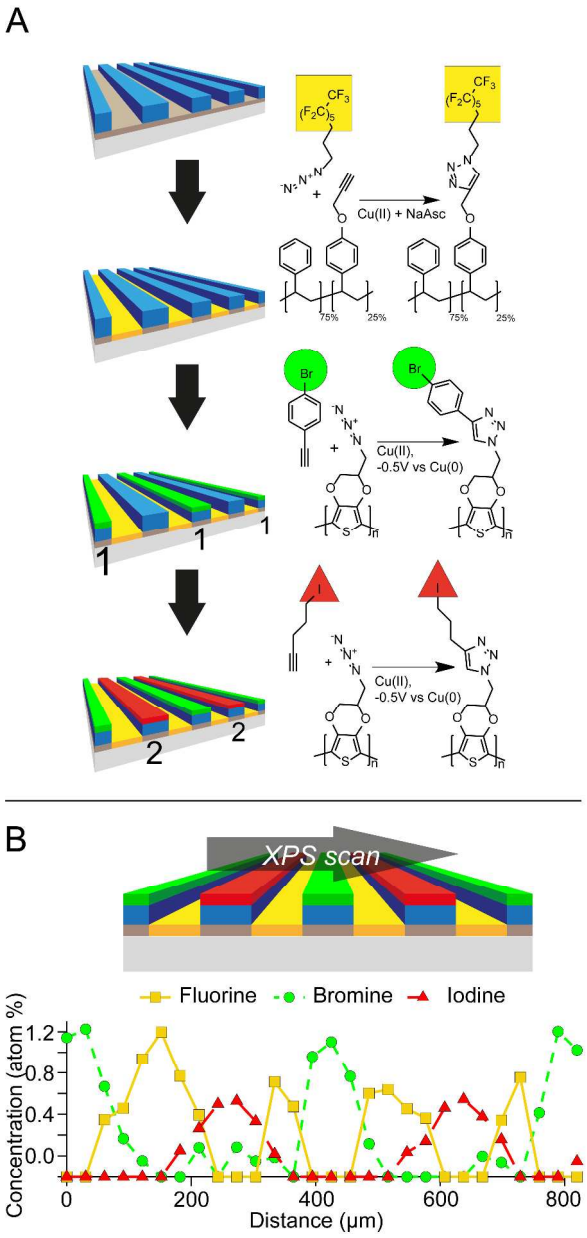

Figure 6. Chemical micropatterning of 3 types of covalently bound surface chemistry in register. A) Re-exposed alkyne-functional polystyrene (PS-alkyne) is covalent modified by tridecafluorononyl azide (fluorine as tracer) using click chemistry after patterning a PEDOT-N_3/ PEDOT film on PS-alkyne into 100 µm wide electrodes. One set of electrodes (marked "1") is then 'electroclicked' with 1-bromo-4-ethynylbenzene (bromine as tracer) followed by electroclicking of the other set of electrodes (marked "2") using 5-iodopentyne (iodine as tracer). Electroclick chemistry is based on the electrochemical reduction of inactive Cu(II) into catalytically active Cu(I) locally at the targeted electrodes. (B) XPS

linescan of the elemental composition across five electrodes (for clarity, only fluorine, bromine, and iodine concentrations are presented).

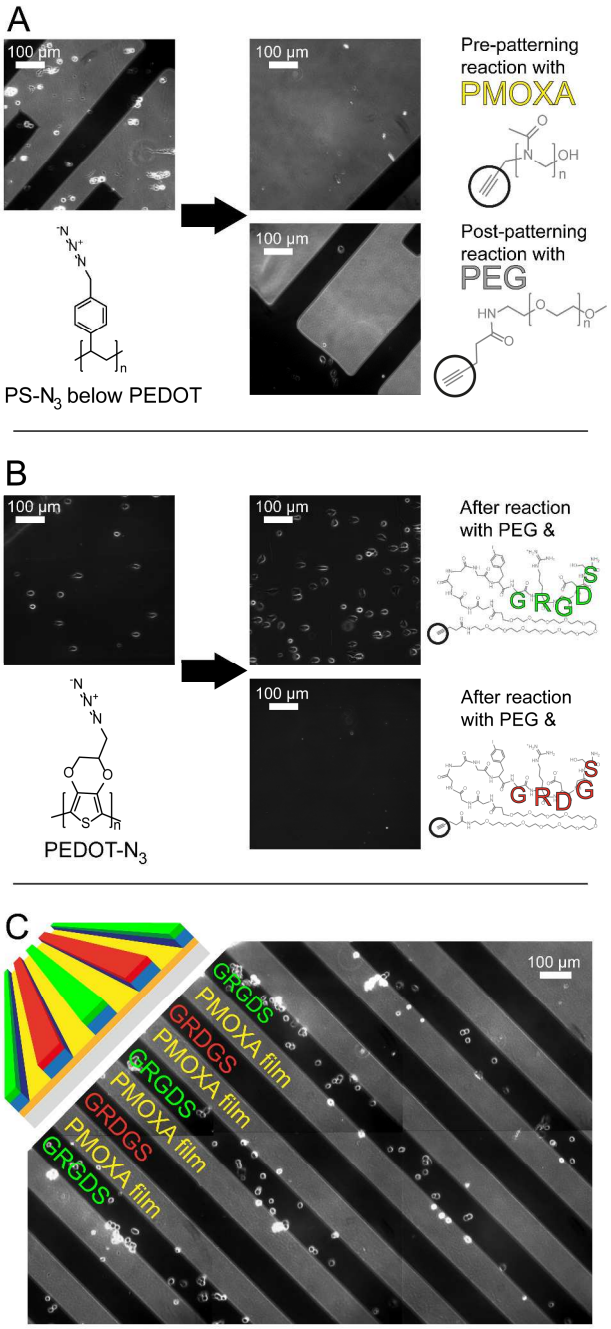

Figure 7. Triple micropatterned biofunctional surface chemistries in register controlling the adhesion of 3T3 fibroblast cells in a microfluidic system. (A) Low cell-binding surface chemistries resulting either from click chemistry coupling of PMOXA-alkyne to a PS-N_3 substrate (left) before PEDOT coating and subsequent reexposure by stamping (upper right) or from click chemistry coupling of PEG-alkyne to a PS-N_3 substrate after PEDOT coating and reexposure by stamping (lower right). (B) Cell adhesion to PEDOT-N_3 films (left) chemically reacted with a mixture of PEG-alkyne and the cell specific peptide alkyne-PEG-G**RGD**S (upper right) versus a mixture of PEG-alkyne and the scrambled peptide alkyne-

PEG-G***RDG***S (lower right). (C) Specific cellular adhesion to PEDOT-N_3/PEDOT microelectrodes electroclicked with alkyne-PEG-G**RGD**S versus corresponding PEDOT-N_3/PEDOT microelectrodes electroclicked with alkyne-PEG-G***RDG***S or the PMOXA-alkyne re-exposed between the electrodes. The PMOXA-alkyne was reacted onto an underlying PS-N_3 substrate before coating with the PEDOT-N_3/PEDOT thin film.

References

(1) Asplund, M.; Nyberg, T.; Inganas, O. Electroactive Polymers for Neural Interfaces. *Polym. Chem.y* **2010***, 1*, 1374-1391.

(2) Kumar, A.; Welsh, D.; Morvant, M.; Piroux, F.; Abboud, K.; Reynolds, J. Conducting Poly(3,4-Alkylenedioxythiophene) Derivatives as Fast Electrochromics with High-Contrast Ratios. *Chem. Mater.* **1998***, 10*, 896-902.

(3) Cataldo, F.; Maltese, P. Synthesis of Alkyl and N-Alkyl-Substituted Polyanilines - A Study on Their Spectral Properties and Thermal Stability. *Eur. Polym. J.* **2002***, 38*, 1791-1803.

(4) Bu, H.; Goetz, G.; Reinold, E.; Vogt, A.; Schmid, S.; Blanco, R.; Segura, J. L.; Baeuerle, P. "Click"-Functionalization of Conducting Poly(3,4-Ethylenedioxythiophene) (PEDOT). *Chem. Commun.* **2008**, 1320-1322.

(5) Daugaard, A. E.; Hvilsted, S.; Hansen, T. S.; Larsen, N. B. Conductive Polymer Functionalization by Click Chemistry. *Macromolecules* **2008***, 41*, 4321-4327.

(6) Luo, S.; Ali, E. M.; Tansil, N. C.; Yu, H.; Gao, S.; Kantchev, E. A. B.; Ying, J. Y. Poly(3,4-Ethylenedioxythiophene) (PEDOT) Nanobiointerfaces: Thin, Ultrasmooth, and Functionalized PEDOT Films with In Vitro and In Vivo Biocompatibility. *Langmuir* **2008***, 24*, 8071-8077.

(7) George, P. M.; LaVan, D. A.; Burdick, J. A.; Chen, C. Y.; Liang, E.; Langer, R. Electrically Controlled Drug Delivery from Biotin-Doped Conductive Polypyrrole. *Adv. Mater.* **2006***, 18*, 577-581.

(8) Richardson-Burns, S. M.; Hendricks, J. L.; Foster, B.; Povlich, L. K.; Kim, D. H.; Martin, D. C. Polymerization of the Conducting Polymer Poly (3, 4-Ethylenedioxythiophene)(PEDOT) Around Living Neural Cells. *Biomaterials* **2007***, 28*, 1539-1552.

(9) Salto, C.; Saindon, E.; Bolin, M.; Kanciurzewska, A.; Fahlman, M.; Jager, E. W. H.; Tengvall, P.; Arenas, E.; Berggren, M. Control of Neural Stem Cell Adhesion and Density by an Electronic Polymer Surface Switch. *Langmuir* **2008***, 24*, 14133-14138.

(10) Svennersten, K.; Bolin, M. H.; Jager, E. W. H.; Berggren, M.; Richter-Dahlfors, A. Electrochemical Modulation of Epithelia Formation using Conducting Polymers. *Biomaterials* **2009***, 30*, 6257-6264.

(11) Kirchmeyer, S.; Reuter, K. Scientific Importance, Properties and Growing Applications of Poly (3, 4-Ethylenedioxythiophene). *J. Mater. Chem.* **2005***, 15*, 2077-2088.

(12) Winther-Jensen, B.; Breiby, D. W.; West, K. Base Inhibited Oxidative Polymerization of 3, 4-Ethylenedioxythiophene with Iron (III) Tosylate. *Synth. Met.* **2005***, 152*, 1-4.

(13) Xu, Y.; Zhang, F.; Feng, X. Patterning of Conjugated Polymers for Organic Optoelectronic Devices. *Small* **2011***, 7*, 1338-1360.

(14) Jiang, L.; Wang, X.; Chi, L. Nanoscaled Surface Patterning of Conducting Polymers. *Small* **2011***, 7*, 1309-1321.

(15) Hansen, T. S.; West, K.; Hassager, O.; Larsen, N. B. Direct Fast Patterning of Conductive Polymers using Agarose Stamping. *Adv. Mater.* **2007***, 19*, 3261-3265.

(16) Devaraj, N. K.; Dinolfo, P. H.; Chidsey, C. E. D.; Collman, J. P. Selective Functionalization of Independently Addressed Microelectrodes by Electrochemical Activation and Deactivation of a Coupling Catalyst. *J. Am. Chem. Soc.* **2006***, 128*, 1794-1795.

(17) Hansen, T. S.; Daugaard, A. E.; Hvilsted, S.; Larsen, N. B. Spatially Selective Functionalization of Conducting Polymers by "Electroclick" Chemistry. *Adv. Mater.* **2009***, 21*, 4483-4486.

(18) Hansen, T. S.; Lind, J. U.; Daugaard, A. E.; Hvilsted, S.; Andresen, T. L.; Larsen, N. B. Complex Surface Concentration Gradients by Stenciled ”Electro Click Chemistry”. *Langmuir* **2010***, 26*, 16171--16177.

(19) Daugaard, A. E.; Hvilsted, S. The Influence of Pendant Carboxylic Acid Loading on Surfaces of Statistical Poly [(4-hydroxystyrene)-co-styrene]s *Macromol. Rapid Commun.* **2008***, 29*, 1119-1125.

(20) Luxenhofer, R.; Jordan, R. Click Chemistry with Poly (2-Oxazoline)s. *Macromolecules* **2006***, 39*, 3509-3516.

(21) Fijten, M. W. M.; Haensch, C.; van Lankvelt, B. M.; Hoogenboom, R.; Schubert, U. S. Clickable Poly (2-Oxazoline)s as Versatile Building Blocks. *Macromol. Chem. Phys.* **2008***, 209*, 1887-1895.

(22) Weber, C.; Becer, R. C.; Baumgaertel, A.; Hoogenboom, R.; Schubert, U. S. Preparation of Methacrylate End-Functionalized Poly (2-Ethyl-2-Oxazoline) Macromonomers. *Polymers* **2009***, 12*, 149-165.

(23) Kagiya, T.; Narisawa, S.; Maeda, T.; Fukui, K. Ring-Opening Polymerization of 2-Substituted 2-Oxazolines. *J. Polym. Sci. Polym. Lett.* **1966***, 4*, 441-445.

(24) Wiesbrock, F.; Hoogenboom, R.; Leenen, M. A. M.; Meier, M. A. R.; Schubert, U. S. Investigation of the Living Cationic Ring-Opening Polymerization of 2-Methyl-, 2-Ethyl-, 2-Nonyl-, and 2-Phenyl-2-Oxazoline in a Single-Mode Microwave Reactor. *Macromolecules* **2005***, 38*, 5025-5034.

(25) Wiesbrock, F.; Hoogenboom, R.; Abeln, C. H.; Schubert, U. S. Single-Mode Microwave Ovens as New Reaction Devices: Accelerating the Living Polymerization of 2-Ethyl-2-Oxazoline. *Macromol. Rapid Commun.* **2004***, 25*, 1895-1899.

(26) Lind, J. U.; Hansen, T. S.; Daugaard, A. E.; Hvilsted, S.; Andresen, T. L.; Larsen, N. B. Solvent Composition Directing Click-Functionalization at the Surface Or in the Bulk of Azide-Modified PEDOT. *Macromolecules* **2011***, 44*, 495--501.

(27) Daugaard, A. E.; Hansen, T. S.; Larsen, N. B.; Hvilsted, S. Microwave Assisted Click Chemistry on a Conductive Polymer Film. *Synth. Met.* **2011***, 161*, 812-816.

(28) Konradi, R.; Pidhatika, B.; Mühlebach, A.; Textor, M. Poly-2-Methyl-2-Oxazoline: A Peptide-Like Polymer for Protein-Repellent Surfaces. *Langmuir* **2008***, 24*, 613-616.

(29) Hoogenboom, R. Poly(2-oxazoline)s: A Polymer Class with Numerous Potential Applications. *Angew. Chem.* **2009***, 48*, 7978-7994.

(30) Pidhatika, B.; Moller, J.; Vogel, V.; Konradi, R. Nonfouling Surface Coatings Based on Poly (2-Methyl-2-Oxazoline). *CHIMIA* **2008***, 62*, 264-269.

(31) Pidhatika, B.; Möller, J.; Benetti, E. M.; Konradi, R.; Rakhmatullina, E.; Mühlebach, A.; Zimmermann, R.; Werner, C.; Vogel, V.; Textor, M. The Role of the Interplay between Polymer Architecture and Bacterial Surface Properties on the Microbial Adhesion to Polyoxazoline-Based Ultrathin Films. *Biomaterials* **2010***, 31*, 9462-9472.

(32) Branch, D. W.; Wheeler, B. C.; Brewer, G. J.; Leckband, D. E. Long-Term Stability of Grafted Polyethylene Glycol Surfaces for use with Microstamped Substrates in Neuronal Cell Culture. *Biomaterials* **2001***, 22*, 1035-1047.

(33) Hersel, U.; Dahmen, C.; Kessler, H. RGD Modified Polymers: Biomaterials for Stimulated Cell Adhesion and Beyond. *Biomaterials* **2003***, 24*, 4385-4415.

(34) Hansen, T. S.; West, K.; Hassager, O.; Larsen, N. B. Integration of Conducting Polymer Network in Non-Conductive Polymer Substrates. *Synth. Met.* **2006***, 156*, 1203-1207.

(35) Winther-Jensen, B.; Chen, J.; West, K.; Wallace, G. 'Stuffed' Conducting Polymers. *Polymer* **2005***, 46*, 4664-4669.

(36) Bernardo, G.; Vesely, D. Equilibrium Solubility of Alcohols in Polystyrene Attained by Controlled Diffusion. *Eur. Polym. J.* **2007***, 43*, 938-948.

(37) Winther-Jensen, B.; West, K. Vapor-Phase Polymerization of 3,4-Ethylenedioxythiophene: A Route to Highly Conducting Polymer Surface Layers. *Macromolecules* **2004**, *37*, 4538-4543.

(38) Tehrani, P.; Robinson, N.; Kugler, T.; Remonen, T.; Hennerdal, L.; Hall, J.; Malmstrom, A.; Leenders, L.; Berggren, M. Patterning Polythiophene Films using Electrochemical Over-Oxidation. *Smart Mater. Struct.* **2005**, *14*, N21-N25.

(39) Sekine, S.; Nakanishi, S.; Miyake, T.; Nagamine, K.; Kaji, H.; Nishizawa, M. Electrodes Combined with an Agarose Stamp for Addressable Micropatterning. *Langmuir* **2010**, *26*, 11526-11529.

(40) Weng, B.; Shepherd, R. L.; Crowley, K.; Killard, A. J.; Wallace, G. G. Printing Conducting Polymers. *Analyst* **2010**, *135*, 2779-2789.

(41) Hansen, T. S.; Hassager, O.; Larsen, N. B.; Clark, N. B. Micropatterning of a Stretchable Conductive Polymer using Inkjet Printing and Agarose Stamping. *Synth. Met.* **2007**, *157*, 961-967.

Supporting Information for:

Micropatterning of functional conductive polymers with multiple surface chemistries in register

Johan U. Lind [†], Canet Acikgöz [‡], Anders E. Daugaard [§], Thomas L. Andresen [†], Søren Hvilsted [§], Marcus Textor [‡], and Niels B. Larsen *[,†]

† Department of Micro- and Nanotechnology, Technical University of Denmark, DTU Nanotech, Ørsteds Plads 345B, 2800 Kgs. Lyngby, Denmark

‡ Laboratory for Surface Science and Technology, Department of Materials, ETH Zürich, Wolfgang-Pauli-Strasse 10, CH-8093 Zürich, Switzerland

§ Department of Chemical Engineering, Technical University of Denmark, Søltofts Plads Building 227, 2800 Kgs. Lyngby, Denmark

Table S1. Efficiency in removing oxidized PEDOT and PEDOT-N_3 from various substrates using post-stamping DMSO washes at different concentrations. Higher DMSO concentration were better at removing oxidized PEDOT and PEDOT-N_3, in accordance with the strong swelling of PEDOT and PEDOT-N_3 in DMSO.[1] Pure DMSO was not included as a wash, since DMSO dissolves many relevant polystyrene based polymers such as PS-N_3. Oxidized PEDOT-N_3 in general seemed harder to remove than regular PEDOT, perhaps due to slower oxidation. Oxidized PEDOT was more difficult to remove from PS-N_3 than from the COC and especially the PMOXA substrates. No detergent was added in this study.

Experimental			Obs.	Contact Angles			XPS atomic composition							
Substrate	film	Wash sol. DMSO %	Visible Film	Static	Adv	Re	C	O	S	N	Si	Na	Cl	Fe
COC	PEDOT	**0**	No	52	62	<15	85.03	11.27	2.56		0.35	0.33	0.45	
COC	PEDOT	**50**	No	73	72	15	89.84	8	1.6		0.56			
COC	PEDOT	**80**	No	82	84	38	92.63	5.86	1.51					
COC	PEDOT	**90**	No	80	86	40	94.2	4.61	1.19					
COC	PEDOT-N_3	**0**	Yes	66	72	<15	53.91	25.72	5.87	12.57	0.97	0.46	0.5	
COC	PEDOT-N_3	**50**	Yes	58	71	<15	53.11	24.8	6.05	13.93	0.99	0.65	0.47	
COC	PEDOT-N_3	**80**	Shade	63	72	<15	65.52	17.86	5.12	10.69	0.45	0.36		
COC	PEDOT-N_3	**90**	No	69	75	<15	74.3	15.85	2.48	4.85	1.66			0.86
COC ref.	none			92	100	81	99.9	0.1						
PS-N_3	PEDOT	**0**	no	65	62	<15	72.95	14.1	3.27	8.4			0.48	0.8
PS-N_3	PEDOT	**50**	Shade	56	61	<15	74.22	11.61	2.85	10.32			0.37	0.62
PS-N_3	PEDOT	**80**	Shade	58.5	71	<15	77.38	9.44	2.63	10.09				0.47
PS-N_3	PEDOT	**90**	Shade	50	66	<15	76.56	10.48	2.74	9.48				0.74
PS-N_3	PEDOT-N_3	**0**	Yes	65	69	<15	52.49	26.56	5.99	13.58	0.82	0.56		
PS-N_3	PEDOT-N_3	**50**	Yes	66	70	<15	52.37	25.79	5.89	13.81	0.93	0.53	0.32	0.36
PS-N_3	PEDOT-N_3	**80**	No	53	67	15	61.41	18.11	5.02	15.16				0.3
PS-N_3	PEDOT-N_3	**90**	No	67	72	<15	65.14	15.6	4.08	14.17		0.35		0.67
PS-N_3 ref.	none			80	86	71	80.5			19.5				
PMOXA	PEDOT	**0**	No	41	57	<15	73.79	10.88	1.46	12.87			0.52	0.48
PMOXA	PEDOT	**50**	No	32	35	<15	77.25	8.03	0.78	13.94				
PMOXA	PEDOT	**80**	No	20	23	<15	76.97	8.24	1.04	13.75				
PMOXA	PEDOT	**90**	No	29	28.5	<15	82.05	7.35	0.67	9.93				
PMOXA	PEDOT-N_3	**0**	Yes	66	70	18	55.95	24.26	5.23	12.28	0.92	0.92	0.44	
PMOXA	PEDOT-N_3	**50**	Yes	64	73	<15	53.11	25.29	5.82	13.66	1.19	0.69	0.24	
PMOXA	PEDOT-N_3	**80**	No	50	47	15	66.56	14.74	3.48	14.78		0.43		
PMOXA	PEDOT-N_3	**90**	No	45	45	<15	74.34	9.41	1.25	14.63		0.36		
PMOXA ref	none			19	20	<15	72.5	9.7		17.8				

Experimental details: PEDOT and PEDOT-N_3 precursor films were spin-coated at 700 rpm and at 2000 rpm, respectively. The stamping solution contained 1.7-2.5 wt% NaOCl. Stamping time of 4 mins and washing time of 10 mins were used. Following the DMSO wash the samples were rinsed in MilliQ water. PMOXA films were made by coupling a PS-N_3 substrate with 1.5 mM alkyne-PMOXA-OH (4000 Da) overnight in 50/50 v/v DMSO/H_2O using 7.5 mM sodium ascorbate and 0.75 mM $CuSO_4$ as catalyst.

Table S2. Efficiency of PEDOT and PEDOT-N_3 removal from COC and PS-N_3 using either a post-stamping 80/20 v/v DMSO/H_2O wash, or using a stamping solution containing 5 vol% Triton-X100 and washing only in water after the stamping. Addition of detergent to the stamp was found to be more efficient in removing oxidized PEDOT or PEDOT-N_3 than washing in DMSO after the stamping. Note that the PEDOT removal is this study was less effective than later results using comparable stamping procedures. This is likely due to incomplete rinsing of the substrates prior to spincoating of PEDOT. The slightly reduced contact angles observed for PEDOT on PS-N_3 stamped with an agarose stamp containing Triton-X100 may not be due to leftover oxidized PEDOT, since other experiments showed that polystyrene substrates became more hydrophilic just by spin coating Clevios-Cb40 (Fe(III)tosylate in n-butanol) and heating, i.e. without any EDOT monomer present. Other non-ionic detergents such as Tween-20 had a similar effect as Triton-X100, whereas the ionic detergent SDS caused coagulation of material in the stamping solution.

Experimental				Contact Angles		
Substrate	film	Triton in stamp	Wash sol. DMSO %	Static	Adv	Re
COC	PEDOT	No	80	80	91	63
COC	PEDOT	Yes	0	85	93	72
COC	PEDOT-N3	No	80	64	76	38
COC	PEDOT-N3	Yes	0	83	89	54
COC ref.	none			92	100	81
PS-N_3	PEDOT	No	80	65	73	25
PS-N_3	PEDOT	Yes	0	72	76	58
PS-N_3 ref.	none			80	86	71

Experimental details: PEDOT and PEDOT-N_3 precursor films were spin-coated at 700 rpm and at 2000 rpm, respectively. The stamping solution contained 1.7-2.5 wt% NaOCl. A stamping time of 4 mins and a washing time of 10 mins were used. After stamping and washing, all samples were rinsed thoroughly in MilliQ water.

Table S3. Efficiency of removal of PEDOT from COC for varying stamping times and NaOCl concentrations. All tested NaOCl concentrations resulted in comparable results using stamping times of 4-8 min. A stamping time of 1 min yielded similar results for NaOCl concentrations ≥0.625 wt%, whereas 0.25 wt% NaOCl did not efficiently remove the oxidized PEDOT.

Experimental				Contact Angles		
Substrate	film	% NaOCl in stamp	Stamp time / mins	Static	Adv	Re
COC	PEDOT	2.5	1	84	91	61
COC	PEDOT	2.5	4	75	92	71
COC	PEDOT	2.5	8	82	88	71
COC	PEDOT	1.25	1	68	82	54
COC	PEDOT	1.25	4	84	97	74
COC	PEDOT	1.25	8	90	92	75
COC	PEDOT	0.625	1	72	88	63
COC	PEDOT	0.625	4	79	82	68
COC	PEDOT	0.625	8	83	93	68
COC	PEDOT	0.25	1	51	43	<15
COC	PEDOT	0.25	4	74	88	65
COC	PEDOT	0.25	8	82	87	64
COC ref.	none			92	100	81

Experimental details: PEDOT precursor films were spin-coated at 700 rpm. Stamping solutions contained 5 vol% Triton-X100. Washing was conducted in MilliQ water. The presented data show less efficient PEDOT removal than later results using comparable stamping procedures. This is likely caused by incomplete rinsing of the COC substrates prior to spin-coating of PEDOT.

Table S4. Efficiency of removal of PEDOT from COC for varying stamping times and NaOCl concentrations, with an added subsequent washing step. All tested conditions efficiently removed oxidized PEDOT, except for 1 min stamping time using 0.25 wt% NaOCl.

Experimental				Contact Angles		
Substrate	film	% NaOCl in stamp	Stamp time / mins	Static	Adv	Re
COC	PEDOT	2.5	1	90	98	82
COC	PEDOT	2.5	4	90	92	80
COC	PEDOT	2.5	8	89	91	80
COC	PEDOT	1.25	1	86	97	78
COC	PEDOT	1.25	4	88	93	82
COC	PEDOT	1.25	8	84	93	78
COC	PEDOT	0.625	1	84	91	78
COC	PEDOT	0.625	4	88	100	78
COC	PEDOT	0.625	8	84	93	78
COC	PEDOT	0.25	1	46	46	<15
COC	PEDOT	0.25	4	88	95	80
COC	PEDOT	0.25	8	86	91	72
COC ref.	none			92	100	81

Experimental details: PEDOT precursor films were spin-coated at 700 rpm. Stamping solutions contained 5 vol% Triton-X100. Washing was conducted for 10 min in 5 vol% Triton-X100 in 10/90 v/v Clevios C-B40/H_2O, followed by rinsing in MilliQ water.

Table S5. Efficiency of removal of PEDOT from COC for varying Triton-X100 concentrations and NaOCl concentrations in the stamping solution. Stamped samples were only washed in MilliQ water. All tested combinations of concentrations resulted in similar removal of oxidized PEDOT, indicating that low (0.2 wt%) Triton-X100 concentrations are adequate for the process.

Experimental				Contact Angles		
Substrate	film	% NaOCl in stamp	% Triton in stamp	Static	Adv	Re
COC	PEDOT	1.5	5	81	93	68
COC	PEDOT	1.5	1	81	90	64
COC	PEDOT	1.5	0.2	75	89	52
COC	PEDOT	0.75	5	79	89	69
COC	PEDOT	0.75	1	76	90	64
COC	PEDOT	0.75	0.2	79	91	61
COC ref.	none			92	100	81

Experimental details: PEDOT precursor films were spin-coated at 700 rpm. Stamping time was 4 min. Washing was only conducted MilliQ water.

Table S6. Efficiency of removal of PEDOT from COC for varying Triton-X100 concentrations and NaOCl concentrations in the stamping solution when including a subsequent washing step. All tested combinations of concentrations resulted in similar removal of oxidized PEDOT, indicating that low (0.2 wt%) Triton-X100 concentrations are adequate for the process.

Experimental				Contact Angles		
Substrate	film	% NaOCl in stamp	% Triton in stamp	Static	Adv	Re
COC	PEDOT	1.5	5	83	90	76
COC	PEDOT	1.5	1	85	93	76
COC	PEDOT	1.5	0.2	85	94	70
COC	PEDOT	0.75	5	89	99	84
COC	PEDOT	0.75	1	89	96	79
COC	PEDOT	0.75	0.2	87	93	77
COC ref.	none			92	100	81

Experimental details: PEDOT precursor films were spin-coated at 700 rpm. Stamping time was 4 min. Washing was conducted for 10 min in 5 vol% Triton-X100 in 10/90 v/v Clevios C-B40/H_2O, followed by rinsing in MilliQ water.

Table S7. Probing the influence of the stamp oxidant (hypochlorite) when stamping directly on PS-N_3 surfaces reacted with PEG or PMOXA. The XPS results show only minor changes in surface elemental composition after being contacted by the hypochlorite loaded stamp.

Experimental				XPS atomic comp.			
Substrate	Coating	film	Stamped?	C	O	S	N
PS-N_3	PEG	-	No	81.94	10.95		7.11
PS-N_3	PEG	-	Yes	81.05	11.24		7.71
PS-N_3	PMOXA-COOH	-	No	75.04	8.84		16.12
PS-N_3	PMOXA-COOH	-	Yes	76.76	8.13		15.12
PS-N_3	PMOXA-OH	-	No	81.31	5.91		12.78
PS-N_3	PMOXA-OH	-	Yes	81.85	5.19		13.23
PS-N_3	PMOXA-OH	PEDOT	Yes	82.44	5.44	0.36	11.76

Experimental details: PS-N_3 substrates were produced as described in the experimental details of the main text. PMOXA films or PEG films, respectively, resulted from overnight reaction of the PS-N_3 substrate in 1.5 mM of alkyne-PMOXA or alkyne-PEG in 50/50 v/v DMSO/H_2O with 7.5 mM sodium ascorbate and 0.75 mM $CuSO_4$. All samples except the last sample with an additional PEDOT coating were stamped using a stamping solution wtih 1-1.5 wt% NaOCl followed by rinsing in MilliQ water. The last sample was further coated by PEDOT prior to stamping, through spin-coating of the PEDOT precursor at 700 rpm. The stamping solution contained 1-1.5 wt% NaOCl and 5 vol% Triton-X100. Washing was conducted for 10 min in 5 vol% Triton-X100 in 10/90 v/v Clevios C-B40/H_2O and in 80/20 v/v DMSO/H_2O, followed by rinsing in MilliQ water.

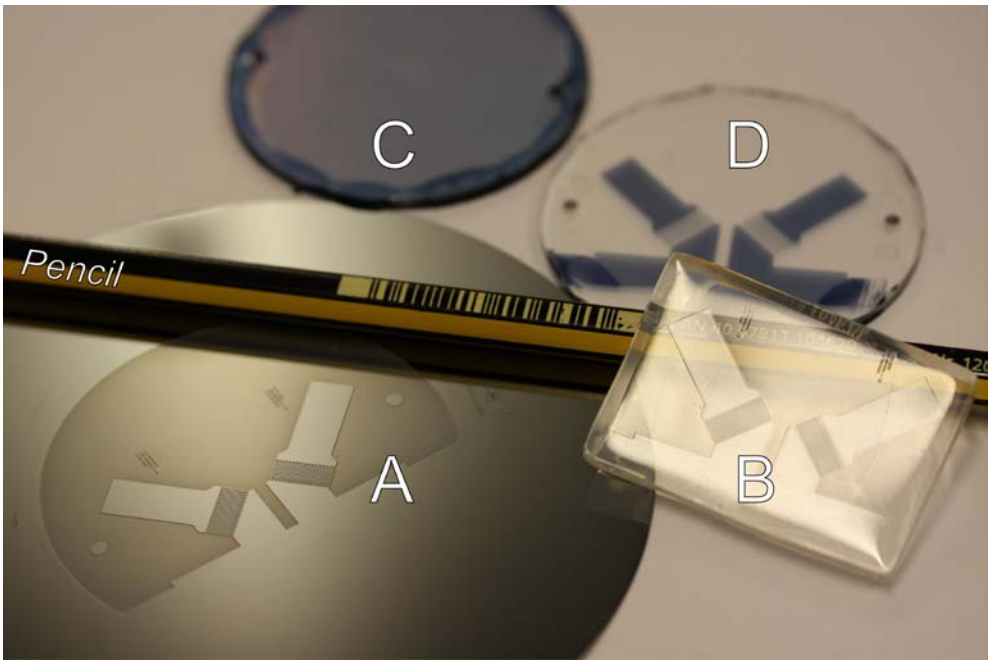

Figure S1. Photograph of the components and materials used for printed deactivation. A pencil is included for scale.
A: Silicon wafer with an inverted relief structure prepared by photolithography and deep reactive ion etching. The wafer serves as a master for making multiple agarose stamps.
B: Agarose hydrogel stamp resulting from replicating the pattern on the wafer. One stamp can be used for patterning multiple PEDOT thin films.
C: PEDOT film on a COC substrate prior to stamping.
D: PEDOT film on a COC substrate patterned by stamping with an agarose stamp soaked in an aqueous solution of 1.5 wt% NaOCl and 0.1 vol% Triton-X100 for 4 mins, followed by washing.

Figure S2. Photographs of PEDOT films on a COC substrate patterned by stamping with an agarose stamp soaked in a solution of 1.5wt% NaOCl and 0.1 vol% Triton-X100 for 4 mins, followed by washing. Pictures A)-C) taken at increasing magnification. A pencil is included for scale in (A).

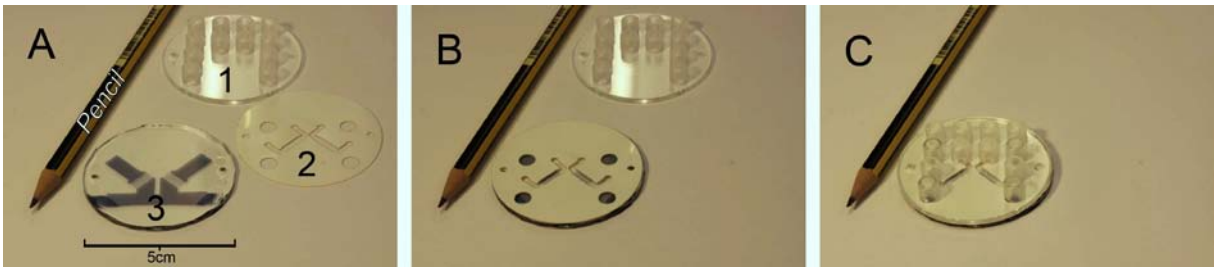

Figure S3. The components of the homemade micro-fluidic chamber. The COC top part containing inlet/outlet connectors (**1**) and the stamped PEDOT electrodes on a flat COC substrate (**3**) is assembled via a laser-cut double-sided transfer adhesive tape defining the microfluidic channels. A) Individual components. B) The structured transfer adhesive (2) is aligned with the electrode connection pads of the bottom plate (3). C) The inlet/outlet connectors of the top part (1) are aligned with the channel structures of the transfer adhesive (2) and the electrode connection pads of the bottom plate (3). A pencil is included for scale.

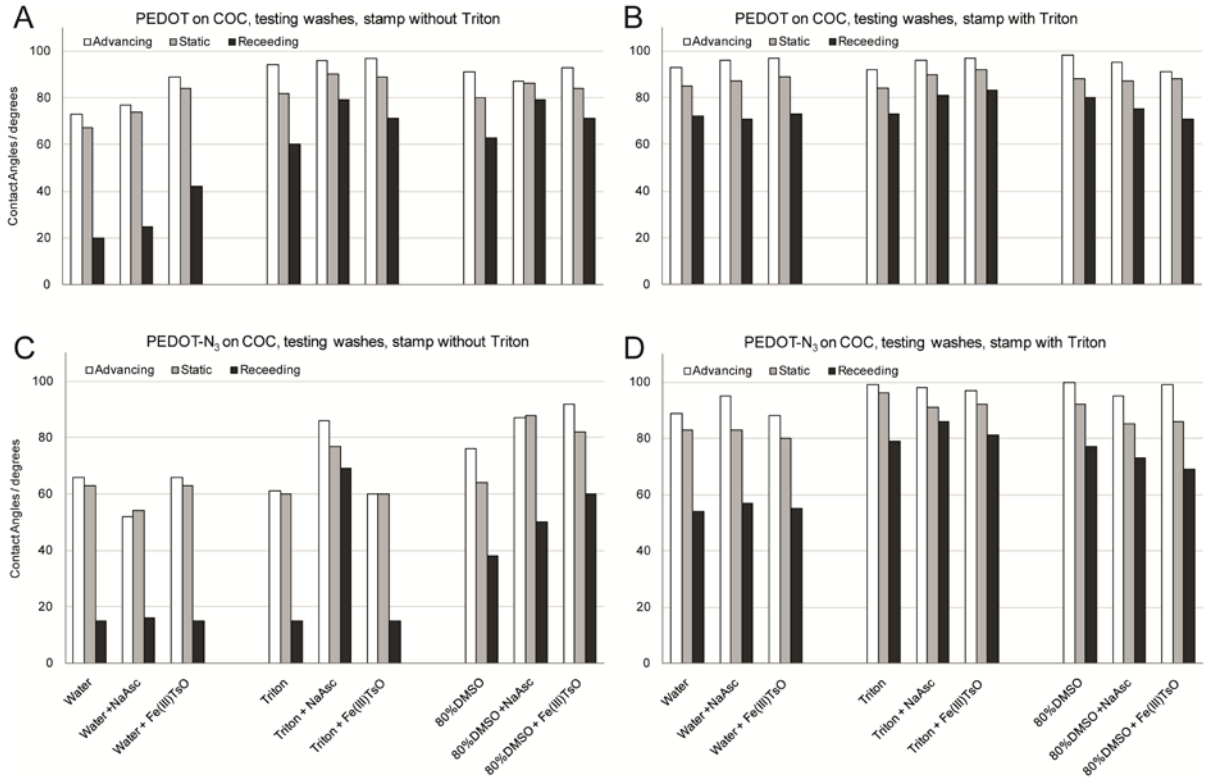

Figure S4. Efficiency of removal of PEDOT and PEDOT-N_3 from COC by adding Triton-X100 to the agarose stamp and/or by adding oxidizing or reducing agents to post-stamp washes. A) Stamping PEDOT on COC, without detergent in the agarose stamp solution. The addition of the reducing agent sodium ascorbate (NaAsc) to the washing solutions had some effect. B) Stamping PEDOT on COC, with detergent in the agarose stamp solution. The conditions in the washing step was of minor importance since removal was good in all cases. C) Stamping PEDOT-N_3 on COC, without detergent in the agarose stamp solution. The addition of sodium NaAsc was effective, and the Triton-X100 wash was found to be superior to washes with 80/20 v/v DMSO/H_2O. D) Stamping PEDOT-N_3 on COC, with detergent in the agarose stamp solution. The washing conditions was of minor importance. The best removal of PEDOT-N_3 was obtained when applying detergent both in the stamp and in the subsequent wash.

Experimental details: PEDOT and PEDOT-N_3 precursor films were spin-coated at 700 rpm and at 2000 rpm, respectively. Stamping solutions contained 1.7-2.5 wt% NaOCl, and additionally contained contained 5 vol% Triton-X100 where indicated. A stamping time of 4 mins and a washing time of 10 mins were used. Washing was conducted in MilliQ water, in MilliQ-water containing 5 vol% Triton-X100, or in 80/20 v/v DMSO/water. These washes contained ~2 wt% NaAsc or 10 vol% Clevios Cb40 (Fe(III)tosylate in n-butanol) where indicated. After the washes all samples were rinsed thoroughly in MilliQ water. For thicker PEDOT-N_3 films, the use of detergent in the stamp seemed to decelerate the oxidation process, even though it assists removal of the PEDOT-N_3 from COC, as seen in figure D. Stamping of samples with thicker PEDOT-N_3 films or sample with PEDOT-N_3 spin-coated on top of PEDOT therefore used a stamp without Triton-X100, with the detergent being introduced along with NaAsc in the subsequent washing step.

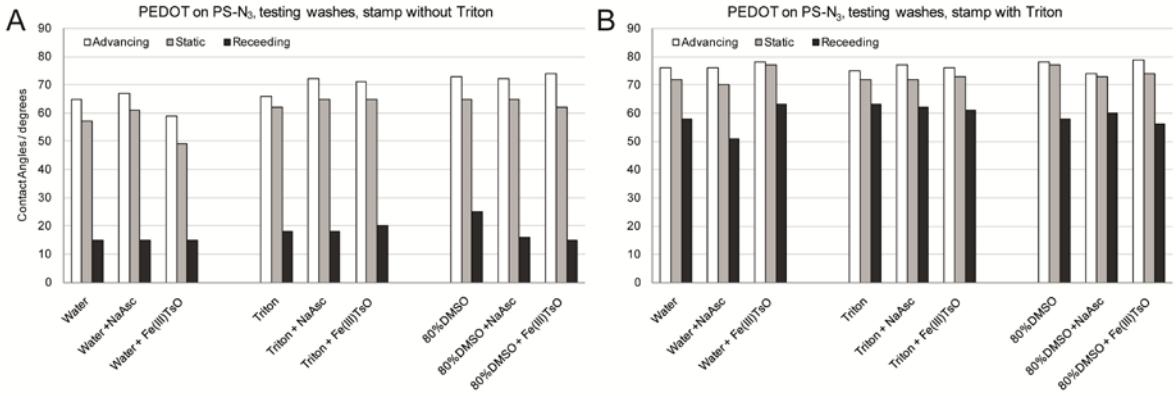

Figure S5. Efficiency of removal of PEDOT from PS-N_3 by adding Triton-X100 to the agarose stamp and/or by adding oxidizing or reducing agents to post-stamp washes. A) Stamping PEDOT on PS-N_3, without detergent in the agarose stamp solution. The oxidized PEDOT was difficult to remove in all cases. B) Stamping PEDOT on PS-N_3, with detergent in the agarose stamp solution. The conditions in the washing step had little significance as long as detergent was added to the stamp.

Experimental details: PEDOT precursor films were spin-coated at 700 rpm. Stamping solutions contained 1.7-2.5 wt% NaOCl, and additionally contained 5 vol% Triton-X100 where indicated. A stamping time of 4 mins and a washing time of 10 mins were used. Washing was conducted in MilliQ water, in MilliQ-water containing 5 vol% Triton-X100, or in 80/20 v/v DMSO/water. These washes contained ~2 wt% NaAsc or 10 vol% Clevios Cb40 (Fe(III)tosylate in n-butanol) where indicated. After the washes all samples were rinsed thoroughly in MilliQ water.

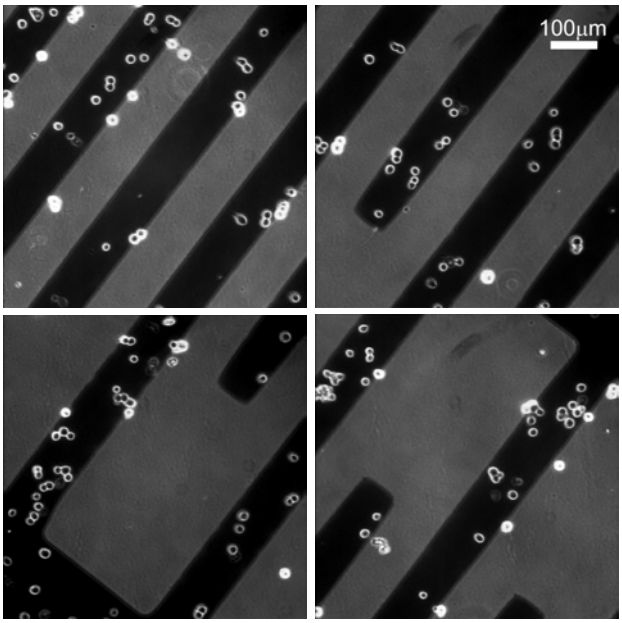

Figure S6. 3T3 cellular adhesion to alkyne-PEG-GRGDS modified PEDOT-N_3/PEDOT electrodes on a PMOXA-functionalized PS-N_3 substrate. The experiments show that cells can be captured specifically onto all electrodes by coupling functional peptides onto all electrodes, and confirm that the binding observed in Fig. 7 on alternating electrodes are in fact due to localized positioning of these peptides.

Experimental details: PS-N_3 substrates were prepared and modified by PMOXA prior to coating by PEDOT, all as described in the experimental section of the main text. After patterned dissolution, the PEDOT-N_3 was functionalized overnight using 2 mM alkyne-PEG-GRGDS in 50/50 v/v DMSO/H_2O with 15 mM sodium ascorbate and 0.5 mM $CuSO_4$. A study of 3T3 fibroblast adhesion to the sample was conducted in an assembled all-polymer microfluidic chamber (see Fig. S3). Fibroblasts at a concentration of 1 mio cells/ml in RPMI were introduced into a chamber pre-filled with HBSS containing Mg^{2+} and Ca^{2+}, and allowed to adhere for 1 h at room temperature. Un-attached cells were washed away by flowing HBSS through the chamber.

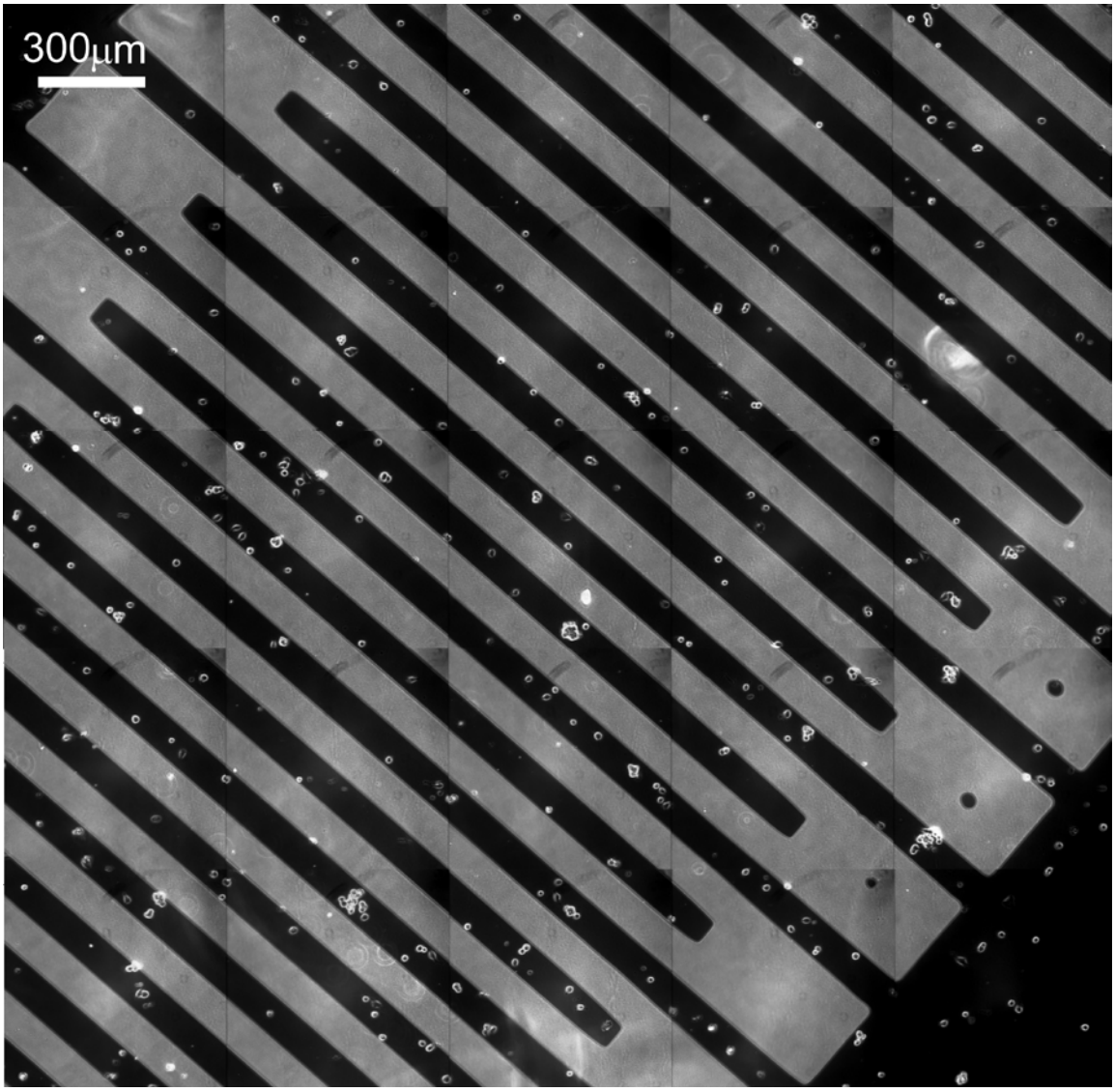

Figure S7. Optical micrograph of 3T3 cells (bright spots) adhering specifically to PEDOT-N_3/PEDOT electrodes (darker areas) on a PS-N_3 substrate (brighter areas). The electrodes were functionalized with high cell-binding alkyne-PEG-GRGDS and the PS-N_3 between the electrodes was reacted with low-binding alkyne-PEG after patterned dissolution. This shows that application of a hidden PMOXA film is not necessary for obtaining a coating between the electrodes which is resistant to cellular binding; conventional PEG films formed after the patterning of PEDOT are also effective.

Experimental details: PEDOT-N_3/PEDOT was deposited on PS-N_3 as described in the experimental section of the main text. PEDOT-N_3 was functionalized overnight using 2.25 mM alkyne-PEG-GRGDS in 50/50 v/v DMSO/H_2O with 15 mM sodium ascorbate and 0.5 mM $CuSO_4$. After stamping, washing, and re-oxidation, the background was functionalized with 5 mM alkyne-PEG (750 Da) overnight in 40/60 v/v DMSO/H_2O with 10 mM sodium ascorbate and 1 mM $CuSO_4$. Following the reaction the samples were re-oxidized and rinsed. A study of 3T3 fibroblast adhesion to the sample was conducted in an assembled all-polymer microfluidic chamber (see Fig. S3). Fibroblasts at a concentration of 1 mio cells/ml in RPMI were introduced into a chamber pre-filled with HBSS containing Mg^{2+} and Ca^{2+}, and allowed to adhere for 1 h at room temperature. Un-attached cells were washed away by flowing HBSS through the chamber.

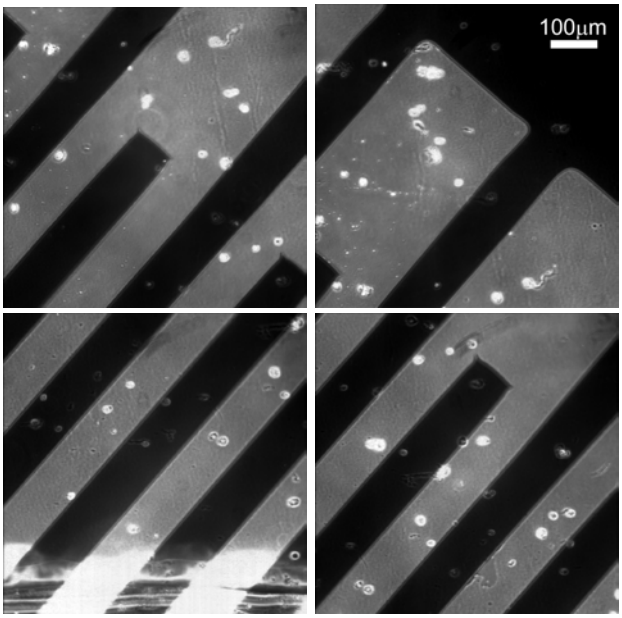

Figure S8. Optical micrograph of the non-specific adhesion of 3T3 cells (bright spots) to un-functionalized PEDOT-N_3 / PEDOT electrodes (darker areas) on a PS-N_3 substrate (brigher areas). The experiments confirm that functionalization of the spacing between the electrodes, as well as of the electrodes, is required for the specific cell capture presented in Figs. 7, S6, and S7.

Experimental details: The micrographs were obtained in the same experiment as that presented in Fig. S7 by observing a patterned but un-functionalized part of the sample. The white shading seen in the bottom of one picture is the transfer adhesive edge of the channel.

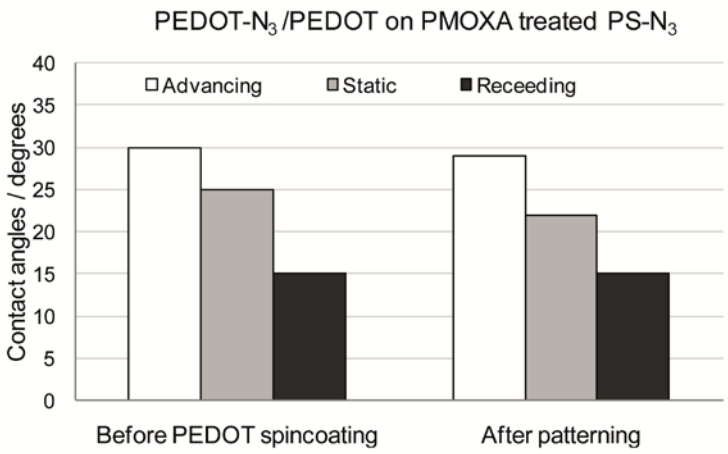

Figure S9. A sample similar to the one used for cellular attachment studies in Fig. 7 and Fig. S6 was fabricated. The water contact angles in the stamped areas were found to be identical to those of PMOXA, confirming the re-exposure of this very hydrophilic coating.

The slightly higher advancing contact angles observed for this PMOXA coating compared to those found for some of the earlier presented PMOXA samples may be due to different PMOXA batches. For the films presented in this graph alkyne-PMOXA-OH (4000 Da) fabricated by a microwave assisted synthesis, along with a subsequent reaction with a alkyne-PMOXA-OH (2000 Da), were used. The earlier presented samples used alkyne-PMOXA-OH (4000Da) synthesized without use of microwave.

Polymer synthesis

Synthesis of 4-(azidomethyl)styrene (PS-N_3) (see Figure S10)

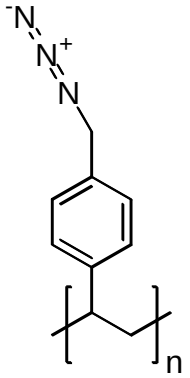

Figure S10. Structure of poly(4-(azidomethyl)styrene (PS-N_3)

2,2'-Azobisisobutyrylnitrile (AIBN, 71.2 mg, 0.4 mmol), 4-(chloromethyl)styrene (10 mL, 71.0 mmol and xylene were mixed in a Schlenk tube and the solution was bubbled through with nitrogen for 30 min. The polymerization was run under a positive nitrogen pressure at 65°C for 18 h. The polymer was precipitated in methanol, filtered and dried in vacuo. The isolated intermediate (poly(4-(chloromethyl)styrene)) was a white powder and was used for the following step without further purification (6.4 g, Mn=30 kg/mol, PDI=1.7).
FT-ATR-IR (cm-1): 3100-2800 (C-H stretch); 1612+1510 (aromatic ring stretch); 672 (C-Cl stretch). 1H-NMR(CDCl3, 300MHz, δH, ppm): 1.39 (m, 2H, CH2-CH); 1.70 (m, 1H, CH-CH2); 4.52 (s, 2H, CH2-N3); 6.49, 7.05 (2xm, 4H, aromatic H). HSQC confirmed the following proton/carbon correlations (δH/δC (ppm)): 1.39/41.6 (CH-CH2); 1.70/38.7 (CH-CH2-ph); 4.52/44.9 (CH2-N3); 6.49/126.4 (aromatic CH); 7.05/127.0 (aromatic CH).

Poly(4-(chloromethyl)styrene) (5.18 g, 34.0 mmol functional group) was dissolved in DMF (100 mL) and NaN_3 (2.75 g, 42.4 mmol) was added to the solution. The reaction mixture was stirred at 40°C for 18 h under nitrogen. After reaction the excess of reagent was removed by precipitation into H_2O. The precipitate was isolated by filtration and rinsed with copious amounts of H_2O and methanol. The solid was dissolved in THF and precipitated in methanol to afford poly(4-(azidomethyl)styrene) as a white powder (4.62 g, 86 %). FT-ATR-IR(cm^{-1}): 3100-2800 (C-H stretch); 2090 (C-N_3 stretch); 1612+1510 (aromatic ring stretch). ^{1}H-NMR($CDCl_3$, 300MHz, δ_H, ppm): 1.39 (m, 2H, CH_2-CH); 1.69 (m, 1H, CH-CH_2); 4.24 (s, 2H, CH_2-N_3); 6.48, 6.97 (2xm, 4H, aromatic H). HSQC confirmed the following proton/carbon correlations (δ_H/δ_C (ppm)): 1.39/44.9 (CH-CH_2); 1.69/40.4 (CH-CH_2-ph); 4.24/54.0 (CH_2-N_3); 6.48/127.7 (aromatic CH); 6.97/127.7 (aromatic CH).
NMR spectroscopy was performed on a 300 MHz Cryomagnet from Spectrospin & Bruker (^{1}H-NMR at 300MHz, ^{13}C-NMR at 75MHz), at room temperature. IR was performed on a PerkinElmer Spectrum One model 2000 Fourier transform infrared system with a universal attenuated total reflection sampling accessory on a ZnSe/diamond composite.

Synthesis of Poly-[4-(prop-2-yn-1-yloxy)-styrene-ran-styrene] (see Figure S11)

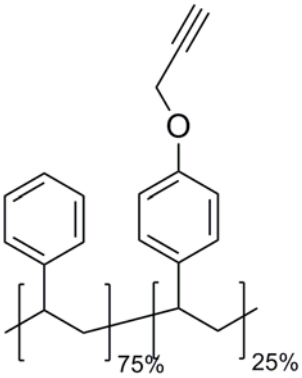

Figure S11. Poly[4-(prop-2-yn-1-yloxy)-styrene-*ran*-styrene] (PS-alkyne)

A randomized co-polymer of styrene and an alkyne-functionalized styrene was synthesized in accordance with our former reports, [2, 3] containing 25% alkyne functional monomer and 75% styrene monomer.

Synthesis of hydroxyl-terminated poly(2-methyl-2-oxazoline)s (see Figure S12)

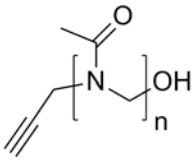

Figure S12. Structure of propargyl-poly(2-methyl-2-oxazoline) (alkyne-PMOXA-OH)

Hydroxyl-terminated propargyl-PMOXA (alkyne-PMOXA-OH) was prepared by living cationic ring opening polymerization as previously described.[4-9] The cationic ring opening polymerization of 2-methyl-2-oxazoline (MeOx) was initiated with addition of propargyl p-toluenesulfonate at initiator ratios of 1:20, 1:50, or 1:100, respectively. The polymerization was terminated with Na_2CO_3/water to obtain hydroxyl-terminated PMOXA. The polymers were purified by dialysis (2 times 24 h; Spectrum Laboratories Inc., Spectra/Por 7). PMOXA-OH was collected as a white solid after lyophilization and characterized by proton nuclear magnetic resonance (^{1}H NMR) spectroscopy (500 MHz, Bruker). By comparing the integrals from the methylene group adjacent to the acetylene group and the methylene groups in the backbone, the degree of polymerizations were found to be approximately 16, 60 and 109, close to the expected values of 20, 50, 100 respectively. ^{1}H NMR (D_2O): δ 4.0 - 4.2 (CH-C-C**H**$_2$-N-), 3.3 - 3.7 (-C**H**$_2$-N(CH_3-C=O)), 1.8 - 2.2 ppm (-(C=O)-C**H**$_3$).

Synthesis of hydroxyl-terminated poly(2-methyl-2-oxazoline) in a Microwave Synthesizer
PMOXA synthesis assisted by microwave was conducted in a similar manner to earlier reports.[10-12] Propargyl p-toluenesulfonate, MeOx and acetonitrile were prepared in a pre-dried microwave vial under inert conditions. The monomer to initiator ratio was 50 and the volume was 20 ml. The vial was capped and heated to 140 °C for 2 min. After the reaction, Na_2CO_3/water was added to terminate the polymerization. The polymers were purified by dialysis (2 times 24 h; Spectrum Laboratories Inc., Spectra/Por 7). Alkyne-PMOXA-OH was collected as a white solid after lyophilization and characterized by proton nuclear magnetic resonance (^{1}H NMR) spectroscopy (500 MHz, Bruker) similar to above.

Synthesis of carboxy-terminated poly(2-methyl-2-oxazoline)s

Carboxy-terminated alkyne-PMOXA was prepared by living cationic ring opening polymerization with a monomer to initiator ratio of 50. MeOx was dissolved in acetonitrile under argon and propargyl p-toluenesulfonate was added at 0˚C under argon. The mixture was then heated to 70˚C for 20 h. Subsequently, the reaction mixture was cooled to room temperature and the reaction was quenched by addition of ethyl piperidine-4-carboxylate for 12 h. The solvent was removed under reduced pressure to yield clear colorless oil. After addition of water, the polymers were purified by dialysis. (2 times 24 h; Spectrum Laboratories Inc., Spectra/Por 7). PMOXA-$COOC_2H_5$ was collected as a white solid after lyophilization. The carboxy ethyl ester (-$COOC_2H_5$) functionalized PMOXA was further reacted with sodium hydroxide solution at pH = 14 and room temperature for 24 h, resulting in alkyne-PMOXA-COOH. The polymers were purified and lyophilized using the same procedure as described above. Proton (^{1}H NMR) spectroscopy was performed to confirm the chemical structure of the synthesized polymers. By comparison the integrals from the methylene group adjacent to the acetylene group and the methylene groups in the backbone, the degree of polymerizations were found to be approximately 55. ^{1}H NMR (D_2O): δ 4.0 - 4.2 (CH-C-C**H**$_2$-N-), 3.3 - 3.7 (-C**H**$_2$-N(CH_3-C=O)), 1.8 - 2.2 ppm (-(C=O)-C**H**$_3$).

Synthesis of alkyne-PEG-GRDGS and alkyne-PEG-GRGDS (see Figure S13):

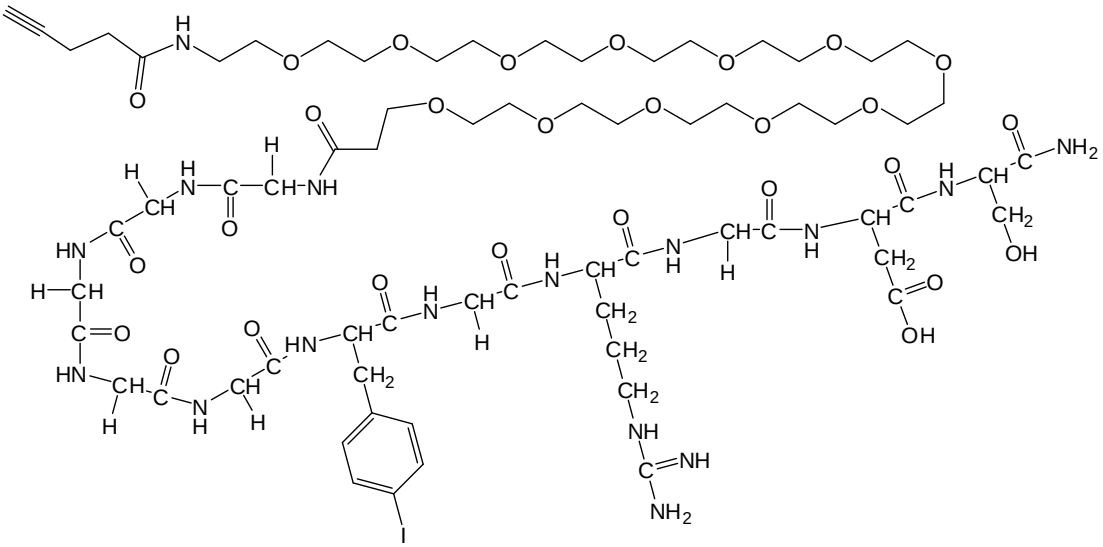

Figure S13. The structure of the alkyne-PEG-GRGDS (similar for "scrambled" alkyne-PEG-GRDGS, except for interchange of the glycine and aspartate moieties). Note the presence of a phenylalanine derivative containing iodine for XPS identification of the molecules.

Pentyne-PEG_{11}-G_5-F(4-iodo)-GRGDS (alkyne-PEG-GRGDS) was made using solid phase synthesis. Base labile Fmoc was used for protecting groups for the amines, and the employed resin was acid labile rink-amide. 2-(1H-7-Azabenzotriazol-1-yl)-1,1,3,3-tetramethyl-uronium-hexafluorophosphate-methanaminium (HATU), Fmoc-Ser(tBu)-OH, Fmoc-Asp(OtBu)-OH, Fmoc-Arg(Pbf)-OH, Fmoc-4-Iodo-Phe-OH, Fmoc-Gly-OH and Rink Amide-AM Resin were bought from GL Biochem (Shanghai, China). Fmoc-NH-PEG_{11}-COOH, *PEG1080*, was acquired from IRIS Biotech (Marktredwitz, Germany). 4-pentynoic acid, EDC, 2,4,6-collidine, trifluoroacetic acid (TFA), triisopropyl silane (TIPS), ninhydrin, piperidine, and all solvents, were acquired from Sigma-Aldrich.

Before reaction, the resin was swelled in dichloromethane (DCM) for 90 min. In each coupling step four equivalents of the new amino acid was used. The amino acid was first mixed with 3.9 equivalent HATU coupling reagent and 8 eq. 2,4,6-collidine in dimethylformamide (DMF), then added to the peptide, and allowed to react for 30 min. The beads were washed 4 times in DMF and 2 times in DCM, each washing step lasting 30 sec. De-protection of the Fmoc group was done by washing twice for 2 min with 20 vol% piperidine in DMF. Kaiser tests were performed to test the presence of free amino groups, between each reaction/de-protection step. The coupling of the PEG segment was done by performing two 1 h long consecutive coupling reactions to ensure a successful binding of the PEG segment. The following pentynoic acid step was also allowed to react for 1 h. The peptide was cleaved from the resin using a solution of 2.5 vol% TIPS, 2.5 vol% Milli-Q water and 95 vol% TFA. A cleaving time of 3 h was used. The cleaving solution containing the peptides was dried on a rotary evaporator. The material remaining was then gently decanted five times using 5 mL diethyl ether.

The product was purified using preparative reverse phase High Performance Liquid Chromatography (RP-HPLC). The RP-HPLC was conducted on a 250 mm x 20 mm C18 column with a bead size of 5 mm and a pore size of 100 Å. Solvent A: 95/5 v/v H_2O/MeOH with 0.1 vol% TFA. Solvent B: 99.9/0.1 v/v MeOH/TFA. The solvents were degassed using a glass filter prior to their use on the RP-HPLC. Solutions of the peptides were made in 50/50 v/v Solvent A/Solvent B. In the RP-HPLC procedure, a linear gradient from 52 vol% to 54 vol% of Solvent A over 16 mins were used. UV detection was set to 206 nm (carbonyl) and 257 nm (phenylalanine). An equivalent procedure was used for the fabrication and purification of the scrambled sequence peptide, *pentyne-PEG$_{11}$-G$_5$-F(4-iodo)-GRDGS (*alkyne-PEG-GRDGS).

Yields after RP-HPLC purification and freeze drying:
Pentyne-PEG$_{11}$-G$_5$-F(4-iodo)-GRGDS, (*alkyne-PEG-GRGDS*): 41.3 mg (16%)
Scrambled Pentyne-PEG$_{11}$-G$_5$-F(4-iodo)-GRDGS, (*alkyne-PEG-GRDGS*): 48.8 mg (19%)
The purity of the products was confirmed by MALDI-TOF MS using a Bruker Reflex IV MALDI-TOF, matrix 50 mg/ml 2,5-dihydroxy benzoic acid (DHB) in ethanol, and 0.1-1mg/mL solutions.

References for Supporting Information

(1) Lind, J. U.; Hansen, T. S.; Daugaard, A. E.; Hvilsted, S.; Andresen, T. L.; Larsen, N. B. Solvent Composition Directing Click-Functionalization at the Surface Or in the Bulk of Azide-Modified PEDOT. *Macromolecules* **2011**, *44*, 495--501.

(2) Daugaard, A. E.; Hvilsted, S. The Influence of Pendant Carboxylic Acid Loading on Surfaces of Statistical Poly [(4-hydroxystyrene)-co-styrene] s. *Macromol. Rapid Commun.* **2008**, *29*, 1119-1125.

(3) Thomsen, A. D.; Malmström, E.; Hvilsted, S. Novel Polymers with a High Carboxylic Acid Loading. *J. Polym. Sci. Polym. Chem.* **2006**, *44*, 6360-6377.

(4) Pidhatika, B.; Moller, J.; Vogel, V.; Konradi, R. Nonfouling Surface Coatings Based on Poly (2-Methyl-2-Oxazoline). *CHIMIA* **2008**, *62*, 264-269.

(5) Pidhatika, B.; Möller, J.; Benetti, E. M.; Konradi, R.; Rakhmatullina, E.; Mühlebach, A.; Zimmermann, R.; Werner, C.; Vogel, V.; Textor, M. The Role of the Interplay between Polymer Architecture and Bacterial Surface Properties on the Microbial Adhesion to Polyoxazoline-Based Ultrathin Films. *Biomaterials* **2010**, *31*, 9462-9472.

(6) Konradi, R.; Pidhatika, B.; Mühlebach, A.; Textor, M. Poly-2-Methyl-2-Oxazoline: A Peptide-Like Polymer for Protein-Repellent Surfaces. *Langmuir* **2008**, *24*, 613-616.

(7) Luxenhofer, R.; Jordan, R. Click Chemistry with Poly (2-Oxazoline)s. *Macromolecules* **2006**, *39*, 3509-3516.

(8) Fijten, M. W. M.; Haensch, C.; van Lankvelt, B. M.; Hoogenboom, R.; Schubert, U. S. Clickable Poly (2-Oxazoline)s as Versatile Building Blocks. *Macromol. Chem. Phys.* **2008**, *209*, 1887-1895.

(9) Kagiya, T.; Narisawa, S.; Maeda, T.; Fukui, K. Ring-Opening Polymerization of 2-Substituted 2-Oxazolines. *J. Polym. Sci. Polym. Lett.* **1966**, *4*, 441-445.

(10) Wiesbrock, F.; Hoogenboom, R.; Leenen, M. A. M.; Meier, M. A. R.; Schubert, U. S. Investigation of the Living Cationic Ring-Opening Polymerization of 2-Methyl-, 2-Ethyl-, 2-Nonyl-, and 2-Phenyl-2-Oxazoline in a Single-Mode Microwave Reactor. *Macromolecules* **2005**, *38*, 5025-5034.

(11) Wiesbrock, F.; Hoogenboom, R.; Abeln, C. H.; Schubert, U. S. Single-Mode Microwave Ovens as New Reaction Devices: Accelerating the Living Polymerization of 2-Ethyl-2-Oxazoline. *Macromol. Rapid Commun.* **2004**, *25*, 1895-1899.

(12) Weber, C.; Becer, R. C.; Baumgaertel, A.; Hoogenboom, R.; Schubert, U. S. Preparation of Methacrylate End-Functionalized Poly (2-Ethyl-2-Oxazoline) Macromonomers. *Polymers* **2009**, *12*, 149-165.